

SOUTH CHINA KARST

1

Zbirka ZRC 19

Chen Xiaoping	Andrej Mihevc
Franci Gabrovšek	Bojan Otoničar
Huang Chuxing	Shi Mengxiong
Jin Yuzhang,	Tadej Slabe
Martin Knez	Stanka Šebela
Janja Kogovšek	Wu Wenqing
Liu Hong	Zhang Shouyue
Metka Petrič	Nadja Zupan Hajna

South China Karst I

1 – Karst Studies of Yunnan

2 – Cave Studies in W Guizhou

© 1998, ZRC SAZU

Uredniški odbor/ Editorial board

Franci Gabrovšek, Martin Knez, Janja Kogovšek, Liu Hong,
Metka Petrič, Andrej Mihevc, Bojan Otoničar, Tadej Slabe,
Stanka Šebela, Zhang Shouyue, Nadja Zupan Hajna

Založil/Published by

Znanstvenoraziskovalni center Slovenske akademije znanosti in umetnosti

Založba ZRC

Za založnika/Represented by

Oto Luthar

Urednik založništva/Managing Editor

Vojislav Likar

Oblikovanje in grafična ureditev /Design and graphic art

Milojka Žalik Huzjan

Tisk/Printed by

Littera Picta, Ljubljana, Slovenia

Tiskano s podporo Ministrstva za znanost in tehnologijo Republike Slovenije.

Published with the support of the Ministry of Science and Technology of the Republic of Slovenia.

CIP - kataložni zapis o publikaciji
Narodna in univerzitetna knjižnica, Ljubljana

551.435.8(510)

SOUTH China karst / [Chen Xiaoping ... [et al.]]

- Ljubljana : Znanstvenoraziskovalni center

Slovenske akademije znanosti in umetnosti, Založba ZRC, 1998. -

(Zbirka ZRC ; 19)

1. - 1998

ISBN 961-6182-86-4 (zv. 1)

1. Xiaoping, Chen

79955456

Po mnenju Ministrstva za kulturo R. Slovenije sodi publikacija med proizvode, za katere se plačuje 5-odstotni davek od prometa s proizvodi.

South China Karst

I

CONTENTS

INTRODUCTION	7
1. KARST STUDIES OF YUNNAN	
1.1. KARST OF YUNNAN..... <i>Huang Chuxing, Liu Hong</i>	11
1.2. THE LUNAN STONE FORESTS..... <i>Huang Chuxing, Martin Knez, Liu Hong, Tadej Slabe, Stanka Šebela</i>	18
1.3. LITHOLOGIC PROPERTIES OF THE THREE LUNAN STONE FORESTS (SHILIN, NAIGU AND LAO HEI GIN)	30
<i>Martin Knez</i>	
1.4. STRUCTURAL CHARACTERISTICS OF SHILIN STONE FOREST	44
<i>Stanka Šebela</i>	
1.5. ROCK RELIEF OF PILLARS IN THE LUNAN STONE FORESTS	51
<i>Tadej Slabe</i>	
1.6. ROCK DISSOLUTION IN STONE FORESTS	68
<i>Janja Kogovšek</i>	
1.7. HYDROLOGICAL CHARACTERISTICS OF THE TIANSHENGAN AREA.....	82
<i>Metka Petrič</i>	
1.8. PHYSICAL AND CHEMICAL CHARACTERISTICS OF GROUNDWATER OF TIANSHENGAN AREA (The wider area of the tracing experiments)	91
<i>Janja Kogovšek</i>	
1.9. TRACING TEST IN THE TIANSHENGAN AREA.....	99
<i>Janja Kogovšek, Liu Hong, Metka Petrič, Wu Wenqing</i>	
1.10. JIUXIANG	113
<i>Martin Knez, Janja Kogovšek, Tadej Slabe</i>	
1.11. A STUDY ON RECENT KARST DENUDATION RATE OF KARST IN SHILIN, STONE FOREST	122
<i>Liu Hong</i>	
1.12. THE ANALYSIS RESEARCH ON SOIL EROSION CHARACTERS IN KARST MOUNTAINS AREA ENVIRONMENT XICHOU OF YUNNAN	127
<i>Chen Xiaoping</i>	

2. KARST STUDIES IN WEST GUIZHOU

INTRODUCTION	137
<i>Zhang Shouyue</i>	
2.1. THE KARST PLATEAU OF EAST YUNNAN AND WEST GUIZHOU	139
<i>Zhang Shouyue</i>	
2.2. THE KARST ENVIRONMENT AND CAVES. RESOURCES OF LIUPANSHUI	144
<i>Shi Mengxiong & Zhang Shouyue</i>	
2.3. HYDROCHEMICAL PROPERTIES OF KARST WATER IN LIUPANSHUI	158
<i>Jin Yuzhang</i>	
2.4. SPELEOLOGICAL EXPLORATION AT TIANSHENGQIAO - NATURAL BRIDGE, SHUI CHENG	161
<i>Gabrovšek Franci, Andrej Mihevc, Bojan Otoničar & Nadja Zupan Hajna</i>	
2.5. KARSTOLOGICAL RESEARCH OF THE CAVE BY XINGCHANG VILLAGE	170
<i>Gabrovšek Franci, Andrej Mihevc, Bojan Otoničar & Nadja Zupan Hajna</i>	
2.6. LITHOLOGIC CHARACTERISTICS OF YEZHONG PLATEAU	175
<i>Bojan Otoničar</i>	
2.7. SOME GEOMORPHOLOGIC OBSERVATIONS OF THE CONE KARST RELIEF IN WEST GUIZHOU	187
<i>Andrej Mihevc</i>	
2.8. EFFECTS OF GEOLOGICAL STRUCTURAL ELEMENTS ON GENESIS OF CONE KARST IN NORTHWEST GUIZHOU	198
<i>Nadja Zupan Hajna</i>	
2.9. CLASTIC SEDIMENTS FROM KARST OF SOUTHEAST YUNNAN AND NORTHWEST GUIZHOU	213
<i>Nadja Zupan Hajna</i>	
2.10. LAND USE IN MOUNTAINOUS KARST AREAS	224
<i>Andrej Mihevc</i>	
2.11. CONCLUSIONS	239
<i>Zhang Shouyue, Andrej Mihevc, Bojan Otoničar</i>	

INTRODUCTION

Members of the Karst Research Institute ZRC SAZU, Postojna, and members of the Yunnan Institute of Geography and Institute of Geology of the Chinese Academy of Sciences gathered the results of karstological researches of south Chinese karst in two projects adopted by an agreement on scientific and technological cooperation between the Government of the Republic of Slovenia and the Republic of China. The projects Karst Environmental Protection and Exploitation of Cave Resources and Study of Stone Forest Genesis, Function and Structures of the Underground Karst Aquifers in Lunan, Yunnan Province were going on from 1995 to 1997. They were made feasible by the Slovene and Chinese Ministry of Science and Technology and supported by Yunnan Provincial Science and Technology Commission, Administration of Stone Forest, and The Ninth Township Scenic Spots and Historical Sites Administrative Bureau, Yiliang County. The researches were carried out near Liupanshui, the western part of Guizhou, in karst between the mountains in Guizhou and Yunnan Plateau, in the area of Lunan stone forests and in cone-karst at Xichou, Yunnan.

The edition of this book was enabled by Research Fund of Scientific Research Centre SAZU and Ministry of Science and Technology of the Republic of Slovenia.



Geographical position of Yunnan and Guizhou

1

South
Karst Studies
China
of Yunnan
Karst

I

1.1. KARST OF YUNNAN

Huang Chuxing, Liu Hong

General introduction

The Yunnan province is situated in the S of the Qinghai-Tibetan high plateau, with 21°09' to 29°15'N latitude, 97°39' to 106°12' E longitude (Figs. 1.1.1., 1.1.2., 1.1.3., 1.1.4., 1.1.5.). It is 910 km long and 884 km wide

territory of 394,000 km². The Tropic of Cancer passes across the Yunnan province. Topographically NW part has high elevations. The highest peak of the Meili Snow mountain range is 6740 m above sea level and is located on the border of Yunnan and Tibet. Towards E, SE and SW, the relief is

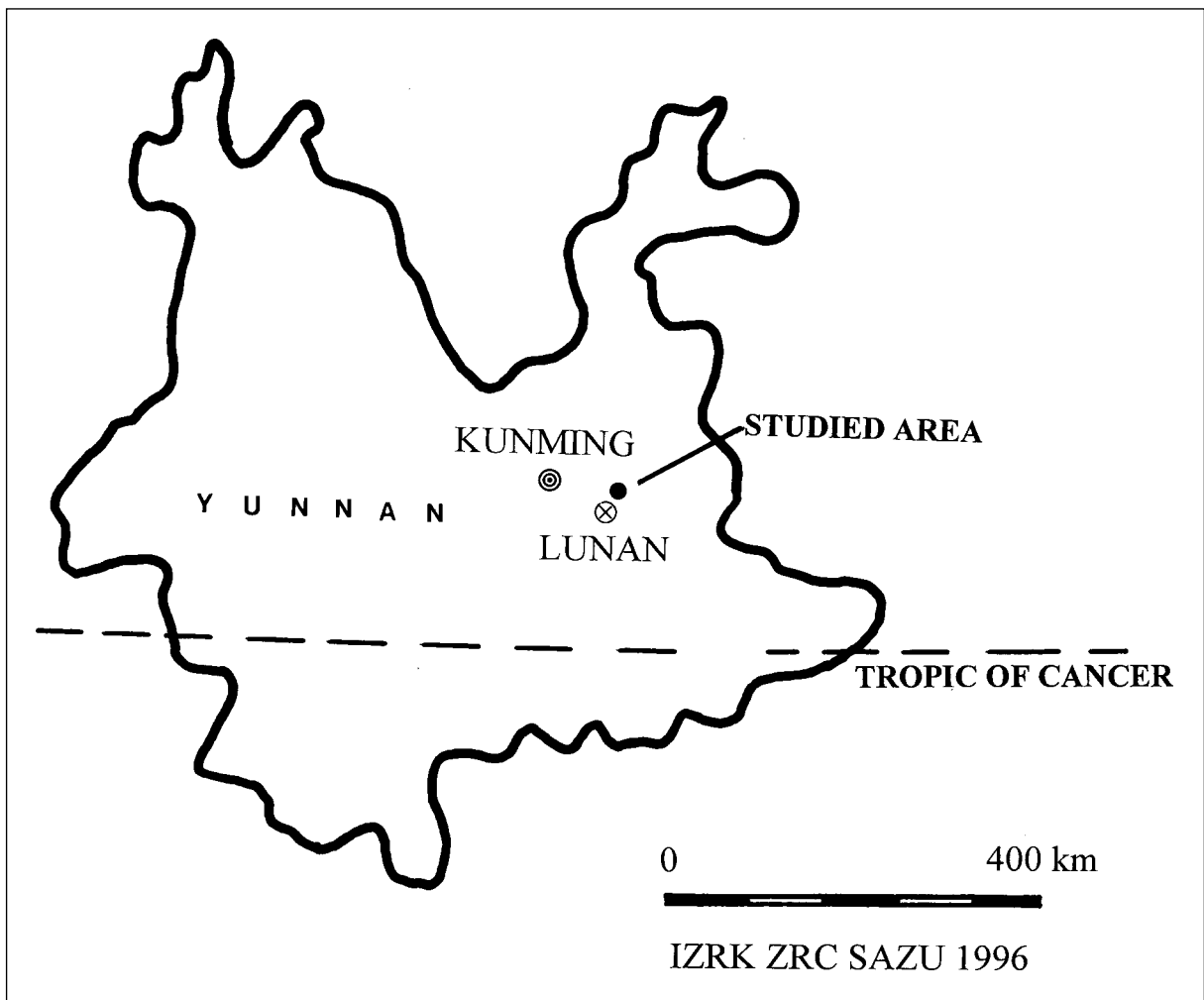


Fig. 1.1.1. The situation of studied area in Yunnan province

lowering gradually, the lowest point is the joint place of the Nanxi river and the Red river with 76.4 m elevation in the Honghe county. The height difference between the highest and the lowest point is 6663.6 m. Generally, the whole Yunnan can be divided into 6 levels. Among them there are three main levels: 1600-1900 m in the N central part, 1200-1400 m in the S central part and 500-900 m in the S. The high plateau and mountains are predominately landforms that occupy 94% of the total area.

According to the variant of lithological characters and geological structures, E Yunnan can be divided into three parts. (1) E Yunnan karst plateau: is composed by gently undulated karst landforms which developed on the Paleozoic and Mesozoic carbonate rocks. Patterns of karst landforms are karst hills, Fengcong shallow depressions and Fenglin poljes. (2) NE Yunnan plateau: is the transit zone from the E



Fig. 1.1.2. Group of Slovene and Chinese researchers. (Photo M. Knez)

Yunnan karst plateau to the Sichuan basin and the NW Guizhou karst plateau. Due to the Wumong mountain range and the Jinshajiang river its tributaries are deeply incised. The plateau surface landforms are very deeply expressed. (3) Central Yunnan red-bed plateau: is located in the W to the Kunming-Shipin county, the outcrop formations are all in the Mesozoic red-beds, landforms are gently undulated and dominated by the down-shape plateau and intermountainous basins.

The climate types are different in the Yunnan province. Influenced by SW monsoon and SE monsoon, the Tibet high plateau and complicated landforms, mainly parts of the Yunnan province, belong to tropic and subtropic high-land monsoon climates. They are characterized by: dry season and wet season, annual temperature difference is small, but daily changes are high; the raining season occurs in summer. By the altitude and elevation increasing, from S to N there are 7 climate zones: N tropics, S subtropics, middle subtropics, N subtropics, S temperate, middle temperate and N temperate zones. The average annual precipitation of the whole province is about 1000 mm. The annual amount of precipitation is around 600 mm to 800 mm in the NW Yunnan, and some of them can occur as snow. In the S tropic and S tropic areas the annual precipitation can reach over 1600 mm. From May to October each year there is a raining season. From November to next April there is a dry season. There is about 80% to 85% of precipitation that occur in the raining season.

There are a lot of rivers and lakes in the Yunnan province, which belong to the Yiluowadijiang river, Nujiang river, Langchangjiang river, Golden river, Yuanjiang river and Nanpanjiang river systems. The strikes of the river are controlled by geological structures and mountain ranges. The average river fall ratios are 1.25‰-3.74‰. For the influence of the monsoon climate, most of the river water quantities have the character of a seasonal change evidently. Meanwhile, the Yunnan province is also one of the five lakes distribution areas of China. There are 37 lakes with water areas over 1



Fig. 1.1.3. Typical karst landscape in Xichou. (Photo M. Knez)

km². Most important are the Dianchi lake, Erhai lake, Fuxianhu lake, Chenghai lake and Luguahu. Those big lakes mostly belong to tectonic lakes. Their arrangement strikes

coincide with the geological structure line strike, from N to S.

The soil types also vary in Yunnan, red soil is the dominate soil type, and it can be



Fig. 1.1.4. A great part of karst territory is picturesque agriculturally cultivated. (Photo M. Knez)



Fig. 1.1.5. One of few real karst poljes. (Photo T. Slabe)

found in almost the whole Yunnan. The soil vertical zoning is very clear. From the bottom of mountains to the top the soil usually appears as the subsequently brick red soil, bright red soil, mountainous red soil (or yellow soil), red-brown soil, yellow-brown soil, brown soil, mountainous podzol, and desert soil. The distances of the varied soil types are very short, somewhere only some hundred meters.

The undulate landforms and different climate conditions make the advantages of the developing varied karst geomorphology and caves. Large river systems and lakes have also formed the local karst solution base-level that controlled the karst landforms evaluation and development.

Geological setting

Lithology

It is observed that karst in Yunnan is developed in Carboniferous, Permian and Upper Tertiary carbonate rocks.

Ren Meier (1983) found that there were Carboniferous dolomite (CaO 33.2%, MgO

15%) and Upper Permian Maokou group limestone (CaO 54.7%, MgO 0.5%) outcropped in the NE Yunnan, but the dolomite rocks were strongly karstified, the depressions, stone-teeth and dolines were strongly developed in them. But on the Maokou limestone they were not developed well. The reason is that the dolomite rock structure is middle-coarse, the particle diameter is 0.5-2 mm, as well as influenced by the ore body heat liquid recrystallisation, its porosity is high. Normally their biotrititic limestone and oolitic limestone have a high porosity and a good water permeability.

Structure

The structure has an obvious effect on the karst development in Yunnan. It has particularly controlled the pattern of Yunnan karst landforms. Structurally, the E district is appropriate to the Yangtzi peneplatform and the southern China platform. For a long time the earth crust is relatively stable, and the thickness of sedimentary strata is very big. From the Upper Proterozoic to the Quaternary strata all are distributive in the

Yangtzi peneplatform. Their thickness range from 2000 m to 4000 m occupies 20%-45% of the total strata thickness. In the S China platform, a great part of the Upper Palaeozoic strata is built of carbonate rocks. The Triassic limestone is widespread. The Summating carbonate strata are 4000-7000 m thick, account 30-60% of the total strata thickness. Distributive carbonate rock areas of these two fields account about 50% of the total land area (Ren Meier, 1983).

The western Yunnan belongs structurally to the geosyncline belt. The thickness of carbonate rocks is 1000 m - 5000 m that account 10-25% of the total strata thickness. Zhongdian and Lijiang of the NW Yunnan belong to the Indosinides folding zone, the carbonate rocks thickness can reach to 4000 m - 7000 m that accounts 20-45% of the total stratum thickness. In the W the karst developed on a more concentrated district as Baoshan, Lijiang, Dali, Lingchang and Xichuangbanna area.

In the E Yunnan platform zone and W geosyncline area the karst development and distribution are obviously different. The E carbonate rocks distribution area of the platform belt is broad, lithologic variety is small and dip is gentle. Karst landforms are well developed. For the W geosyncline belt the carbonate rocks distribution area is narrow and the surface karst is not developed. It is characterized by low hills and corrosive denuded mountains. There is no typical karst morphology developed.

At the inner sub-zone field the structural control action is still more evident. The structure line has controlled the whole karst landforms pattern. The most typical example is the Xichou county, Wenshan.

The neotectonic movement is quite strong and has a great impact on the genesis and evolution of the geomorphology in Yunnan. The neotectonic uplift movement raised the lower Yunnan peneplain to the elevation level of the present plateau. On the W side rivers cut in the surface and formed the gorges that separated high mountains. A strong fault movement happened and reactivated some old faults, while the structure uplifted. Under the structure block-faulted movements a series

of block mountains and fault basins were formed. The Dongchuan Xiaojiang fault is an active large fault, there are high block mountains on both sides of the fault and the fault itself appears as a valley or fault basin.

Intensive and frequent earthquakes are another appearance of the neotectonic movement. In Yunnan there are 1-2 earthquakes a year of over 6 grades.

Karst geomorphology in Yunnan

The karst geomorphology is limited in solution rocks, limestone, dolomite, gypsum, anhydrite and rock salt distribution areas. The carbonate karst surface prevails in Yunnan. Areas with the gypsum or fossil salt karst are smaller.

China is one of the karst most developed country in the world, the carbonate rocks outcrop area is over 1,250,000 km² (*China karst research* group, 1979). Three provinces Yunnan, Guizhou and Guangxi are intensive and typical karst areas where the karst occupies 320,000 km² of the total area, i.e. 28.9% of the total area, and the karst area in Yunnan includes 110,900 km².

Considering the scale and extent of the developed karst the Yunnan province can be placed along the 102° E longitude line and the Honghe river. The karst landforms density distributes in E parts. But in the W area the karst areas are scattered and untypical. The Yunnan province has different karst landform types, from S to N, tropic karst, temperate karst and alpine frigid karst are presented disciplinary. The Lunan Shilin (stone forest), Yiliang Jiuxiang Cave system, Gangnan Babao Fenglin-basin scenery, and the Zhongdian Baishuitai Adarce platform which is more than 3000 m above the sea level, are representatives of the Yunnan karst.

Karst forms

Fengcong-Depression

is a composition of the conterminal base karst cone and depressions. The depression

area is normally smaller than 0.5 square kilometers and has clay draping and a sinkhole at its bottom. The normal relative altitude of Fengcong is smaller than 100 meters. It is the most developed karst form in Yunnan. Construed by the depression depth it can be divided into the Fengcong shallow depression and the Fengcong deep depression. From watershed to the river valley the Fengcong depression forms changes from the Fengcong shallow depression to the Fengcong deep depression. The depth of the depression increases from 50 m to 150 m or more (Song & Liu, 1992).

Fengcong Valley

is composed by karst cones and valleys among them. It mainly distributes at the watershed area where a large spring or an underground river comes out of the karst plateau on both sides of rivers. It widely distributes in the E and SE Yunnan. For instance, it is well developed along the Chouyang river in Xinjie of Xichou and Malipo counties.

Hillock Depression

is composed by Conterminous base hummock alternated by depressions. Compared with the Fengcong depression, here the karst develops normally weakly. Topographically there is an undulation of the hill state, and the relative high difference is less than 50 m. Terra rossa developed well and was widely distributed in the watershed areas of the E and SW Yunnan.

Fenglin Basin and Valley

are composed by karst peaks which are base free on the valley or basin plain. Their relative height difference is 200 m and less. It is mainly distributive at the SE Louping county, Pingyuanjie basin, Gangnan's Babao basin and Luxi areas of the E Yunnan and the SE Yunnan. They are also common in

Menglian, Mengding and Bingma of Baoshan of the W Yunnan.

Residual Hill and Paniform

is a later period phase of the karst development. It is formed by the Fenglin evolves toward karst hummock by further abrasion, and the basin evolves to paniform. It is draping of red brick clay that has funnels, dish-like depressions and the blocked sinkholes distribution. There are also some stone-teeth developed nearby residual hills and isolated peaks. It is mainly distributed in the Shilin period abrasive paniform in Lunan-Luliang-Louping and Zhongheyang-Pingyuanjie areas.

Yunnan karst development stages

After the carbonate rocks were lifted up the karst phenomena developed widespread. Taking into account the Yanshan movement which has had a deep impact on the Yunnan geologic and landform evolution as a boundary, the karst can be divided into four stages: Pre-Cambrian ancient karst stage, Old Palaeozoic ancient karst stage, Later Palaeozoic ancient karst stage, and Old Mesozoic ancient karst stage (*China Karst Research*, 1979). In Cenozoic the karst can be divided into different stages: plateau stage, stone forest stage and canyon stage.

Plateau Stage

Its genesis and development is concerned with the whole landform evolution history of Yunnan. The end of the Mesozoic Yanshan movement has made the Yunnan present day fundamental outline of landforms. Palaeogene Himalaya movements occur in a large area with up-lifts and a fault activity. Before the Miocene movements Yunnan was relatively quiet in the tectonic sense. In that period almost the whole of Yunnan belonged to the tropical climate field, and the rivers activity was weak, the

uniform denudation of landforms and shallow karstification prevailed.

Stone Forest Stage

The second period of the Himalaya tectonic activity happened during Miocene to Pliocene by uplifting and fault movement. During the Pliocene mesophase Mengzi, Datunhai, Caoba, Jijie and Dazhuang were most probably linked together and became a lake. In the Upper Tertiary lake face sedimentation of the Ciyang group the coal beds are represented. In lifting the ascended zone formed a wide range of the Fenglin depression, Fenglin basin, stone forest and large-scale poljes typical karst senility landscapes. Topographic undulation is small, with the height difference of 100-300 m. This karst landform plane is called the stone forest period landform. Some also call it »lake basin stage« (Yunnan agricultural division Office, 1987). In Quaternary neotectonic lifts up ascended and block break motion made the denuding abrasion face of the stone forest stage distributed at different elevations. The Nanpanjiang river upstream ample watershed area is the best preserved karst denudation plane in China. There are shallow depressions, dolines and funnels, as well as residual karst lakes, the Yuehe lake, Jijianhe, and the stone forest in Lunan for instance. The S debasement of elevation from the N in the NE Yunnan is 2100 m, and in Kunming-Shizong 1800 -1900 m. In Lunan and Yiliang it is distributed at the height of 1700 -1800 m.

Canyon Stage

This stage was developed in Quaternary. In the E the Nanpanjiang river and the Yuanjiang river formed canyons and river valleys which developed therein multiple level terraces and nick points. The vertical karstification is reinforced in downward river valley districts of the nick point where the underground water level descends and the aeration zone thickness increases. Dolines and the Fengcong deep depression morphology were developed by that. The depth of shafts can reach up to several hundred meters. In Niupeng Yanzidong in Mengzi for instance, affected by the Lushihe river incision, the cave reaches 267 m of depth. The groundwater yielded deep runoffs and developed multilayered caves and underground river systems.

In the downstream far from nick points there is another new landforms type developed. In the upstream above the river nick point or watershed area the retrogressive erosion of rivers has not yet strongly affected districts. The stone forest stage landforms face is gradually disintegrated or broken up. As a consequence it has yielded the phenomena of karst landforms from the river valley to the watershed area an ordinal appearance young stage - mature stage - old stage. Landform features of this stage the karst has not formed yet. They are in a developing phase.

To sum up, the present karst landforms of Yunnan is formed mainly on account of the stone forest stage that recreates through a later stage, especially reactivating karst during the canyon stage.

1.2. THE LUNAN STONE FORESTS

Huang Chuxing, Martin Knez, Liu Hong, Tadej Slabe, Stanka Šebela

A stone forest (Fig. 1.2.1.) is a unique form of pinnacle karst (Ford & Williams 1989, 337). The pinnacles that are crisscrossed with fissures and cracks are composed of rock pillars (Song Lin Hua 1986; Habič 1980, 109) and stone teeth (Song Lin Hua 1986; Song Lin Hua & Liu Hong 1992). Stone teeth are smaller protuberances less than five meters high; tall teeth are higher than three meters, and short teeth are lower than one meter (Song Lin Hua & Liu Hong 1992). They are divided according to their shape into canine teeth, molar teeth,

and ridge stone teeth (Song Lin Hua & Liu Hong 1992). The pillars range from five to fifty meters tall and are of various forms. Along with former and current factors of formation, their shape is determined primarily by their composition, stratification, and the way the rock has been crushed. In uniform rock, the pillars are usually broader at the bottom, if they have not been narrowed by the subcutaneous dissolving of carbonate rock, of course, and become narrower especially at the top. Mushroom-shaped pillars are formed when the lower beds are



Fig. 1.2.1. Shilin stone forest. A stone forest is a unique form of pinnacle karst. (Photo M. Knez)

thinner, densely fissured, and when the rock is very porous or made of dolomite; in short, they decay faster. A stone forest develops in thickly-stratified, relatively pure limestone whose layers are inclined no more than 15° and crisscrossed with a network of vertical fissures. A stone forest does not occur on distinctly crushed rock.

Song Lin Hua (1986, 6,7,8) distinguishes three types of stone forests according to their position. In lowlands and valleys, large forests with intervening sinkholes and hollows are formed. Underground waters flow below them, they are periodically flooded, or water flows through them. Forests on the tops of hills are lower (10-30 m), their pillars grow from a common foundation, and the sediment that covered them was thin. Forests on the slopes of hills are an intermediate form between these two types.

In most cases, a stone forest is described as a form of covered or subjacent karst (Chen Zhi Ping et al. 1983) or cryptokarst (Maire et al. 1991; Sweeting 1995, 125). The carbonate rocks on which pinnacles occur were covered by thick sediment which decisively influenced the development and form of the stone forest. Depending on the sediment, a forest can be denuded, covered, or buried. Hantoon (1997, 311) describes stone forests as an epikarst form.

Large stone forests are a characteristic form of polytropical and subtropical climate conditions (Song Lin Hua 1986, 3,5).

The stone forests in Lunan have been relatively well and comprehensively studied, and some of the more distinct rock forms on pillars have been described. These descriptions found in the literature are included in the chapters on individual rock forms. We have not found, however, a comprehensive description of the rock relief, but the obstacle might be the Chinese language. We devoted the studies to the forms of pillars in different types of lowland stone forests and specifically to their rock relief that reveals the factors of their formation and often of their development as well. We supplemented and also modified previous explanations of the origin of some rock forms, but, of course, the study must be continued and individual hypotheses verified.

The rock relief described is characteristic of larger stone forests that were originally covered with sediment and soil, then stripped and transformed by rainwater. The rock relief of smaller pinnacles that were originally formed under the ground was formed in a similar manner.

The Lunan stone forests

The Lunan stone forests are among the most remarkable in the world. The Shilin Central Forest spreads over eighty hectares, while larger and smaller stone forests are distributed over an area of 350 km² (Chen Zhi Ping et al. 1983; Zhang Faming et al. 1997a). The tourist sections of the Lunan stone forests are visited by more than a million people every year. They are a unique and integral natural and cultural landscape where the Sani minority lives, now partly from tourism.

The geological structure of rock in the wider area of Lunnan is revealed as a series of interchanging ridges and depressions (tectonic troughs) in a north-south direction. It is generally well-known that the eastern and central parts of the region were fully elevated during the Cenozoic and now comprise vast, high plateaux. It is mostly Early Palaeozoic and Triassic carbonate rock which extends above all over east Yunnan. At the same time we find individual smaller carbonate areas in some parts of west Yunnan (Zongdian, Dali and Licang) (Sweeting 1995).

The rock in some parts of the Lunnan area is of a very monotonous structure, although in some places a variegated alteration of diverse types of limestone and dolomite can be found in the geological profiles. This is reflected in the process of selective carbonate corrosion and erosion, and thus in the shape and morphological appearance of particular stone columns, larger blocks of rock and the landscape relief.

The main characteristics of carbonate rock are: a high concentration of carbonates, great thickness, and the great age of the rock which forms the vast carbonate complexes. They are mostly of the platform

type and are distinguished by a high level of purity, regularity in the distribution of various carbonate types, and uniform thickness. In addition, one of the characteristics of this rock is that, due to its age, it felt the strong effects of diagenetic processes. These characteristics are directly reflected in the hydrological response of the bedrock, as well as in the general development of the karst.

In the Lunnan area the basic features of carbonates appear at a number of levels. One of the more significant features is undoubtedly its Early Permian age. Typical stone forests generally develop in ridge biomicrite and biosparite deposited on the gentle sloping of shallow-water coasts. This carbonate rock, additionally characterised by thick layers and a uniform chemical composition, is thought to be best for the formation of high stone columns. The particular stratigraphic and lithologic features which were found in the geological profiles additionally contribute to the formation of remarkable shapes. The preliminary analyses carried out this year assisted in solving several presuppositions (Knez 1997c).

In various climatic and geological conditions, three different types of karst have formed:

- a tropical rain forest karst in the south;
- a tectonic depression (graben) karst;
- a high plateau karst with »stone forests«.

Tropical rain forest karst

The vastest peripheral tropical area in China stretches out across Xishuangbann province. Two karst areas stand out: Mengla province, an area covering around 500 km², and the territory along the Lancang river (450 km²). In Mengla province, Permian and Middle Carboniferous grey massive limestone, biolithic limestone, pseudooolitic limestone, bioclastic limestone and Triassic dolomite limestone prevail. The carbonate layer deposit is over 2000 m thick. Under the influence of the humid tropical climate, the limestone underwent intensive karst processes during the Quaternary. The characteristics of the karst

landscape along Lancang river is reflected in numerous depressions and blind valleys where stone teeth, as well as individual stone columns, are quite frequent.

Tectonic depression (graben) karst

Karst in tectonic depressions (Song Lin Hua & Liu Hong 1992) is a very widespread occurrence in the wider Lunnan area, where there are at least 28 divided parts, none of which is less than 100 km². The largest is the so-called Kunming basin (named after Kunming, the capital of Yunnan province), exceeding an area of 1100 km² and with a water-collecting hinterland of over 3000 km². The loose rock covering in Kunming basin is approximately 1000m.

High plateau karst with »stone forests«

»Stone forests« indicate a specific type of karst landscape with characteristic groups of standing limestone columns reaching a height of over 50 m. Limestone columns usually stand on a gently wavy base.

A comprehensive and diverse system of water courses (Zhang Faming et al. 1997a, 5) developed under the forests. The form and height of the pillars in the forest are characteristic of the individual type of rock and their topographical position (Zhang Faming et al. 1997b, 73).

Mangin (1997, 106) believes that the epikarst of the stone forest reaches a depth of 100 meters. The Lunan forests originated largely through the dissolving of the rock underground by water from the soil which contains biotic CO₂ and sediment. The water enlarges the fissures and separates rocks. Under the acidic soil, wide and deep cracks occur between the pillars as well as deep channels on their walls (Yuan Daoxian 1997). The uncovered carbonate rock is reshaped by rainwater. First, teeth appear and from them, a forest (Song Lin Hua 1986, 13). I studied the rock relief in three selected, dissimilar Lunan forests.

Originally, there was limestone, already karstifying (Yu Jinbao, Yang Baoguo 1997;

Song Linhua, Wang Fuchang 1997, 433) and covered by Permian basalt and tuff which influenced the shape of the forest, and rock that in some places underwent metamorphism (Song Linhua, Li Yuhui 1997; Ford et al. 1996, 34). Water percolated through the basalt and tuff and began the development of the underground karst. In the Mesozoic, part of the limestone was denuded (Song Linhua, Wang Fuchang 1997, 433). In the Oligocene and Miocene, stone blocks rose and dropped, and in lower areas the karst relief was reshaped by erosion (Yu Jinbiao, Yang Baoguo 1997). In the Eocene, the Lunan graben collapsed, depositing thick layers of lake sediment (Chen Zhi Ping et al. 1983; Zhang Faming et al. 1997a, 433). In the tropical climate, thick layers of laterite soil appeared on the sediment (Sweeting 1995, 124; Ford et al. 1997, 112). In the Pliocene, the current stone forest

began to develop (Yu Jinbiao, Yang Baoguo 1997, 66). In the Quaternary, a large proportion of the sediment was dislodged but remained in the fissures.

With the development of the underground water courses, pillars began to develop from the teeth (Fig. 1.2.2.) (Zhang Faming et al. 1997a). The level of the underground water played an important role in the development of the forest (Ford et al. 1997, 114). The oscillating underground water widened the fissures (Yuan Daoxuan 1991).

The Shilin (central) stone forest (Fig. 1.2.3.) is situated between 1625 and 1875 meters above sea level. The forest is located in a lowland with underground waters that lie close to the surface and rise up to ten meters after heavy rain. The majority (70-80%) of the annual 936.5 mm of precipitation falls between June and October (Chen

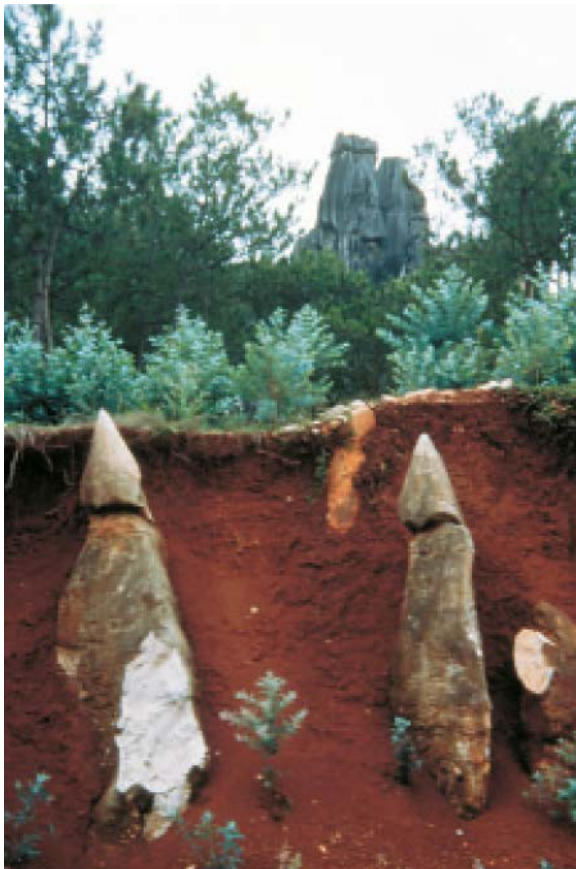


Fig. 1.2.2. Shilin stone forest. With the development of the underground water courses, pillars began to develop from the teeth. (Photo T. Slabe)

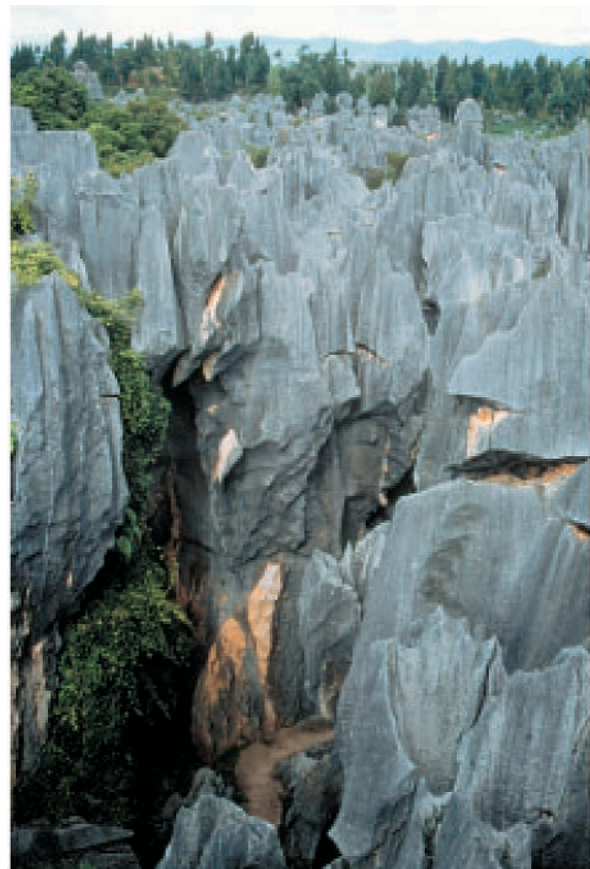


Fig. 1.2.3. The Shilin Central Forest is situated between 1625 and 1875 meters above sea level. (Photo T. Slabe)

Zhi Ping et al. 1983). The mean temperature is 16.3°C and varies from -2°C to 39°C. The pillars are tallest in the central part of the lowland where the surface waters run into the underground. There is more sediment on the margins of the stone forest (Sweeting 1995, 125). Habič (1980, 110) defines it as shallow karst. In the lower part of the stone forest (Fig. 1.2.4.), water also runs on the surface.

The Shilin (central) stone forest developed on thickly layered and vertically fissured Lower Permian carbonates of the Maokou period composed of limestone and dolomite in the lower part. In the middle of the pillars are also concretions of chert. The limestone is sparry and bioclastic and in some places slightly dolomitized (Sweeting 1995, 125). The limestone layers are mostly five meters thick and inclined by 5°. The lithological characteristics were studied by Knez (1997c), and the characteristics of tectonic fracturing by Šebela (1996).

The pillars in the central part of the forest in the lowland are as tall as 35 meters.

In the middle area, they mostly stand close together; between them are cracks mostly one to five meters wide, while on surrounding larger surface areas, they also stand individually (Fig. 1.2.5.). They are therefore the remains of carbonate rock between fissures and are shaped accordingly. Their cross sections are square and triangular, as well as oblong and narrow. The dense fissuring of the rock resulted in smaller pillar cross sections. The pillars whose lower parts are composed of thinner and fissured beds are mushroom-shaped and as a rule have pointed tops starting at the same level. Those pillars that were subcutaneous below ground have somewhat more squarish tops. The pillars are also dissected along bedding planes and along longer-lasting levels of sediment and soil. Notches along bedding planes are often jagged, a reflection of the stylolite formation of the rock. Pointed and blade-like pillars with sharp tops and ridges dominate. Through laboratory tests on the shaping of pinnacles in gypsum, Dzulinski, Gil, and Rudnicki (1988, 8) determined that pillars acquire a pyramidal shape when the

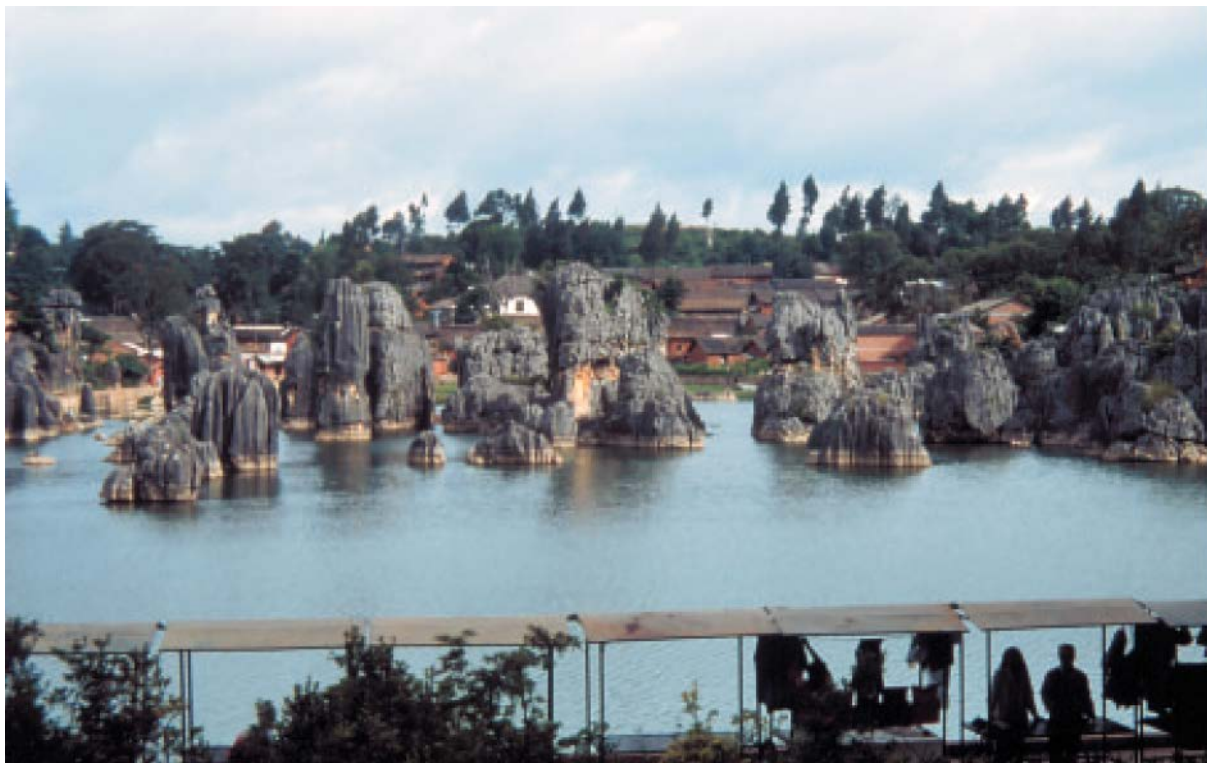


Fig. 1.2.4. Shilin stone forest. In the lower part of the stone forest, water also runs on the surface. (Photo M. Knez)

cracks between them widen. The shape of pillars on evenly composed carbonate rock should be pyramidal and sharp: the purer the limestone, the sharper the shape of the pillar. On relatively evenly composed carbonate rock, the action of rainwater hollowed distinct rock forms across the subcutaneous rock relief.

The **Naigu stone forest** lies twenty kilometers east of the Shilin (central) stone forest and is also an important tourist attraction. The pillars, 20 to 30 meters tall, are tower-like with mostly square cross sections and with many short, pointed tops. The pillars are often linked in rows between distinct faults. Between larger rock masses are individual, sometimes narrow pillars (Fig. 1.2.6.). The cracks between the pillars have been eroded to various widths, from a few centimeters to ten meters and more. The tops of pillars (Fig. 1.2.7.) united into extensive towers are at a uniform level. Many pillars, particularly individual pillars, are mushroom-like. The edges of the pillars are often curved, only the ridges between channels are sharp. Along the bedding planes,

they are indented by distinct cracks. Their rock relief is less distinct and unique because of the uneven composition of the rock, especially the smaller rock shapes, and the rock surface is rough.

That the forest developed on Qixia rock is reflected also in its form and rock relief. The lower sections of the pillars are composed of thicker beds of limestone and their forms are more rounded, medium-thick beds of limestone lie above them and the pillars are narrower, and the upper sections of the pillars are composed of dolomite limestone (Ford et al. 1997, 115).

In most cases, the form of the subcutaneous stone teeth does not reflect the different composition of the rock. They are either rounded or pointed like the subcutaneous teeth on other rock. Only the largest differences in the composition of the rock stand out.

Below the forest is a Baiyun tourist cave (Fig. 1.2.8.) where it is possible to read many periods of their development from the rock relief. Water currents flowed through the flooded passages with a speed of 0.5 m/s



Fig. 1.2.5. Shilin stone forest. Between pillars are cracks mostly one to five meters wide, while on surrounding larger surface areas, they also stand individually. (Photo M. Knez)



Fig. 1.2.6. Shilin stone forest. Between larger rock masses are individual, sometimes narrow pillars. (Photo T. Slabe)



Fig. 1.2.7. Naigu stone forest. The tops of pillars united into extensive towers are at a uniform level. (Photo M. Knez)

(Kranjc 1989). This is confirmed by the basalt gravel in the cave and in front of it and by smaller scallops that do not have very distinct forms. They were covered by the fine-grained sediment which filled the cave. On the ceiling are large above-sediment ceiling channels (Slabe 1995, 61) that are several meters in diameter as well as above-sediment anastomoses. The extensive above-sediment anastomoses, whose surface measures several square meters, therefore have several levels (Slabe 1995). The smallest channels are three centimeters in diameter and the largest fifty centimeters, while those with five to ten centimeter diameters dominate. The above-sediment ceiling forms indicate the long-term reshaping of the cave by water flowing across the fine-grained fill. The cave in the heart of the park is part of the cavernous karst underground below the stone forest and indicates periods of rapid outflow of water from the surface and the carrying away of the sediment that covered the limestone. There were relatively long periods when the cave was filled with fine-grained sediment and the surface above it was flooded. This indicates the intermittent growth of the stone forest.

Examples of distinctive, mostly mushroom-like, 30-40 meter high pillars are found in the **Lao Hei Gin stone forest** (Fig. 1.2.9.), twenty kilometers northeast of the Shilin Central Forest. The tallest pillars are in the lowest part of the forest, from where the largest quantity of sediment was washed away. The stone pillars can be divided into larger rock masses that are criss-crossed by thinner fissures and have many smaller pointed tops and individual pillars separated by extensive patches of sediment. The individual pillars have the form of square towers or are mushroom-like. They are frequently composed of several blocks, the remains of layers of rock between bedding planes and fissures. The central part of the pillars quickly crumbles into fine debris and disintegrates. The rock disintegrates mostly in grains which makes the rock surface rounded; it is only angular under the thin flakes. The rock is porous, and the central sections of the pillars are interwoven with numerous tubes that are

from one centimeter to one meter and more in diameter. The rainwater shapes the rock relief on the tops of the pillars and the more voluminous base, that is, on the sections where the rock is most resistant to decay. The rock relief is therefore the reflection of the composition and tiny fissuring of the stone which was first shaped below the ground for a long period and then reshaped by rainwater.

Sinkholes often occur between pillars and in them, caves. Thirty to fifty meters below the surface, water currents in the nearby caves flow with a discharge to 3 m³, and exceptionally up to 4-6 m³. As a result, in this forest the water can flow off the surface due to the developed underground water network, taking with it the sediment and soil from the limestone and dolomite.



Fig. 1.2.8. Naigu stone forest. Below the forest is a Baiyun tourist cave where it is possible to read many periods of their development from the rock relief. (Photo T. Slabe)

In August 1996 we carried out speleomorphological researches of some horizontal caves near Lunan Stone Forest. We visited 3 horizontal caves, 2 of them were mapped for the first time, the map of **Baiyun cave** (Naigu Stone Forest) existed before.

The Naigu stone forest lies north from the Shilin (Lunan) Stone Forest and is tourist arranged. Naigu means »black« in the Sani language. An area of 7.38 km² has been opened to tourists in 1986. It consists of two parts (E and W part) with a path about 6 km long winding through the high and steep rock pinnacles. There are magnificent topography, primitive simplicity, unusually shaped rock formations, jadeite-colored lake water, spectacular caves enchant tourists.

By a tourist visit of the Naigu Stone Forest the visit to the horizontal Baiyun cave is included. The cave is 500 m long and opened for public visits from 1989. General strike of the cave is N-S. The water flow strike was also from N to S. It is a typical

phreatic passage which is today in vadose conditions.

In the area of the Naigu Stone Forest we find 7 caves. Beside others these are: Zhiyun cave, Dieyun Rock cave, Jibailong cave. None of them is longer than 1 km.

On the SE edge of the Naigu Stone Forest the **Xin Shi Dong** cave was measured (Fig. 1.2.10.) on 22 July 1996. Before our visit the cave was closed with a big rock for the protection of the flowstone inside against vandalism. The measurements of the cave were done by dr. Stanka Šebela, mag. Metka Petrič and Mr. Huang. Studies of percolated waters were done by mag. Janja Kogovšek. Coordinates of the entrance are 24° 54' 05" N and 103° 21' 30" E, with the elevation of the entrance 1785 m. General strike of the cave is N-S. Inside the cave the water flow is not active any more, but because of precipitation the water can be found in pools. The water level can rise occasionally (also to 2 m) what can be concluded from the level of red sediments on cave walls.



Fig. 1.2.9. Examples of distinctive, mostly mushroom-like, 30-40 meter high pillars are found in the Lao Hei Gin stone forest. (Photo M. Knez)

The measured cave length is 175.5 m, the depth is 6.5 m. From the low entrance 0.6 x 1 m we reach the entrance collapse chamber. The cave is rich in flowstone. There are many columns which divide the wide passage (up to 12 m) into more parts. The thickness of the ceiling above the cave is not big, not thicker than 10 m, the ceiling in the cave is low, not higher than 3 m.

Xin Shi Dong was developed in the Permian limestone, which strike and dip in the N part of the cave is 310/5. At all the cave ceilings we can observe planes similar to tectonic structures which are in fact plains caused by sediments. The cave was filled up with sediments which were later removed. In the SE part the cave ceiling lowers to less than 0.9 m and becomes impass-

able. Between numbers 10 and 9 we find massive gourls showing strike of the water flow from N towards S, NW-SE.

On the wider area of the water tracing experiment N from the Lunan Stone Forest the number 7 represents the **Guan Yin Dong** cave (Fig. 1.2.11.). In fact it is a spring cave in the E edge for which we would need a boat or divers. This cave is intersected by a bigger collapse doline (Fig. 1.2.12.), which is continuing into a ponor cave on the W side. This cave is accessible and was measured on 20 July 1996 by dr. Stanka Šebela, Liu Hong, Chen Xiaoping, mag. Metka Petrič. Within the speleological studies there were also involved dr. Tadej Slabe, dr. Knez Martin and mag. Janja Kogovšek.

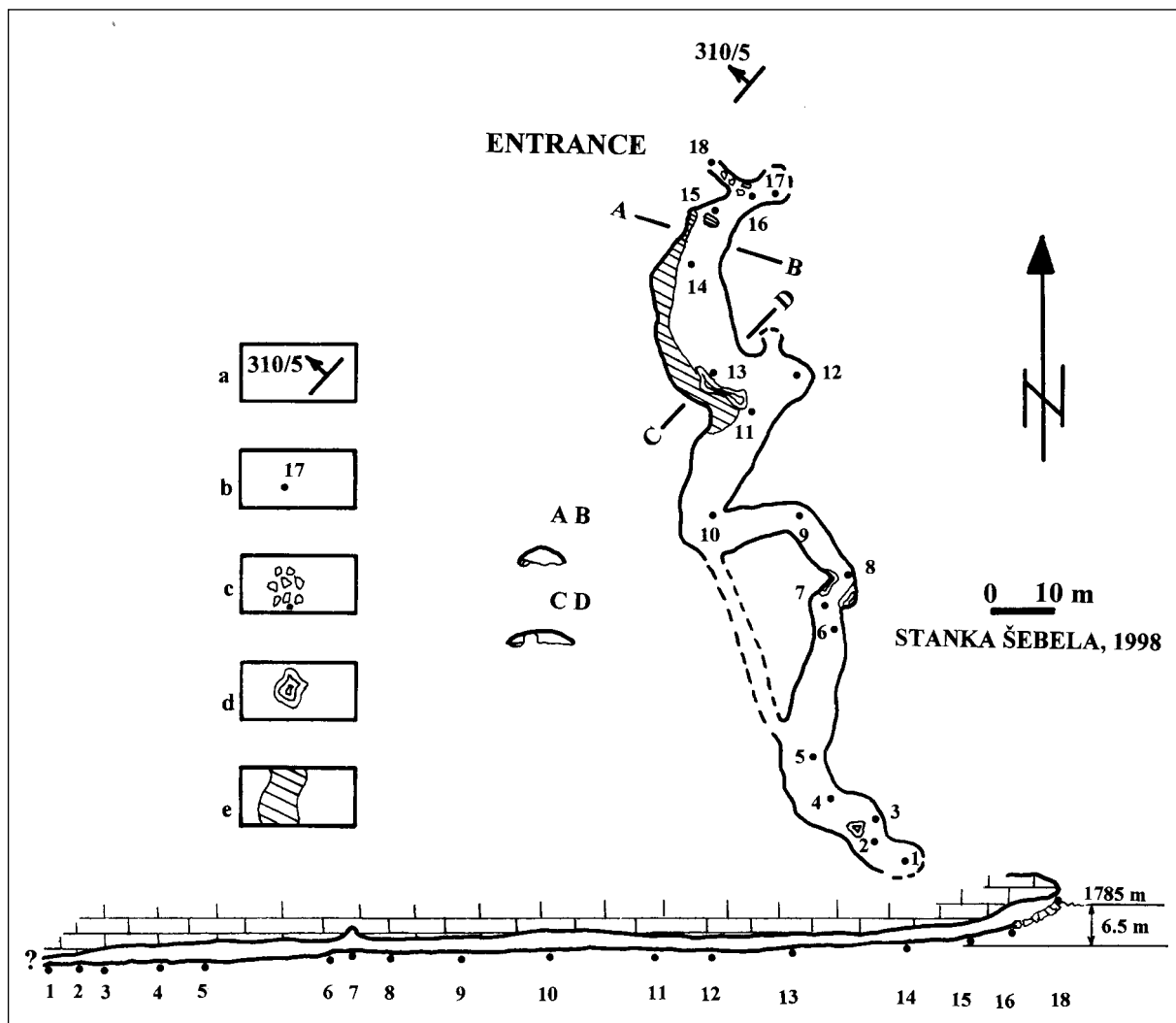


Fig. 1.2.10. Map of cave Xin Shi Dong (ground plan, longitudinal and cross sections); a-strike and dip of bedding planes, b-point of cave measurements, c-collapse blocks, d-flowstone, e-lake.

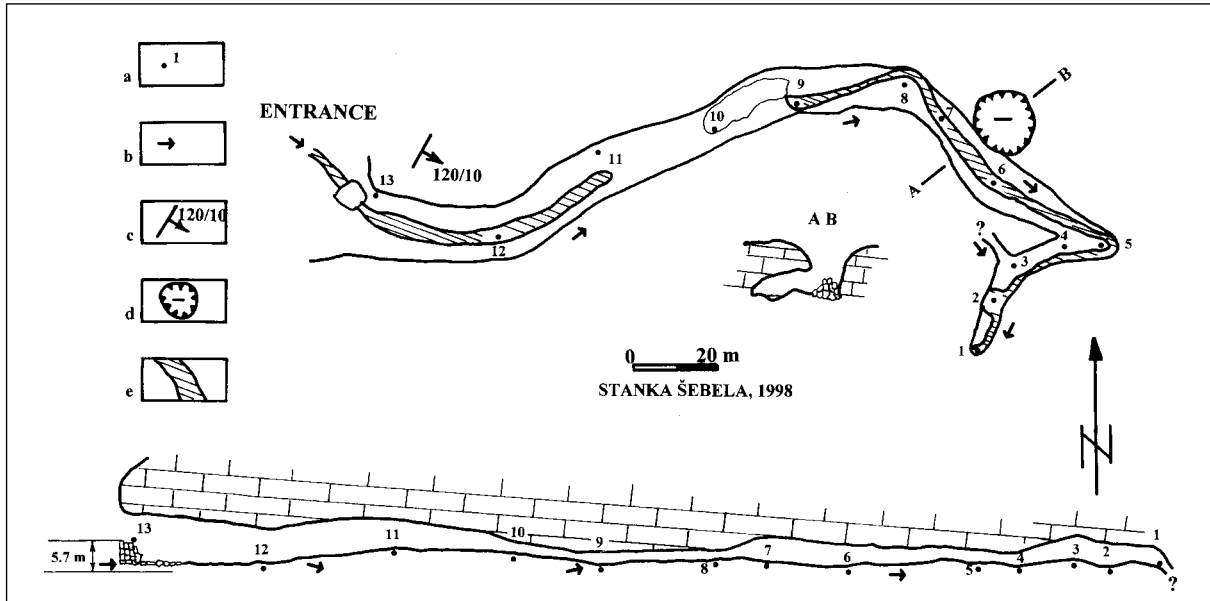


Fig. 1.2.11. Map of cave Guan Yin Dong (ground plan, longitudinal and cross sections); a-point of cave measurements, b-direction of water flow, c-strike and dip of bedding planes, d-collapse doline, e-water flow.

The Guan Yin Dong cave is 239.2 m long and 5.7 m high. It is still an active ponor cave which was measured in the scale of 1:500. The water flow strike is towards S

with more cave passages curves. There are 2 principal passage strikes, NW-SE and NE-SW. Between the points 7 and 6 there is a collapse doline, 15 m wide, with the mate-



Fig. 1.2.12. Collapse doline and entrance into Guan Yin Dong cave. (Photo S.Šebela)

rial fallen into the cave. That is the shaft with 10 m of depth.

The cave is developed in the Permian limestone with strike and dip 120/10 at the entrance. The thickness of bedding is 1 m. In the entrance the principal fissures are 90/90 and 10/80-90. Strike and dip of bedding in the spring cave on the E side of the collapse doline is 200/5-10. Directly through the middle of the collapse doline there is an anticline axis in the general strike N-S. The development of the collapse doline, that is a collapse of the former cave ceiling, is connected with folding deformations and formation of the anticline and fissures.

The entrance of Guan Yin Dong is 23.5 m wide and 13-15 m high. At the entrance there are remains of an old mill. On 20 July 1996 we measured the discharge of the sinking stream into the cave which was 30 l/s. The passage in the entrance of the cave is not higher than 8 m. The water flow sinking at the point 11 appears again at the point 9. At the point 3 from the NW side passage a smaller water flow joins the prin-

cipal passage. The point 1 is the final siphon. Between the points 12 and 9 there are massive gours which are oriented in strikes towards NE and SW.

The underground water level is in accordance with horizontal caves which were explored in the depth of 30 m. There are cave systems which are speleologically not explored yet, but results of the tracing experiment test have shown that there are pretty good direct connections. The thin roof above cave passages which can be from 10-15 m high is in many places collapsed, what caused that horizontal caves can be accessible by shafts (15-60 m deep) or from dolines or collapse dolines. General strike of the water flow is towards S. Horizontal caves survived the phreatic phase and the period of fillings in with sediments and replacement of sediments. Common are massive gours and flowstones which overlay sediments. A small dip of bedding planes 5-10° corresponds to the orientation of the horizontal passage, but meandering of the passage inside bedding is determined by structural elements.

1.3. LITHOLOGIC PROPERTIES OF THE THREE LUNAN STONE FORESTS (SHILIN, NAIGU AND LAO HEI GIN)

Martin Knez

General characteristics of carbonate rock in the Lunan stone forests

The most characteristic of the Chinese stone forests is undoubtedly the one situated in the direct vicinity of the city of Lunan (Lunan Shilin). The stone columns there have distinct sharp peaks. The columns are generally higher than 10 m.

Stone forests, in general as well as in the Lunan area, potentially develop in very

thick-layered and chemically-pure limestone. Some data indicates that Lunan stone forest developed in carbonate strata to over 30 m thick (Chen et al 1985; Habič 1980; Mihevc 1994; Song 1986; Song & Liu 1992; Sweeting 1995; Waltham 1984). The thickness of layers in other stone forests in southern China is much smaller (only around 2 m).

Lunan stone forest developed in Early Permian limestone (Maokou formation).



Figure 1.3.1. Shilin stone forest. Lunan stone forest is located on a wavy karst plateau 1720-2000 m above sea level. (Photo M. Knez)

The rock was very leveled; despite this, the sloping of the layers did not exceed 10° on average. In some stone forests the average slope of the layers is up to 20° . It has been found that if the slope of the strata exceeds 15° , large stone columns cannot develop (Song 1986). Varying tectonic pressures caused the development of numerous fissures which form a dense network (cf. Šebela 1996; cf. Kogovšek et al 1997).

The research was not only based on sampling rock from individual stone columns, as it was paid most attention to the contact of various rocks in the geological column. In some cases this contact was revealed by the stronger corrosion of a particular part of the profile, which was morphologically expressed in the rock. Finding contact between lithologically diverse rocks was often based on continuous sampling.

We discovered that in selective corrosion, various levels of porosity play a special role in Lunan stone forest. In some places it was macroscopically noticeable that individual areas of the geological profile, i.e. the stone columns, essentially underwent more potent corrosion and erosion effects. Research carried out at the microscopic level, although not yet complete, confirms this fact.

The lithostratigraphic conditions in Shilin stone forest

The carbonate rock in Shilin stone forest (Fig. 1.3.1., 1.3.2.), which has an area of 11 km^2 (Salomon 1997) does not change through the geological profile from the structural and textural points of view, with the exception of some short sections. All the samples studied by microscope revealed that the 250-million-year-old rock had been altered a great deal by diagenetic processes. The fossil remains are mostly unrecognizable, even though they are not tectonically damaged. The dip of the strata, which is mostly around 5° (Fig. 1.3.3.) and rarely more than 10° , indicates minor regional movement. At the same time, the results of microscopic observations indicate that the dip of the strata today most likely reveals



Figure 1.3.2. Shilin stone forest. The peaks of some columns over 30 m high are very sharp due to homogenous and compact rock. (Photo M. Knez)

only a relatively short phase of the inclining of the terrain in a non-vertical direction and/or that the blocks remained undamaged between the not-very-densely-located fractures. Irrespective of this, we find numerous tiny, calcite-filled fissures in which no noticeable shearing movements have occurred. Calcite veins can be difficult to locate macroscopically due to the purity and crystalline nature of the bedrock carbonate. The regionally vast gentle anticlinal elevation of the rock happened during a number of phases and periods. Other researchers also point out that there had been a number deformations of the Permian rock (cf. Yuan 1991).

Geological column is divided into 4 sequences: A, B, C and D. Total thickness of geological profile (stone column) under study is 37 m.



Figure 1.3.3. Shilin stone forest. The dip of the layers in Lunan stone forest is less than 5°. (Photo M. Knez)

Sequence A

Sequence A is 7 m thick.

The lower part of the sequence, i.e. the base of the stone column, is of biopelmicrite to biopelmicrosparite limestone of the wackstone type (samples 1251, 1252, 1253, 1254, 1255, 1256).

Fragments of various bioclastics prevail among the allochemes: uniserial, biserial and fusulinid foraminifers, shellfish, snails and other unidentifiable organisms. Especially characteristic of Shilin limestone are separate whole and crushed fusulinid foraminifers. In some places we noticed evidence of bioturbation. The numerous pellets are mostly no larger than 0.09 mm; most frequently their average size is 0.045 mm. Larger snails measure up to 7 mm in diameter. Smaller plasticlastics most likely occur among intraclastics.

Of the types of porosity the most common are moldic and shelter porosity. There are no calcite veins, although frequent secondary porosity is noticed.

Fossil remains comprise 20% of the rock, pellets and pelletoids up to 10%, and fusulinid foraminifers (whole and crushed) less than 1%.

Drusy mosaic calcite predominates in the directly precipitated calcite (orthochemical component), fills the inside of whole and well-preserved large fossils, replaces shells and fills individual caves. The anhedral to subhedral calcite crystals are 0.09 mm to 0.7 mm large (on average 0.27 mm). The calcite forms a mostly ksenotopic structure.

Chips of large fossils (e.g. fusulinid foraminifers) are more damaged on the bottom side; signs of endolithisation are noticeable.

Hollows in micritic intraclasts are frequently found to be filled with large mosaic crystal calcite. Filled hollows usually point to gravitation cement.

The geopetal filling of fenestrae with internal sediment underneath and large crystal sparite above and outside the clastics is also characteristic of the section of the geological profile.

Due to the position of the large crystal calcite in the fenestrae, there is no doubt that the strata are in a normal position.

One metre above ground, i.e. one metre above the present point of the exposed stone column, we notice pelbiomicrosparite to pelbiosparite limestone of the grainstone type (sample 1257).

Among the allochemical components, pellets and pelletoids are by far the most frequent, comprising over 90%. The first have a diameter of 0.09 mm, the latter from 0.09 mm to 0.18 mm, exceptionally up to 0.23 mm. There were no noticeable intraclasts in this part of the geological profile. The biogenetic component is represented mostly by fragments of various fossil remains. Larger pieces of thick shells are exceptionally well preserved.

The orthochemical component (sparite) is among the allochemes in the form of granular cement. The size of calcite crystals is between 0.045 mm and 0.32 mm, the average size being around 0.09 mm. The limestone is of a very homogenous and compact nature; no calcite veins were noticed.

Three metres above the base of the profile the lithologic features of the limestone change noticeably. It passes from a pelsparite to a biointramicrite limestone of the wackstone to packstone type (sample 1258).

Bioclastics prevail in the slightly recrystallised rock, taking up 35 to 40% of the volume. They are mostly approximately foraminifers (0.09 mm) and fragments of various fossils. Plasticlasts with a grain diameter of 0.36 mm to 1.35 mm appear only exceptionally.

Grain direction in the rock is very distinct. The longer axis is parallel to the stratification.

Sample 1259 was taken 5 m above the profile base. The limestone is of the biomicrite type without apparent fossil material. Exceptionally small foraminifers appear. Sparite fields of granular calcite are stratified in levels parallel to the stratification. There are no calcite veins.

Just below the top of the sequence we find pelsparite limestone (sample 1960). Pellets are the dominant allochemical com-

ponent in the rock, taking up around 90% of the rock volume. Granular sparite crystals, around 0.09 mm in size on average, form cement. Some fenestrae in the very washed-out pelsparite have a diameter of around 0.9 mm, and the size of the mosaic sparite crystals is up to 0.45 mm.

Sequence B

Sequence B (divided from sequence A by a bedding-plane) forms a whole and, from the point of view of lithology, is much more evenly built. It is necessary to stress the fact that the area bordering on sequence A, i.e. the section above and below the bedding-plane that divides the sequences, is of limestone with the same features. The thickness of the sequence is 13 m.

At the beginning of the sequence we find, as we did at the top of sequence A, pelsparite limestone (sample 1961). The two sequences differ mainly in the level that the cement is washed-out. Pellets are also the dominant allochemical component in the rock, taking up around 90% of the rock volume. Granular sparite builds the cement, which is less washed-out than the sparite in sample 1260.

Individual calcite veins (between 0.09 mm and 0.23 mm thick, Fig. 1.3.4.) are present in the sample; they are filled with two generations of sparite crystals.

In the middle of the sequence a belt of chert nodules, a few metres wide, is visible (samples 1263, 1264, 1273) (Fig. 1.3.5.). All the nodules have a characteristic zone structure. On the outside, dark and light belts can be distinguished, the latter being wider. The dark and narrower zone contains a major part of the carbonate component. This is most likely caused by the silification of the carbonate component. Numerous carbonate intrusions occur in the zones of silified rock.

The upper part of the sequence (sample 1262) is comprised of slightly washed-out pelbiointramicrite of the wackstone type. The rock is quite diagenetically altered, so many primary forms and features are impossible to define clearly.



Figure 1.3.4. Shilin stone forest. Individual calcite veins are present in the sample; they are filled with two generations of sparite crystals. (Photo M. Knez)

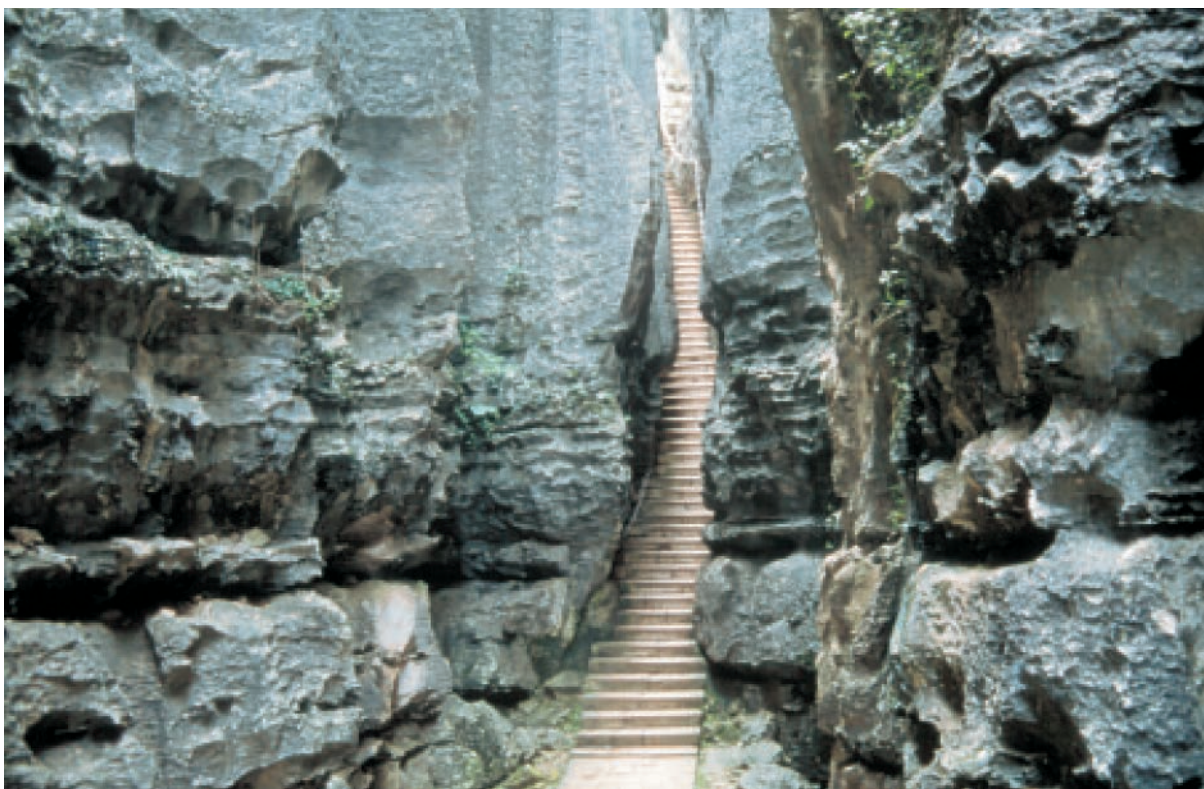


Figure 1.3.5. Shilin stone forest. In the middle of the sequence a belt of chert nodules, a few metres wide, is visible. (Photo M. Knez)

Among the allochemes, pellets and pelletoids prevail; there are fewer fragments of various bioclastics: uniserial, foraminifers, shells and other unidentifiable organisms. In some places on the bioclastics we notice signs of bioturbation. The numerous pellets are mostly no larger than 0.09 mm; most of them have a diameter of 0.045 mm. Smaller plasticlastics probably occur among the intraclastics.

Of the orthochemical components, drusy mosaic calcite prevails, fills the inside of whole and well-preserved large fossils, replaces shells and fills individual caves and fissures. Anhedral to subhedral calcite crystals are between 0.23 mm and 1.8 mm in size. Here, calcite builds a mostly ksenotopic structure.

Sequence C

Sequence C (divided from sequence B by a bedding-plane, Fig. 1.3.6., 1.3.7.) is monotonous from the lithologic point of view and is not noticeably different to the rock and sequence below it. It is 13 m thick.



Figure 1.3.6. Shilin stone forest. Sequence C is monotonous from the lithologic point of view and is not noticeably different to the rock and sequence below it. (Photo M. Knez)



Figure 1.3.7. Shilin stone forest. Detail from Figure 1.3.6. (Photo M. Knez)

The rock in the lower part of the sequence has the same features as the rock observed in the upper section of sequence B (samples 1265, 1266, 1271). The most apparent difference is only in the orthochemical component, where micrite calcite grains were generally found to be slighter.

In the upper section of the sequence we noticed individual non-transparent minerals up to 0.23 mm in size, and individual euhedral calcite grains.

Sequence D

The thickness of sequence D varies from 3 to 5 m due to its conical peaks, which are most exposed to atmospheric influences (Fig. 1.3.8.).

The carbonate sedimentation has not changed noticeably in this part of the geo-

logical column. The top of the sequence, i.e. of the stone column, is of biopelmicrite limestone of the wackstone type (samples 1267, 1268, 1269, 1270).

Among the allochemes, fragments of various bioclastics, which are difficult to identify due to moderate recrystallisation, prevail: various foraminifers and fusulinid foraminifers, shells, snails, etc. In some places on the bioclastics we notice signs of bioturbation. Pellets are mostly no larger than 0.14 mm; most of them have a diameter of 0.09 mm.

Of the orthochemical components, drusy mosaic calcite prevails, filling the inside of whole and well-preserved large fossils, replacing shells and filling individual caves.

In the samples from the upper sequence of the geological column we find somewhat more calcite veins. Their thickness ranges



Figure 1.3.8. Shilin stone forest. The thickness of sequence D varies from 3 to 5 m due to its conical peaks, which are most exposed to atmospheric influences. (Photo M. Knez)



Figure 1.3.9. Naigu stone forest. C characteristic relief of rock surface. (Photo M. Knez)

from 0.09 mm to 0.7 mm. They are mostly filled with one generation of sparite crystals. Calcite veins are not evenly filled in all places, and allow for the observation of interparticle and fracture porosity.

The lithostratigraphic conditions in Naigu stone forest

Naigu stone forest covers an area of 8 km² (Salomon 1997). It is composed of rock from the Qixia formation, which alters a few times through the geological profile (Fig. 1.3.9.). Changes in colour, stratification, porosity and intrusions are noticeable at several points. The base of the lowest exposed part of the Qixia stone forest (where lies Baiyun karst cave, Fig. 1.3.10.) is composed of light-brown-to orange massive and homogenous carbonate. Rock that is less resistant to corrosion and erosion follows in the profile; it makes up a leaner portion of the column beneath an otherwise wider and more resistant upper part.

Geological column divided into 6 sequences: A, B, C, D, E and F. The total thickness of the geological profile (stone column) under study is 51 m.

Sequence A

Sequence A is 2 m thick.

The base of the stone column is formed from a very recrystallised pelbiomicrite to pelbiomicrosparite of the grainstone type (sample 1274).

Although the rock is called pelbiomicrite, a well-preserved fossil inventory is extremely rare. The rock underwent dolomitisation and, on the outside, has a grainy and simultaneously speckled appearance. The speckles in the rock, with a diameter of between 1.3 mm and 12 mm (about 4 mm on average), are in fact non-dolomitised or less dolomitised fields in a dolomitised foundation.

In some places in the nearly 100%-dolomitised foundation we find idio-

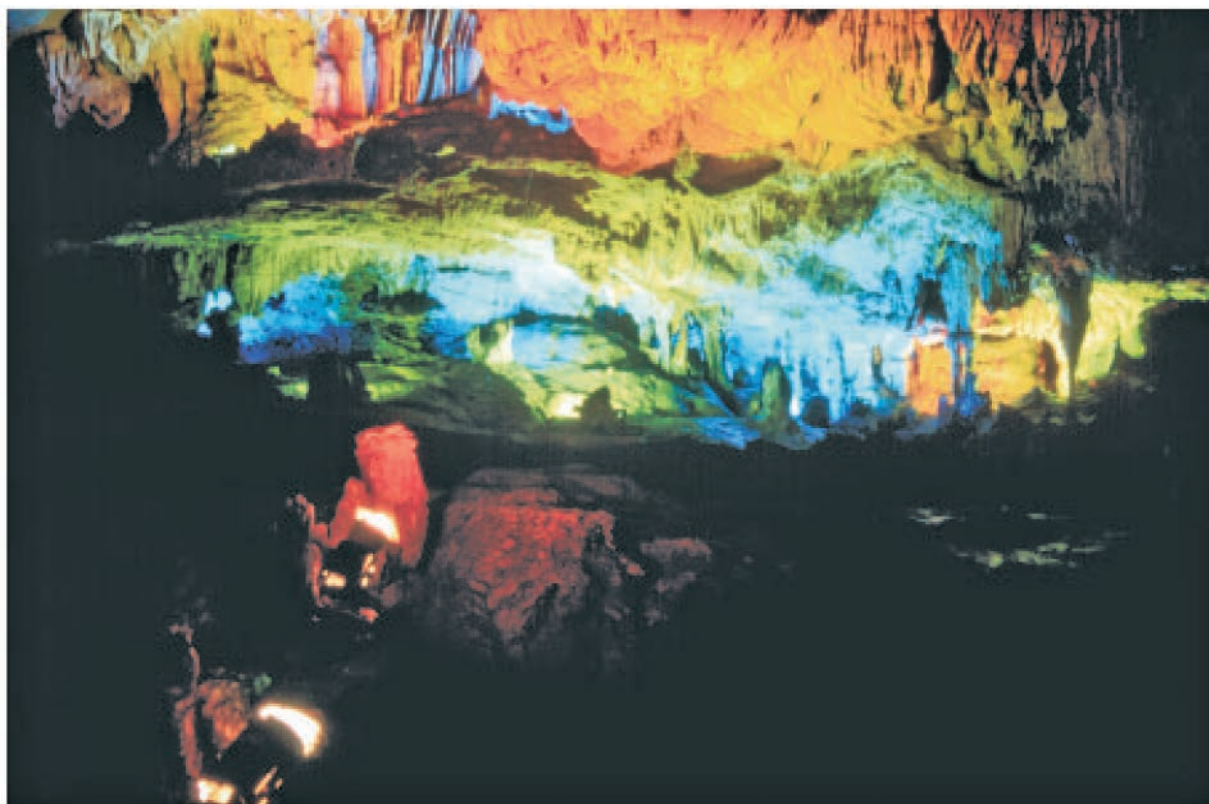


Figure 1.3.10. Naigu stone forest. Baiyun cave below Naigu stone forest. Varicoloured lighting is characteristic of Chinese caves. (Photo M. Knez)

morphic euhedral grains of dolomite, enclosed in micrite and/or microsparite. In general, the structure of the foundation, as well as of the speckles, is ksenotopic and slightly hipidiotopic (the latter only in some places).

Sequence B

Sequence B is 2 m thick.

Over sequence A is pelmicrite limestone of the mudstone type (sample 1275). The rock is of an extremely homogenous structure. No larger concentrations of individual intrusions are noticeable. The rock does not have calcite veins or secondary porosity.

Pellets are evenly distributed in the micrite foundation. They frequently give the impression of being parallel with their longer axis. The average diameter of the allocheme pellet grains is 0.07 mm. Beside

the pellets, less numerous fields of sparite crystals appear in the micrite foundation; most of them are no larger than 0.14 mm.

Sequence C

Sequence C is 5 m thick. Above sequence B is pelmicrite limestone of the mudstone type (sample 1275).

Overlying sequence is a micrite to sparite carbonate of the mudstone to grainstone type (samples N1, N2, N3, N4.). The rock is extremely hard and not weathered in its interior even though bands are macroscopically clearly visible. It has been found that the foundation of the rock (that is the proportionally larger part) is nearly pure calcite, while the bands are dolomite. In the middle of the sequence a belt of chert nodules, a few metres wide, is visible (Fig. 1.3.11., 1.3.12.).

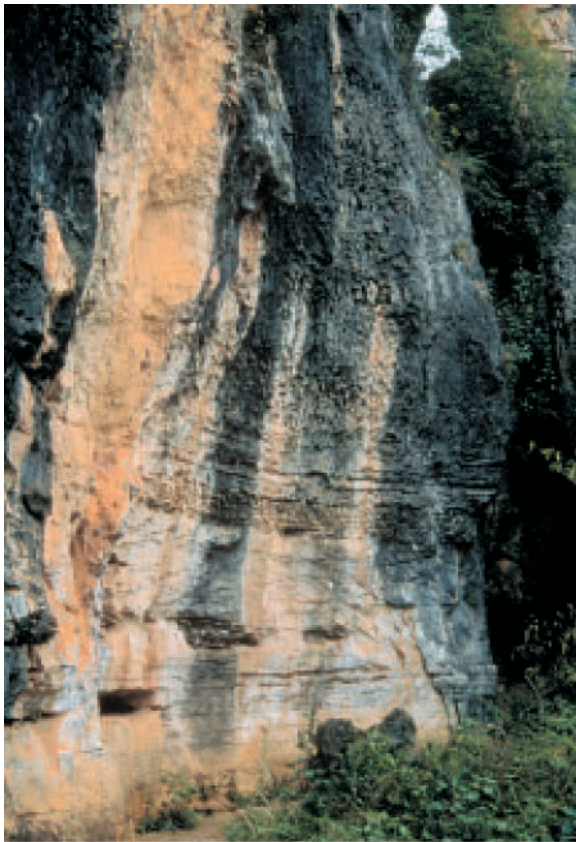


Figure 1.3.11. Naigu stone forest. Various lithologic characteristics of the rock are reflected in the morphology of stone columns. (Photo M. Knez)

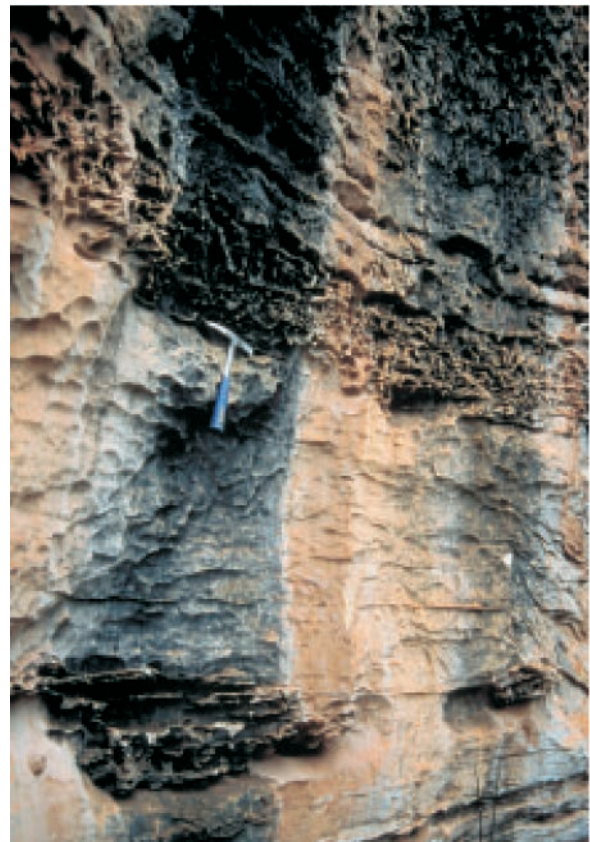


Figure 1.3.12. Naigu stone forest. Detail from figure 1.3.11. (Photo M. Knez)

Sequence D

Sequence D is 5 m thick.

The primary limestone is heavily altered by the process of diagenesis – by means of a microscope we were able to observe subhedral to euhedral grains of dolomite in the rock which form the hipidiotopic to idio-
tropic structure (samples 1276, 1277). We can call the rock dolosparite of the grainstone type as there are no fossil or pellet interclasts. The dolomite grain size ranges from 0.09 mm to 0.9 mm, on average 0.23 mm. The dolomite grains are generally extremely pure and translucent. There are remainders of calcite among the dolomite grains, but not exceeding 15% of the rock. Fillings of fine fissures are also of calcite.

Sequence E

Sequence E is 5 to 10 m thick, it was 7 m thick at the location where the sample was taken.

The rock is a biopelmicrite to biopelmikrosparite of a mudstone to wack-

stone type (samples 1278, N5, N7) and contains numerous cherts, with the longer axes measuring between a few centimetres to over 10 cm, in singular horizons. Growth of crystals has been very widespread in the carbonate rock, so the fossil remains are barely distinguishable. In some of the larger ones (0.7 mm) we can observe nicely represented shelter porosity.

In the rock in the vertical direction we find a number of contacts of very thick micrite mass and biosparite to biomikrosparite mass in which we found numerous tiny fossil remains, these are not definable due to extensive crystal growth.

Sequence F

Sequence F is 5m thick.

Sequence F does not differ essentially from sequence E. In some points it is thickly meshed with calcite veins with a thickness of 0.02 mm to 0.045 (samples 1297, 1280, N8, N9). We found numerous contacts of calcite and dolomite rock in the vertical direction. The dolomite parts (dolomicro-



Figure 1.3.13. Laoheigin stone forest. Rock in the lower sections of the stone columns is more porous than the upper sections, which is reflected in the morphological image. (Photo M. Knez)

sparite to dolosparite) of the wackstone to grainstone type are built of subhedral to euhedral dolomite grains, which form a hipidiotopic to idiotopic structure.

Sequence G

Sequence G has a thickness of 20 to 30 m, it was around 25 m thick at the location where the sample was taken.

This is the thickest more or less homogeneous rock mass in which dolomite and calcite areas are intertwined at irregular contacts and positions (samples 1281, N10, N11, N12, N13). On the exterior they form a characteristically rough surface (T. Slabe, chapter 1.5.; cf. Slabe 1995), while on the interior the situation is very complex and complicated due to extremely strong diagenesis activity and shattered rock.

In general the rock is a biomicrosparite to biosparite or biodolomicrosparite to biodolosparite. Of the allocheme components, bioclastics are very poorly preserved, there are signs of it being worm-eaten, and signs in some places of moldic porosity.

The lithostratigraphic conditions in Lao Hei Gin stone forest

Lao Hei Gin stone forest (Fig. 1.3.13., 1.3.14.) is located around 20 km north of Shilin. Individual stone columns and large blocks modified by corrosion and erosion are spread across an area of only 2 km². The columns are morphologically similar to the columns in Naigu stone forest (Fig. 1.3.15., 1.3.16.).

The geological column is divided into 4 sequences: A, B, C and D. The total thickness of the observed geological profile (stone column) is 26 m.

Sequence A

Sequence A is 7 m thick.

The lower part of the stone column is composed of a heavily recrystallised dolosparite to dolomicrosparite of the



Figure 1.3.14. Laoheigin stone forest. Rapidly decaying stone columns. (Photo M. Knez)

grainstone type (samples L1, L2). The primary limestone is heavily altered by diagenesis – under the microscope we could observe subhedral to euhedral grains of dolomite in the rock, these compose the hipidiotopic to idiotopic structure. The dolomite grains are from 0.14 mm to 0.9 mm large, on average 0.27 mm. The dolomite grains are mostly of a light-brown colour in translucent light, although singular larger grains are extremely pure and almost completely translucent. In a few percent of the dolomite crystals, autogenic overgrowth is clearly visible. There is 6% calcite substance in the rock. Secondary porosity is considerable.

Sequence B

Sequence B is 8 m thick.

Sequence B does not differ considerably from sequence A. Above sequence A is also



Figure 1.3.15. Laoheigin stone forest. Stone columns stand in a number of groups on a slightly anticlinal structure. (Photo M. Knez)

a heavily recrystallised dolosparite to dolomicrosparite of the grainstone type (samples L3, L4, L5).

The dolomite (dolomicrosparite to dolosparite) of the grainstone type is built of subhedral to euhedral dolomite grains, which compose a hipidiotopic to idiotopic structure. The essential difference between the rocks from both sequences is that the rock from sequence B is secondarily porous to a considerably greater extent. The dolomite crystals are on average smaller than the crystals in sequence A (0.23 mm) - even approximately 0.09 mm in the upper part of the sequence - and at the same time less pure.

Sequence C

Sequence C is 5 m thick.

The rock is limestone, only about 10% of the rock is dolomite crystals (sample L7). In the vertical direction the rock immediately passes into biopelintramicrosparite to biopelintramicrosparite. The fossil remains are generally not well preserved, only in



Figure 1.3.16. Laoheigin stone forest. Some cave sections are seen in the lower part of the columns. (Photo M. Knez)

some parts are there better preserved singular foraminifers and thick-shelled snails. There is no noticeable secondary porosity.

Sequence D

Sequence D is 6 m thick.

Sequence D is composed of rock which is practically identical to that of sequence A and represents the top of the stone column. The rock is heavily recrystallised dolosparite to dolomicrosparite of the grainstone type (samples L8, L9, L10). The primary limestone is heavily altered by diagenesis – we can observe subhedral to euhedral dolomite grains composing a hipidiotopic to idiotopic structure. The grains of dolomite are 0.09 mm to 0.23 mm large, on average approximately 0.18 mm. The dolomite grains are mostly of a light-brown colour in translucent light, although singular larger grains are extremely pure and almost completely translucent.

Among the more important differences we can observe more frequent rounded and unfilled fissures from 0.09 mm to 0.18 mm in width, and a considerably lower dolomite content at the top of the column on account of calcite.

Conclusions

The opinions on the effect of lithology on the morphology of the karst, and on individual stone columns and stone blocks, are interesting. Some karst researchers (Zhang 1997) maintain that there is no influence from the carbonate composition and rock structure on the development and form of the karst and its formations. The author also points out that stone forests may develop in dolomite as well as limestone, with or without chert intrusions, and that

they can develop on carbonate rock of diverse structural and genetic types. Others (Salomon 1997) are of the opinion that the particular features of the lithostratigraphy (cf. Knez 1994, 1995, 1996, 1997a, 1997b) are an essential factor in development and formation, and present a morphological image of karst formations, through the whole process from stone teeth to stone columns.

There was not found any literature concerning detailed microscopic research into samples from geological profiles of the stone forests under examination. Despite this, one of the studies mentions that some microscope sections have been prepared from samples from Shilin stone forest. However, it was impossible to find out if the eventual results of the microscope analyses are obtainable. In the parts of the geological profile which it was possible to examine in the direct vicinity of Shilin, it was found that the microscopic analyses did not show larger biostratigraphic changes in the rock. Lithologic anomalies were of greater significance in all three stone forests.

Even though the results of calcimetric analyses are frequently contained in research results, detailed research involving microscopic and calcimetric analyses of contact in lithologically diverse rock, where selective erosion is often clear, was not found. To illustrate, there are outlined the results of calcimetric analyses of two carbonates (Knez 1997c). That sample A and sample B are, in fact, two different rocks in the profile (there was no vertical distance between them, they have been in contact) could be noticed only because of their slightly different colour.

With regard to macroscopic and microscopic analyses of rock from three stone forests in the vicinity of Lunan, it was found that the type of rock was clearly reflected in the selective corrosion and erosion of

SAMPLE	CaO*	MgO	Calcite	Dolomite	Total carbonate	CaCO ₃	MgCO ₃	CaO/MgO
A	51.76	3.23	84.38	14.75	99.13	92.38	6.75	16.02
B	32.41	20.16	7.82	92.21	100.00	57.87	42.13	1.61

Table 1.3.1. Example of two carbonate rocks; intensive corrosion occurred in contact.

*All values in %, except in the last column.

carbonate, and thus in the form and morphological appearance of individual stone columns and larger stone blocks.

The calcimetric analysis (Table 1.3.1) was performed by Mateja Zadel at the Karst Research Institute ZRC SAZU.

1.4. STRUCTURAL CHARACTERISTICS OF SHILIN STONE FOREST

Stanka Šebela

In the sense of geological investigations of Stone Forest turistical part of Shilin was structural-lithological mapped. In July 1996 measurements of strike and dip directions of bedding planes as also principal tectonic zones was accomplished. Final aim was basic structural-geological map with statistically determined frequency of directions of tectonic zones and bedding planes.

Geological data

»Stone forests« belong to karst plateaus in eastern Yunnan (Sweeting 1995). Devonian and Permian limestones are covered by Eocene (and possibly Miocene) lake muds and clays and a deep lateritic soil cover.

The Lunan Stone Forest consists of Permian limestones and dolomites. Accord-



*Fig. 1.4.1. The Lunan Stone Forest-bedding planes are gently deformed to syncline
(Photo S. Šebela)*



Fig. 1.4.2. Stone pillars in Lunan Stone forest (Photo S. Šebela)

ing to geological map (1:50.000) the beds in park gently dip from 2° to 8° , in average for 5° and strike towards west. In the base the Devonian beds are overthrust to the Permian beds.

In limestone open synclines (Fig. 1.4.1.) and anticlines with dips from 3° to 17° may be seen. Where the limestones are thick-bedded and strongly jointed, rock columns up to 30 m high can be formed (Sweeting 1995).

The stone pillars (Fig. 1.4.2.) are developed in the Lower Permian Maokou (354 m thick) and the Qixia (100 m thick) limestones. Both of these limestones are very uniform in composition and are thickly bedded.

The Maokou is a platform, sparitic and bioclastic limestone (Song Linhua 1986). It is slightly dolomitized in places. The Qixia is a massive reef limestone and also dolomitic.

Widely spaced fractures are critical to the formation of the stone forest. If the carbonate rock mass has been tectonically stressed and has developed sets of oblique

fractures, the structural weakness of the rock makes it difficult for tall pinnacles to remain stable. The main sets of rock fractures are close to vertical (Zhang Shouyue 1997).

The outlines of the pillars are related to the directions of the jointing, the main joints at the Lunan Stone Forest being $N20^{\circ}W$, $N50^{\circ}W$ and $N50^{\circ}E$. The $N20^{\circ}W$ joints are pre-Cenozoic and are filled with calcareous tufa, but the other joints are Cenozoic in age and are open vertical intersecting fissures which cut the sub-horizontal Maokou limestones (Sweeting 1995).

Lunan Stone Forest lies east from Jiu-Xian-Shiyakou fault which makes part of Xiaojiang folded belt. Geological elements of the fault are 70-80/60.

Local water table in the Lunan area are Sword Peak Pond, Lotus Flower Pond and Stone Forest Lake (Fig. 1.4.3.). The superficial and underground waters drain into Bajiang, towards S and SW. The underground water flows in epiphreatic channels.



Fig. 1.4.3. One of ponds in Lunan Stone Forest (Photo S. Šebela)

Water level in Sword Peak Pond and Lotus Flower Pond may increase for 10 m.

The situation of the Lunan Stone Forest is determined by movements along Jiu-Xian fault zone. These movements controlled the deposit of Eocene rocks and permitted gentle covering of Permian limestones. More than 500 m thick layer of red loam was deposited in the Lunan area.

Modern stage of karst development includes the late Miocene to the Holocene, some 7 to 4 million years ago. This stage corresponds to intensive uplifting of the Tibet plateau and records the appearance of deep valleys (Miocene - Holocene). The uplifting of the Earth crust in the Tertiary and the Quaternary played an important role at karst development in southern and western China. It caused the changes in karst water level. Continental crust of China is intensively affected by neotectonic movements (the modern Himalaya's displacements) which is important for development and various types of karst in China (Zhang Zhigan 1980).

Ford et al. (1997) describe that karst developed in Lower Permian carbonates

was buried by terrestrially erupted Upper Permian tuffs and basalt lavas (Emeishan Formation). Remnant basalt patches are up to 50 m thick in Shilin area but 600 m thick near Kunming.

Measurement of fissures in the Lunan Stone Forest

I measured dip and strike of fissures in the area of the Lunan Stone Forest. Limestone pavement is formed along the most frequent trendings of fissures.

In a rose graph (Fig. 1.4.4. and Table 1.4.1.) is shown the frequency of the fissure directions. Out of total number of fissures (N=202) the direction $315-330^{\circ}$ (NW-SE) is the most common (20.79%). The second place (15.34%) occupies the direction $45-60^{\circ}$ (NE-SW) and the third one (14.35%) the direction $285-300^{\circ}$ (NW-SE).

Poorly are represented the directions N-S although regionally important geological structure lines are of this direction. This fact implies the idea that the area of stone forest lies among stronger faults; a block is

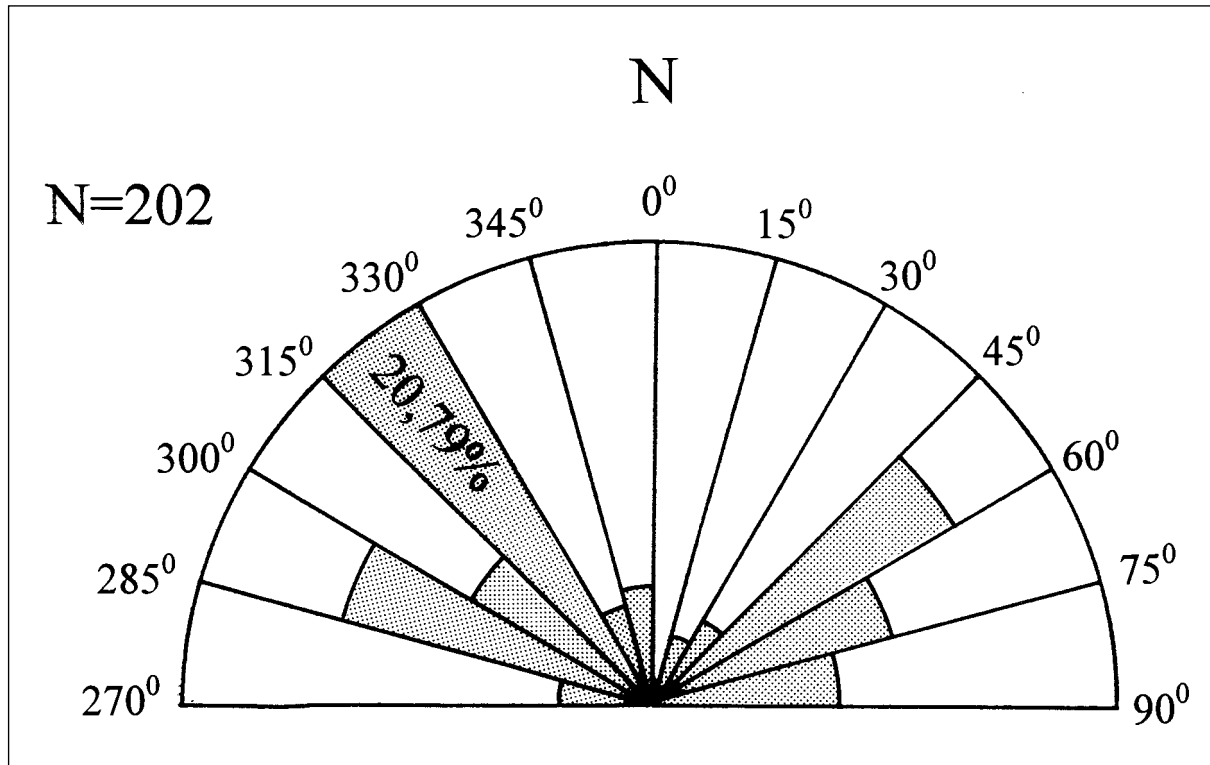


Fig. 1.4.4. Rose graph of jointings in the Lunan Stone Forest (N=202)

broken in two main jointings, NW-SE and NE-SW.

When the pathways in the park were made the fissures among the pinnacles were used and thus the main tourist ways are concordant to fissures in a limestone (Fig. 1.4.5.).

It is typical of the fissures to dip very steeply, almost vertically (80-90°).

According to Sweeting (1995) the main joints are N20°W which differs for at least 10° from mine measured and analysed data.

In the book Karst of China (1991) Yuan Daoxian summarizes the researches done by Zhang Shouyue (1983) who was the author of a linear structures map in the Lunan Stone Forest. According to this map the most frequent tectonic structures are N50°W.

In a central part of the Lunan Stone Forest (Fig. 1.4.6.) the most expressed dip direction is 50° and transverse dip direction 140°, 160° and 180°. In eastern part of stone forest the dip direction 80° (N10°W) prevails. West from touristically displayed pathways in the Lunan Stone Forest there is a thicker layer of red loam deposited in a val-

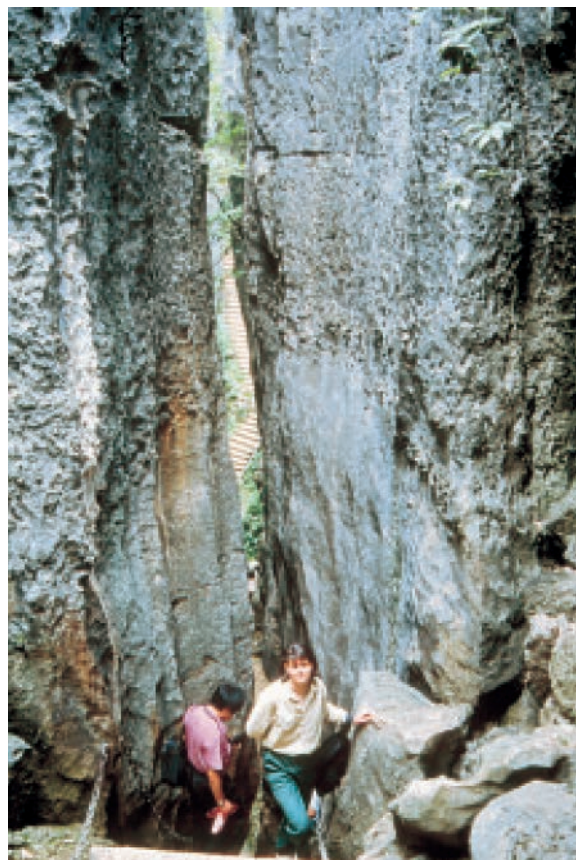


Fig. 1.4.5. The fault zone in the Lunan Stone Forest (Photo S. Šebela)

ley, oriented to 110° (N 10° E). South from the Stone Forest Lake and along the southern touristic pathway the direction of the jointing is $0-20^{\circ}$ (E-W, N 80° W, N 70° W).

During field mapping I could not determine bigger displacements along some joints. It is fact that on the mapped area (Fig. 1.4.6.) there is not an uniform direction of joints intersecting all the others. Thus we perceive that directions NW-SE are intersected by directions NE-SW and vice versa. The relative age of the main joints in the Lunan Stone Forest thus cannot be determined for sure.

Measurement of layers in the Lunan Stone Forest

I measured 52 dips and strikes of strata. The results are shown in structural-geological sketch (Fig. 1.4.6.), in Schmidt net (Fig. 1.4.7.) and in rose graph (Fig. 1.4.8.). The main direction of strike is NW and W (Fig. 1.4.7.).

Due to small dipping of beds lithological column is accessible in a thickness of 200 m. In its lower part, accessible in the eastern part of the Stone Forest and also in its central part through deep fissures it contains limestone with inliers of cherts jutting

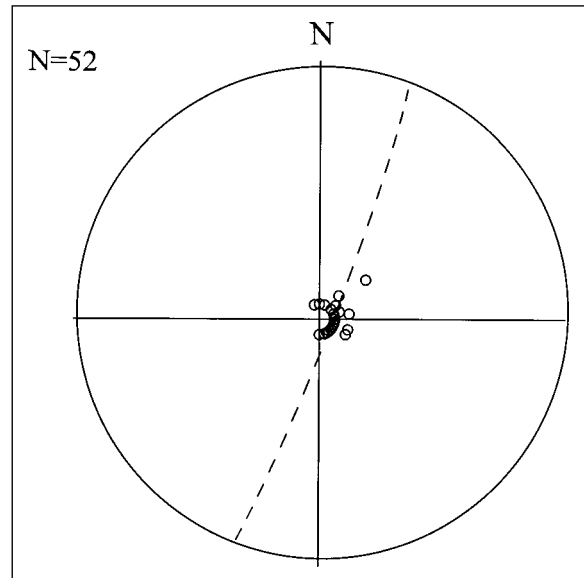


Fig. 1.4.7. Schmidt's net - the layers of limestone in the Lunan Stone Forest (N=52)

out of a limestone. The layers in upper part of the lithological column are the least stable in case of earth-quakes. It is evidenced by numerous collapse blocks that had fallen into the fissures during the earth-quakes of the last decades.

At least 21.2 % of limestone layers have direction N $16-30^{\circ}$ E (Fig. 1.4.8. and Table 1.4.2.) striking westwards for 5 to 20° , in average for 5° .

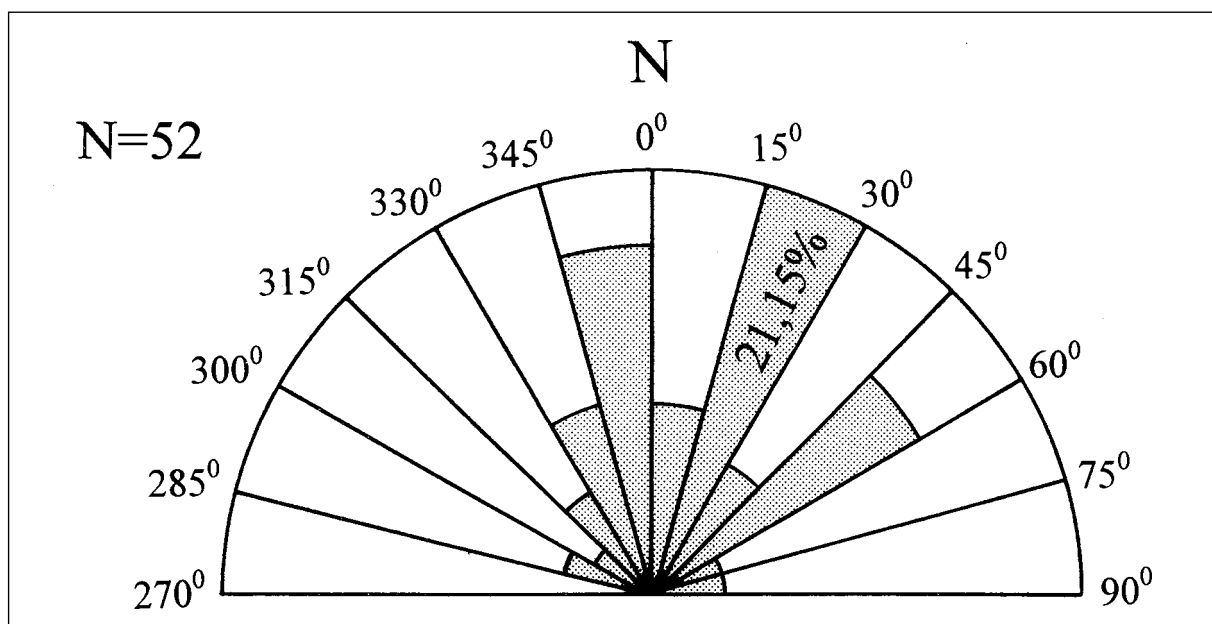


Fig. 1.4.8. Rose graph of layers in the Lunan Stone Forest (N=52)

direction	no. of measurements	%	position
1-15°	0	0	12
16-30°	5	2.47	11
31-45°	8	3.96	9
46-60°	31	15.3	2
61-75°	22	10.9	4
76-90°	17	8.4	6
271-285°	8	3.96	9
286-300°	29	14.4	3
301-315°	19	9.4	5
316-330°	42	20.8	1
331-345°	10	4.95	8
346-0°	11	5.44	7

Table 1.4.1. Statistical evaluation of fissures trending in the Lunan Stone Forest (N=202)

In the southern part of the stone forest (Fig. 1.4.6.) the layers of limestone dip not only towards NW and W but also towards SW.

As already Sweeting (1995) pointed out the structures in the limestones of the Lunan Stone Forest are open synclines and anticlines. The anticline ridge is the most obvious in S and SE part of the Stone Forest (Fig. 1.4.6.).

Conclusions

The stone pillars or pinnacles that form a stone forest developed below soil, the fissures widened and later some typical below sediment features developed.

By measuring geological elements of strike and dip of fissures in the Lunan Stone Forest and by basic statistical data processing it was established that in the Lunan

direction	no. of measurements	%	position
1-15°	5	9.6	4
16-30°	11	21.2	1
31-45°	4	7.69	6
46-60°	8	15.4	3
61-75°	2	3.8	8
76-90°	2	3.8	8
271-285°	0	0	12
286-300°	2	3.8	8
301-315°	1	1.9	11
316-330°	3	5.76	7
331-345°	5	9.6	4
346-0°	9	17.3	2

Table 1.4.2. Statistical evaluation of the direction of layers in Lunan Stone Forest. N=52

Stone Forest three main directions of fissures prevail. These are 315-330° (NW-SE), 45-60° (NE-SW) and 285-300° (NW-SE). As the main regional tectonic structures are directed N-S the area of the Lunan Stone Forest presents morphologically slightly elevated terrain between two stronger fault systems inside which the limestones jointed in three main directions. The fissures that widened below the sediment cover are displayed as pinnacles of the stone forest since the sediment cover had been removed.

The layers of Permian limestones strike towards NW and W dipping for 5 to 10°, they are gently folded into several smaller anticlines and synclines.

To attain a more complex explanation of tectonic conditions it would be necessary to widen the researches over the borders of touristic part of the Lunan Stone Forest.

1.5. ROCK RELIEF OF PILLARS IN THE LUNAN STONE FORESTS

Tadej Slabe

Rock relief is often a significant reflection of the conditions under which various factors and processes shape carbonate rock. The rock relief indicates the formation of the coat of the rock which composed of rock forms (Slabe 1995). The rock is shaped by one of the factors or exhibits traces of several different factors that wear away the rock either simultaneously or sequentially. The characteristics of the formation of the stone forests and partly their development as well are therefore reflected in the rock relief of pillars in the stone forests. On decaying and non-homogenous rock, characteristic rock relief frequently does not appear or is less distinct. The composition of the rock also dictates the roughness or smoothness of the rock surface.

Many individual rock forms carved by rainwater as well as some subcutaneous forms have been described in detail and the research on them so far has been summarized in the books *Karst Geomorphology and Hydrology* (Ford & Williams 1989) and *Karren Landforms* (Ed. Fornós & Ginés 1996), and more works are mentioned in

the descriptions of individual rock relief. My intention was to supplement the list of rock forms on the pillars of the stone forests and expand the knowledge of the less studied rock forms, to add special features of the stone forests, and to describe the rock relief of the forests, defining it as traces of their development. During the classification of cave rock forms (Slabe 1995), I determined that it is more sensible and useful to combine them according to the factors and processes which shaped them and the surroundings in which they appeared and not just according to the characteristics of the forms. I therefore did the same in this work (see table below). In naming them, I frequently add the most important characteristic of their origin to the basic forms.

Subcutaneous rock forms on the pillars of the stone forest

The importance of subcutaneous dissolving of carbonate rock in forming the Lunan stone forest has been stressed by al-

SUBCUTANEOUS ROCK FORMS			SUBCUTANEOUS ROCK FORMS RESHAPED BY RAINWATER	ROCK FORMS CARVED BY RAINWATER
<i>Under sediment and soil</i>	<i>Under thin layers of soli and vegetation</i>	<i>On the level of soil</i>		
subcutaneous tubes				
subcutaneous small and large channels	subcutaneous small and large channels	bells and half-bells		small and large channels small and large recesses
subcutaneous scallops	subcutaneous small and large recesses	notches		solution pans

Table 1.5.1. Rock forms that comprise the rock relief of pillars in the stone forests

most all of its researchers. Rock pillars are originally formed below the sediment and soil and then reshaped by rainwater. The majority of researchers also enumerate and briefly describe individual rock shapes formed below the ground. I have added the adjective »subcutaneous« to the majority of the characteristic rock forms, an expression very graphically applied to karst forms of this type by Gams (1971). Gams (1997, 324) also stresses the speed at which carbonate rock dissolves below the soil. I already described, named, and attempted to explain the formation of cave rock forms that occur in contact with fine-grained sediment (Slabe 1995). In most cases, subcutaneous rock forms could be called epikarst forms because they are linked to the characteristic formation of stone forests in this part of a karst area.

The importance of water—which becomes rich in CO_2 as it percolates through the soil—in shaping the rock under the soil is stressed although this influence is presumed to decrease after two or three meters. However, I have observed that the influence of water percolating along the contact point between rock and soil reaches deeper in individual places, a fact related to the degree of permeability. J. Kogovšek (chapter 1.6.) established that water that has percolated through the soil and a cave ceiling has greater hardness than rainwater at the contact with the rock, which indicates the influence of the soil on the water. Hantoon (1997, 311) divided the permeability of epikarst into its permeability at the contact between sediment and rock, its permeability through rock, and finally its permeability through sediment containing clay, which should be low. According to Hantoon (1997, 313), the dissolving of carbonate rock is most efficient below sediment. Song Lin Hua (1986, 9) also brings up the importance of the recurrent corrosion capability of the water where water that has percolated through the soil mixes with saturated water running along the junction between rock and soil. Large subcutaneous channels are therefore dissected by horizontal notches. Song Lin Hua also states (1986, 9) that the speed of the forma-

tion of the forest in areas with organic material in the soil is ten times greater than those on the tops of the hills. Zhang Shouyue (1997, 79) determined that corrosion notches and niches were formed under the sediment. According to the frequency of distinct turns in subcutaneous channels below soil and large horizontal subcutaneous notches, I conclude that the junction with the rock is often poorly permeable and the corrosion is distinctly more effective at the level of the soil and underneath it. Below the subcutaneous channels, which are wide in the upper part, and the horizontal notches, there are often smaller winding channels. Of course, the size of subcutaneous rock forms is also influenced by the quantity of sediment in the cracks between the pillars and the period of their formation. The largest channels occur when the level of the sediment lowers gradually but evenly.

Rock forms whose origin is linked to the fine-grained sediment and soil that entirely or partially covered the pillars in the period of their formation, I divided (see table) into those that originate deeper under the ground, that is, completely subcutaneous rock forms, those that originate under a thinner layer of soil and vegetation, and those that originate at the surface of the soil and are composed and directly shaped by rainwater. Old subcutaneous rock forms reshaped by trickling water also survive higher above the ground. However, we must distinguish between the subcutaneous shaping of rock that is specifically the consequence of the composition of the rock, its joint frequency and stratification, that is, the points of weakness in the rock, from subcutaneous rock forms created by characteristic factors. Due to relatively even dissolution of the rock below the soil and the sediment, the rock is rounded so that the subcutaneous forms are of the same type and the surface of the rock seems relatively smooth to the eye or characteristically rough on the variably composed or recrystallized carbonates. Under great magnification, the under-sediment rock surface, as a rule, is distinctly finely rough due to the even corrosion of the grained rock (Slabe 1994).

Below the sediment and soil, **large** (Fig. 1.5.1.) and **small subcutaneous channels** occur. Vertical channels range from twenty centimeters to one meter and more in diameter (Chen Zhi Ping et al. 1983, 605). They occur when larger amounts of water continuously flow along the permeable contact with the rock. The largest channels can be wide and shallow and also deep along fissures where the channels are most frequent. The size of the diameter of the semi-circular subcutaneous channels can vary. Deep under the soil and sediment, the large channels are often distinctly narrower. Therefore, the rock dissolves fastest at the upper part of the soil and sediment. Along the more distinct fissures, a subcutaneous shaft with soil at the bottom can occur in the middle of the pillar.

In Lao Hei Gin, subcutaneous channels may be preserved on the harder stone tops and feet. They are several meters wide and up to half a meter deep and dissected by small subcutaneous recesses. Channels are visible at all heights only on pillars that are close together. The pillars are therefore undercut and overhang considerably. On the

upper parts of the pillars, the subcutaneous channels are distinct only on lower pillars that have not been denuded long enough for the rainwater to reshape them to a larger degree. As a rule, they no longer exist in the denuded middle sections of the pillars due to the fine disintegration of the rock.

Smaller channels (Fig. 1.5.2., 1.5.3.) five to twenty centimeters in diameter cross the wall at various angles and can have winding shapes. They are evenly wide along their entire length or wider at the contact with other channels. They can also be linked in a network.

Channels also occur in the lower sections of the pillars in the Shilin Central Forest which is composed of layers of limestone with large lenses of chert in them. There are no minor rock forms on them. Larger rounded and shallow channels are also found on the pillar walls in Naigu. Smaller rock forms are not found on such rock or they are indistinct due to the composition of the rock or its decay.

Channels therefore appear under sediment and soil, and when the level of the sediment drops, the denuded parts of the



Fig. 1.5.1. Large subcutaneous channel (Photo T. Slabe)



Fig. 1.5.2. Small subcutaneous channels (Photo T. Slabe)

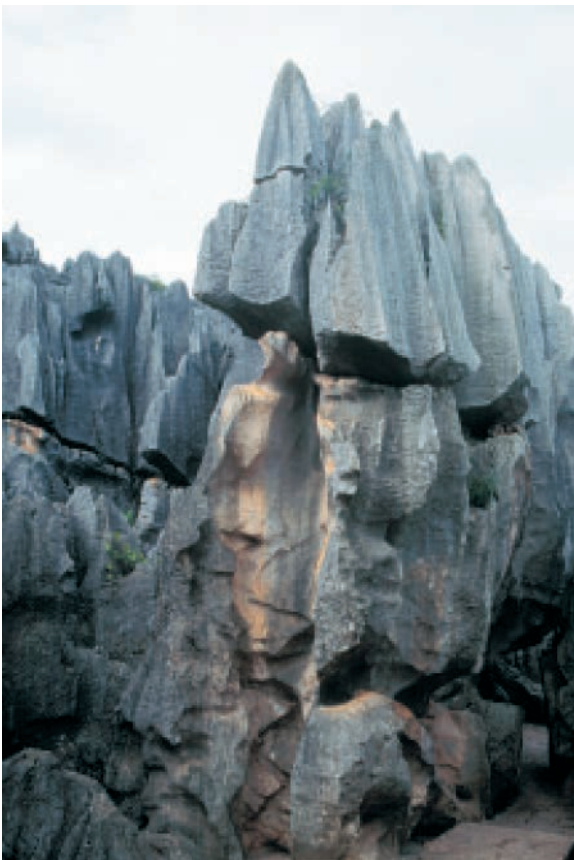


Fig. 1.5.3. Subcutaneous channels (Photo T. Slabe)

pillars are reshaped by rainwater. Their surface is therefore dissected by small recesses. Below deep channels formed by rainwater on the tops of pillars, their lower parts under overhangs are shallow and wider, only partly reshaped by rainwater.

As a rule, the most winding are subcutaneous small channels (Fig. 1.5.3.) between one and five centimeters in diameter. Small channels often run obliquely down the walls and curve by as much as 90°. They either stand individually or are connected in characteristic rhombohedral grids.

Subcutaneous large and small channels develop mainly through the soaking of the soil and sediment at the permeable contact with the rock and not through distinct minor streams, a fact reflected by the network of small channels and their dissection with small horizontal notches. Small tubes through which water flows occur only at the bottom of channels. At the contact point, the dissolving of the rock is more distinct and longer lasting. The size and the shape of the large and small channels are dictated, along with the composition of the rock, primarily by the permeability of the



*Fig. 1.5.4. Subcutaneous channels
(Photo T. Slabe)*

contact with the soil and the quantity of the water flowing over the contact point. The less permeable the contact is, the more winding small channels develop. The character of the contact between the wall and the soil can vary or change in places. Winding small channels can therefore occur on the walls of larger channels (Fig. 1.5.3.). At poorly permeable contact points, subcutaneous channels are the largest along the level of the sediment and soil, while below it they narrow quickly. Gams (1997) also establishes a connection between the growth of underground caverns and the permeability of their fill. In old caves without ceilings, the contact between the clay and the wall has not been reshaped in most cases from the period of the fine corrosion of the rock when the moist fine-grained sediment was deposited (Slabe 1997).

Unique vertical or horizontal subcutaneous channels (Fig. 1.5.4.) with semicircular or omega-shaped cross sections appear at

the bottom of the cracks between the pillars or teeth where the fissures are wedged out or where the channels crisscross the tops of larger subcutaneous teeth (Fig. 1.5.5.) or lead from subcutaneous recesses (Fig. 1.5.5.). The water flowing along permeable contacts with the rock accumulates at the bottom of cracks and recesses, and the soil therefore preserves its ability to dissolve the rock for a longer period.

Under a thinner layer of soil, in most cases in the vicinity of large and small subcutaneous recesses, there are, as a rule, gradually sloping channels with semicircular bottoms. They occur with the accumulation of the water that percolated through the soil. Underneath the soil, they also deepen quickly when only their bottom is covered. On larger rocks, systems of channels developed. Smaller subcutaneous channels unite radially into a larger channel due to the gravitational flow of the water. In the following chapter, channels will be described that formed due to the draining of water from subcutaneous recesses and from solution pans on the tops of the pillars. The vegetation was removed and the water carried away the weathered debris.

Subcutaneous channels must be distinguished from the subcutaneous channel-like notches that are merely the consequence of stratification and the way the rock has been crushed.

The largest **subcutaneous scallops** are a unique feature, similar to large and open scallops with smooth walls. Their diameters are fifteen to fifty centimeters and they are shallow. As a rule, they are found on overhanging surfaces (-5° to -20° ; Fig. 1.2.3.). Most frequently, they are slightly deeper on the upper side and connected in a network. Larger recesses also occur on overhanging walls of pillars that have been exposed to rainwater for a longer period. For the time being, I am of the opinion that they developed during contact with fine-grained sediment. This supposition is also proven by rock dissected by recesses whose yellow surface is rounded and smooth. Such is often the case on rock at the contact with sediment or soil and when the water drains from it. They are also similar to the subcu-



Fig. 1.5.5. Subcutaneous channels (Photo T. Slabe)

taneous rock forms that can be observed at distinct fissures along which cracks develop filled with soil and which have been denuded by land works in Kras (Slovenia). Along fissures crisscrossing the rock or at distinct bedding planes, recesses of this type as a rule do not occur, but rather a semi-circular channel develops beside them. It appears that the recesses occurred because of the distinct flowing of the water along the contact with the rock and the percolation of water through the porous soil and sediment. Soil or sediment of this type often contains particles of rock or rubble. Along-sediment recesses also occur frequently on the walls of caves filled by fine-grained sediment. In the stone forests, they are visible only in individual places.

For the moment, I can conclude—though I will also try to verify this with tests with gypsum—that large and small channels occur mostly due to the percolation of water at the contact of the rock with the less porous sediment and soil, while recesses occur at distinctly porous sediment and soil when a larger quantity of water trickles

down the contact and simultaneously percolates through the soil and sediment. The latter can be found only rarely in the Lunan stone forests.

Under the thin layer of porous soil that covers the rock in some places only in spots and elsewhere entirely, hemispherical **small and large recesses** (Fig. 1.5.6.) occur. The former are one to five centimeters in diameter, the latter are larger. They occur due to the percolation of water through the soil. The water moistens the soil in the small recesses and, as a rule, enlarges them in a hemispherical way when the rock is surrounded by fine-grained sediment or soil. The recesses in most cases lie side by side or are already connected. The subcutaneous channels described often lead from them. From recesses on level surfaces, solution pans can be formed when the majority of the soil is washed away. Trudgill (1986, 468) says that the subcutaneous recesses and channels only occur underneath acidic soils.

Separately, we can single out rock shapes that occur at long-lasting levels of



Fig. 1.5.6. Subcutaneous recesses (Photo T. Slabe)

sediment and soil. These are **subcutaneous notches, bells, and half-bells** shaped by rainwater that trickles to the bottom and then flows between the rock and the soil.

Smaller subcutaneous notches, ten to twenty centimeters in diameter, have the form of semicircular horizontal channels, except their upper edges are sharper in most cases while the lower edges are rounded, assuming, of course, the entire subcutaneous notch has not been reshaped by rainwater. Larger subcutaneous notches (Fig. 1.5.7.; undercut notches - Waltham 1984, 182; Ford et al. 1997) are indented into the rock by one meter and more, and the largest I have seen are up to one meter high. The lower part of the notches is undercut as the rock has been subjected to faster, longer-lasting dissolving under the moist ground and is therefore rounded and smooth. The bottom of the notch is horizontal and the upper part lowers toward the bottom in a semicircular fashion. The upper part of the notch has been reshaped due to the trickling of rainwater. Notches can be seen at various heights of the pillars at

long-lasting levels of soaked ground. Smaller and exposed notches are more distinctly reshaped by rainwater while larger notches are less distinctly reshaped.

Half-bells (Fig. 1.5.8.) occur below channels that lead larger quantities of rainwater trickling down the pillars to the sediment. Above the soil and sediment, the expansions have characteristic bell-shaped and half-bell-shaped forms. Their shape and size are linked to the quantity of water reaching the soil, the permeability of the contact between the rock and the soil, and the duration of the level of the soil or sediment. When formed along a distinct fissure, the upper part of the channel can also be a tube, while the wall is only weathered at the area of expansion. The walls of bells from which the soil was recently removed are dissected with oblong subcutaneous recesses reaching up to one meter in diameter. Large bells also occur between the pillars. The upper parts of half-bells and bells are reshaped by trickling water that gives them the distinct semicircular form. Below, above the soil, the bell-shaped expansions most frequently



Fig. 1.5.7. Subcutaneous notch (Photo T. Slabe)

gradually narrow into subcutaneous channels. First, smaller semicircular notches occur, and larger notches then grow during the slow lowering of the level of sediment. The rapid lowering of sediment causes these forms to remain hanging on the walls of the pillars. Poorer permeability of the contact below the notches and subcutaneous bells is also proven by small subcutaneous channels.

In short, notches and bells occur when more water flows to the contact with the soil or the sediment surrounding the pillars than the contact or the unevenly porous sediment can immediately conduct, and the dissolving of the rock at this spot is therefore faster.

The forms described are distinguished from the notches that occur because of the often faster dissolving of the rock along the bedding planes that are almost horizontal in Shilin. As a rule, these notches are narrower and often relatively deep in relation to the diameter of the opening.

Cracks occur along the vertical fissures that crisscross carbonate stone in various

networks, and between them are **subcutaneous stone teeth**. The cracks often have their cross sections in variously wide and deep V-shapes. At their bottoms, subcutaneous channels are frequent. With densely distributed teeth, only narrow cracks can occur, from 0.2 to 0.75 meters in diameter and usually up to two meters deep. Such stone teeth are stubby under the ground and on the surface. Narrow and pointed teeth occur, though, when the crack-like notches between them are up to two meters wide and more than five meters deep. In the latter case, only narrow and relatively low points reach the surface. Of course, there are numerous intermediate variations. The differences in their shapes are the consequence of the properties of the fissured rock, the type of sediment, and the duration of the dissolving of the rock under the ground. The type and composition of the stone is not reflected in the shape of the subcutaneous stone teeth as much as on the surface where it defines the shape of the pillars and to a large degree their rock relief as well. Subcutaneous stone teeth are

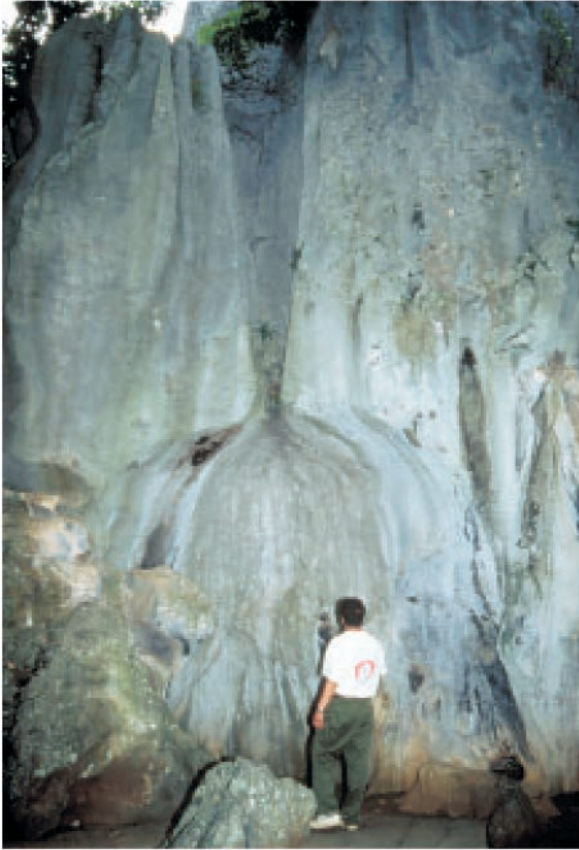


Fig. 1.5.8. Subcutaneous half-bells
(Photo T. Slabe)

quite regularly pointed and rounded. Such is the case in the Naigu and Lao Hei Gin forests. They have semicircular subcutaneous rock forms, while fissures or bedding planes also show here along which semicircular notches occur. The water therefore reaches and shapes the underground teeth relatively evenly.

The water flowing along the contact of rock and soil or percolating through the soil to the rock accumulates in the recesses that occurred at weak points in the rock, and from there it flows down the stone teeth. Subcutaneous channels occur at the bottom of the cracks between the teeth, they can cut across the tops of the stone teeth, or they can appear as outflow channels from subcutaneous recesses. However, due to the lowering of the level of the soil, the soil been preserved only on the bottoms of channels where water has deepened and expanded them.

The pillars in the stone forests are often crisscrossed by **subcutaneous tubes and**

anastomoses that originated at distinct bedding planes, fissures, or in porous rock. Water also deposited sediment in the originally small tubes that became wider in the process.

The pillars in the Lao Hei Gin stone forest are perforated by tubes in their middle and lower sections, that is, in layers of distinctly porous rock, while these are practically non-existent on the tops and at the feet of the pillars. They penetrate deeply into the rock, and some run through the pillars. The bottoms of the semicircular tubes, on top of which are often smaller above-sediment channels, are clayey if they are situated in the layer of sediment and soil. Above-sediment ceiling channels occurred when the level of the subcutaneous tubes was under the soil. The tubes were filled with sediment, above which smaller quantities of water flowed. The size of the tubes, which reach 1.5 meters in diameter, and their branching, indicate the long duration of the formation. Individual systems are the size of smaller caves.



Fig. 1.5.9. Subcutaneous tube (Photo T. Slabe)



Fig. 1.5.10. Subcutaneous tube (Photo T. Slabe)

The majority of subcutaneous tubes (Fig. 1.5.9.) in the pillars of the Shilin stone forest are smaller. They occurred at fissures in the middle sections of the pillars. Only individual tubes are larger, reaching up to two meters in diameter. In most cases, their cross section has the shape of a horizontally elongated ellipsis. As a rule, there are channels (Fig. 1.5.10.) on their bottoms formed when the level of the sediment encircling the pillars dropped and the water flowed only along the bottoms of the channels.

In Naigu, large tubes occurred at the contact between the harder and non-fissured tops and the lower, thinner layers of rock. In most cases, they are not larger than one meter in diameter, although some are genuine tunnels.

Rock forms carved by rainwater on the pillars of the stone forest

The most beautifully developed rock relief with rock forms of this type is found in the Shilin (central) stone forest. In the

relatively pure and thickly layered limestone with relatively even composition, unfissured, and not particularly dolomitized, distinct rock forms developed due to rainwater. The most distinct and diverse is the rock relief formed by rainwater on the upper five meters of the pillars, while the tracks of trickling water on vertical and slightly inclined walls reach all the way to the feet. There are also surfaces, however, that the rainwater does not reach directly. Deeper notches occurring at bedding planes or levels of sediment of longer duration are smooth or have points only on the initial part of their ceiling. J. Kogovšek (chapter 1.6.) identified the significance of various types of rain that influence the speed of the dissolving of the pillars due to variations in the thickness of the film of water they create on the rock.

The first subgroup of rock forms directly or indirectly shaped by rainwater consists of **small and large channels**. On the upper parts of pillars, small channels (Fig. 1.5.11.; Rillenkarrren – Bögli 1981; Sweeting 1995; Chen Zhi Ping et al. 1983)) are found



Fig. 1.5.11. Small channels carved by rainwater (Photo T. Slabe)

on evenly fine-grained rock. Semicircular (parabolic – Glew and Ford 1980) small channels, one to three centimeters wide and from several centimeters to several dozen centimeters long, run parallel to one another, that is, linked in a network. The more evenly fine-grained the stone is, the more regular the forms of the small channels and the straighter the ridges between them are. The curvature of the ridges and the dissection of small channels into small recesses, a characteristic of small channels especially on steeply inclined surfaces (Slabe 1995), are the result of the composition and recrystallization of the rock. Small channels occur on sloping and gently inclined surfaces. Glew and Ford (1980, 27) established that they occur on surfaces inclined from 12° to 70° . On gently inclined surfaces, they are similar to one another and equal, while on steeper rock surfaces they unite into larger, mostly shallow channels (Fig. 1.5.11.; Regenrinnenkarren) that are therefore distinctly ribbed in the upper part. Small channels, connected in this way can also be found in caves formed under a

thin flysch cover (Slabe 1995). On steep pointed pillars, only shallow less distinct small channels dissecting larger channels occur on the ridges. On wider tops of the pillars, the water from the small channels flows into shallow, wider, and gently inclined channels (Fig. 1.5.11.). Small channels occur when the film of water is still thin and does not prevent rain from direct contact with the soluble rock; however, when the film is thick enough, flat surfaces (Glew & Ford 1980, 25) or the channels described above occur that are therefore a characteristic form below the small channels. The small channels in the Naigu stone forest are only found on dolomite limestone tops of pillars. They are winding and their ridges are not level. They are often arranged radially around lenses of slower dissolving rock. In the Lao Hei Gin stone forest, the rainwater flows down a network of one to two centimeter deep and similarly wide at the top small notches that occur along thin, densely distributed fissures. The ridges between them are narrow but rounded. Forti (1977, 10) determined the various sizes of

small channels on different rock. The most regular forms occur on micrite (Forti 1977, 11). As a rule, this applies to all rock forms on evenly fine-grained rock (Slabe 1995).

Individual small channels and channels that most frequently have diameters up to fifty centimeters are of different origin. The first, whose diameters reach up to fifteen centimeters, are characteristic of the steep and vertical upper sections of pillars. Small channels unite in them (Fig 1.5.11.). They are frequently dissected only by less distinct horizontal ridges. They begin on sharp tops or ridges and can unite in a larger channel that is straight or widens downward, the case especially on ridges. On the tops of the pillars are forms that are often similar to open funnels with gently sloping sides covered with small channels, while larger channels occur on the steeper walls below them. This is the most frequent form found on rock tops in general, not just in the Lunan stone forests. For the moment, I judge that the funnels are the legacy of subcutaneous channels. That is, semicircular subcutaneous channels wider at the top most frequently indent the stone teeth. The channels also occur due to the outflow of water from only slightly inclined and shallow channels that occurred on more extensive tops of pillars below small channels (Fig. 1.5.11.). The walls of the upper sections of pillars are thus entirely dissected with small channels and channels with only smaller or larger ridges between them. On stocky tops of pillars there are frequent subcutaneous recesses, although solution pans prevail after rapid denuding. Channels occur due to the outflow of water from either. Larger and deeper channels on the tops of the pillars widen in a funnel-like manner. The form of individual large and small channels of different sizes is also the consequence of the composition and joint frequency of the rock on which they occur and the inclination of the surface into which they indent. Their form is therefore also the legacy of the subcutaneous dissolving of the rock. Channels with diameters of one to fifty centimeters also occur as walls of deepening solution pans or subcutaneous recesses. They end with rocky jags that are the re-

mains of the bottoms of the solution pans. According to Habič (1980), the deep channels with sharp edges also found on fallen pillars developed in a more humid climate with heavy downpours. Large channels in the Naigu stone forest are more shallow and rounded, and their ridges are less sharp. Smaller channels are not often found on this characteristically composed rock. In the Lao Hei Gin stone forest where small channels are indistinct or even non-existent due to the composition of the rock or its decay, individual channels full of small cracks occur along vertical fissures.

The second subgroup of rock forms hollowed by rainwater trickling down the walls of pillars are various **small and large recesses** on vertical and overhanging walls where the rock is unevenly composed or fissured on inclined surfaces and **ceiling points** on the overhangs. I have previously described these forms as they occur on cave walls (Slabe 1995). They occur due to the way water trickles on rough or fissured rock. In most cases, evenly fine-grained rock that has not been reshaped by other factors is almost vertical and relatively smooth (Slabe 1990). Researchers who have described recesses (Sweeting 1995; Chen Zhi Ping et al. 1983) classify them as small (with only one-centimeter diameters), medium (five to fifteen centimeters in diameter), and large (with diameters reaching thirty centimeters). Their size probably reflects the speed of the water flowing down the rock and its hydraulic characteristics (Sweeting 1995). I have attempted to supplement their observations and more accurately define the origin, size, and shape of recesses. Small and large recesses also dissect the walls of large and small channels where the recesses are of the same width. These are often smaller rock forms occurring inside larger forms.

According to their size, I divide them into small recesses with diameters from 0.5 to five centimeters and large recesses most frequently having diameters between five and ten centimeters. We can learn more about them from their division according to the manner of occurrence and shaping. Small and large recesses of this type occur

due to the trickling of water down rough rock surfaces with varying inclinations. Their development, especially of the smallest, is therefore determined by the relatively even fine-grained composition of the rock down which the water trickles swirling along the rough surface. Small channels on vertical walls are dissected by short small recesses of the same width. Their edges are therefore jagged. Small recesses are also found on the walls of vertical channels and linked in columns. They are similarly arranged on the ridges of pillars. Their arrangement into lines indicates smaller quantities of water trickling down the vertical rock. In narrow cracks between pillars, small recesses on the projecting parts of the rock can be also obliquely oblong, one centimeter wide and three centimeters long, indicating a strong air current that influences the direction of the trickling water. There are small recesses on overhanging walls that are deeper on the flowing side and joined in a network. Most frequently, they are 0.5 centimeters long and one centimeter wide. They are relatively deep and therefore have distinct edges. On the overhangs, the recesses are smaller below channels where a larger quantity of water flows faster with diameters up to one centimeter, while on the surrounding overhanging surface of the same inclination, they can be larger with diameters reaching three to five centimeters. On the ceiling, small recesses pass into ceiling points. These usually have a triangular cross section with rounded tops. They occur due to the uneven dissolving of the grained rock under a thin layer of water flowing across the ceiling. The water accumulates on particles of rock protruding from the ceiling, but because it is less corrosion-effective, the distinction between the ceiling points and the small recesses between them increases (Slabe 1995, 79). Characteristic small recesses occur along tiny vertical fissures. They usually have a teardrop shape (Slabe 1995, 97).

The walls above horizontal bedding planes are dissected in a characteristic semi-kettle fashion. The large recesses are three to twenty centimeters in diameter. Smaller

ones are hemispherical, while larger ones have flat, circular bottoms constituting the upper layer of the lower bed. Above the bottom is an overhanging wall. Large recesses are usually teardrop shapes hollowed into the wall and composed of small recesses that occurred due to the trickling of water toward the bedding plane. Large recesses grow from the bottom up and often occur side by side.

The largest recesses, up to thirty centimeters wide, occur on overhanging walls and were, as I conclude for the moment, formed at the contact with fine-grained sediment and soil surrounding carbonate rock, and are therefore not the consequence of rainwater trickling down the overhanging walls of the pillars.

The occurrence of small and large recesses is determined particularly by the grainy composition, joint frequency, and stratification of the rock, while their size and shape is influenced by the different quantities of water that trickle down the surface of rock of different inclinations at various speeds. On vertical and inclined rock surfaces, smaller amounts of water unite into streams, while small and large recesses and ceiling points develop on overhanging rock surfaces due to the characteristic gravitational spreading of the water. According to research done so far, it does not appear that the size of the small and large recesses is only the trace of the speed of water over rough surfaces (Sweeting 1995, 127) or that large recesses are just a variation of smaller ones, as is the case in caves where streams of water flow over different rocks and hollow out scallops (Slabe 1995).

I believe that the largest recesses occurring on the overhanging walls of pillars were formed under fine-grained sediment and soil.

On the pillars, there are also various **solution pans**. These are small depressions formed by rainwater on horizontal or gently sloped surfaces of the rock. They range from one centimeter to one meter and more in diameter and can be equally deep. The smallest, up to ten centimeters in diameter, are usually hemispherical with mostly flat bottoms. They often occur side by side with

thin rims between them. The largest solution pans occur along fissures between pillars, and their forms are dissected accordingly.

Solution pans are frequently most distinct on the tops of lower formerly covered pillars that were recently denuded. They were covered with soil and vegetation, and the pillars retained horizontal tops. Subcutaneous recesses therefore in most cases developed into solution pans. The development of subcutaneous recesses into solution pans was also identified by Gams (1971, 32) and Zhang Shouyue (1997, 79). On the walls of such pillars, the previously described subcutaneous channels formed under the soil also occur.

In the Lao Hei Gin and the Naigu stone forests, the solution pans have various forms and their edges are jagged as a result of the properties of the rock. In the Lao Hei Gin stone forest, solution pans develop from small recesses occurring under the vegetation, as the development of solution pans is usually described (Perna 1996, 393). Small solution pans up to ten centimeters wide and two to three centimeters deep on the tops of the pillars developed in lenses of more rapidly dissolving rock. Solution pans on various rock have been described by Forti (1972).

Deepening solution pans and subcutaneous recesses often occur on the walls of pillars, and above them are channels that are actually their former walls. Such solution pans can also be small, only one centimeter in diameter. They look like the bottoms of small channels of different lengths and therefore can be found at various heights of the wall.

Algae and soil are often found in solution pans, which accelerates their growth. This is also proven by the quantity of dissolved limestone which is higher in solution pans (Sweeting 1995). The contents of dissolved carbonates in the water in solution pans and the change during rain has been studied by J. Kogovšek (chapter 1.6.).

The properties of the rock, particularly its composition and joint frequency, have a distinct impact on rock relief hollowed by rainwater and on its **surface**.

The surface of distinctly unevenly composed rock is rough, while the surface of fissured rock is angular due to fine crumbling. On distinctly rough rock surfaces, there are none of the characteristic described forms hollowed by rainwater that are smaller than the constituent parts of the rock or are their traces of irregular forms. This is especially true of dolomite or dolomitized carbonate rock and limestone with chert. Small channels therefore usually do not occur, although channels of medium size occur on more finely rough surfaces. Large channels, apparently originally subcutaneous, are relatively shallow and of irregular form and are found on the roughest surfaces. Ring-like solution hollows (Chen Zhi Ping et al. 1983) often occur around the bulbs of chert. In the Naigu stone forest, dissected solution pans occur on the tops of pillars with relatively wide and flat tops, while indistinct irregular small channels are found only in the sections of the most evenly grained rock. The tops of the small channels are made of the bulbs of slowly soluble rock. The majority of the rock surface is relatively coarsely rough due to the composition of the dolomite limestone (Ford et al. 1997). Differences in sedimentation, mostly bedding planes, are reflected in the rock relief.

I classify the roughness of the rock surface in the Naigu stone forest into three form varieties. From the surface of pointed tops in the middle part of the forest, relatively densely distributed oblong points protrude, one to three centimeters long. On such rock, only medium and large channels occurred, while small channels only occurred on individual sections. In the lower parts of the pillars, »bulbs« protrude from the rock. The bulbs, whose surface measures ten and more square centimeters, are rarely pointed and protrude up to three centimeters from the rock. Between them are large surfaces of the basic rock plane. The surface of protuberances and the rock between them is rough. Larger notches indent the protuberances, and smaller recesses whose diameter reaches at most one centimeter are found in the rock between them. Thinner dissected plates also pro-

trude from the rock surface. They reach up to ten square centimeters and in most cases are connected with narrow belts of protuberances. The proportion of the surface of the protuberances is equal to the proportion of the rock between them. The surface of the protuberance is dissected by small recesses up to one centimeter wide. Ford, Salomon, and Williams (1997, 115) believe that the protuberances also occurred through recrystallization around small holes that were probably filled with gypsum originally. M. Knez states, while studying the pillars, that roughness of the rock is controlled by being strongly tectonically broken, recrystallized and dolomitized.

Rock surface formed under vegetation on the pillars of the stone forests

Rock surface under vegetation and a thinner layer of soil is of varying roughness, and subcutaneous small recesses and small channels are found under somewhat thicker layers of soil.

The rock below compact vegetation and thinner or only patchy soil is often corroded into forms dictated by the composition, by the way the rock has been crushed, and the stratification of the rock. Up to two centimeter wide, in spots only slightly deeper, oblong small notches reflect the diverse stratification of the rock and bedding planes. Finely and densely crushed rock is dissected by a network of equally-sized small notches (Fig. 1.5.12.). Often, only the broader tops of the shorter pillars or their lower parts and the notches along bedding planes are formed like this, in short, formerly overgrown parts. Above the described dissections, small and large channels and small recesses dominate if the rainwater is able to flow across the rock relatively unhindered. The same rock is either smooth or dissected with rounded small recesses if it was reshaped under the soil.

The rock surface under the vegetation is often dissected by one millimeter small recesses. On the tops of pillars in the Lao Hei Gin stone forest, small recesses developed under moss with diameters of one to



Fig. 1.5.12. Rock surface formed under vegetation (Photo T. Slabe)

ten centimeters and up to five centimeters deep. A large proportion of the pillars are covered by lichen and moss, the dark surface of the Naigu stone forest is the consequence of algae on the rock (Ford et al. 1997, 114), and the rock surface is therefore characteristically finely corroded (Slabe 1995). Moses and Viles (1996) establish the importance of biologically created nanomorphology, but in spite of the fact that small recesses develop under lichen, rain still decisively shapes the rock. Fiol, Fornós and Ginés (1996) draw attention to the great importance of the mechanical removal of larger pieces of rock isolated by biocorrosion under the algae that covers the small channels.

Small and densely distributed subcutaneous recesses and subcutaneous channels (described among the subcutaneous rock forms) developed under the vegetation and soil. Biocorrosion also accelerates the development of solution pans described with the forms hollowed by rainwater.

Channels formed due to the draining of water from subcutaneous recesses on the tops and gently sloping parts of the pillars and strongly corroded rock surfaces indicate the considerable importance of the long-lasting covering of the rock by a thin layer of soil and vegetation for the formation of the rock relief.

Conclusion

In the rock relief of pillars in the stone forests, there are crisscrossed traces of the original shaping of the rock under the soil and sediment, marks indicating the lowering of level of soil and sediment, and traces of later more distinct reshaping of the pillars by rainwater, largely, of course, on the tops. This type of rock relief is best seen on the pillars in the Shilin Central Forest, that is, on relatively evenly composed carbonate rock. With the lowering of the level of the sediment and soil surrounding the carbonate rock, the original subcutaneous rock relief of the stone forest pillars has been in some places more and in others less effectively reshaped by rainwater.

Subcutaneous rock forms are divided into three types. The first rock forms occur under sediment and soil, the second occur at the level of sediment and soil, and the last occur under thin layers of soil that covers the rock in places. Through the pillars, subcutaneous tubes of various sizes occurred along fissures or bedding planes under the ground. Distinct subcutaneous forms testify to the efficient dissolving of carbonate rock under the ground. Below sediment and soil, larger and straight as well as smaller and winding subcutaneous channels occurred along the contact of the soil and rock due to the flow of water. Large subcutaneous recesses occur on vertical or overhanging walls because the rock is surrounded by porous sediment and the contact between them is more permeable. Also the frequent overhanging narrowing of pillars below their tops is the consequence of the more rapid dissolving of carbonate rock under the soil and sediment. At long-lasting levels of soil and sediment, horizontal subcutaneous wall notches and subcutaneous half-bells formed due to rainwater trickling steadily down the walls of the pillars and then slowly flowing along the contact with the soil. Subcutaneous small recesses and channels occurred under thin layers of soil due to the percolating of water through it.

Small channels formed on the sharp tops, as a rule occurring in funnel-shaped notches that developed from the beginnings of former under-sediment large channels. On steep walls, they combine into large channels. Large channels also occur below funnel-shaped notches and when the water drains from subcutaneous recesses and solution pans. Vertical and overhanging walls are also dissected by various small recesses hollowed by rainwater and on the most overhanging sections by ceiling points. Solution pans occur on gently sloping sections. The progressive reshaping of the rock relief is also indicated by composed, originally subcutaneous channels whose upper parts have been reshaped by rainwater and whose lower parts continue into artificially opened and wider subcutaneous channels. The contact at a long-last-

ing level of soil and sediment is bell-shaped and the wall is overhanging.

That the pillars were overgrown is best seen on broader tops, on gently sloping walls, and just above the ground. Rock surfaces that were overgrown are characteristically finely corroded.

The rock relief is most easily readable on the pillars in the Shilin Central Forest, that is, on quite evenly composed carbonate rock. The varieties of characteristic rock relief and, of course, the shapes of the pillars and their development were dictated primarily by the properties of the rock. On the tops of the Naigu stone forest, unique small channels occurred due to the composition of the rock, while on the tops of the Lao Hei Gin stone forest, they occurred due to tiny fissures. The rock surface of the pillars in the Naigu stone forest is rough, with large surfaces of slower soluble parts of the rock protruding from it. Even the channels hollowed by rainwater mainly occurred only along vertical fissures. The rims of solution pans are strongly jagged. Subcutaneous forms are less distinct and dissected. Along the bedding planes in the Naigu stone forest and in the middle part of the pillars in the Lao Hei Gin stone forest where the rock is most porous, large tubes occurred that penetrate the pillars.

Under the ground, fissured carbonate rock is shaped into subcutaneous karren (Fig. 1.2.2.). Between the cracks are rock teeth and smaller pillars with characteristic rock relief containing subcutaneous rock forms. Subcutaneous channels with semicircular or omega-shaped cross sections and subcutaneous recesses first occur under the soil and sediment. These forms can also crisscross the tops of subcutaneous teeth. With the lowering of the level of the soil, in most cases the result of the development of an underground water network below the forest, protuberances emerge and are further reshaped by rainwater. From the rounded channels and cracks cutting across the tops of subcutaneous teeth, sharp funnel-shaped

notches begin to form along with small channels on them. As the level of sediment and soil lowers, the reshaping continues downwards. The rock forms hollowed by rainwater are originally determined by the initial subcutaneous forms.

The rock relief reveals the way the stone forests were formed and presents the course of their development. Rock forms that develop at the level of soil reflect the duration of the soil level at particular points in time. Rock forms of this type captured in the walls therefore reveal periods of the intermittent lowering of the level of the soil. We must also be aware of man's impact on the stone forests, especially in those open for tourists where the cracks between the pillars have been deepened in many places. I also link the rock relief on the pillars with the rock relief in the caves below the forest. Here too we find characteristic traces of distinct changes in their permeability. Signs of fast water flowing through the tunnels alternate with the filling of the caves with pebbles or fine-grained sediment over which above-sediment channels occurred. The flow of water through the caves in certain periods was small. I believe that the water also occasionally flowed on the surface between the stone pillars and that the level of sediment remained unchanged for long periods. In most places, the level of underground water below the forest is close to the surface, which means that more recent factors can quickly cover the traces of older factors. This type of comparison and reading of the rock relief as the traces of the development of the stone forest therefore calls for further in-depth research, more precise comparison of the levels of characteristic cave and surface rock forms, and comparison with other developmental indexes such as various sediments. I also plan to continue the research on the origin and development of the stone forests and their rock relief with laboratory tests using gypsum to verify many other hypotheses.

1.6. ROCK DISSOLUTION IN STONE FORESTS

Janja Kogovšek

In July 1996 we studied the precipitation and carbonate rock dissolution characteristics in Shilin stone forest and in Naigu stone forest in the vicinity of Lunan. The average annual precipitation is approximately 800 mm, the average relative humidity is 75 % and the average annual temperature is 15.6 °C. The annual amount of precipitation has been very variable through the years, although over 80 % of all annual precipitation occurs during the rainy season, roughly from June to October, during the period with higher temperatures.

We took and analysed rain samples repeatedly, we examined recent dissolution of stone blocks during rain and the dissolution in cups in Shilin stone forest and the intensity of carbonate rock dissolution by vertical movement of precipitation from the surface to the vadose zone into the underground Baiyun and Xinshidong caves in Naigu stone forest and into Jiuxiang cave.

Research Methodology

Samples of rain were taken in Shilin stone forest near the hotel and placed into polyethylene containers. We analysed them immediately. The samples for examining the dissolution of stone blocks in Shilin stone forest were taken from the base of the selected blocks, while it was raining. The percolated water in the caves was in most caves sampled directly from the cave ceiling. We measured larger discharges by using a stopwatch and a measure, and estimated smaller discharges by the quantity of water caught in a certain amount of time.

While we took samples in the field, we also measured the water temperature to the exactness of one tenth of a degree and the specific electric conductivity (SEC) to $1\mu\text{S}/\text{cm}$ (July 1996 with an LF 91 - WTW apparatus, September 1997 with LF 196) and also the pH of the samples (pH 90 - WTW apparatus).

The comparison and intercalibration of both conductivity meters indicated a fairly good correspondence. In the area of 150 to 250 $\mu\text{S}/\text{cm}$ we defined from 1 to 0 % excessively low numbers and in the area of 250 to 500 $\mu\text{S}/\text{cm}$ for 0 to 1 % excessively high numbers.

Carbonate, Ca and Mg content, as well as overall hardness were determined titrimetrically according to standard methods (Standard Methods of the Examination of Water and Wastewater 1992).

Rain composition

Yuan Daoxian (1991) described the following rain composition: pH, calcium, magnesium, sodium, and chlorides, sulphates, nitrates, and ammonium for some of the areas of China, but not for the Yunnan area. He studies the effect of the bedrock and the effect of human activities such as smoke and pollution caused by cement plants and stone-pits. He also states that the content of calcium in the rain is notably higher in karst areas, that is over 5 mg/l (or 12.5 mg CaCO_3/l) higher than in non-karst areas, where it is below 0.1 mg/l.

We took the first samples and made the first measurements of rain in Shilin stone

forest in July 1996. A total of 87 mm of rain fell from July 9th to 14th. The atmosphere was well washed on the evening of July 16th, when it started to rain again. We estimated that approximately 10 mm of rain fell before midnight, and by our measurements an additional 42 mm during the period from midnight to morning, which was when we took the first rain sample. The rain continued occasionally throughout the day and added up to 14 mm, which was when we took the second sample. Our measurements were in correspondence with those from Dakenyan precipitation station, according to their data 56.6 mm of rain fell on July 16th and 11 mm on July 17th, giving altogether 67.6 mm.

Light rain fell for the next time on the night between July 20th and 21st in the form of a slow drizzle. We measured 3.5 mm in Shilin stone forest, the Dakenyan station measured 5.5 mm. Somewhat more rain fell the following night, we measured 10 mm, and the Dakenyan station 26.5 mm. Observing the water table level while taking samples the following day confirmed to us that in Dakenyan, which is located at a distance of seven kilometres and at Shilin stone forest NE area more rain had fallen due to occasional local differences.

In all cases we took samples of rain from the time when it began to rain until it stopped. This way I analysed the composite rain samples. The results of the measurements are presented in Table 1.6.1. The atmospheric temperature during the day and during the night altered only slightly around the value of 20 °C. The SEC of the samples was in reciprocal proportion to the amount of rain. This seems logi-

cal due to the fact that air pollution was washed from the atmosphere by light or heavy rain and smaller or larger dilution effects were caused. When the SEC and pH values were low (on the night between July 21st and 22nd) the rain contained only 0.12 meq/l (6 mg CaCO₃/l) of calcium and magnesium. During the drizzle on July 20th, we measured a slightly higher SEC and pH, which leads us to conclude that the value of carbonates was probably also higher at that time.

On our next visit on September 25th 1997 there was drizzle, so that only 7 mm of rain fell during the day. The rainfall was heavier in the afternoon, and continued at intervals throughout the next day. The temperatures dropped sharply, we measured only 14 °C. 25 mm of rain had fallen in all, and we analysed it (Table 1.6.1.). The rain contained 0.2 meq/l of calcium and magnesium (10 mg CaCO₃/l). It rained for the following two days with occasional interruptions, during this period 10 mm of rain fell containing 14 mg CaCO₃/l.

Measurements and analyses of precipitation in Postojna in the period from 1985 to 1987 indicated a variation of the SEC between 10 and 285 µS/cm, the average value being 45 µS/cm. Rain with a higher SEC, containing more calcium and carbonates, also had higher pH values. We assigned this to the Borea wind, that is to the dissolution of carbonate particles in the air. The average values of the sum of calcium and magnesium in the rain was 6.8 mg CaCO₃/l and the average pH 4.5. We occasionally recorded noticeably higher values of sulphates, nitrates and chlorides (Kogovšek & Kranjc 1988).

Time of sampling	Quantity of rain	T	SEC	pH	Carbonates	Ca+Mg
	mm	°C	µS/cm		meq/l	meq/l
16.-17.7.96	42	19.5	29	7.15	0.12	0.06
17.7.96	14	18.5	44	7.95		
20.-21.7.96	3.5	20.5	76	8.24		
21.-22.7.96	10	19.0	44	7.18		0.12
25.-26.9.97	25	14.0	17	7.12	0.12	0.20
26.-28.9.97	10	20.5		7.72		0.28

Table 1.6.1. The characteristics of rain in Shilin stone forest.

Carbonate rock dissolution in Shilin stone forest

Habič (1980) compares Shilin stone forest to the rilled surface of the Dinaric karst except that in Stone forest it exists in a larger scale. The rilled weathered surface is formed in thick-layered gently sloping Early Permian limestone, shaped by rainwater as well as its lithological composition, and the layers and fractures in the rock. Karst water is near the surface and thus floods part of the area between the rock ceilings. The lower parts of columns become dissolved to a higher degree because they come into contact with soil, and this type of corrosion probably took place beneath an argilliferous cover. The dissolution of columns in Shilin stone forest is most intense in the more exposed areas, where the rainwater is channelled. Some light-coloured, yellow-brown areas that remained untouched by the rainwater are noticeable.

Song Linhua (1986) describes the composition of the Shilin stone forest limestone with the maximum thickness of the layer being 30 m, and the main conditions for the development of stone forests. These are thick and pure limestone, an only slight sloping of the layer (maximum 15°), a web of vertical fractures, a non-homogeneous cover of soil, and soil that is damp and has a high CO₂ content.

Yuan Daoxian (1991) described some general characteristics of limestone and dolomite in Yunnan. For the area of Kunming, he established a lower aridness index due to the fact that more rainfall combined with high temperatures and CO₂ content in the soil causes increased limestone dissolution. The speed of dissolution of limestone covered by soil is twice as fast compared to the rock above the surface that is not covered by soil. The measurements we made in Stone Forest confirm this.

Thickening of small solution basins or dishes-kamenitzas

M.M. Sweeting (1995) described small solution basins or dishes-kamenitzas on the

surface in Shilin stone forest, up to 1 m long and deep, and still deepening.

During our visit to Shilin stone forest in July, I noticed that the small solution basins and dishes-kamenitzas were filled up to a different degree in the morning hours following occasional drizzle overnight. The measurements of temperature, SEC and pH of the water in them revealed to what degree the water dissolved the carbonate rock. Most of the small solution basins had fallen leaves and other dead vegetation at their bottom, and those near the tourist path also contained garbage, all of this affecting dissolution. Some of the small solution basins were overgrown, the thin cover of soil and vegetation holding quite a lot of water, this also being a form of carbonate dissolution in small solution basins. We took some successive samples for the chosen small solution basins A and B to establish the dissolution of the rock in the given conditions. Solution basin A was not overgrown, it was 50 cm wide and only a few centimetres deep. During the second sampling the water was not as deep and the water was filled with tiny larvae. Solution basin B was not overgrown, and was larger in length (over 1 m), and the depth of the deepest part was 25 cm. The results of the measurement are set out in Table 1.6.2.

The highest dissolution, that is the highest carbonate content measured in the solution water basins, was 2.84 meq/l, which adds up to 142 mg CaCO₃/l, although most likely this is not the highest value. We measured the value of 3.68 meq/l due to dissolution on rock columns. After successive observations of the solution basin B, we noticed a proportionate increase of the concentration of dissolved rock (measurements of SEC) with the lowering of the water surface (Fig. 1.6.1.), when evaporation is present, causing concentrating of the solution also due to this effect. During a noticeable drop in temperatures in Autumn 1997, we measured a notably lower SEC, and this indicates the effect of temperature. We did not measure the humidity, although we assume that it was relatively high. The Figure 1.6.2. shows dependence between



Fig. 1.6.3. Solution basins in Shilin stone forest. (Photo J. Kogovšek)

Dissolution of rock columns in Shilin stone forest

During rainfall the precipitation water falls on up to 40 m high bare columns, trickles down them and is accumulated at their base on argilliferous soil (Fig. 1.6.4.). As the rain comes into contact with the rock, it begins to dissolve it. During the rainfall on July 21st and 22nd 1996 I managed to take a few samples of this water and analyse it.

On the night between July 20th and 21st 1996 only 3.5 mm of rain fell in the form of drizzle. The water trickled slowly down the columns, causing the rate of dissolution (the amount of dissolved limestone in a certain quantity of rainwater) to be higher than that measured the following night during which the rain was more intensive and amounted to 10 mm of rainfall. Early in the morning of July 21st I took a sample of water in the pool formed beneath a 15 m block – point G. On July 22nd I took a sample beneath the 7 m high block at point H. For comparison I took a sample of water dripping directly from the block (H*), but it did



Fig. 1.6.4. Rock columns in Shilin stone forest. (Photo J. Kogovšek)

Place	Length m	Precipitations mm	Temperature °C	SEC μS/cm	pH	Carbonates meq/l	Ca+Mg meq/l	Delta SEC μS/cm
G	15	3.5	19.2	428	8.02	3.68	3.92	352
		10	19.9	325	7.83	2.84	3.04	281
		25	14.5	271	7.8	1.68	2.31	254
H	7	10	18.8	232	8.44	2.08	2.24	188
H		25	12.1	186	8.52	1.82	1.92	169
H*	7	10	19.1	230	8.56	2.00	2.24	186

Table 1.6.3. Measurements of stone block dissolution taken at their base at points G and H.

not differ from the one in the pool at its base. The characteristics of the rainwater have already been described. All the measurements and analyses made at the bases of blocks G and H are presented in Table 1.6.3. The non-carbonate hardness was 7% in all cases. The content of dissolved carbonates as well as the total hardness are proportionate to the SEC. The content of magnesium is low, below 0.1 meq/l.

During the drizzle each litre of water on the 15 m high block (point G) dissolved 190 mg of CaCO_3 (3.8 meq/l), and during heavier rainfall only 105 mg CaCO_3 (2.1 meq/l). We presumed that the drizzle contained 6 mg CaCO_3 , as this was the value obtained by measurements the following night.

In half the distance at point H 106 mg CaCO_3 /l (2.12 meq/l) was dissolved. This means that 1 litre of rain dissolved one fourth less limestone than at point G. The proportion of dissolved limestone in one litre of water taken from the base of the block was over 25% higher than during heavy rainfall. However, the estimation of the dissolution effect in heavy rainfall based on these measurements is, due to the almost three times greater amount of rainwater, over two times higher.

Similar to the situation for dissolution elsewhere in karst landscapes, we established that dissolution of carbonate rock depends primarily on the amount of water. Gams (1980) and Habič (1968) studied the interdependence of mass and volume discharge for karst flows in the Slovenian karst. Flow in the vadose zone (Kogovšek 1986) indicated a linear correlation between dissolved and removed carbonates and the volume of the water in the flow, that is from precipitation.

Stone block dissolution after the removal of soil and vegetation in Shilin stone forest depends on factors such as the amount of rainfall, rain composition and temperature, and rain intensity, which affects the thickness of the water film on the carbonate blocks. The amount of limestone a certain amount of water will dissolve when it trickles down the block depends on the height of the block and/or the length of the path of the water, because the balance is not usually present when the water reaches the base of the block.

We can expect stronger dissolution effects during slow, light precipitation since the rate of dissolution reaches higher values. A high rate of dissolution is thus added

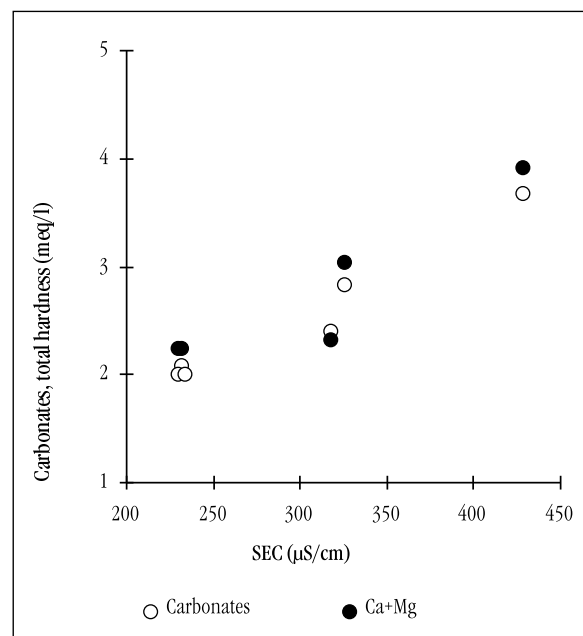


Fig. 1.6.5. Dissolution of columns in stone forest (Points G and H): SEC is proportionate to the content of carbonates and/or to the total hardness.

to the determining influence of the amount of precipitation on limestone dissolution.

Fig. 1.6.5. presents the constant and low non-carbonate hardness and linear correlation of SEC and carbonate and/or total hardness, without additional influence of vegetation and soil that could increase the effects of dissolution, although these probably affect only dissolution on soil-covered limestone.

Characteristics of percolated water in caves

Precipitation water percolates first through a thin or thick layer of soil with vegetation. If this is absent, it percolates directly through variously thick carbonate rock and appears in the form of percolated water in caves. All that takes place on the way to the cave is reflected in the composition of groundwater in the cave.

Carbonate rock dissolution is affected, aside from the composition and amount of rain, by the soil cover with its vegetation. To understand the influence of the soil cover, we took samples of the soil on the surface and determined the content of carbonates, organic carbon, and phosphates (Table 1.6.4.). To determine which components of precipitation can be rinsed from the soil, we occasionally soaked the ground samples into distilled water (5g in 500 ml for six days) and after spinning them, we determined the content of the following in

Sample	Carbonates	Organic C	P ₂ O ₅
	%	g/100g	mg/100g
Stone forest	0	0.39	24
P1- near Maoshuidong	1.08	1.7	48
P2 - near Guanyindong	0.8	1.4	28

Table 1.6.4. Soil analyses.

Sample	pH	Calcium	Magnesium	Silica	Chlorides	Nitrates	Phosphates
		mg/100g	mg/100g	mg/100g	mg/100g	mg/100g	mg/100g
Stone forest	6.65	50	3.6	170	5	9	1
P1- near Maoshuidong	6.3	20	1.2	78	5	2.2	0.2
P2 - near Guanyindong	8	8	2.4	99	5	11	0.4

Table 1.6.5. Some components of soil soluble in water.

the water solution: chlorides, nitrates, sulphates, silica, calcium, magnesium and pH. The results are presented in Table 1.6.5.

During our visit to the Baiyun, Xinchidong, Wayao and Jiuxiang caves in Yunnan, we took a number of samples of groundwater, carried out measurements of temperature, pH and SEC and some other analyses (Fig. 1.6.6.), which indicate basic groundwater characteristics in this part of the Chinese karst.

Yuan Daoxian (1991) established the carbonate hardness of groundwater in the Muyuanfu cave (Guilin) between 1.6 and 5.7 meq/l (100 - 350 mg HCO₃⁻/l), however we were not able to obtain any figures for Yunnan to verify our measurements.

Baiyun Cave

The Baiyun Cave is located in the Naigu stone forest. Ford et al. (1997) established that the basis of the Naigu stone forest is homogeneous grey limestone. Overlying it is a layer of approximately 1.5 m of medium layered massive dolomite limestone. Because the groundwater also reflects the composition of the rock through which it percolates, the chemical analyses of carbonate, calcium and magnesium content carried out outline the type of rock.

Percolation water

The ceiling in Baiyun cave is only a few meters high, yet it is several tens of meters thick. The cave is well encrusted due to numerous and small-scale drips, and in some places there are smaller trickles of percolated water. From the cave entrance to its end, a clear stream runs parallel to the tourist path. We visited the cave on July 18th



Fig. 1.6.6. Water samples analysis. (Photo J. Kogovšek)



Fig. 1.6.7. Sampling of percolation water at Point G in Baiyun cave. (Photo M. Knez)

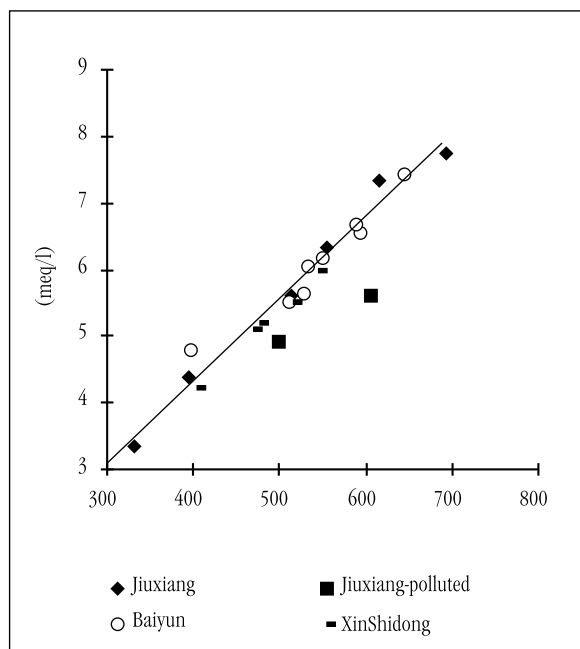


Fig. 1.6.8. Total hardness and SEC of percolation water.

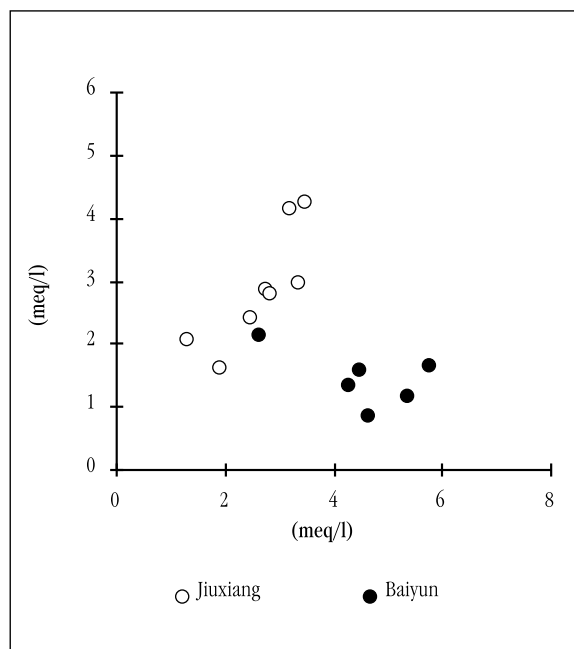


Fig. 1.6.9. Calcium and magnesium in percolation water.

1996, following two days of heavy rainfall which caused heavier discharge. A sample of the percolation water G-96 was taken

from the ceiling (Fig. 1.6.7.). The discharge of this tiny trickle amounted to 100 ml/min. The water travelled a little less than 1 m

Cave	Place	Dischar. ml/min	T °C	SEC μS/cm	pH	Carbonat. meq/l	Ca meq/l	Mg meq/l	Total h. meq/l	Ca/Mg	Noncar.h. meq/l
Jiuxiang	A - 97			331	8.40	3.36	1.28	2.07	3.35	0.6	
	B - 96	70	20.0	605	8.40	5.12	2.72	2.88	5.60	0.9	0.48
	B - 97		17.2	500	8.15	4.75	2.47	2.44	4.91	1.0	0.16
	C - 97	100	15.9	615	8.03	5.28	3.19	4.15	7.34	0.8	1.06
	D - 97			692	7.68	7.70	3.47	4.27	7.74	0.8	
	E - 96		17.5	514	7.80	5.04	2.80	2.80	5.60	1.0	0.56
	E - 97		15.9	556	7.70	5.75	3.35	2.99	6.34	1.1	0.59
	F - 97		15.2	394	8.40	4.21	1.88	1.62	4.39	1.2	0.18
Baiyun	G - 96	100	17.3	550	7.75	6.08			6.16		0.08
	G - 97	50	17.6	594	7.44	6.32	5.35	1.19	6.54	5.5	0.22
	H - 97	10		645	8.03	7.05	5.75	1.67	7.42	3.4	0.37
	I - 96	400	18.0	590	7.15	6.52			6.68		0.16
	I - 97	50	16.4	527	7.97	5.43	4.27	1.36	5.63	3.1	0.2
	J - 97	100	16.4	532	7.88	5.63	4.47	1.59	6.06	2.8	0.43
	K - 97			398		4.54	2.63	2.16	4.79	1.2	
	L - 97		16.8	511	7.63	5.59	4.63	0.88	5.51	5.3	
Xinshidong	M	3	20.4	405	8.45	4.00			4.24		0.24
	N	20		478	8.15	4.88			5.20		0.32
	O	10		515	8.40				5.52		
	P	80	19.8	545	7.53	5.76			6.00		0.24
	R		18.6	470	7.52				5.12		
Wayao	S		16.2	355	8.27	2.75	3.31	0.2	3.51		0.76
	T		15.9	461	8.11	3.77	4.59	0.16	4.75		0.98

Table 1.6.6. The characteristics of percolation water in Jiuxiang, Baiyun, Xinshidong and Wayao caves.

through the air and then fell onto an encrusted dripstone beside the tourist path, where evidence of flowstone deposition was noticeable. Characteristics of percolation water are presented in Table 1.6.6. and Figs. 1.6.8., 1.6.9.

During our visit in September 1997, as we recorded smaller discharge of percolation water along the cavern than in July 1996, we took a sample of the spurt G (G-97) again. It resulted in higher values of SEC and hardness, which is probably the reflection of the nature and lower discharge speed through the cavern ceiling. The ratio between the carbonate and magnesium content was 5.5. Only a few meters away we sampled dripping H-97 with the highest SEC and hardness of the percolation water in the cave. The carbonate hardness was 7.05 meq/l, the total hardness was 7.42 meq/l. The ratio between the carbonate and magnesium content was lower in comparison with trickle G, which indicates a higher proportion of magnesium dissolution when compared to calcium.

Flowstone gours

In July 1996 we took a sample of trickle I-96 located somewhat deeper in the cave, with the discharge of 400 ml/min. It dripped into a gour, then the water successively spilled over into some lower lying gours. SEC measurements indicated a notable decrease in values, and from this we concluded that there was a noticeable deposition of carbonates, that is growth of gours. In the next gour the SEC decreased by 13%, to the third by an additional 11%, and to the fourth by another 11%. So, in the distance of a few meters the SEC decreased by a whole 35%. Because there were no visible possible polluters above the cave, we concluded that the changes of the SEC are proportionate to the carbonate content. This assumption could, of course, be confirmed only by parallel analyses. This percolation water had the highest values for carbonate content (6.25 meq/l) and highest total hardness (6.68 meq/l) of all our measurements of percolation water made in July 1996 in



Fig. 1.6.10. Small gours in Baiyun cave - Point K. (Photo T. Slabe)

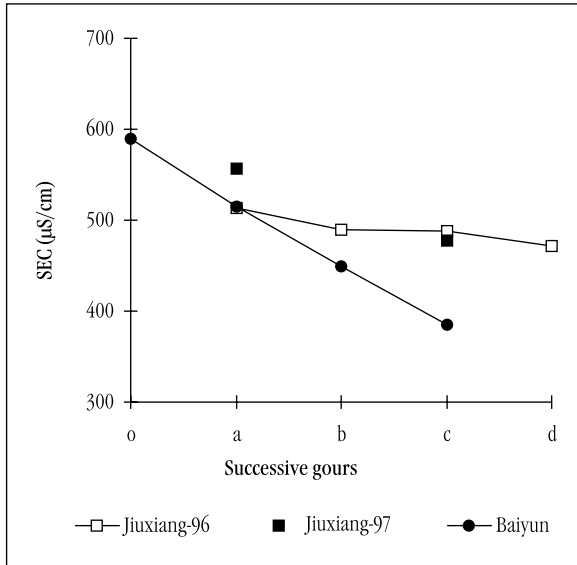


Fig. 1.6.11. Flowstone deposition in the gours in Baiyun cave and in small gours in Jiuxiang cave.

this area of the Yunnan karst. The non-carbonate hardness was very low, but we were unfortunately not able to determine the calcium content due to lack of adequate equipment.

In September 1997 this trickle was dripping slowly, and the gours were only partially filled with water, running from the stream, so we sampled the water of 1 meter distanced dripping with the discharge of approximately 50 ml/min I-97, which had a lower SEC value and lower hardness than

I-96. We sampled a 3 m distanced tiny spurt with a discharge of 100 ml/min and somewhat higher hardness than the dripping I-97. We conclude that they were the reflection of a different type of percolation. Both trickles had a lower calcium/magnesium ratio, similar to the trickle H.

In September 1997 we took samples of water in smaller gours in the beginning of the cave at point K (Fig. 1.6.10.). Through successive gours the SEC gradually decreased from the first to the fourth gour, in total by 61 µS/cm. During this time, 56 mg CaCO₃ from 1 liter of water were deposited (Fig.1.6.11.). However, the carbonate content of the inflow water (4.54 meq/l) was relatively low, as the inflow water into the gours at point I, I_o-96 reached the value of 6.52 meq/l (Table 1.6.7.), and the inflow into the large gour in Jiuxiang cave (D-97) even 7.7 meq/l (Table 1.6.6.).

Stream

All percolation water in Baiyun cave was oversaturated and everywhere visible signs of fresh flowstone deposition due to the trickling of water were noticeable. The stream (L), which accompanies visitors alongside the tourist path from the beginning to the end of the cave, also has a high content of carbonates and calcium. The

Cave	Place	Dischar. ml/min	T °C	SEC µS/cm	pH	Carbonate meq/l	Ca meq/l	Mg meq/l	Total h. meq/l	Ca/Mg	Noncar. meq/l
Jiuxiang	Eo - 96		17.5	514	7.80	5.04	2.80	2.80	5.60	1.0	
	Ea - 96		17.8	489							
	Eb - 96		17.8	488							
	Ec - 96		18.0	472							
	Eo - 97		15.9	556	7.70	5.75	3.35	2.99	6.34	1.1	0.59
Baiyun	Eb - 97		15.7	477	8.24	4.9	2.35	2.84	5.19	0.8	0.29
	Io - 96	100	18.0	590	7.15	6.52			6.68		
	Ia - 96			515							
	Ib - 96			450							
	Ic - 96			385							
	Ko - 97			398		4.54	2.63	2.16	4.79	1.2	
	Ka - 97			385							
	Kb - 97			375							
Kc - 97			337		3.65	2.07	1.6	3.67	1.3		

Table 1.6.7. Flowstone deposition in the gours in Baiyun cave and in small gours in Jiuxiang cave (E).

content of magnesium is somewhat lower. The calcium/magnesium ratio is 5.3. The water does not contain solid soil cover particles, as was already established for other flows. I conclude that the stream is a heavier trickle of the discharge of percolation water. Its water is oversaturated and deposits flowstone, the SEC decreasing by $25 \mu\text{S}/\text{cm}$ over a distance of some 400 m through the cave. The cave managers appropriately led this water to the nearby stalagmite and into the flowstone gours at point I, which both remain without fresh water flow during the dry season. But they probably did not verify the content of the water beforehand. Already on the three meter distance to the stalagmite the SEC decreases by $42 \mu\text{S}/\text{cm}$, which means relatively rapid flowstone deposition.

The highest carbonate content in percolation water in the area of Slovenia was recorded in Karst caves, in Škocjanske jame cave as 6.3 meq/l and in Vilenica cave as 6.6 meq/l, though for dripping with discharge of just a few ml/min (Kogovšek 1984).

Xinshidong and Wayao caves

We explored Xinshidong cave, which is not open for tourists, located in Naigu stone forest on July 22nd.

The surface above the cave Xinshidong is covered with a thin layer of soil and visible rocks grown over with grass and thin bushes. The height of the cave ceiling is only to a few meters, and we noticed visible signs of the water level occasionally almost reaching it. Numerous small drips in the cave were probably caused by the heavy rainfall the previous night. The cave is located near the surface, as the ceiling is only 2 m thick at the entrance and approximately 10 m thick further into the cave.

We noticed numerous tiny drips with the discharge of a few ml/min and only a few larger ones. The largest discharge, 80 ml/min, came from the trickle P located in the deepest part of the cave (near Point 10 on Fig. 1.2.10.). Measurements and analyses indicated an increase of SEC, dissolved carbonate content and total hardness in the

direction from the entrance towards the end of the cave, that is with the increase of the cave ceiling thickness (Table 1.6.6., Fig. 1.6.12.). This means that on the thin parts of the ceiling saturation and/or oversaturation of percolation water does not occur.

Sample R (at Point 11) is water from a small lake in the lowest part of the cave, its characteristics reflect percolation water collecting on an impermeable bottom with fine sediments. Similar to the Jiuxiang and Baiyun caves, the percolation water also has a low non-carbonate hardness.

Similar characteristics of percolation water were measured in the Wayao cave, which is located in the direct vicinity of a road, which is a source of pollution. The percolation water, percolating through an approximately 3 m thick ceiling (S) reached lower hardness values than deeper in the cave where the ceiling is around 8 m thick (T). In both samples we noticed a lower non-carbonate hardness than with other percolation water, a higher content of chlorides and sulphates (Table 1.6.6.).

Chemical composition of all examined water in the area of Lunan

Fig. 1.6.13. indicates the dependency of SEC and carbonate content and total hard-

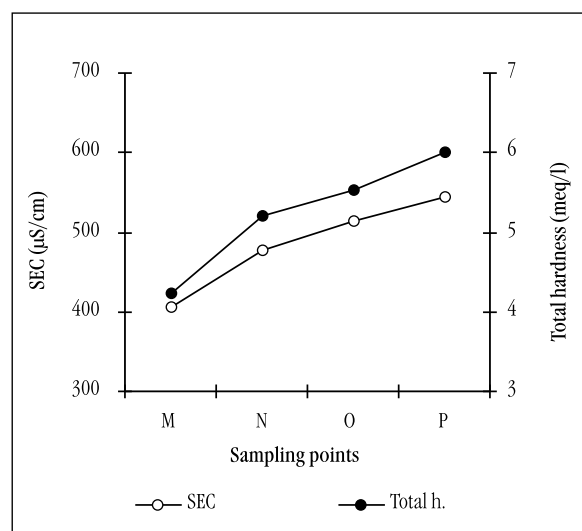


Fig. 1.6.12. Xinshidong cave: total water hardness and SEC increase with cave ceiling thickness.

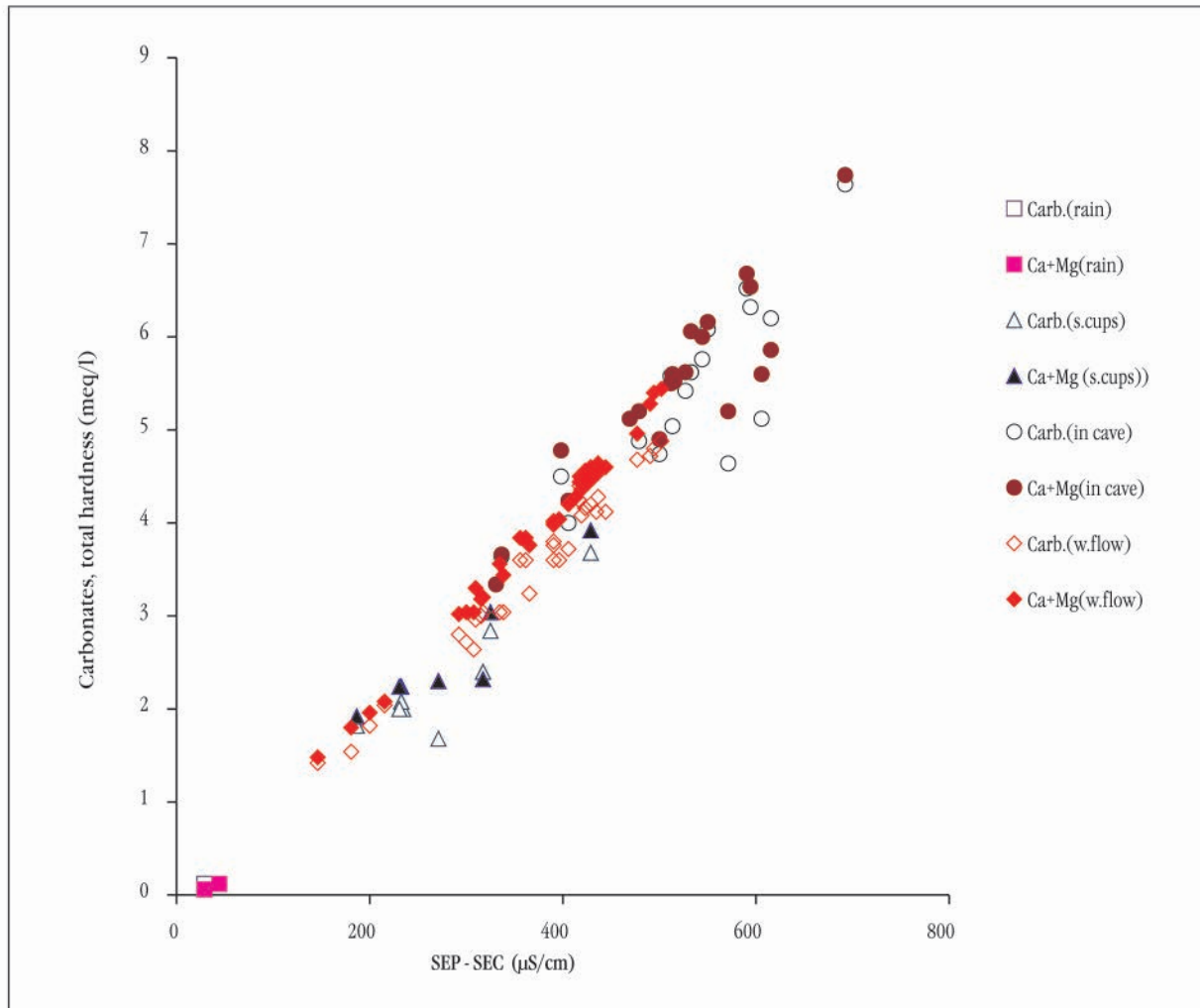


Fig. 1.6.13. Carbonate content and total hardness in dependance of the SEC in rainwater, in gours and at the base of columns in Shilin stone forest, in percolation water in the aforementioned caves and in groundwater flow.

ness of all performed measurements, of the rainwater as well as of water in gours and trickling water on columns in Shilin stone forest, percolation water on columns in Shilin stone forest, percolation water in caves and karst groundwater flows. There is a linear correlation between SEC and total hardness and carbonate content, even though dolomite water with a Ca/Mg ratio of 0.8 and water with a Ca/Mg ratio of 18 are present.

The percolation water in the larger chamber in Juxiang cave, which we assume is polluted, stands out. A somewhat larger difference between the total and carbonate hardness (non-carbonate hardness) was found for the groundwater flow at Point a to the spring of Dalongtan - 5.

Conclusive findings

Rainfall observation in the Shilin stone forest area in Yunnan showed that a large amount of precipitation may fall in a relatively intensive form (July 1997, 40 mm in 6 hours) or a slow rain, with the daily amount below 10 mm. The specific electric conductivity of the rainwater amounts from 17 to 76 $\mu\text{S}/\text{cm}$, pH from 7.1 to 8.25, the total calcium and magnesium content ranged from 3 to 24 $\text{mg CaCO}_3/\text{l}$. Yuan Daoxian (1991) states that the calcium content in rainwater in the Chinese karst is notably higher than in non-karst areas and exceeds 12.5 $\text{mg CaCO}_3/\text{l}$. The soil cover,

that is non-soluble components in it that can be rinsed by rain, contribute significantly to carbonate rock dissolution on overgrown karst. These are primarily silicates, nitrates and chlorides.

We sampled the percolation water (together 25 samples) in four caves in July and September in various hydrological conditions. Percolation water in the Jiuxiang cave reached the ratio of Ca/Mg from 0.6 to 1.2, similar to the Mai Tian river which submerges into it. The specific electric conductivity, which reflects the amount of dissolved substances, ranged from 331 to 692 $\mu\text{S}/\text{cm}$, the carbonate content was 3.36 to 7.7 meq/l and total hardness from 3.35 to 7.74 meq/l. The highest hardness value was recorded in percolation water filling the large gours in Jiuxiang cave in September in the period of high water levels. A higher value of magnesium in comparison with calcium was measured in it, which is something we have never measured in the Slovenian karst. Due to the fact that percolation water reaches its highest hardness values in the beginning of the season, similar to the spring water in this karst, we assume that we would have recorded additionally higher values if measurement was carried out in that period.

It is interesting that the water inflow to the gours in Škocjanske jame cave has the highest hardness of all water in the cave, that this flow is occasional and occurs only after precipitation, that it is abundant, and of long duration. However, the water in Škocjanske jame cave has low magnesium content, and the hardness is approximately 15% lower compared to the

water that flows to the large gours in the Jiuxiang cave.

The percolation water in Baiyun cave reflects a different rock composition than Jiuxiang cave the Ca/Mg ratio value ranges from 2.8 to 5.5. The water is oversaturated and deposits flowstone. In September 1997 discharges were lower than in July 1996. In September we measured higher values of hardness and specific electrical conductivity at point of comparison G. This probably reflects the predominance of the manner of percolation in conditions of the less filled trickle hinterland in comparison with seasonal variations. The seasonal variation of hardness could be verified only by more frequent measurements throughout the year. In Xinshidong cave we sampled water that had percolated through the 2 to approximately 10 m thick cave ceiling. Measurements confirmed the increase of hardness, that is the various rates of saturation or oversaturation of the water as proportionate to the increase of the ceiling thickness.

The measurements of flowstone deposition in gours in the Jiuxiang and Baiyun caves indicated that in the short distance through a few gours of approximately 3 m, 20% (56 mg CaCO_3) to 35% of the total carbonates is deposited from one litre of percolated water. The stream that runs through Baiyun cave also deposits flowstone, and is classified into percolation water in regard to its chemical composition. This is also the reason it is being used to fill gours and a nearby stalagmite, which both have a low inflow of percolation water. This is not possible in the case of the Mai Tian river in the Jiuxiang cave.

1.7. HYDROLOGICAL CHARACTERISTICS OF THE TIANSHENGAN AREA

Metka Petrič

Evaluation of the basic hydrological characteristics of the wider area of Tianshengan village in the north-eastern part of Lunan province was programmed as the basis for planning the tracing experiment, which was to give more accurate answers to questions concerning the groundwater flow regime in studied karst aquifer. The existing data concerning the hydrological conditions were completed by new obser-

vations in the field and analysis of precipitation measurement data and groundwater discharge.

Hydrological conditions

The hydrological scheme of the discussed area includes surface streams and lakes, large and small karst springs, and

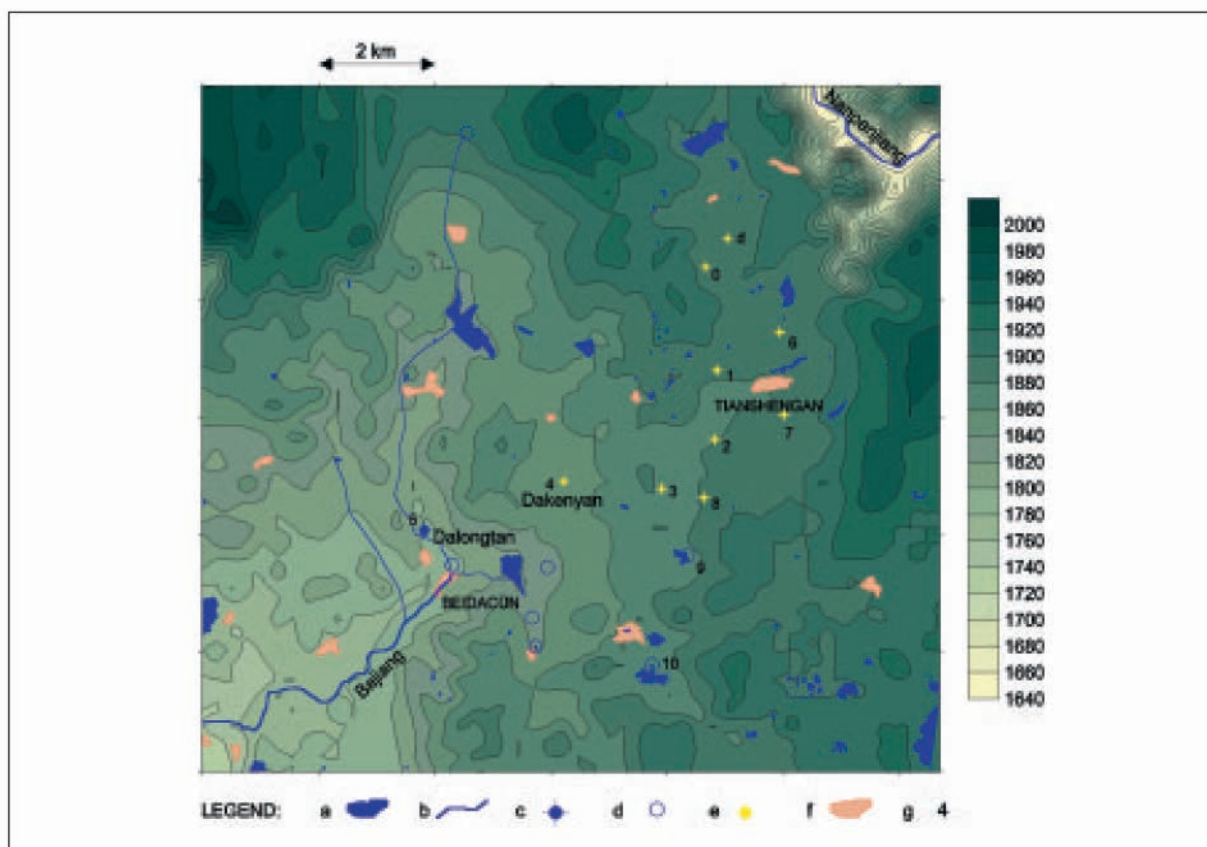


Fig. 1.7.1. Hydrological map of the Tianshengan area (a-lake, b-surface stream, c-bigger spring, d-smaller spring, e-shaft with underground water flow, f-village, g-mark of the hydrological object - see also chapter 1.9.).

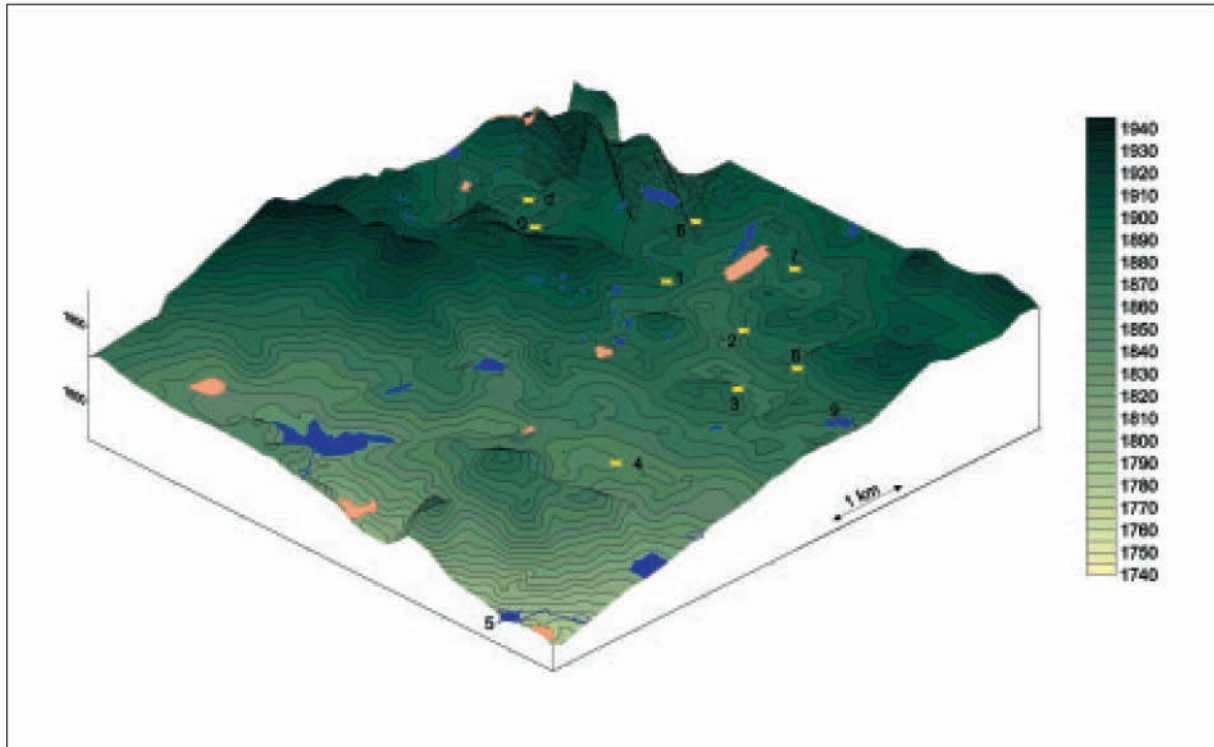


Fig. 1.7.2. Relief map of the tracing test area (legend on Fig. 1.7.1.).

groundwater streams (Figs. 1.7.1., 1.7.2.). The most important spring is Dalongtan at 1810 m above sea level with an estimated discharge from 0.24 to 4.6 m³/s (verbal account). Approximately 4 and 5 km to the south-east on the eastern part of the aquifer there are another two interesting springs: Changshuitang (marked as 9) 1866 m above sea level, and Xiniutang (marked as 10) 1863 m above sea level. During the time of our field research, it was not possible to evaluate discharge of the first spring as the water flows directly into a lake. The other one was evaluated during various hydrological conditions as 100 l/s to 1 m³/s. These values are not valid in extreme hydrological conditions, but for a shorter period of a medium water table level in July 1996. We have no data for discharge of other springs.

In the recharge area of Dalongtan, groundwater discharge is measured at the Dakenyan hydrological station located in a vertical shaft around 2.5 km north-east of the spring. The data for the period of August 1993 to August 1996 show discharges ranging from 12 l/s to 6.28 m³/s.



Fig. 1.7.3. Bajiang river before Dadieshui waterfall. (Photo J. Kogoušek)



*Fig. 1.7.4. Dadieshui waterfall.
(Photo J. Kogovšek)*

The surface stream which is formed by water from the Dalongtan spring, flows into Bajiang river (Fig. 1.7.3.). It runs over the more than 90 m high Dadieshui tufa waterfall (Fig. 1.7.4.). Bajiang river is one of the influxes of Nanpanjiang river and represents the erosion base of the discussed area. Also the water from other karst springs in the western part of the territory charge surface flows, which head towards the south or south-east and flow to Bajiang river. There are no surface flows in the eastern part.

Numerous lakes play a special role. As the whole area of study is cultivated, with rice, tobacco and corn fields predominating, the lakes are important primarily for the irrigation of agricultural land. The lakes have formed both as a natural accumulation of karst water and artificially by damming surface flows.

Groundwater is also used for irrigation. Pumps for supplying water to the irrigation systems are located in seven vertical shafts cutting the groundwater flow, although usually only three stations are active (Fig. 1.7.5.). All seven operate only at the end of



Fig. 1.7.5. Pumping station. (Photo A. Mihevc)



Fig. 1.7.6. Reservoir and irrigation channels. (Photo J. Kogovšek)

the dry season, when a large amount of water is needed for irrigating rice fields. The largest pump has the capacity of 50 l/s, the smallest 2.5 l/s. The pumped water is stored in open or closed reservoirs in higher locations, then the water is led by the force of gravity through channels to the lower-lying fields (Fig. 1.7.6.).

The source of recharge of the karst system is precipitation, with its distribution in wet and dry seasons. For the area of the high karst plateau of east Yunnan the average annual precipitation in the period 1980-1992 was 796 mm, of this 80% to 88% in the wet season. For the smaller area of the village of Tianshengan data are available for daily precipitation for the period of three years, from August 1993 to August 1996, measured at the precipitation station located in Dakenyan. The annual precipitation in 1994 and 1995 was 1133 mm and 727 mm. The characteristics of precipitation are discussed in detail later.

Hydrological analysis of measured values of daily precipitation and discharge

In the wider area of Tianshengan village the hydrological parameters are regularly measured at the Dakenyan station (Fig. 1.7.7.). In the vertical shaft, which cuts through the main groundwater flow approximately 2.5 km north-east of Dalongtan spring, there is a pump and nearby the gauging profile for underground discharge measurements which began to operate in August 1993. Discharges are measured four times daily. The procedure is such that the measurer reads the water level in profile off a measuring staff. Based on these figures he calculates the discharge from a pre-made discharge curve. The average daily value is obtained as the average of four measurements (at 6.00, 12.00, 18.00 and 24.00). At the location of Dakenyan, precipitation is also measured with a rain gauge once daily at 8 a.m. There are no data on the quality of



Fig. 1.7.7. Dakenyan measurement station. (Photo T. Slabe)

measurement instruments and accuracy of measurements, which is why an estimate of measurement error is not possible. In the further analysis, data supplied by the measurement stations were used.

The daily data on discharge and precipitation for the period of three years from August 1st 1993 to August 21st 1996 were collected (Fig. 1.7.8.). The division into wet and dry seasons is clear for discharge and precipitation. The wet season begins in May and ends in October, the rest of the year is the dry season. This distribution is repeated through the entire observation interval. Each wet - dry cycle lasts approximately one year. Precipitation of varying duration and intensity also occurs during the dry season, but during this time discharge in underground channels does not increase significantly. There is interesting data for the day of December 2nd 1994, when despite the daily precipitation quantity of 59 mm being the second largest measured, the discharge measured at Dakenyan station practically did not increase. We can say that be-

side the quantity and intensity of precipitation, the distribution of precipitation in time is a significant influence on the discharge curve.

The periods of high waters are short, the attained maximum is followed by a steep decrease and a longer period of middle and low waters. With the exception of extreme values, discharge is less than 2 m³/s. During the wet season, precipitation occurs in intervals of 1 to 3 days (exceptionally longer), and the periods without rainfall in between are 1 to 9 days long. The effect of pumping on discharge is not noticeable due to small capacities and occasional operation of individual pump stations. Extremely dry periods in the time when all seven stations are operating to irrigate fields are the exception.

The characteristic values of precipitation are presented in Table 1.7.1. for the observation period from August 1st 1993 to August 21st 1996. We can present the total annual value for this interval only for 1994 and 1995, but already these data point to a

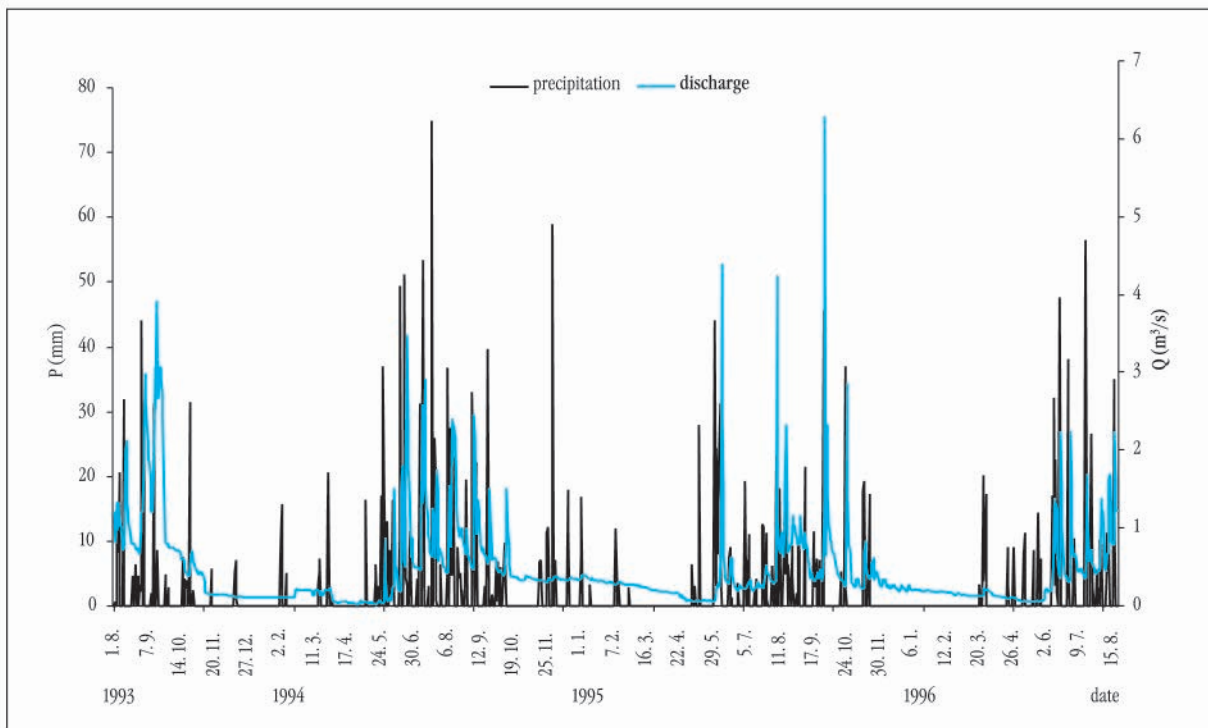


Fig. 1.7.8. Diagram of daily precipitation and discharge for the period of 1.8.1993 to 21.8.1996.

high variation of annual precipitation quantities, between 1133 and 727 mm. The maximum daily precipitation was 72 mm, measured in July 1994. The whole observation period was 1117 days long, and of these 902 days were without rainfall (283 days in 1994, and 301 days in 1995).

Discharge characteristics are described in the second part of the table. The value of 12 l/s is recorded as the minimal value. But there are some difficulties connected to measuring this parameter. The total quantity of pumped water from underground flow is, during extremely dry conditions, practically equal to discharge and there is

Precipitation	P_{annual} (mm)	P_{mean} (mm)	P_{max} (mm)	days with $P=0$ mm
1993-1996		2.4	75	902
1994	1133	3.1	75	283
1995	727	2.0	46	301
Discharges	Q_{min} (m ³ /s)	Q_{mean} (m ³ /s)	Q_{max} (m ³ /s)	
1993-1996	0.012	0.47	6.28	
1994	0.012	0.45	3.48	
1995	0.012	0.42	6.28	

Table 1.7.1. Characteristic values of precipitation and discharges

no water in the measurement profile at Dakenyan station. Discharges for this period are thus an estimation based on the quantity of pumped water. Determining the minimal value of 12 l/s is thus somewhat questionable and represents merely an approximate estimation. During the highest water table level in October 1995, 6.28 m³ of water per second flowed through the measurement profile. The discharge peak does not correspond in time to the precipitation peak, which was recorded in July 1994. A similar discordance can be noticed in comparing average recorded daily discharges and daily precipitation. The second parameter is not usually used to describe the characteristics of the time function of precipitation and is adopted here only because it makes comparing precipitation and discharge in the entire observation period possible. This comparison shows the average daily precipitation value in the period of August 1st 1993 to August 21st 1996 to be in between the value for 1994 and 1995. The mean discharge is higher in the entire observation interval than in both singular years. Again, it can be concluded that beside the quantity and intensity of precipita-

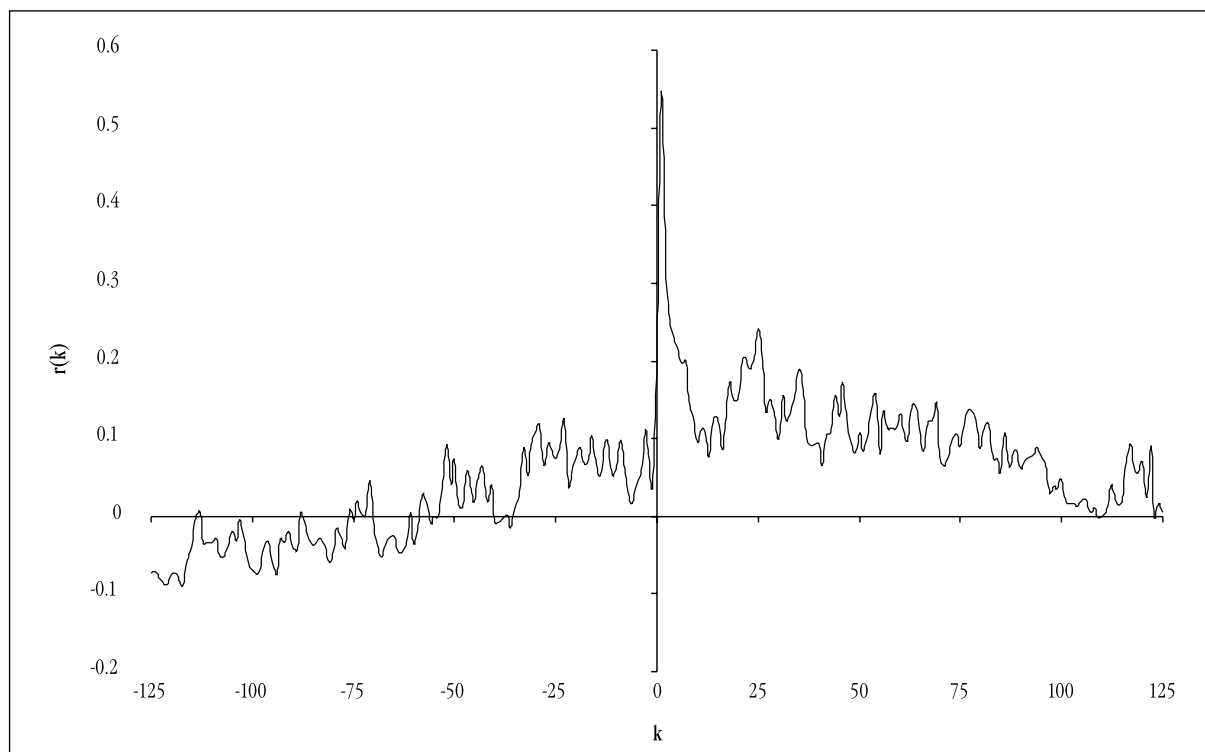


Fig. 1.7.9. Cross-correlogram.

tion, the distribution and consequently the state of water reserves in the karst aquifer has an important effect on groundwater discharge in subterranean channels.

To determine the interdependency of precipitation and discharge, I calculated the cross-correlogram of both time functions (Fig. 1.7.9.) with the Stochastos program by A. Mangin and D. D'Hulst (Mangin 1984). The calculations confirmed that the correlation coefficient is not high, reaching the maximum value 0.55 while taking into account the one-day retardation of the reaction of discharge to precipitation. The curve has a pointed form with a rapid dip of the correlation in the first days, then the curve slope decreases. The pointed form in the beginning indicates the existence of karst channels, which rapidly drain infiltrated precipitation. The decline of the curve slope in the second part points to the conservation of precipitation information over a longer period of time and a slower function of percolation through the fissure network.

Particularly are examined the characteristics of two hydrological years from May

1st 1994 to May 16th 1996. The hydrological years in the observed climatic conditions have a characteristic shape, which is periodically repeated in the wet season - dry season system (Fig.1.7.8.). The values of the comparison between annual precipitation and mean discharges for two hydrological years with special emphasis on the relations between dry and wet seasons are presented in Table 1.7.2.

Due to not having data concerning precipitation and discharge in the previous period, I cannot compare the characteristics of the two studied hydrological years with averages of many years. Based on data for two years, large amplitudes of annual

	P (mm)	Q_{mean} (m^3/s)
1.5.94 - 12.5.95	1125	0.48
13.5.95 - 16.5.96	760	0.38
wet season 1994	919	0.74
dry season 1994/95	196	0.30
wet season 1995	675	0.55
dry season 1995/96	95	0.18

Table 1.7.2. Comparison between precipitation and discharge for two hydrological years.

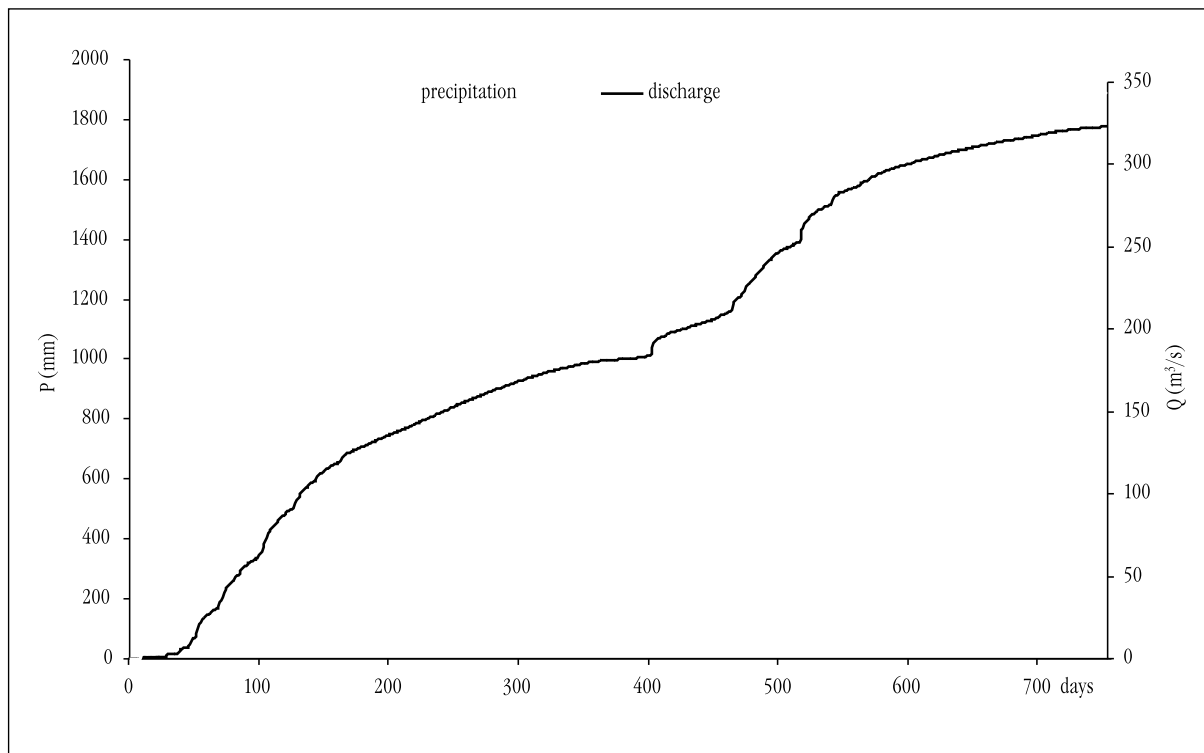


Fig. 1.7.10. Cumulative curves of precipitation and discharge for the period of two hydrological years.

values of both parameters can be presupposed. Following a relatively wet first year, the precipitation decreases by 32% and discharge by 21% the next year.

I also compared the dry and wet seasons of both years and found large differences. The dry season of 1994/1995 had approximately two times more precipitation as the dry season of 1995/1996, and the mean discharge was also approximately two times greater (0.30:0.18). The wet season of 1994 was significantly wetter than in 1995 ($P=919:675$ and $Q=0.74:0.55$). 1995 had marked discharge peaks, as the consequence of a less even precipitation distribution. Due to a relatively large amount of precipitation in the dry season in 1994/1995, the decrease in discharge is lesser in this period.

Based on data concerning daily discharge and precipitation in the period of the two hydrological years from May 1st 1994 to May 16th 1996 two cumulative curves were also drawn. They present the total volume of water drained from the basin, that is the total quantity of precipitation in the selected time interval (Fig.

1.7.10.). The distribution into dry and wet seasons is clearly visible from these curves. Inside of individual intervals the curve is relatively constant, and the curve incline is much greater for the wet than for the dry season.

Conclusions

A review of the basic hydrological characteristics of the Tianshengan area was conducted. The main drainage routes are subterranean channels near the surface. Groundwater runs toward karst springs, among which Dalongtan, located south-west of Beidacun village, is the most important.

Based on daily precipitation measurements at Dakenyan station and discharge in the ganging site at the same station, some other basic hydrological analyses were carried out. I compared records of daily data for the whole interval of measurements from August 1st 1993 to August 21st 1996 and for the period of two hydrological years, from May 1st 1994 to May 16th 1996. For precipitation and discharge, the divi-

sion into the wet and dry season is clearly visible. The wet season begins in May and finishes in the end of October, while the rest of the year is the dry season. This distribution is apparent also from the cumulative curves of precipitation and discharge.

From the interval of two hydrological years, the mean annual quantity of precipitation was 942 mm, the minimum discharge

12 l/s, the mean discharge $0.47 \text{ m}^3/\text{s}$ and the maximum discharge $6.28 \text{ m}^3/\text{s}$. We found a characteristic regime with a short duration of high discharge and longer periods of intermediate and low waters. The effect of precipitation on discharge is obvious, although the connection depends on numerous factors, which should be more accurately determined in this next phases of research.

1.8. PHYSICAL AND CHEMICAL CHARACTERISTICS OF GROUNDWATER OF TIANSHENGAN AREA (The wider area of the tracing experiments)

Janja Kogovšek

Prior to performing the first tracing experiment in the Lunan area we analysed the accessible karst water flows in the larger Tianshengan area. While taking samples, we determined temperature, specific electric conductivity (SEC) and pH (Figs 1.8.1. and 1.8.2.) in the field, and later on in the laboratory the content of carbonates, calcium and magnesium by procedures described in

chapter 1.6. We attempted to determine the main characteristics of the water, and similarities and differences which would indicate possible directions of groundwater movement, as an aid in planning the tracing experiment.

Water samples were taken from potential injection Points a, b, c and d (Quighuadong), in caves and in vertical shafts



*Fig. 1.8.1. Measurements of temperature, pH and SEC and water sampling.
(Photo J. Kogovšek)*

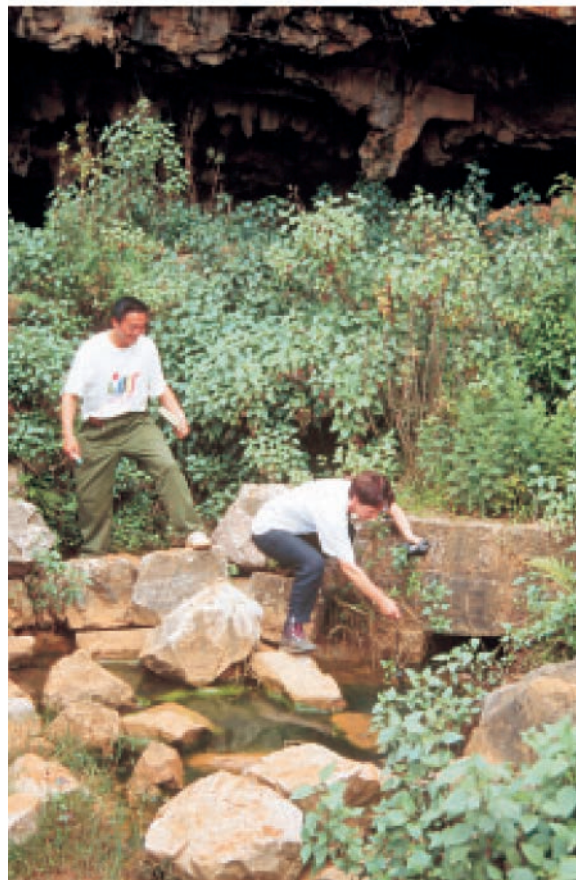


*Fig. 1.8.2. Water sampling at Point 7.
(Photo J. Kogovšek)*

Place	Date	H	T °C	SEC μS/cm	pH	Carbonates meq/l	Ca+Mg meq/l	Ca meq/l	Ca/Mg
a	15.7.96		17.7	490	7.2	4.72	5.28		
b	15.7.96		17.2	501	7.3	4.88	5.44	4.48	
c	15.7.96		17.4	494	7.4	4.80	5.40	4.48	
d	15.7.96		17.6	334	7.6	3.04	3.56	3.04	5.8
	26.9.97	high	13.1	181	7.4	1.54	1.80	1.52	5.4
0	15.7.96	low	17.4	417	7.6	4.40	4.45	3.76	5.4
	19.7.96	higher	18.4	362	7.4				
	23.7.96	higher	18.2	374	7.5				
1	16.7.96		17.5	420	7.7	4.08	4.48		
2	16.7.96	low	17.6	424	7.4	4.16	4.56		
	17.7.96	high	18.0	339	7.3	3.04	3.44		
	23.7.96		18.0	417	7.3				
	27.9.97	high	15.2	310	7.4	2.96	3.31	2.91	7.3
3	16.7.96	low	17.6	429	7.6	4.20	4.60		
	19.7.96		18.3	400	7.3				
	23.7.96		18.1	401	7.4				
	27.9.97	high	15.6	316	7.4	3.00	3.19	2.91	10.3
4	15.07.96 12	low	19.7	444	7.6	4.12	4.60	4.24	11.8
	16.07.96 20	low	17.6	436	7.5	4.28	4.64		
	17.07.96 18	high	17.9	308	7.4	2.64	3.04		
	19.07.96 18		18.4	365	7.3	3.24	3.76		
	20.07.96 06			390		3.60	4.00		
	20.07.96 18			406		3.72	4.20		
	21.07.96 06			421			4.40		
	21.07.96 18			426			4.44		
	22.07.96 06			420			4.36		
	22.07.96 18			413			4.28		
	23.07.96 13	higher		378	7.3				
	25.09.97 00		17.6	390	7.4	3.77	3.99	3.71	10.6
5	17.7.96	higher	19.7	397	7.5	3.60	4.04		
6	16.7.96	low	18.3	318	7.3	3.04	3.20		
	19.7.96	higher	19.8	309	7.3				
	26.9.97	high	14.8	200	7.6	1.82	1.96	1.80	11.3
7	16.7.96		18.0	300	7.4	2.72	3.04		
	19.7.96		18.5	305	7.3				
8	16.7.96		17.4	434	7.5	4.12	4.52		
9	17.7.96	low	17.9	477	7.0	4.68	4.96		
	19.7.96	high	18.0	400	7.0				
	23.7.96		17.9	418	7.1				
	27.9.97		17.7	417	7.2	4.25	4.51	4.27	18
10	17.7.96	high	18.9	215	7.4	2.04	2.08		
	19.7.96		20.5	335	7.2				
	21.7.96		19.6	362	7.2	3.60	3.84		
	23.7.96		19.1	368	7.3				
	27.9.97	higher	14.5	293	7.5	2.81	3.03	2.70	8.2
10a	21.7.96		20.7	355	7.6	3.60	3.84		

Table 1.8.1. Measurements and analyses of all taken samples in the tracing area (H – water table level (low, high, very high), T – temperature, K- carbonate content, Ca+Mg – total hardness, Ca – calcium content).

between the injection point and the final spring of Dalongtan accessible water flow at points: 0 (Yanshidong), 1 (Maoshui-

dong), 2 (Shihuiyao), 3 (Xiangshuidong), 4 (Dakenyan), 7 (Guan Yindong) and from springs 5 (Dalongtan), 9 (Changshuitang)

and 10 (Xiniutang) (Figs. 1.9.1., 1.7.1., 1.7.2.).

On July 15th and 16th 1996 we took samples during low water levels. Only at Point 9 was there also a low water table on July 17th, which reached an estimated 50 l/s on July 19th - the highest recorded during our observations. At Point 10 the highest discharge was on July 17th, we estimated it to be 0.5 m³/s. On July 21st it underwent a steep decrease. Sampling on July 17th and 19th took place during a high or very high water level in most sampling points. The water level was only estimated, due to the fact that measurements of discharge exist only for Point 4 - Dakenyan.

In September 1997 we repeated the sampling in the sampling Points 2, 3, 4, 6, 9 and 10. The water levels were high, at points 2, 3 and 6 even the highest among all the measurements and sampling during July 1996 and September 1997.

Temperature

In July 1996 the temperature measurements revealed a relatively constant temperature during a low or medium water level, which was in the interval of 17.2 to 17.6 °C

from point a to Point 4. The pH was in the interval from 7.2 to 7.7. Only at Points 6, 7 and 8 we did measure somewhat higher temperatures. During a high water level following rainfall we measured some tenths of a degree higher temperatures at most sampling points (18 to 19 °C), which reflect the influence of warmer precipitation at these points, as then the water does not cool off in such degree - due to faster movement underground - as it would in the case of slower movement and a lower water level. At spring 9 we did not record noticeable differences, while the temperature at spring 10 was 0.7 °C lower, which might reflect the pressing out of older water (Tables 1.8.1., 1.8.2.).

In September 1997 we found generally lower temperatures, from 13.1 to 17.7 °C. Spring 9 had a temperature of 17.7 °C, which is only 0.3 °C less than at nearly the same water level in July 1996. Small variations of temperature of this spring during the year point to longer water retention in the hinterland and strong moderation of precipitation effects. At Point 10 we measured a temperature of only 14.5 °C, which it is still necessary to verify. Otherwise, it is evident that the subterranean stream flow from Point d to Point 4 gradually becomes warmer.

Place	At low water level								At higher water level				
	T	SEC	pH	Carb.	Ca+Mg	Ca	Ca/Mg	Noncarb.	T	SEC	pH	Carb.	Ca+Mg
a	17.7	490	7.2	4.72	5.28			0.56					
b	17.2	500	7.3	4.88	5.44	4.48	4.7	0.56					
c	17.4	494	7.4	4.80	5.40	4.48	5	0.60					
d	17.6	334	7.6	3.04	3.56	3.04	5.4	0.52					
0	17.4	417	7.6	4.20	4.45	3.76	5.8	0.25	18.4	362	7.4		
1	17.5	420	7.7	4.08	4.48			0.40					
2	17.6	424	7.4	4.16	4.56			0.40	18	339	7.3	3.04	3.44
3	17.6	429	7.6	4.20	4.60			0.40	18.3	400	7.3		
4	17.6	444	7.6	4.12	4.60	4.24	11.8	0.48	18.4	365	7.3	3.24	3.76
5									19.7	397	7.5	3.60	4.04
6	18.3	318	7.3	3.04	3.20			0.16	19.8	309	7.3		
7	18	300	7.4	2.72	3.04			0.32	18.5	305	7.3		
8	17.4	434	7.5	4.12	4.52			0.40					
9	17.9	477	7.0	4.68	4.96			0.28	18	400	7.1		
10	19.6	362	7.2	3.60	3.84			0.24	18.9	215	7.4	2.04	2.08

Table 1.8.2. Physical and chemical characteristics of groundwater in the wider tracing area during low and high water tables in July 1996

Water hardness and SEC at low or medium water level

The carbonate content of all observed points was, during a low or medium water table in July in the interval of 2.72 to 4.88 meq/l and the total hardness from 3.04 to 5.44 meq/l. The SEC reached the values from 300 to 500 $\mu\text{S}/\text{cm}$ and the non-carbonate hardness from 0.4 to 0.6 meq/l. Only at Points 6, 7, 9 and 10 did we find a lower non-carbonate hardness. The Ca/Mg ratio was around 5 at Points b, c, d and 0, and at Dakenyan (4) it was 11.8. All physical measurements and chemical analyses of sampled water are presented in Table 1.8.1.

The results of the determination of the carbonate content, total hardness and SEC during a low water level (Table 1.8.2., Fig. 1.8.3.) indicate that the water does not flow from Point d in the direction of Point c as was previously assumed. Later, the tracing experiment indicated the flowing from Point d to Point 0. Based on the chemical analyses we can assume that water from Points a, b and c also runs to Point 0. We assume the ratio of the quantity of water from direction d and the quantity from direction a, b and c during a low water table amount to approximately 1:1.

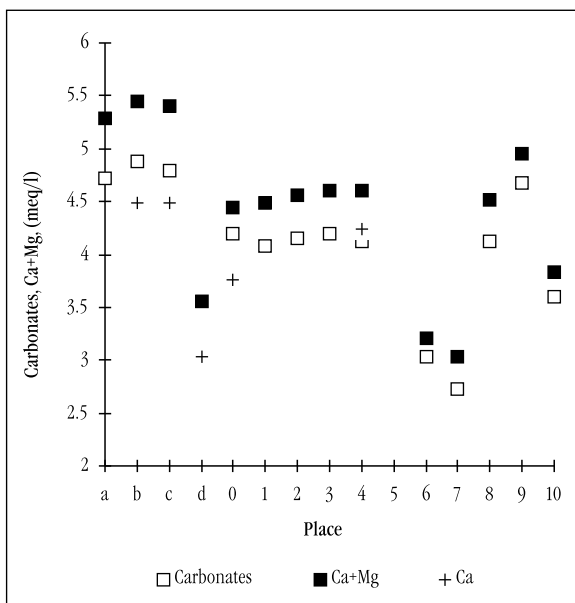


Fig. 1.8.3. Water characteristics at measurement points during low or medium water levels.

The water composition at successive Points 1, 2, 3, and 4 indicates the direction of the underground flow through successive points. Water from the spring at Point 9 has a similar composition, but this connection has not been confirmed by the trace experiment. We did not take samples at Point 8, but we assume that the water flows in the direction of Point 3. Points 6 and 7 deviate strongly by a notably lower carbonate content, total hardness and SEC (Fig. 1.8.3.). We do not exclude the possibility of the connection of water at Point 6 with the spring at Point 10, but for the tracing in July 1996 we used sodium chloride as a tracer, which does not render reliable results when used for longer distances. This is the reason we injected uranin in the second tracing experiment on September 26th 1997.

Water hardness and SEC at high water level

During a high and very high water level in July 1996 the carbonate values were up to 1.56 meq/l lower, and the SEC values up to 147 $\mu\text{S}/\text{cm}$ lower than at a low water level, except at Points 6 and 7, where the SEC difference was minimal. At Point 3 the differ-

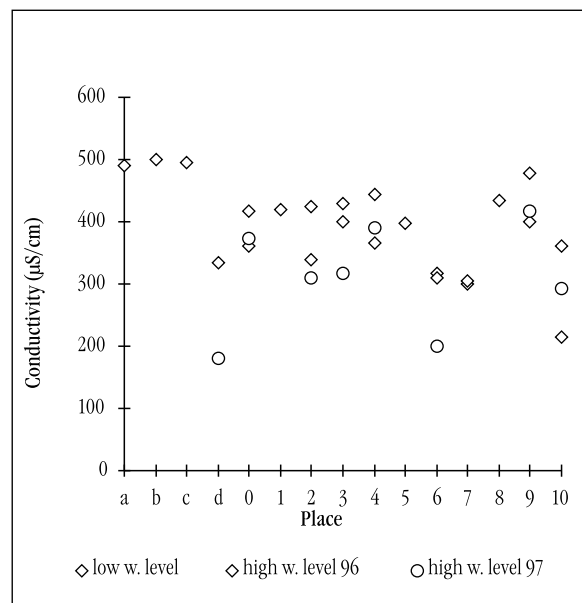


Fig. 1.8.4. SEC of water at measurement points during very high and during low water levels.

ence was only 29 $\mu\text{S}/\text{cm}$, while the difference at Point 0 was a whole 55 $\mu\text{S}/\text{cm}$. By tracing using sodium chloride we found that water drained from Point 6 to Point 2 and then successively to Points 3, 4 and 5. Tracer waves of uranin and sodium chloride (breakthrough curves) appeared at Point 2 simultaneously and travelled in the direction of spring 5 simultaneously – thus we did not notice differences between either tracers. The comparison of the SEC at Point 0, 2 and 6 indicates a notable proportion of water at Point 2 from direction 6 during a high and very high water level, which is probably not present during a low water level, that its proportion is insignificant (Figs 1.8.3., 1.8.4.).

In the fall of 1997 during high discharge the SEC at Point 6 decreased to 200 $\mu\text{S}/\text{cm}$, at Point d to 181 $\mu\text{S}/\text{cm}$ with a corresponding decrease of carbonates to 1.82 and 1.54 meq/l, respectively and total hardness. These were the lowest measured values, although insufficient comparable measurements were made to allow us to study seasonal variations of hardness.

The calculated Ca/Mg ratio at the successive points also indicates that water from Point d flows to Point 0. The elevated value at Point 2 indicates the mixing with water from direction 6 with a larger Ca/Mg ratio, which somewhat increased on its way to Point 3, but did not change significantly to Point 4.

Characteristics of the water pulse of underground water flow at Dakenyan

During a low water level ($Q = 0.35 \text{ m}^3/\text{s}$) the groundwater flow at Dakenyan had a carbonate content of 4.12 meq/l and total hardness of 4.6 meq/l, which means a non-carbonate hardness of below 0.5 meq/l. The water has primarily a high calcium content (4.24 meq/l) and low magnesium content (0.36 meq/l), so the Ca/Mg ratio is 11.8.

In July 1996 we installed an electronic temperature and SEC monitor with a data saver (TC instrument, DAS company). We wished to follow the water pulse, that is to define the characteristics of ground water

flow at the Dakenyan point (4) following precipitation and during increase and later decrease of its water level. Its water appeared later in the Dalongtan karst spring (5). This underground water flow was later accurately traced from its upper flow in the karst hinterland NE of spring (from Point d) by using the fluorescent tracer uranin. We also examined its flow velocity in individual sections (chapter 1.9.).

Regular discharge measurements are made at the hydrological station at Dakenyan four times daily, and after July 19th the measurements took place every two hours for the tracing experiment. Our measurements, carried out at one-hour intervals, included temperature to an accuracy of 0.1 °C, and SEC to an accuracy of 0.1 $\mu\text{S}/\text{cm}$. Parallel to this, we took some samples for total hardness and carbonate content analysis.

With regard to the data provided by the meteorological station at Dakenyan, where the daily quantity is measured at eight o'clock in the morning, 56.6 mm of rain fell on July 16th, an additional 11 mm on July 17th, in sum 67.6 mm of rain. On the night between July 21st and July 22nd, 26.5 mm of rain fell.

From July 1st, when it reached the value of 0.963 m^3/s , the groundwater discharge decreased until July 16th, when it reached its lowest value of 0.354 m^3/s . Heavy rainfall on the night between July 16th and July 17th triggered a fast reaction of the discharge, which reached, during our measurements carried out every six hours, the highest value of 2.24 m^3/s by the following day at noon. This was probably not the highest value. We assume that water began to flow together from the wider hinterland due to heavy rainfall and caused, in the beginning, the displacement of old water. This points to the delay of the SEC decline by a few hours after discharge had already increased. The discharge increase is followed by the decrease of the SEC and total hardness, and later as discharge decreases, the SEC increases again. Precipitation (11 mm) before midday triggered a repeated slight increase of discharge ($Q = 1.53 \text{ m}^3/\text{s}$) without a noticeable SEC decrease, which slowly increased to the starting-point value until July

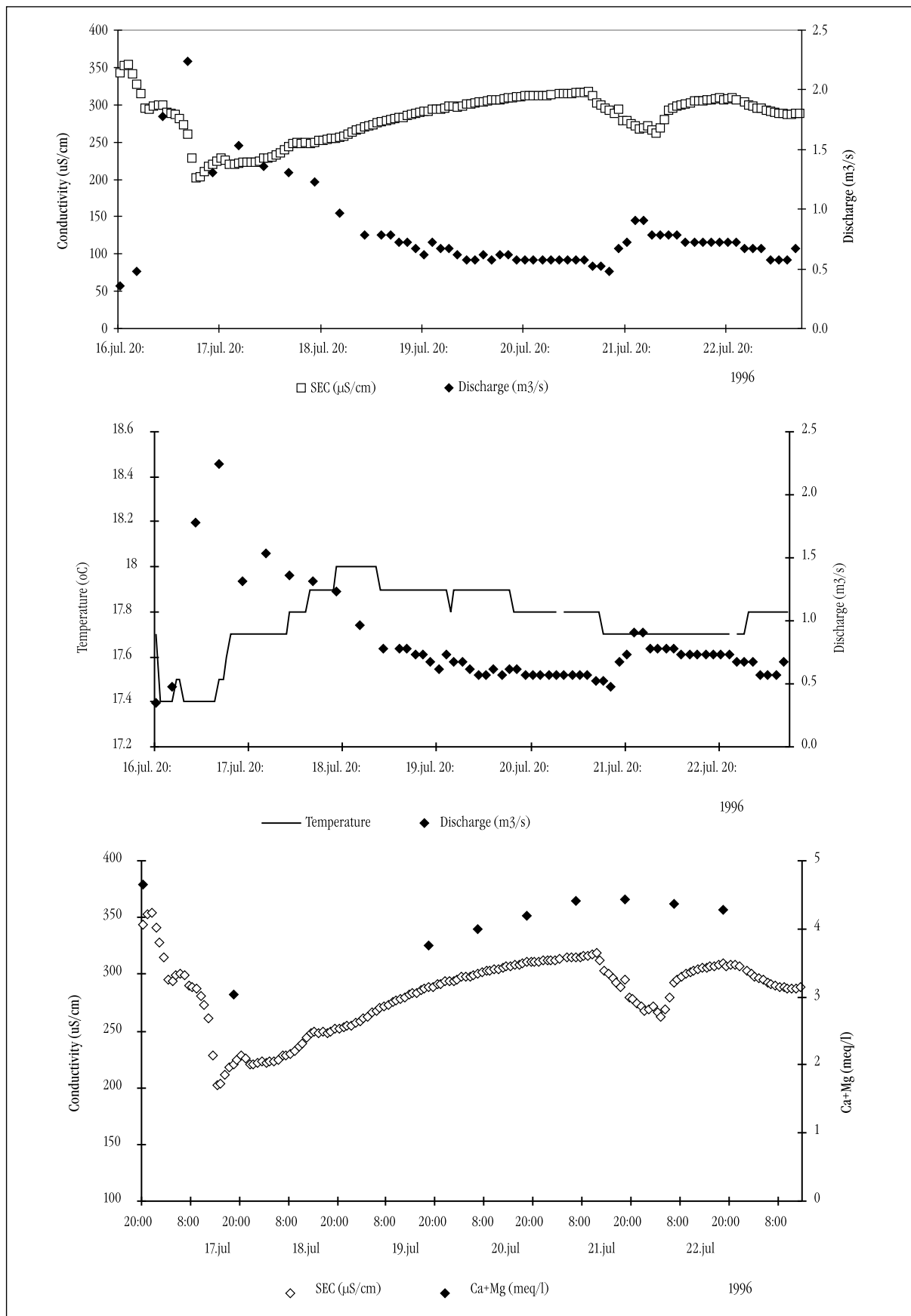


Fig. 1.8.5. Accurate recording of discharge, temperature and SEC with occasional analyses of total hardness of groundwater flow at Dakenyan (4) in water pulses in July 1996.

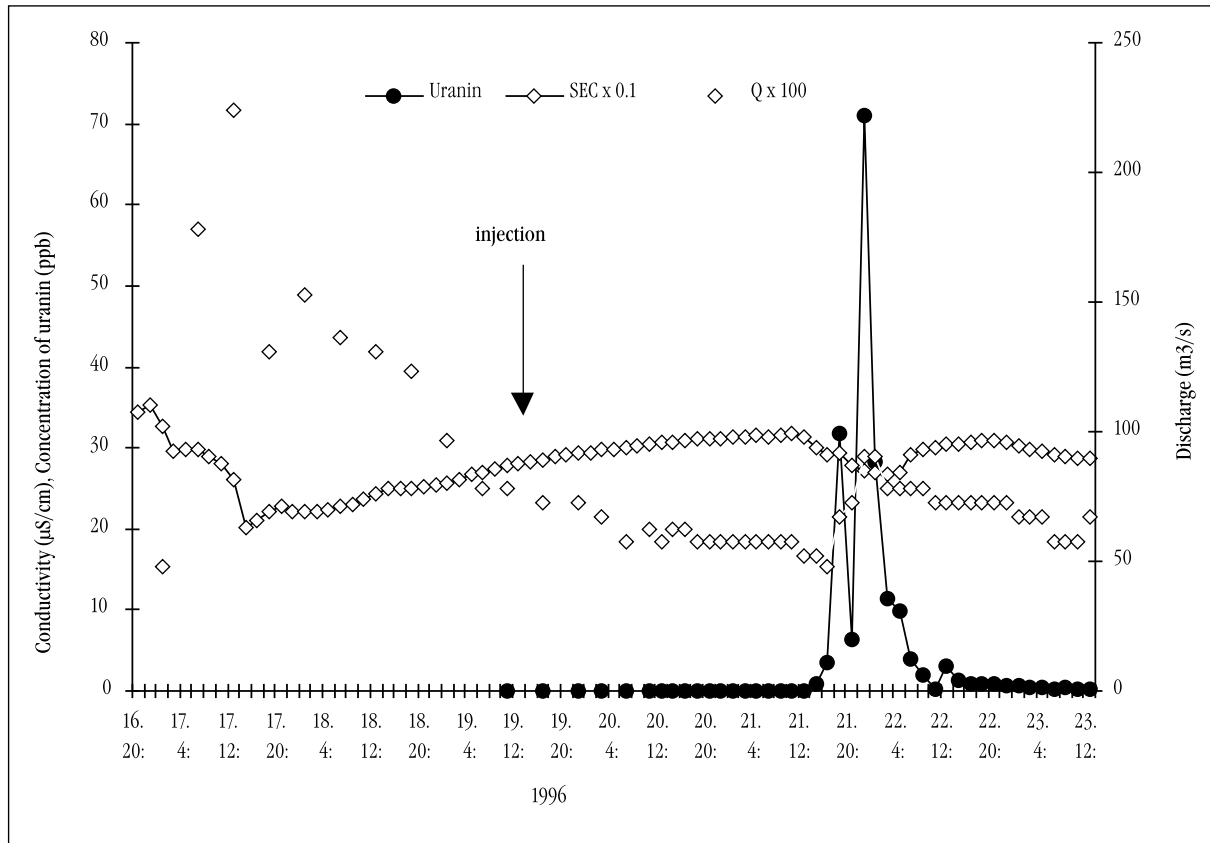


Fig. 1.8.6. Stream flow at Dakenyan: comparison of discharge, SEC and uranin appearance in July 1996.

21st, when it again began to rain in the evening (26.5 mm) and discharge increased to 0.902 m³/s, and then gradually declined. We recorded in this last water wave a smaller decrease of the SEC before the increase of discharge, which might point to the influence of differences in precipitation in the area of groundwater inflow (Fig. 1.8.5.), indicating complex recharge from various directions changing with precipitation and hydrological conditions.

When discharge increased six times its previous value in the first water pulse, the total hardness and carbonate content decreased by 1.6 meq/l, approximately one third of its previous value, a similar amount to the SEC. Similar changes have been found for karst flows in Slovenia. The temperature dropped during the increase of discharge, and then gradually increased. All these changes took place in the range of 0.6 °C.

Accurate recording of discharge, SEC and temperature (Figs. 1.8.5., 1.8.6.) clearly

indicate the conditions in which the tracing with uranin and sodium chloride were carried out (chapter 1.9.). Uranin was injected at Point d at the final section of a larger water pulse, when discharge slowly declined. Simple tracing breakthrough curves formed in these conditions at Points 0, 1 and 2 (Fig. 1.9.12.). The tracing curve at Point 3 was more flattened, as the water had to pass over the Tianshengan fault, and was formed with regard to a constant, lower discharge. At Point 4 we found the first traces of uranin at the lowest discharge and a slight decline in the SEC. The rain, which later caused a smaller water pulse at Point 4, pushed the tracer and accelerated the formation of two peaks on the uranin breakthrough curve. More frequent sampling, every hour or half hour, would have rendered a complete answer to the question whether there are possibly two smaller inflows in the groundwater hinterland.

But we did definitely find that the tracing experiment determined the velocity of the flow in conditions of discharge decrease in the range of 1 to 0.5 m³/s and also, that the velocity of the flow in section 3-4 would be somewhat less under these conditions than we calculated for the tracing performed in July 1996 (chapter 1.9.). The reason of higher velocity in sections 3 - 4 is a later rain event.

The comparison of precipitation and discharge of the flow demonstrates a rapid reaction of the flow. The flow velocities of water, as in the tracing experiment, are also relatively high during low and medium water levels, from 2.1 to 23 cm/s. This is why we can expect even higher flow velocities during very high water levels, which in the case of possible pollution means rapid spreading of pollution, that is a very short reaction time.

1.9. TRACING TEST IN THE TIANSHENGAN AREA

Janja Kogovšek, Liu Hong, Metka Petrič, Wu Wenqing

The study polygon near the village Tianshengan in the Lunan province is predominantly agricultural area with frequent problems of water shortage. This typical karst aquifer has plenty of underground water, but the time distribution of the quantities of stored water is disadvantageous. A rainy period from May to October is followed by a long dry period, in which the water reserves are often not large enough for the irrigation of the mainly rice fields. Therefore the agricultural production of the area is very low and problems with water supply for the villages are also frequent.

To resolve this problem, different surface and underground water accumulations are created. To the west and east of Tianshengan two reservoirs are already used, but their capacities are too small. Therefore the possibility of constructing a new reservoir has to be studied. For this purpose some basic hydrogeological characteristics of the area must be delineated first.

As one of the research methods a tracing test was proposed in order to find out underground water flow characteristics in the studied karst aquifer. This was done in July and August 1996. It was the first such experiment in the Tianshengan surroundings, so our goal was predominantly to define the main underground flow and to get some basic information required for planning a more complex tracing and other tests in future.

Natural background

The climate of the Lunan area can be classified as subtropical with an average an-

nual precipitation of 796 mm, average relative humidity of 75.3% and average annual temperature of 15.6° C (for the period 1980 - 1992). The amount of total annual rainfall varies considerably and for the observed period between 1980 and 1992 it ranges from 542 mm (1992) to 1066 mm (1991). Each year can be divided into dry and rainy season. The dry season from October to April has only 12 to 20% of total annual precipitation.

The polygon for the tracing test covers of 50 km² and is located in a broader area of the Shilin stone forest (Fig. 1.9.1.). The altitudes range between 1920 m in the east to 1750 m in the west. The relief undulates very gently. On the slopes of depressions and hills, stone teeth are developed, from 0.5 to 5 m high. Also, pinnacles more than 20 m high can be seen in this area near the Dakenyan.

The basic hydrogeological features of the discussed area are summarised from the hydrogeological map, produced in 1993 by the Water and Electricity Survey & Plan Institution of Quijing - Yunnan (Fig. 1.9.1.) The central part of the studied territory, with an area of approximately 100 km², consists of Carboniferous and Permian carbonate rocks, among them is a narrow belt of chert sandstone and schist marl, which divides the aquifer to the east and west part. Limestone and oolitic limestone, which underwent the karstification process and are highly permeable, are the prevailing carbonate rock. They are characterized by the karst-fissured porosity type. The main drainage routes are underground channels, which compose a heterogeneous karst-fis-

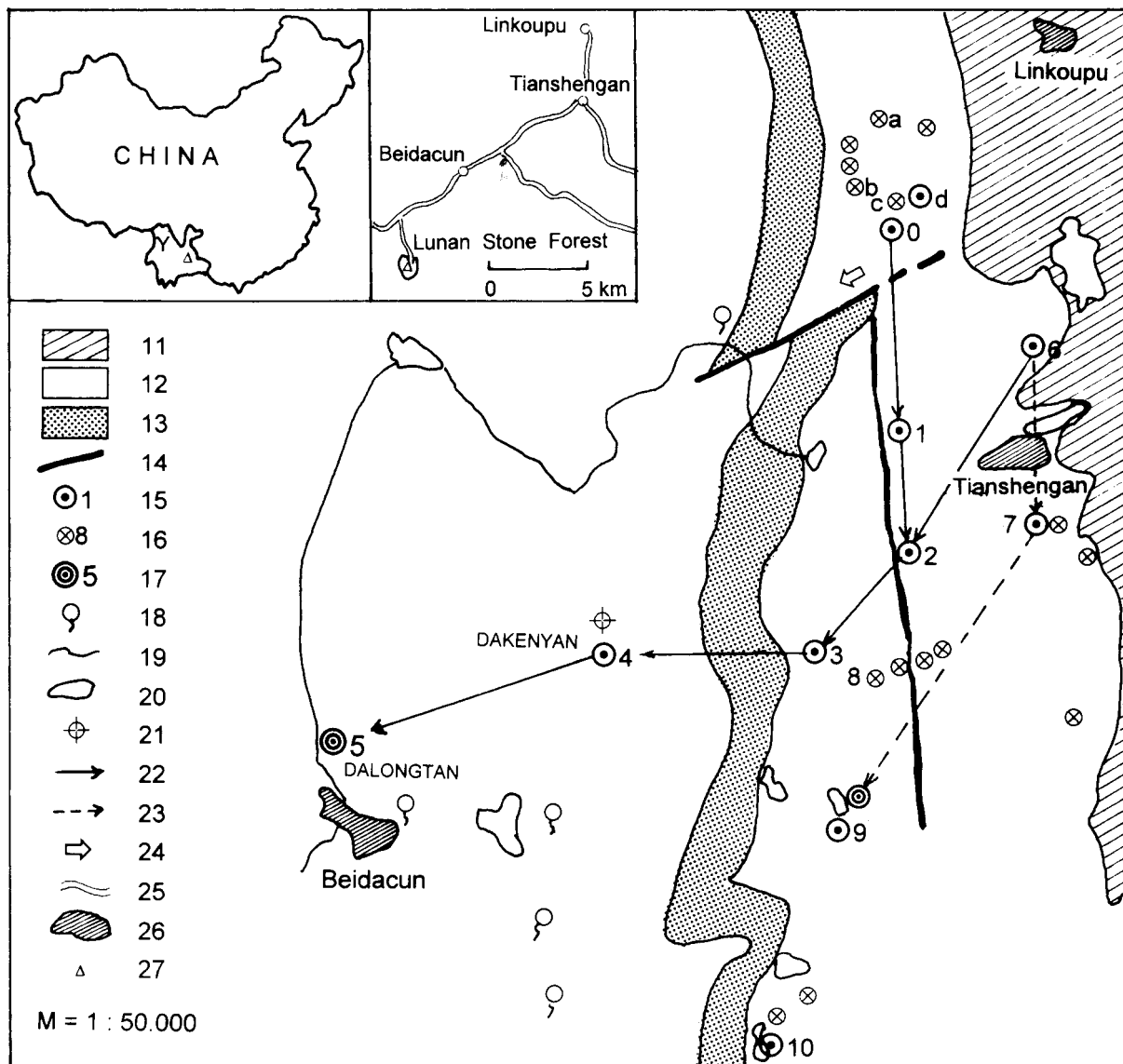


Fig. 1.9.1. Hydrogeological map

11. Precambrian noncarbonate rocks, 12. Carboniferous and Permian carbonate rocks, 13. Lower Permian clastic rocks, 14. fault, 15. cave or shaft with underground water flow - a sampling point, 16. cave or shaft with underground water flow, 17. karst spring - a sampling point, 18. small spring, 19. surface stream, 20. lake or water reservoir, 21. precipitation station, 22. on the base of tracing test proved direction of underground water flow, 23. on the base of tracing test supposed direction of underground water flow, 24. possible direction of underground water flow, 25. road, 26. village, 27. Shilin stone forest

sured system together with a network of fissures. Secondary porosity is well developed and the storage capacity is low. Large karst channels with constant or occasional groundwater flow are located near the surface and accessible through numerous vertical shafts. At low waters the channels are only partially filled with water, and the groundwater level is up to 30 m below the surface during drought. In the wet season

the water can completely fill the channels and during the highest water table level even flood the lower lying fields. The water flow transports large amounts of sediment, which is deposited in the channels when the transport capacity of the stream decreases. The consequence of this process is thick layers of sediment in the caves.

The thickness of the belt of quartz sandstone and shale marl is 20 to 30 m. The rock

is poorly permeable, but because it is tectonically fractured and the layer is thin, it does not act as an impermeable barrier. Based on fundamental field research in vertical shafts on both sides of the belt, it is possible to conclude that the groundwater flow continues from the eastern into the western part of the karst aquifer. This assumption was confirmed by the tracing experiment.

The carbonate rocks are bordered by Precambrian sandstone and tuff in the north-east. Cut approximately 300 m deep into it is the Nanpanjiang river, which is hydrologically separated from the examined karst aquifer because of impermeable layers in the base. Also classified into the group of impermeable rock are singular patches of Lower Permian basalt and tuff, and Eocene claystones and siltstones on the western and north-western boundaries. They do not, however, affect the hydrogeological conditions in the studied part of the aquifer in the vicinity of Tianshengan village.

In the studied area two faults are important: Tianshengan fault in the N-S direction and the Shibanshou fault in the NE-SW direction. Several shafts and caves with underground flow, that were observed during the tracing test, are distributed along the Tianshengan fault.

The karst aquifer is recharged in two ways: diffuse infiltration of precipitation through fissures in the carbonate surface, and point infiltration through swallow holes. It discharges concentrated through springs; Dalongtan spring (Figs. 1.9.2., 1.9.3.) near Beidacun village south-west of Tianshengan village, is most important. Similar to Dalongtan, karst water is collected by numerous other smaller springs, but their capacities and sizes of recharge area are unknown. During periods of high water table, flow-over points are activated at various heights, and through these the aquifer discharges. Due to the small regulation capacity of the system, there is too much water during wet seasons, with floods occurring, and a shortage of water during dry



Fig. 1.9.2. Dalongtan spring (Point 5) at low water level. (Photo A. Mihevc)

seasons. The ratio of minimal and maximal discharge is large.

Basing on explorations of karst caves and passages that are accessible from the surface we assumed the directions and basic properties of the underground water flow. Regime of recharge and underground flow was evaluated by daily data of precipitations of the area and by discharges at underground gauge station from August, 1993 to June, 1996 (Chapter 1.7.). The discharges are measured in the underground karst channel at the Dakenyan pumping station (Fig. 1.9.4.), which is situated 2.5 km north-eastern of the spring. The water levels are observed four times a day and from these values a mean daily discharge is calculated. The precipitation station is also at Dakenyan and the daily precipitations were measured for the same period. The most important spring Dalongtan, is situated in the south-western part of the area at an altitude of 1810 m. As yet there are no exact data about the capacity of this spring.

For the planning of the tracing test first some basic hydrological characteristics of the studied area had to be defined. The possible expected discharges were estimated on the base of the characteristics of the measured discharge at the Dakenyan station. The maximum discharge there was $6.28 \text{ m}^3/\text{s}$ and the average discharge $0.47 \text{ m}^3/\text{s}$. In May 1996 the measuring profile in Dakenyan was empty, but it is hard to define the minimum discharge, because in the dry period it is largely controlled by the quantity pumped by different pumping stations.

The tracing test was planned for July, 1996, so the characteristic values for this month were compared also. The maximum discharges were $2.92 \text{ m}^3/\text{s}$ in July, 1994 and $0.52 \text{ m}^3/\text{s}$ in July, 1995. Although we have the data only for a short period, a great variability of hydrologic conditions can be observed. On the basis of these values the broader interval of expected discharges in the time of tracing test has been predicted



Fig. 1.9.3. Dalongtan spring (Point 5) at high water level. (Photo J. Kogovšek)



Fig. 1.9.4. Meteorological and hydrological stations at Dakenyan. (Photo A. Mihevc)

and used in constructing the plan of the experiment.

On the base of described data about the studied polygon the tracing test was planned.

Tracing test

Hydrological conditions at the time of the tracing test

After the injection of tracer on July 19th, 1996, the discharges were measured at the Dakenyan station at shorter time intervals than usual: between July 19th and 25th every two hours, and from July 26th to 30th, every four hours. The values obtained are presented in Fig. 1.9.13., together with the con-

centration curves, and were used for the quantitative analysis of the experiment. At the time of injection the discharge was 0.783 m³/s. No water for irrigation was pumped at the pumping stations in this area.

The characteristic discharge values for the time of tracer test between July 19th and August 18th, were compared with the values of the two previous years (Tab. 1.9.1.). On the basis of this comparison the observed period in 1996 can be defined as average; only the extreme maximum discharge was lower than in previous years.

At the time of the tracer test daily precipitations were measured also. The total amount (P_{tot}) was 160.9 mm and the maximum daily value (P_{dmax}) 35.1 mm. Comparison with the same period of the years

Time interval	Q_{min}	Q_{mean}	Q_{max}	P_{dmax}	P_{tot}
July 19 - August 18, 1996	0.393	0.817	2.24	35.1	160.9
July 19 - August 18, 1994	0.426	1.064	2.40	75	271.9
July 19 - August 18, 1995	0.214	0.689	4.25	23.3	124.3

Table 1.9.1: Hydrological situation at the time of the tracing test.



Fig. 1.9.5. Injection of Uranin on July 19 1996 at the Point d (Quighuadong). (Photo S. Šebela)



Fig 1.9.6. Injection of NaCl on July 19 1996 at Point 6 (Wayadong). (Photo J. Kogovšek)



Fig. 1.9.7. We sampled the karst water at 9 sampling points. (Photo J. Kogovšek)

1994 and 1995 shows the same picture as for the discharges. In 1995 the total amount and the maximum daily precipitation were lower, and in 1994 higher than in the observed period in 1996. Therefore we can characterize this 1996 year as an average without extreme values.

On July 3 1996 10.4 mm of rain fell. The next intensive rain occurred on July 16 in the evening and continued during the night to the next morning; 56.6 mm of rain fell. Rain continued to fall the next morning but less heavy as there were only 11 mm of rain. The next rain followed on July 21 when 5.5 mm fell and on July 22 when 26.5 mm fell. Up to the end of July it rained three more times with a few mm of rain only. In the first three days of August 28.1 mm of rain fell, and from July 8 to 11 an additional 38.8 mm in total; heavier rain occurred on August 16 and 17 when 35 and 15.7 mm fell.

The rainfall in the middle of July increased the discharge of underground flow considerably and it reached $1.7 \text{ m}^3/\text{s}$ at Point 4; the water transported huge amount of soil and was of an intense orange-brown

colour. On July 19 when we decided to inject a tracer, the discharge was decreasing and was $0.783 \text{ m}^3/\text{s}$. It continued to decrease over the next few days and it reached the initial value not earlier than after the rain of July 22. By the end of August the discharge decreased slowly and after the rain it increased again to $1.23 \text{ m}^3/\text{s}$.

The tracing test

Inspection of the area where we planned the water tracing indicated possible injection points and springs and places where the appearance of the tracer would be probable. We measured temperature, SEC and pH and took blind samples and samples for determination of carbonate, calcium and magnesium levels.

On a basis of these first measurements and analyses we assumed that the water flows from Point d - Quighuadong towards Point 0 - Yanshidong and not in a direction towards Point c as had been supposed earlier (Fig. 1.9.1.). The analyses suggested that water



Fig. 1.9.8. The sampling at Point 2 (Shihuiyao) - in a shaft. (Photo J. Kogovšek)

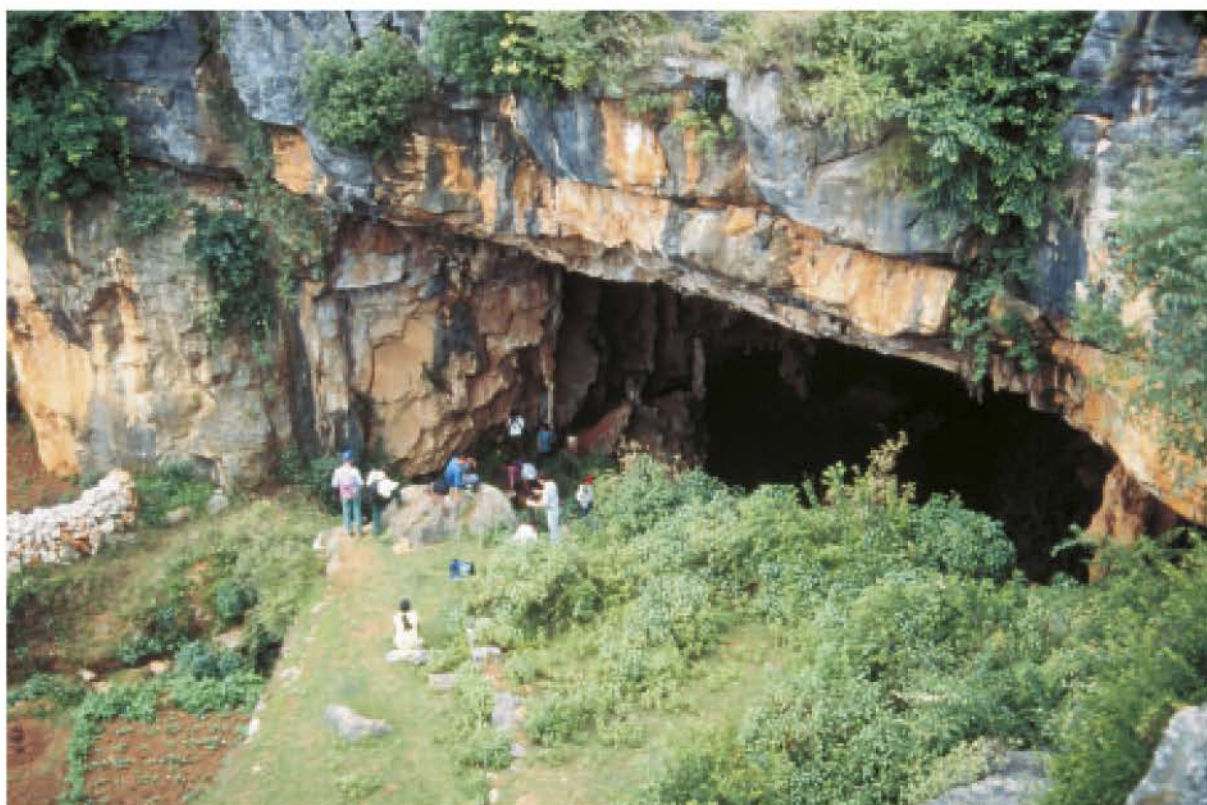


Fig. 1.9.9. The sampling Point 7 (Guanyindong) - in front of the cave. (Photo J. Kogovšek)



Fig. 1.9.10. The sampling at Changshuitang spring - Point 9. (Photo J. Kogovšek)



Fig. 1.9.11. Sampling at Xiniutang spring - Point 10. (Photo J. Kogovšek)

flows from the Point 0 towards Points 1 - Maoshuidong, 2 - Shihuiyao (Fig. 1.9.8.), 3 - Xiangshuidong and 4 - Dakenyan up to the Dalongtan spring at Point 5 (Figs. 1.9.2., 1.9.3.). We assumed that water at Points 6 - Wayaodong, 7 - Guanyindong (Fig. 1.9.9.) and the springs 9 - Changshuitang (Fig. 1.9.10.) and 10 - Xiniutang (Fig. 1.9.11.) had a different origin but we did not exclude the probability of connection. Possible injection points could be points a, b, c and d; as the most favourable conditions existed at Point d where discharge was approximately 30 l/s we chose that one. The second injection point was Point 6 which is a stream in the Wayaodong cave, having a discharge of 5 l/s.

Injection of tracers and water sampling

On July 19 1996 from 10.35 to 10.40 a.m. we injected 2 kg of Uranin that was dissolved in 50 l of water into a stream at the Point d (Fig. 1.9.5.). On the same day from 12.30 to 12.40 we also injected 100 kg of dissolved NaCl at Point 6 (Fig. 1.9.6.).

Referring to the previous analyses of rainfall and discharge we made a sampling plan. Point 4 was sampled in most detail.

For the first 7 days we sampled every 2 hours, later every 4 hours and then every 6 hours then every 12 hours and after 15 days once per day (Fig. 1.9.7.).

At Points 0 and 3 we started sampling every 2 hours and at Point 1 and 2 every 4 hours. To define precisely the maximal concentrations of Uranin and the time when it appeared we should need slightly more frequent sampling at Points 1 and 2. We also sampled at Points 5, 7, 9 and 10.

The results of Uranin tracing

Uranin appeared at consecutive Points 0, 1, 2, 3, 4, and 5 as shown in Figure 1.9.12.. At other observed Points 7, 9 and 10 Uranin was not detected and we may exclude the possibility of bad connection with these points as we used relatively great quantities of tracer.

The flow velocity for single sections of central runoff towards the Dalongtan spring (5) were calculated from air distance and time when maximal concentrations of Uranin appeared at single points (dominant velocities). Real velocities thus might be higher. (Table 1.9.2.)

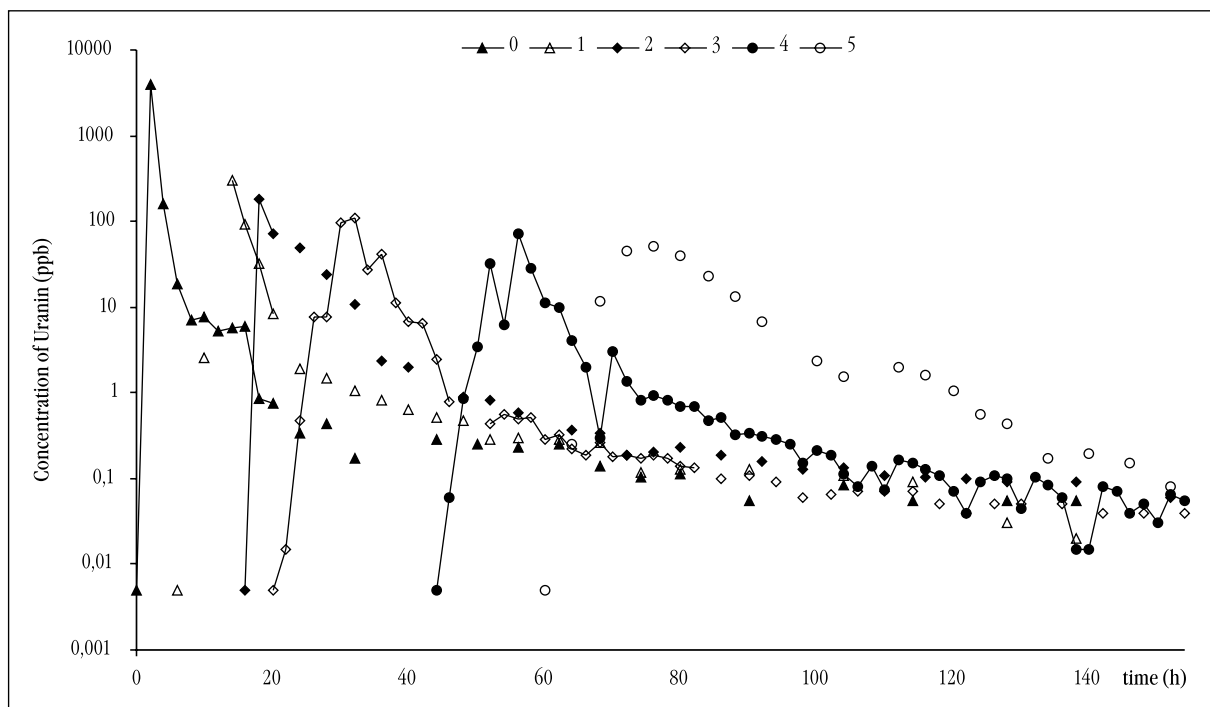


Fig. 1.9.12. Breakthrough curves of Uranin at the points 0, 1, 2, 3, 4, and 5.

Distance	Distance (m)	URANIN			NaCl		
		Time (C _{max}) (h)	Velocity _{domin}		Time (C _{max}) (h)	Velocity _{domin}	
			(m/h)	(cm/s)		(m/h)	(cm/s)
d - 0	500	0.6	830	23.0			
0 - 1	1800	11	164	4.5			
1 - 2	1050	8	131	3.6			
2 - 3	1250	16	78	2.2	16	78	2.2
3 - 4	1850	24	77	2.1	24	77	2.1
4 - 5	2450	20	123	3.4	22	111	3.1
6 - 2	2000				17	118	3.3
6 - 7	1500				13.5	111	3.1
6 - 9	4050				200	21	0.58
d - 5	8900	80	112	3.1			

Table 1.9.2. Air distance, time of tracer's travel in respect to maximal tracer's concentration and dominant velocity of Uranin and NaCl between observed points

The fastest water flow appeared in the initial part of its route between the Points d and 0; the slowest was between Points 2 and 4 where it passes over impermeable rocks. After this section its velocity rises up to spring 5 again (Fig. 1.9.1.). The average velocity between injection Point d and the Dalongtan spring (5) is 3.1 cm/s. A tracing experiment in Wulichong subsurface drainage system in Mengzi County, Yunnan shows the average velocity between 0.6 and 49 cm/s. Water tracings in the Slovene karst

(Habič et al. 1990, Novak 1991, Habič & Kogovšek 1992), when the tracer was injected directly into the water flow, indicated flow velocities between 0.2 and several cm/s, and in rare cases only the flow velocity reached values as high as 10 cm/s.

We studied more in detail the Uranin appearance at Point 4 (Dakenyan) where every 2 hours we also measured discharge and daily rainfall. Figure 1.9.13. shows the breakthrough curve of Uranin and relative recovery. By the end of July the Uranin con-

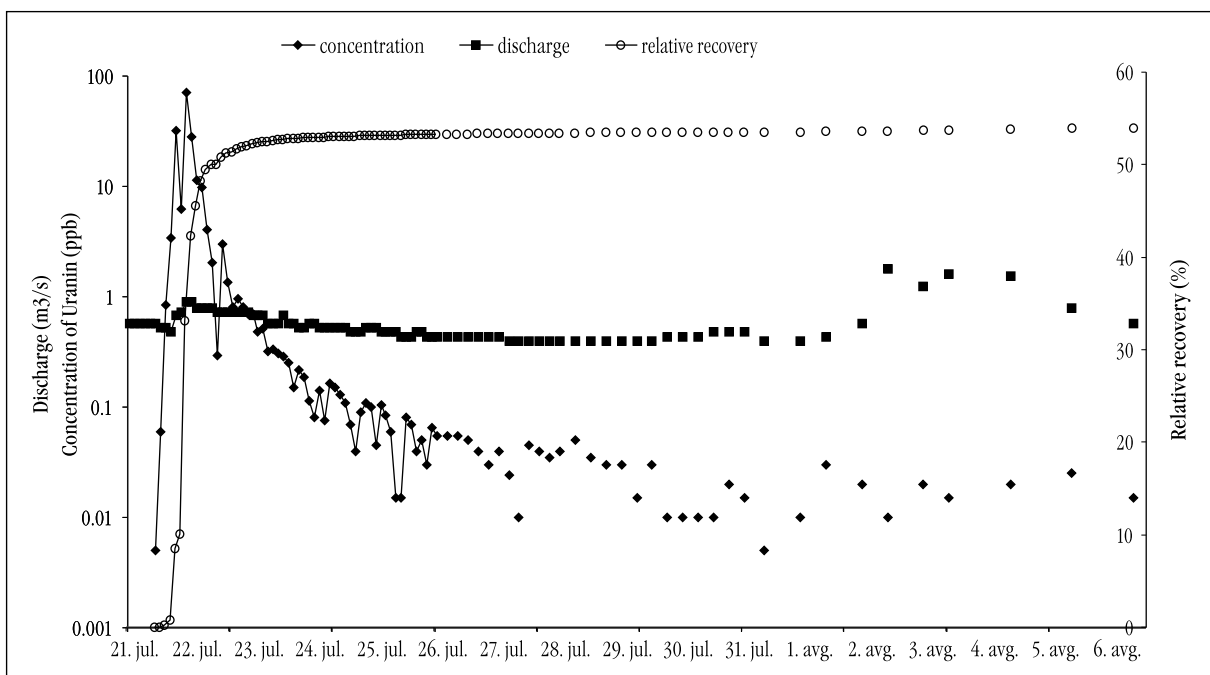


Fig. 1.9.13. Discharge, breakthrough curve of Uranine and relative recovery of Uranin at Dakenyan Point 4.

centration decreased to 0.01 mg/m^3 . Heavier rainfall at the beginning of August increased the drainage and washed out the remained Uranin. The Uranin concentration rose to 0.070 mg/m^3 , yet it decreased by the middle of August to 0.01 mg/m^3 . By the middle of August, namely one month since the injection, the returned quantity of Uranin was more than 1100 g, more than 55%. Some of remaining tracer was probably washed off later after each rainfall but we did not continue sampling.

The results of tracing by NaCl

As a second tracer the only one available was NaCl. Injection at Point 6 and observations at the above-mentioned springs showed the water flow to be towards Point 2 and towards spring 5 as already assessed by Uranin (Fig. 1.9.14.). Dominant flow velocity up to Point 2 was 3.3 cm/s ; other velocities to the Points 3, 4 and 5 were practically the same as those given by Uranin. At Points 7 and 9 we sometimes noticed in-

creased chloride levels (Fig. 1.9.15.) but only on a few occasions so we cannot state that these points are connected. We may conclude that drainage from Point 6 towards Point 7 is very probable as the flow velocity obtained from the results would be 3.1 cm/s ; drainage towards Point 9 is very questionable as there the flow velocity would be only 0.6 cm/s . More frequent sampling or a greater amount of tracer, or a more suitable tracer would probably give clearer picture. It is most probable that water flows from Point 6 in two directions, towards Points 2 and 7; this gives a higher dilution effect and consequently lower concentrations which must be considered in future. These results indicate a need to repeat the water tracing from Point 6 with a more suitable tracer.

No increase was noticed at Point 10. Even from the physical measurements and chemical analyses obtained we cannot suggest possible connections which could be used for future tracing tests. But we noticed the very different reactions to rainfall of the discharges at springs 9 and 10.

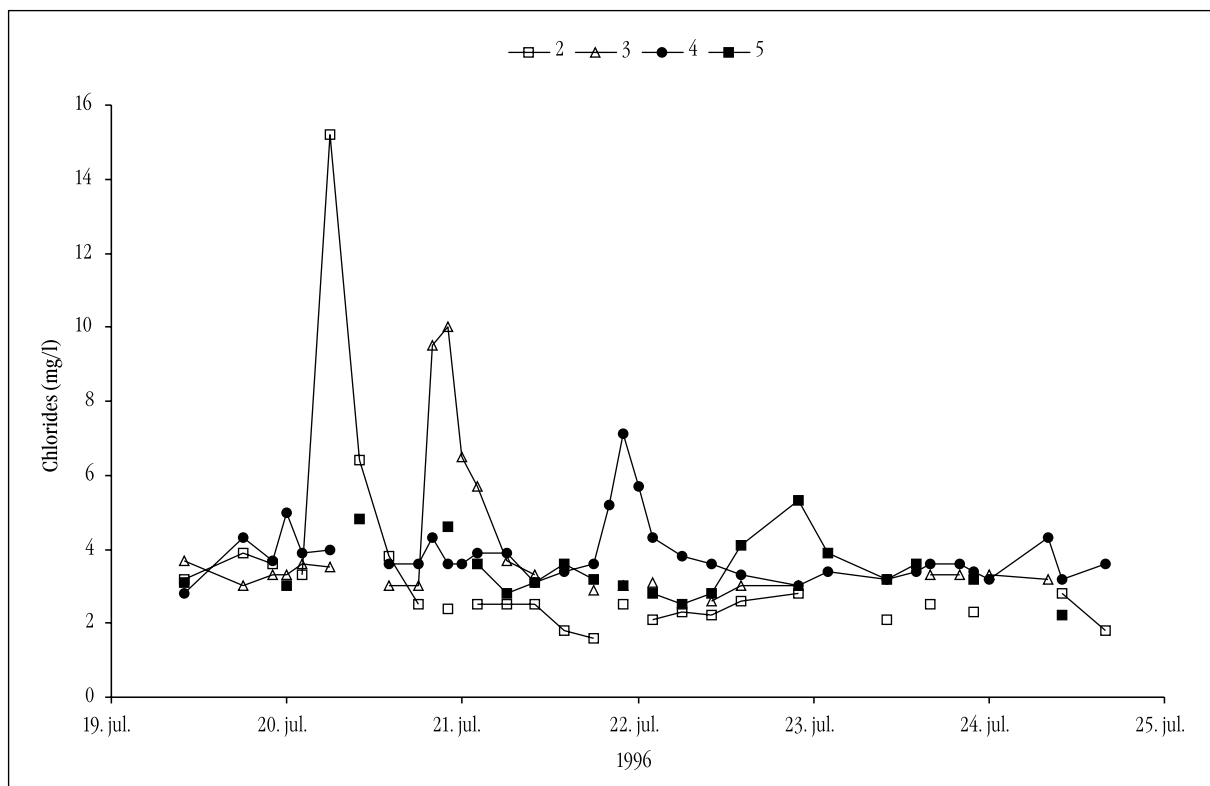


Fig. 1.9.14. Breakthrough curves of NaCl at the Points 2, 3, 4 and 5.

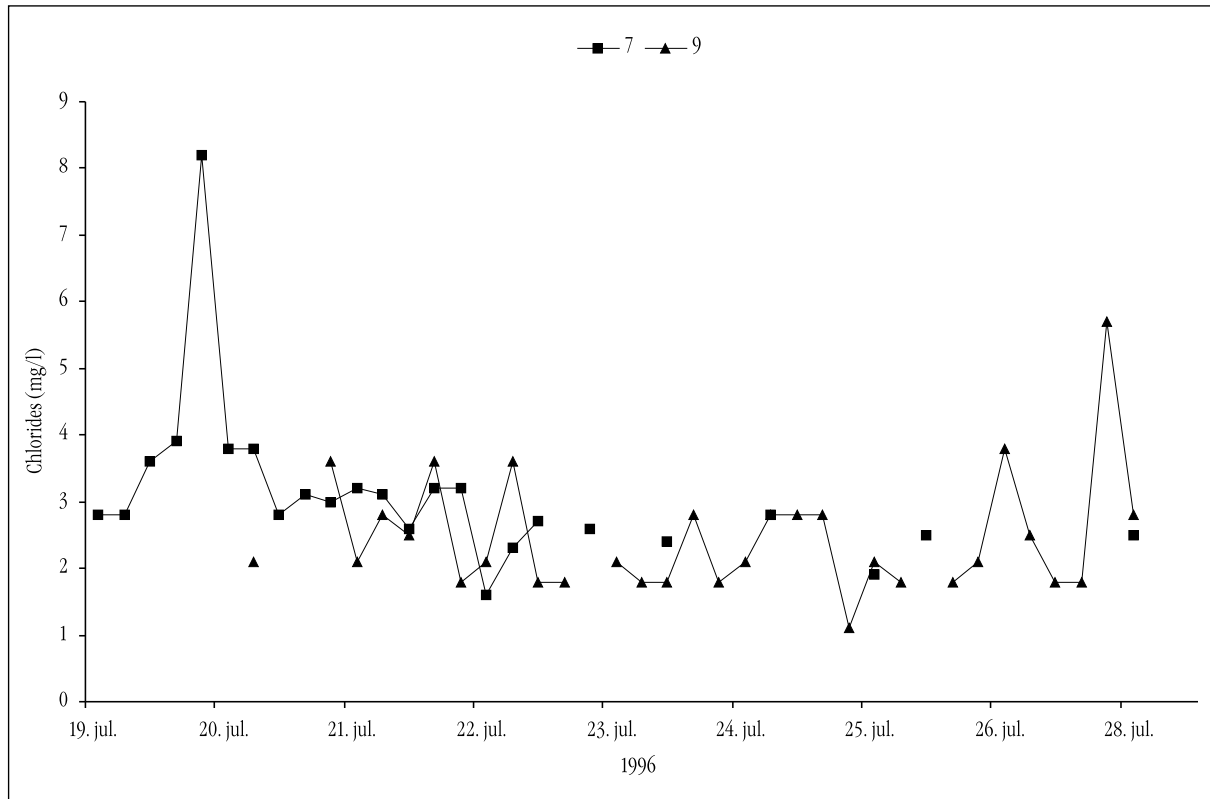


Fig. 1.9.15. NaCl appearance at Points 7 and 9.

Conclusions

In the studied area the underground karst channels are well developed not deep below the surface. They may be observed at various locations where shafts and caves reach the underground flow and they are proved by high flow velocity which was established by water tracing during medium high water level. When discharge is high, drainage may be still faster which is an important fact due to be considered for eventual pollution. The flow velocity slightly diminishes when water reaches the belt of non-carbonate rocks. Stated velocities predominantly vary between 2.1 and 4.5 cm/s, the average velocity for the whole section is 3.1 cm/s, and they correspond to values given for underground waters of southern China by Yuan Daoxian et al. (1991) and Song Linhua et al. (1993): medium values of more mm/s and maximal from several cm/s to more ten cm/s.

In spite of well-developed underground passages, fast drainage and fact that we injected a tracer directly into the under-

ground flow, the returned quantity of tracer is relatively low. Uranine adsorption into soil studied by laboratory experiments did not show any possibility of an important tracer adsorption. This is why we admit a possibility that a part of underground flow was not included in the sampling after tracing test. It seems probable that a part of water flows along the Shibanshou fault through a belt of non-carbonate rocks and feeds smaller springs or superficial flow on its western side. The maximal decrease of tracer concentration was noticed between the Points 0 and 1. Similar conclusion indicate the stated main directions of underground flow N-S and E-W and comparison with underground flow between Points 3 and 4 (Fig. 1.9.1.).

Comparing the discharges at Points 4 and 5, which were due to changeable hydrologic conditions only estimated, we noticed considerable increase in discharge of the Dalongtan spring. We assume that the observed underground flow from NE direction is not the only feeding source of this spring.

As already mentioned, the described water tracing test gave us only some basic information regarding the properties of the underground water in the treated area but it also raised a series of interesting questions. Let us quote only some of them: does the water drain along the Shibanshou fault and if this is the case, what is its rate? What

role does the flow passing Points 6 and 7 play and where is its continuation? Is there any connection between springs at Points 9 and 10 in spite of our negative results? The answers may be obtained by new investigations which are already planned by Chinese experts for the future.

1.10. JIUXIANG

Martin Knez, Janja Kogovšek, Tadej Slabe

Jiuxiang is an underground cave open for tourists, 90 km from Kunming, the capital of Yunnan and 20 km north of Stone Forest. Cave visitors gather in a pleasantly arranged reception hall. The tourist path runs parallel to the surface and subterranean canyon and then continues into the vast chambers. The Mai Tian river flows into the cave and flows in the canyon bed (Figs. 1.10.1.,

1.10.2.). Deeper into the cave there is an interesting double waterfall, the tourist path passes through numerous passages and large chambers with flowstone formations, of which the large gours across a vast slope in a chamber stand out. The visit to Jiuxiang cave gave us an impression of similarity to Škocjanske jame cave in Slovenia.

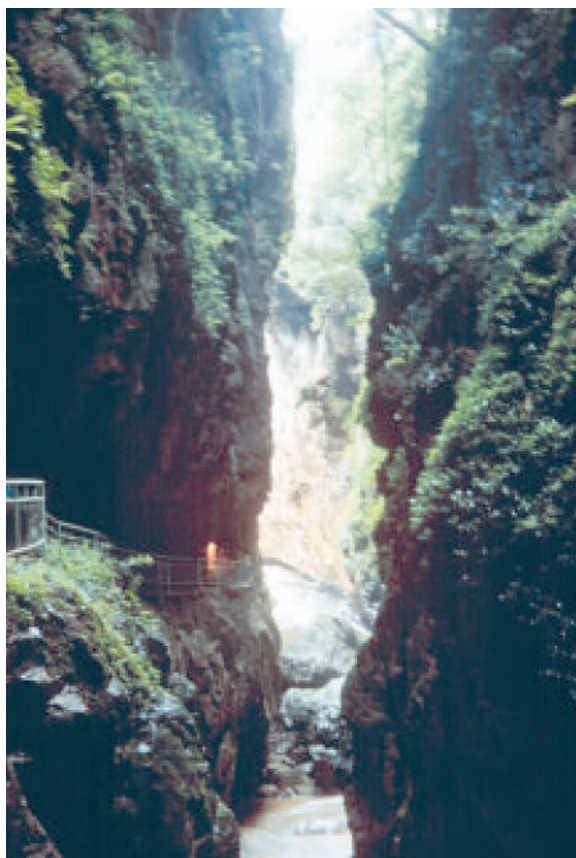


Fig. 1.10.1. The Mai Tian river at the entrance in the Jiuxiang cave. (Photo S. Šebela)



Fig. 1.10.2. The Mai Tian river. (Photo J. Kogovšek)

Lithostratigraphic characteristics of the rock in the cave

Nine locations for taking samples were chosen in the cave (Fig. 1.10.3.) in the areas where we observed a change in lithology or outstanding bedding-plane (Figs. 1.10.4., 1.10.5.). Eight samples were taken from the cave walls and one from the underground river bed (a siliceous sandstone pebble). The samples were microscopically examined. A complexometric analysis was done on all the samples.

Microscopic inspection of the thin sections revealed characteristic stromatolite and/or biopelmicrite to biopelsparite dolomite of the boundstone type (biolitite), standard microfacies 20 (SMF 20). Among the biogenic components the skeletons of blue-green algae prevail. Pelitic rock and rock derived from pelitic metamorphism processes are represented in the rock by only a few percent, exceptionally up to 10 percent. Besides singular non-transparent minerals, there are no allochemes in the sample.

The rock in the second part of the cavern gradually and continuously changes from stromatolitic biolite into characteristic laminite, standard microfacies 19 (SMF 19). The rock in this section does not contain biogenic components. Here and there we found fenestrae filled with chert.

In general we found that among the otherwise simple lamination, areas with frequent pelitics and areas with characteristic fenestrae are found. Despite the fact that in the thin sections the lamination is clearly expressed, in the exposed rock on the surface, here and there it is macroscopically completely blurred.

Of the types of secondary porosity, fenestral, intercrystal and vugy porosity are most common.

Calcimetric analyses showed that the total carbonate values vary from nearly 100% (99.29%) at point 2 to more than 80% (81.23%) at point 9. The difference to 100% is always the insoluble remainder. At the Ca/Mg value between 1.42 and 35.75 we found that the proportion of CaO in the sample ranged from 24.96% to 52.72% and the pro-



Fig. 1.10.3. The cave interior illuminated by many-coloured bulbs. (Photo M. Knez)



Fig. 1.10.4. One of the most important bedding-planes in the entrance part of the cave. (Photo M. Knez)



Fig. 1.10.5. Detail of figure 2. (Photo M. Knez)

portion of MgO in the sample ranged from 1.61 to 21.36%. From the calculation it follows that the proportion of calcite in the samples is between 0% and 90.08% and the proportion of dolomite in the samples between 9.25% and 99.59%. Seven out of eight carbonate samples are almost completely pure dolomite.

The colour of the rock in most of the cavern is between N4 and N6 by the Rock colour chart.

Rock relief in the cave

The cave rock relief is composed of various rock formations: ones that indicate initial water flowing at lesions formed by slow stream flow which used to run through the cave, ones that are signs of a faster flow present today, and the sign of slow flows of water above the fine particle alluvial sediment.

The remnants of the anastomoses between the rock strata, some cm to dm wide grikes, show how the cave began to form.

The anastomosis network is most usually visible as cut off grikes in a rock frame. The orifice is frequently widened into pans formed by a slower water flow which flooded the cave and whirled around the dissections.

Traces of the early phase of the cave development, when a slow stream flowed through the flooded cave, are ceiling and wall pans on the frames of passageways which were not deformed by disintegration. Small, higher located and currently dry passage ways are dissected into spongy forms (Fig. 1.10.6.). On their frames we find ceiling and wall pans, and from this protrude rounded horns, dissected by rock bridges. All these forms are traces of slow water flow through porous or cleaved rock. Traces of slow water flow are also on the passageway ceilings, which deepened the water flow with a free water table. This is what most effectively forms the cave today.

Fast water flows chisel small facets and potholes (Fig. 1.10.7.). In a part of the cave, flutes on alluvial sediment (Slabe 1995) are preserved, indicating that the cave or at

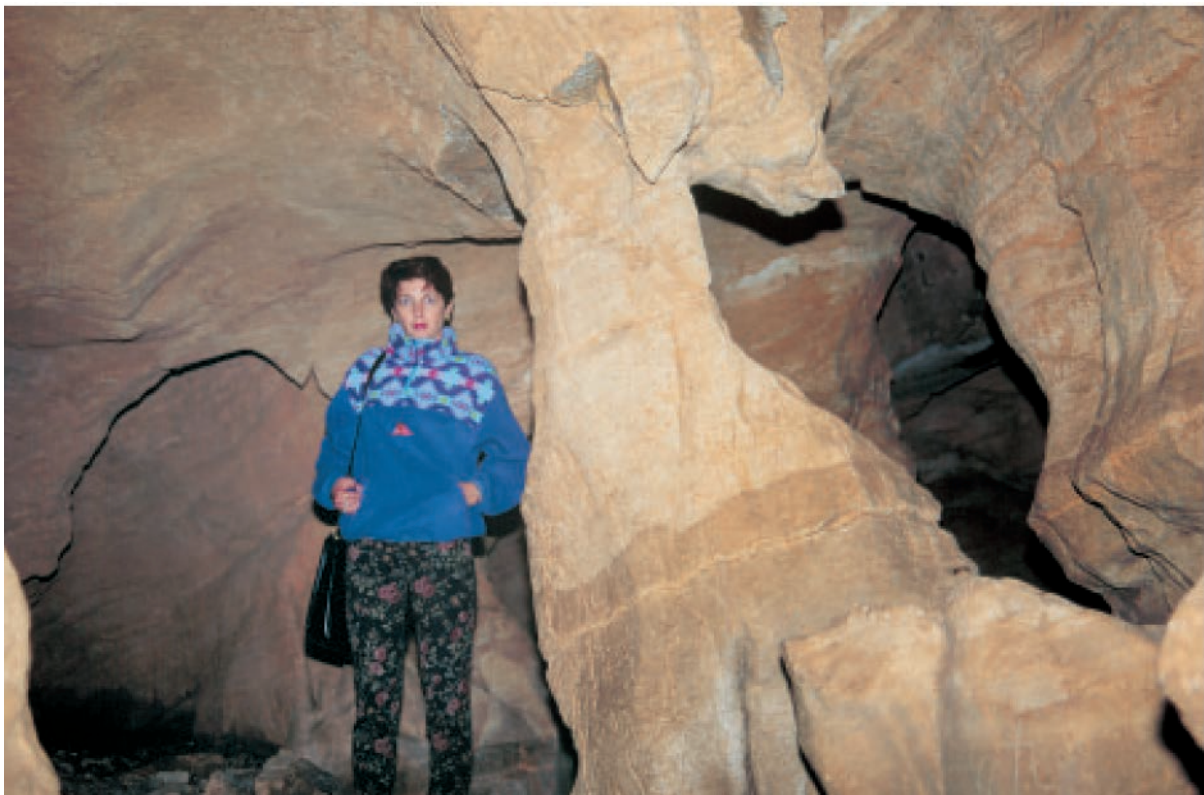


Fig. 1.10.6. The passage shaped by slow water flow. (Photo T. Slabe)



Fig. 1.10.7. Scallops due to fast water flow. (foto T. Slabe)

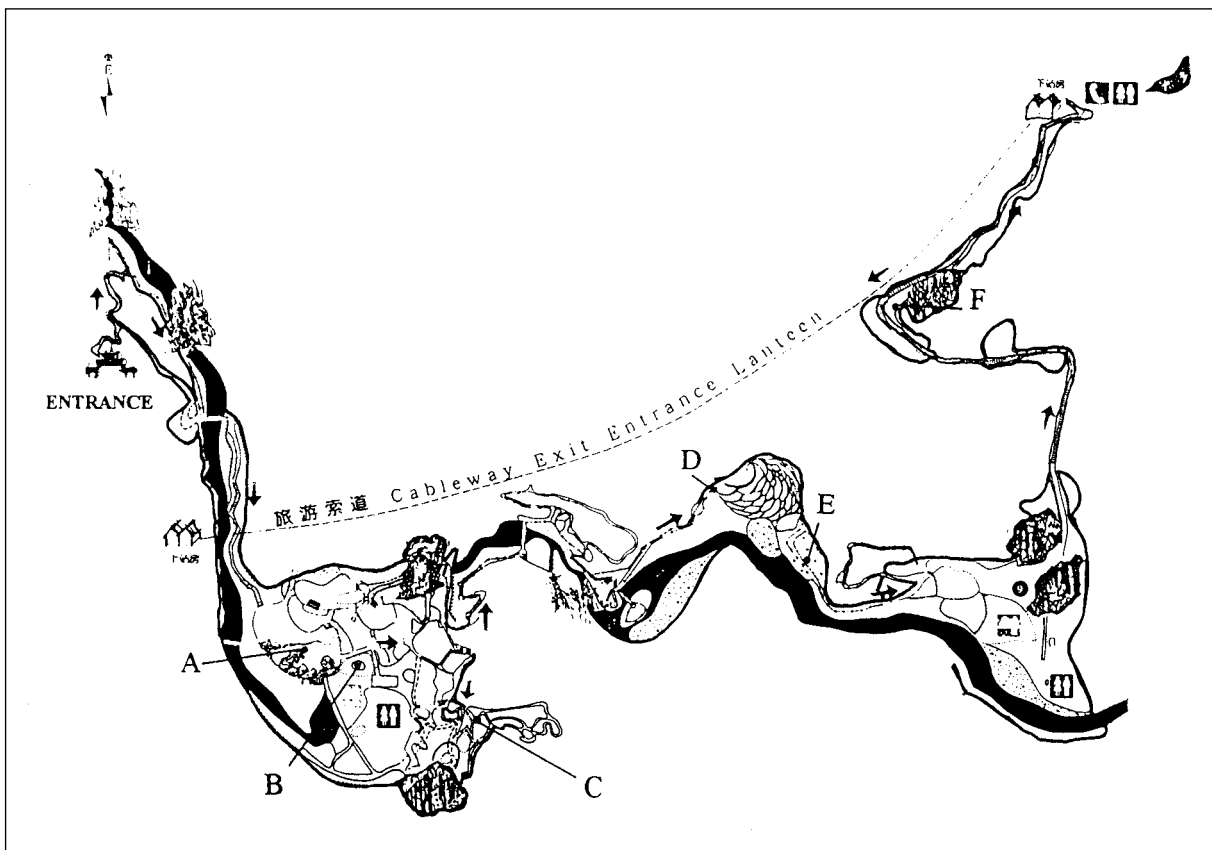


Fig. 1.10.8. Jiuxiang cave: sampling points of percolation water A, B, C, D, E and F.

least a part of it was filled with fine particle sediment, across which small water flows ran and cut characteristic forms into it. The rock relief reflects the most evident stages of the development of the cave. The cave developed from a network of grikes in rock strata. Slower flows, which completely flooded the cave enlarged and formed some of the initial grikes that then grew into passages. This period was relatively long in duration, which is reflected in the size of the middle passageways with traces of slow water flow. The water flow began to deepen the cave because of the lowering of the underground water table. It was occasionally flooded and during heavier flood periods it was filled with fine particle sediments. When the cave was filled for a long period of time, the water flowing above the sediments left marks on the passageway ceiling. The process of fast water flow cutting into the bottom of the rock continued from then on and remains the main factor in forming the cave.

Water in the cave

The Jiuxiang cave has a submerged river and percolation water supplied by precipitation. There had been no heavy precipitation two weeks previous to our visit in July 1996. We noticed a number of drips and tiny trickles and took three samples of percolation water (Fig. 1.10.8.). We also took a sample of Mai Tian river (Fig 1.10.9.). During our next visit in September 1997 we again took a sample of Mai Tian river, four samples of percolation water and inflow water to the large and small gours.

Mai Tian river

On July 13th 1996 Mai Tian river water taken from in front of the swallow hole at 13.00 was medium-turbid, the discharge was somewhat higher, the temperature measured was 20.1°C, specific electric conductivity (SEC) 184 µS/cm and pH 8.26. Be-



Fig. 1.10.9. Sampling of the Mai Tian river. (Photo M. Knez)

fore doing further analyses we filtered the sample through the blue ribbon filter, but it remained turbid even after filtration, which indicates the presence of very fine solid particles. The water contained 1,76 meq/l (107 mg HCO_3^-/l) of carbonates and 0.88 meq/l (17.6 mg Ca^{2+}/l) of calcium. The magnesium content was the same as the calcium content, so the Ca/Mg ratio (Ca and Mg in meq/l) was 1, which indicates that the river water is supplied from a dolomite area.

We took a sample from Mai Tian river in the same spot next year on September 23rd during a slightly higher, although decreasing water level. Lower temperatures in this season caused a lower river water temperature, which was 17.7°C, the SEC was 147 $\mu\text{S}/\text{cm}$ and the pH 8.95. The water contained 1.42 meq/l of carbonates, 0.84 meq/l of calcium and 0.64 meq/l of magnesium, the Ca/Mg ratio thus being 1.3. In comparison with percolation water in the cave, the SEC and hardness values of the river water were noticeably lower.

Percolation water

The Ca/Mg ratio of water in the samples from Jiuxiang cave was also around 1, indicating that precipitation water percolates through dolomite rock and/or dolomitised rock. Sample A-97 (Table 1.10.1., Fig. 1.10.8.) was taken on September 1997 from a drip from the cave ceiling with a discharge of around 10 ml/min, located on top of the stairs in a passageway leading from a canyon to an otherwise very dry part of the cave. We took sample B-96 in July 1996 from a heavier drip, which was almost a trickle, with a discharge of approximately 70 ml/min falling from the 5 m high ceiling into a collector in the vast room (Fig. 1.10.10.). The immediate measurement of the SEC indicated high values, and due to this we assumed a possible pollution source on the surface. A subsequent comparison of carbonate content and total water hardness of this sample with the other ones indicated the same. After visiting the cave we took a chair lift to the starting point. We found that



Fig. 1.10.10. Sampling of percolation water at point B. (Photo J. Kogovšek)

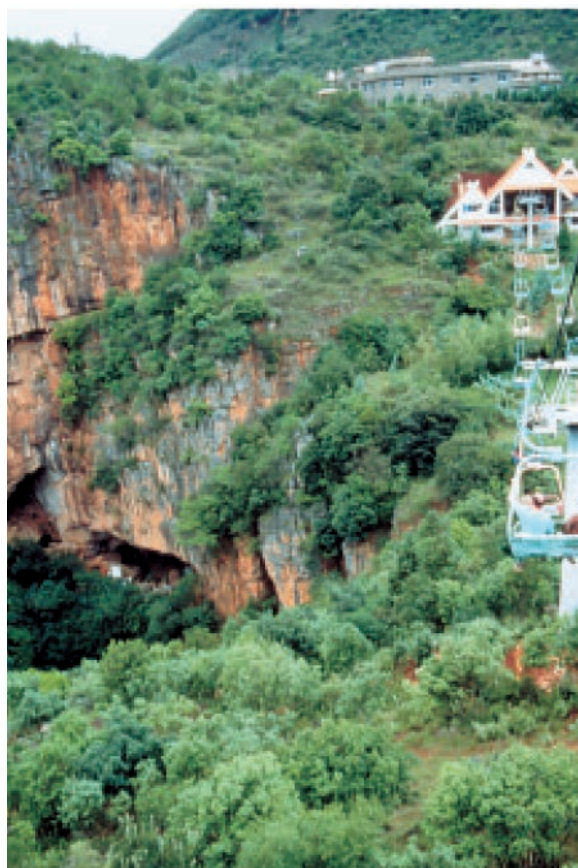


Fig. 1.10.11. View to Jiuxiang cave from chair lift at the end of our visit.
(Photo J. Kogovšek)

the end station of the chair lift is located approximately above the room where we had taken the sample (Fig. 1.10.11.). This is how pollution from the surface is possible. Unfortunately, we were unable to carry out the analyses of the content of nitrates, chlorides and sulphates, which could confirm our assumptions.

In September 1997 we took another sample of the B-97 water and found the val-

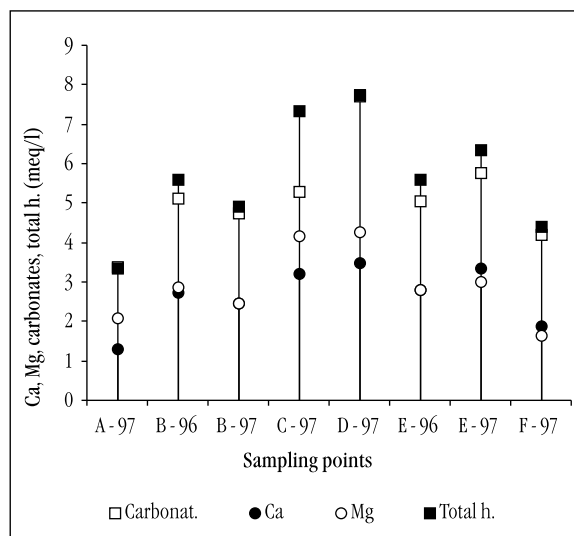


Fig. 1.10.12. Carbonate, calcium, magnesium level and total hardness in percolation water.

ues of SEC and total hardness to be lower, 9 mg/l of chlorides and a higher content of sulphates, which were determined only qualitatively. Measurements and analyses are presented in Table 1.10.1. and Figure 1.10.12. The heavier drip at point C in the side passageway had a high SEC and chiefly an increased hardness. It also contained 6 mg/l of chlorides, but the sulphates were not higher. Unfortunately, we were once again not able to determine the nitrate content.

Flowstone deposition in gours

Jiuxiang cave is adorned with variously large flowstone gours in four different locations. The largest gours are on a vast slope and are several times larger than the ones found in Škocjanske jame cave. These gours,

Place	Discharge ml/min	T °C	SEC μS/cm	pH	Carbonat. meq/l	Ca meq/l	Mg meq/l	Total h. meq/l	Ca/Mg
A - 97			331	8.40	3.36	1.28	2.07	3.35	0.6
B - 96	70	20.0	605	8.40	5.12	2.72	2.88	5.60	0.9
B - 97		17.2	500	8.15	4.75	2.47	2.44	4.91	1.0
C - 97	100	15.9	615	8.03	5.28	3.19	4.15	7.34	0.8
D - 97			692	7.68	7.70	3.47	4.27	7.74	0.8
E - 96		17.5	514	7.80	5.04	2.80	2.80	5.60	1.0
E - 97		15.9	556	7.70	5.75	3.35	2.99	6.34	1.1
F - 97		15.2	394	8.40	4.21	1.88	1.62	4.39	1.2

Table 1.10.1. Measured parameters in percolation water in the Jiuxiang cave.

like those in Škocjanske jame cave, do not have a regular flow of water. Smaller gours, which are continuously filled with water, are at their base.

During our September 1997 visit we managed to take a sample of water that flows into the larger gours, this is sample D-97. This water contains noticeably more dissolved carbonates in comparison with the flow into the smaller gours (Eo) and thus we can expect more intense deposition (Table 1.10.1.). But the gours were only half filled with water. The previous year in July, when the rainy season had hardly begun, there had been no flow. This is why it would be advantageous to direct the water to fill all the gours after precipitation, that is when the inflow is active. For the further maintenance of the gour, a small amount of oversaturated water would suffice, depending on the extent of evaporation.

Measurements and analyses of the inflow water (D-97) indicated the highest measured SEC and hardness values of our analyses of percolation water in the Slovenian and Yunnan karst. Due to the fact that hardness varies throughout the year with the highest values at the beginning of the rainy season, similar to the spring flows in this karst, we assume that we would have measured even higher values during that period. Analyses indicated higher values of magnesium in comparison with calcium (in meq/l), which we have never found in the Slovenian karst. The diversity of percolation water composition through the length of the cave indicates a varied geological structure, which will probably be confirmed by detailed rock analyses, for which numerous samples have been taken.

During our first visit in July 1996 we took samples of water in smaller, lower lying gours, that is the inflow water to the first

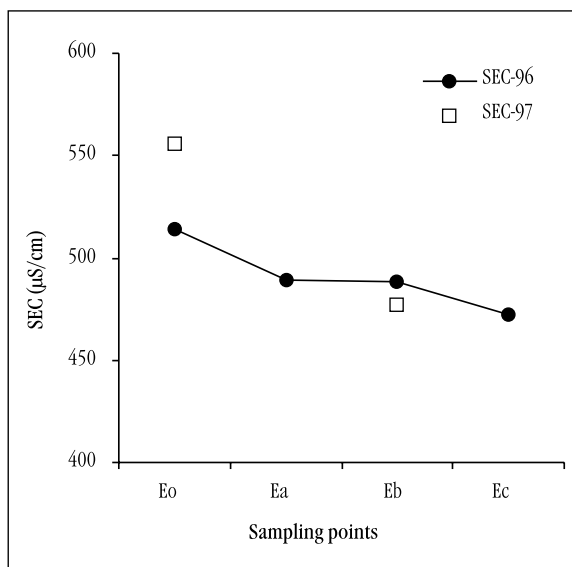


Fig. 1.10.13. Flowstone deposition in small gours in Jiuxiang cave.

gour (Eo-96) and carried out measurements in lower subsequent gours (Fig.1.10.13). The SEC measurements indicated a subsequent decrease of values, which is why we assume flowstone deposition, that is recent growth of the gours. Since we did not manage to take a sample of the water before the first gour, we assume that it has an even higher SEC and/or higher carbonate content. In Autumn 1997 we measured higher values in the first gour, which probably indicate an even heavier deposition in the recent conditions.

To 'revive' the larger gours oversaturated water would be required, that is water with a high carbonate content. Mai Tian river water, which usually transports a large amount of solid particles is not adequate, because it has different chemical composition with only a fifth of the carbonate and total hardness and could cause dissolution of the gours.

1.11. A STUDY ON RECENT KARST DENUDATION RATE OF KARST IN SHILIN, STONE FOREST

Liu Hong

Previous studies

Research into the corrosion of carbonate rocks mainly uses three methods:

1. To calculate the weight of dissolved carbonate per unit drainage area either by measuring river run-off with its concentration of dissolved rock and the boundaries of the river basin, or to calculate from the rate lowering of the rock surface, using the formula:

$$X=4ET/100$$

where X is the solution rate ($\text{m}^3/\text{km}^2/\text{year}$ or $\text{mm}/1000 \text{ year}$), E is run-off (dm) and T is the average concentration (mg/l).

2. By using tablets of carbonate rock of standard weight, noting their structural characteristics and exposing them in the field. They are then reweighed after a known period and the loss in weight is the amount dissolved in that time. From that the volume dissolved can be obtained and can be converted into rate of surface lowering.

It was suggested by Gams (1981) from analyzing 1500 tablets in eight countries and Day (1986), from test results in Wisconsin (USA) and in the Brasil, that:

(a) The amount of solution is generally greater on tablets placed in the soil than on the surface or above it. The solution rate depends more on the difference between precipitation and evaporation than the temperature.

(b) The solution rate is highest in humid tropical area.

(c) The influence of different rocks is greater than the effect of climate.

(d) Even in areas where solutional denudation is very active, the effect of mechanical erosion may also be very clear.

Yuan (1988) measured the solution rates on 12 tablets under different climatic conditions on the ground surface and also 20 and 50 cm deep in the soil. He concluded that:

(a) In damp climates the tablets in the soil are denuded more than the surface above it. This result is associated with biotic action and the high concentration of CO_2 in the soil.

(b) The case with which water can penetrate the soil has an important effect on solution rate.

Yuan's results give average solution rates for tablets buried in the soil at depths of 20 and 50 cm 33.96 mg/100d and 32.05 mg/100d respectively. For tablets on the ground the average solution rate was 14.46 mg/100d, and for tablets 1.5 m above the ground it was 16.42 mg/100d. The solutional denudation rate obtained from tablet tests is usually less than that calculated from water hardness and run-off data (Williams & Ford 1989).

3. Direct measurement of the denudation rate by micrometrical method.

This is usually suitable only for measurement over long periods. It has been used by the Karst Research Institute in Postojna to measure the surface denudation rate in Snežna jama cave NW Slovenia.

The authors of China Lunan Stone Forest Karst Research (1997) have calculated a denudation rate by combining the result of water hardness, change of rock volumen and weight, rate of fissure development and rate of formation of karst fractures. They conclude that it is between 32 and 73 mm/1000y in the Shilin stone forest, using Cor-

bel formula, they calculated the denudation rate in Luoping county, 99 km west of Lunan stone forest as 51.53 mm/1000 years. This figures may be compared with those obtained by Yuan (1989) above.

Methodology

Rock samples were obtained from the Permian Maokou limestones. They were prepared as 88 tablets 5 cm diameter and 0.5 cm thick, which in July of 1996 were placed in various parts of Shilin stone forest. To allow for the possible effect of soil depth (5 to 50 cm), hydrological conditions and locations, the tablets were located in depressions located on hillsides of various gradients, at their edges, on their slopes and in the soil of the bottoms. Some of tablets were placed in water, as at Sword Pool. 45% of the tablets were recovered about a year later, in September 1997. After washing, the tablets were dried and weighed (with an accuracy to 0.0001 g). The weights lost indicate the solution rates under present climatic and hydrological conditions in Shilin stone forest.

Segment type	near base	midslope	near summit
Staircase	0.0521	0.0213	0.0216
Broken Cliff	0.0215	0.0110	0.0260
Inclinal bedrock	0.0527	0.0217	0.0305
Talus	0.0303	0.0201	—

Table 1.11.1. Tablet weight mean losses (g/y) by slope segment type and location (From Micheal Day, 1986).

Central section fissures of pillar	Vegetation cover				Roofing with no vegetation		
	0.0153				0.0103		
Buried under soil	5 mm	10 mm	15 mm*	20 mm	30 mm	40 -50 mm*	average
	0.0197	0.0315	0.1209	0.0293	0.0469	0.2947	0.1807
Peak of pillar	average weight loss*		Maximum		Minimum		
	0.0654		0.3878		0.0156		
Earth's surface	rainwater not easy drenching			rainwater easy drenching			average
	0.0013			0.0454			0.0160

Table 1.11.2. The average weight loss (g/y) statistics in Shilin stone forest.

* Deducts these tablets that weight losses caused by mechanical disintegration clearly, the average weight loss is 0.0196 g/y and 0.0622 g/y respectively and 0.0369 g/y is the average value for the stone column's top.

Results

The maximal denuding rate occurs at the tablets buried in the soil and the lowest at tablets interspersing at rock dissolutional fissures where the rain is not easy drenching. The denuding rate of tablets placed at the stone crests or in woods, is in the middle.

Maximal loss weight occurs under Ashima stone pillar (20 cm in the soil) with 1.8946 g/y. The minimal value (0.0068g/y) presents at »hog bajie ate watermelon« stone crest's rock fissure, buried 5 cm under the thin soil. This except chemical denudation, weight loses primarily owing mechanical broken. As a result of corrosions along porousness and fissures of rock ongoing first of all, it may cause the rock drop-out possibly. It has been found that with the proportion of dolomite increasing in limestone the mechanical disintegrative quantity of limestone increases too (Gao Zhang et al. 1986). Additionally, there is a relationship between rock's micro-fissures developing degree and mechanical disintegrative amount, the mechanical disintegrative quantity can occupies 27% of whole denuding quantity (Weng Jintao 1987).

Comparing with the work of Michael Day (1986) in Belize Karst depression, both results correspond. The surroundings of these tablets that were placed at stone column in study area are similar with that steep cliff of Michael Day's, and the weight loses are conformable too (Table 1.11.1., 1.11.2.).

If we omit their placing surroundings, the 45 pieces tablets mean that the weight loss is 0.1221 g/y. After deducting 7 pieces

maximize value samples, the average weight loss is 0.0454 g/y. These samples placed in stone column central sections where the rain can not easily reach the dissolve loss quantities are quite smaller than others.

During the testing period, there are also some rainfall samples collected for analyzing the quality of precipitation in the Shilin stone forest area (chapter 1.6.). In the study area the cave roof percolation waters were also taken and analyzed (chapter 1.6.).

Discussion

Precipitation is the main controlling factor on the rock (chemical) denudation. For a good understanding the effect of precipitation on the stone forest development, some tablets were laid at rock stone pillar fissures. A part is opened to precipitation drip washing, and others not for the contrast specially. The average corrosion quantity for those tablets lying at the surface where not easy pouring rainwater is 0.0013 g/y, but for those where the rains may directly pour is 0.0454 g/y. Both are nearly 35 times different.

For those tablets placed at the central section of the stone column where there is not easily directly to get rain the mean denuding weight of the rock sample is 0.0058 g/y. The average loss weight for those put at the stone pillar upper part is 0.0438 g/y. Rainwater from the stone column top underwashing drowns and forms a quick-speed flow that is not yet come up to a saturated state. This is very helpful for the rock surface ionic carry and CO₂ supply, and can enhance the chemical denudation speed of carbonate rocks (Yu Jinbiao et al., 1990). It is one of the main reasons for the development dashing groovy on stone columns. The quantity and runoff speed are limited owing to the tested samples placed partially near the upstream of the canal, it is hardly able to reflect any very big variant. Both of weight losses have a difference of barely 7.5 times. Flattening dissolve grooves or denuding, and it seems they are widely developed at the central section of the stone pillar along the rock stratum bedding planes in

the Shilin stone forest, it is formed under the soil buried or under water conditions. Even if the rock is covered up by the soil, if the rain water unables direct-acting at the burial places, the denuding amount of its is also very low, in Nantainman only 0.0015 g/y. Compared with the average denuding amount of the under soil, it is 120 times lower.

For rainfall features of the stone forest area, there are torrential rains, as well as mizzly rainfalls (chapter 1.6.). The torrential rain has a big rainfall amount but the endurance time is short. It plays a very important role in forming of stone column surface ditches. Its contacting time with rocks is brief, in contrast to small rainfall amounts mizzly, the denuding-quantity of the former should be smaller than that of the latter. Therefore, the length of the rain-water-rock action time and the amount of precipitation have a determinant action on the carbonate rock corrosion process. This is in tune with the Yuan's research (1988).

The karst features caused by the creature action at carbonate rocks is called the biotic karst. The majority of the rocky surface is not completely bare, but is covered by a thin layer lichen, algae or other stone surface, fissure and inter-rock organism. By now, their machine-processing on the carbonate rock denuding is not yet wholly understood. It may be connected with the excretory organic acid, raising of the relative humidity and CO₂ emission. Danin's (1983) study in Israel shows that orchid algae can yield a dissolving rate of 5 mm/ky. Once for a time it is agreed that vine and wood growing on the stone column have very big effect on the chemical denudation procedure of the stone column. Earlier some tablets were specially placed under vines or trees of the stone pillars, for taking measure of the liana's effect onto the stone column.

After the precipitation passes through the crown and tree trunks, the acidity of rainwater can be grown up (Yu Jinbiao 1990), and it consequently has enhanced its chemical denudation ability. 7%-43% of the total rainfall is hindered by transpiration. Stones pillar surface micro-figures are a lit-

tle bit different between the pillars with the vegetation and those without vegetation. The stone pillars with plants appearances are not very fluent. The surface up and down is greater than the one with no vegetation. This is because dripping water of a crown is unlike the meteoric water that can uniformly act on the rock surface. Commonly, there are small corrosion pits developed on the rock surface of 1 cm depth and the diameter from 1 cm to several cm. At the Major and Minor stone forest, because of the stone column superficies' plants cleavage, all might eye out it in the reserve prints. The surface of the stone column appears with white color, but other pillars with no vegetation covered present black-ash color. It may related to the vegetation keeping off the rainwater and sunshine, as well as related possibly to microbio selective living.

The rock under woods is awkward to have rainwater uniformly brushed during the light rain. Only during the downpour hours the precipitation is able to yield a strong action on under rocks. Therefore, the chemical denudation amount of those tablets which are placed under the plants is not as high as the supposed amount, the average value is 0.0153 g/y (Table 1.11.2.).

The root system of the vegetative growth pitches into rock gap deeply, and this procedure contributes to the rainwater ingoing, yielding corrosion and mechanical spallation. Therewith, plant root systems dissolve out organic acid and yield strong chemical denudation action on carbonate rocks. Occasionally, there are fluting figure forms at the plant root system or liana adhesive places. This kind of figures can normally be seen in the Shilin after the woods or vines of the stone column were cleaned out. Except for its acidity increase and denuding ability reinforces after the meteoric water the transition through tree trunk and crown, it may be also concerned with the moisture of that place, and the holding-up time is longer than other places owing to the root or vine coherence.

At the places where vine and rock touch there grow out fibrous roots acting on the rocks. There are samples laid under vines

and at the joint positions of the vine and rock, unfortunately, there are only two pieces preserved. They all have fibrous roots (lateral roots) growth. Due to the limited time, these two samples' corrosion quantities were not very high, 0.0209 g/y and 0.0156 g/y respectively.

The tablets buried at the depression side slopes (gradient 20°-25°, burial depth 30 cm) have an average loss weight approached to 0.0804 g/y. The tablets mean denuding amount is 0.1326 g/y. The samples at the top gentle district of the depression with the same burial depth, the mean loss weight is only 0.021 g/y. From top to bottom, the loss weight of the tablets has increased progressively 3.8 times and 6.3 times respectively.

Besides hydrological and topographical factors, it is a concern with soil behaviors. On the top there are cypresses and pine trees growing, and under them there develops loosely humid earth having a worthwhile penetrating property of water. Under the effect of the dry-wet season clear climate, the surface layer soil moisture during the dry season is terrible low, that is to say that the procedure of chemical denudation speed is very low, too. For the depression central slope area, the grasses grow well on the surface, but the depth of the soil is relatively thinner. The depth of the samples buried is almost to the rocky zone. The earth could hold certain humidity during the dry season. At the bottom of the depression the soil viscosity is high and easily hardened. In most cases the water holding property and penetrating ability are not all equal to the former, but in the wet season there can form impermanent storing water, soil moisture all along very high. Meanwhile, the water penetrating capability along the border of rocks and soil (sediment) is very high that approximated to the conduit level. In the Busaoshan area the weight loss of tablets with 10 cm, 20 cm, 30 cm and 40 cm burial depth in the bottom of the hollow are all over 0.2 g/y.

According to the weight loss statistics, the average corrosion speed of the earth surface and the top of stone pillars is 10.4 mm/ky in the Shilin stone forest area and

the under earth mean speed is 28.77 mm/ky. There are 2.7 times different between them. That is to say that the Shilin stone forest under soil still keeps growing by the speed of 18.37 mm/ky. Reckoning on this speed, if the stone forest could develop to the nowadays' dimension, over 30 m of stone pillars, it will need about 1630 thousand years, equivalent to the Middle Pleistocene period. This coincides with the results by Liu Xing(1998) and the authors of China Lunan Stone Forest Karst Reseach(1997). By means of ESR dating, they think the stone forest predominately developing period is Middle Pleistocene. The ESR date of Dadieshui waterfall ancient river course adarce sediment is 1350 thousand years old, that is to say that the Shilin stone forest and Dadieshui cascades are the offspring of the same period karst.

Conclusion

Deducting the influence of the rocks, the rainfall is the main motivation of the karst developing. In most cases the amount of carbonate rocks denuding of the under-earth is 2-3 times bigger than that of the earth surface. The undersoil denuding is regarded with the edaphic water-holding behavior and landforms sites. The vegetation activity is not as big as preconceptional in-process of the stone forest development. According to the today karst developing speed, the Shilin stone forest mainly developed period is Middle Pleistocene. It is the offspring of the corresponding periodical karst with the Dadieshui waterfall.

1.12. THE ANALYSIS RESEARCH ON SOIL EROSION CHARACTERS IN KARST MOUNTAINS AREA ENVIRONMENT XICHOU OF YUNNAN

Chen Xiaoping

The karst environment is a special physical environment. Specially, there is mainly a distribution of tropic and subtropic karst mountain areas in the Yunnan-Guizhou Plateau and Guangxi area, China. It has a complex geomorphological character, steep slope and rugged mountain, thin soil layer, widely spread stoneteeth, discontinuous soil layer, lesser vegetation cover, deep underground water and dry ground. Thus, it shows a fragility of the low environment capacity, high variant sensitivity of the ecosystem, small elasticity of the catastrophe duration threshold value. Due to the high density of population, limited farmland and influenced by the unreasonable human being activity of the denuded forest, it results in the soil erosion increasingly in the karst mountain area. And it leads to the originally thin soil layer erosion, poor farmland, bare rock and waste mountain which have extended with an obvious desert trend and resulted in a disastrous effect to a worse ecosystem, lack of water, drought or excessive rain disaster aggravation, deposited and destroyed farmland, danger to the water conservancy and traffic facilities, and danger to the local social economic production and life. It is seldom researched, specially about the soil erosion in the karst mountain area environment, and it is still weak at present. Even the problem related to the soil erosion in the karst mountain area, it is still judged through the non-karst erosion level. It is often concluded that the karst area has a character of a slight erosion. It gives a bad influence on water and soil conservation in the karst mountain area. Therefore, it is important to think high of carrying out the

research work. This paper is based on the observation research work by the author in the typical research area in the peak-cluster depression area in the Southeast of Yunnan. The soil erosion problems on characters, reason, erosion level index and prevention and control in the karst mountain area is analysed and discussed.

The soil erosion character in the karst mountain area

The soil erosion actuality and latent dangerousness

The soil erosion widely arisen. The erosion area is up to 2/3 of the total area in the karst mountains. Due to the fragility of the karst mountain environment, it comes to a result that once the key element "forest-soil system" is destroyed, the soil erosion will certainly aggravate.

At present, many forest vegetation is destroyed in the wide karst mountain except in some karst forest nature reserves, and provide a wide condition for the soil erosion. According to the research works by Cai Zongxin(1989), it shows that the karst soil erosion area in the Guangxi area is up to 69,742 km², it occupies 90% of the total karst mountain area. The annual mean eroded modulus is 265.5 t/km². The total eroded amount in one year is more than 18,000,000 t. According to the statistics the soil erosion area is more than 70% in the peak cluster mountain area in the southeast of Yunnan. The annual mean modulus in one year is up to 380 t/km². The soil ero-

sion area is up to 253km² in the erosion researched region of the peak cluster mountain, Xichou county (Song Linhua, et al. 1991, Synthetical research on the water, soil and biological resource in the karst peak cluster area). It occupies 76% of the total area in the region. The annual mean eroded modulus is 387.7 t/km², and the annual eroded amount is up to 98,100 t or similar. (Tab. 1.12.1.)

The soil erosion grade of intensity in the karst mountain area is mainly middling and strong erosion. Regardless the proportion-distributed area or amount, the middling and strong erosions are both proper. This reflects the soil erosions in a serious situation in the karst mountain area. Among the soil erosion distribution area in the Guangxi province, the erosion area serious is like the middling one up to 11,794 km². The homologous erosion amount is 17,100,000 t. These occupy a part of 80% of the total erosion area, and 95% of the total erosion amount. In the erosion research area in the peak cluster mountain of Xichou in the southwestern Yunnan the middling and the strong erosion area is 208km², and they occupy 82.2% of the total erosion area. Its erosion amount is 95,850 t, and occupies 91.7% of the total erosion amount.

The latent dangerous degree of the soil erosion is extremely serious. Influenced by the steep slope, and the special soil forming factors in the karst mountain area, the slope soil layer is often shallow and slight. The average soil layer thickness is 30–150

cm on the peak-cluster slope in the western Xichou (Tab. 1.12.2.), and less thick, only 30-60 cm, in the Nonggang peak-cluster slope of Guangxi. By the steep slope condition, and by no protection of the forest the soil layer erosion would arise more seriously, and the erosion intensity would increase rapidly. According to the observation of the erosion serious site of the Longtan peak-cluster slope of the western Xichou on 6 June 1998 the erosion amounted to 72 t/hectare, and was formed after a storm with the duration of one hour and precipitation of 35 mm/hour. It is equal to the intensity grade of a short dated extreme erosion of 7200 t/km² and the soil layer was eroded to the depth of 5.7 mm. Generally, the bare soil belt with a relative thickness of the steep peak-cluster has an extremely strong soil erosion. The annual eroded depth range to the soil layer is from 5 cm to 10 cm, and at rare places there can be 30 mm. The surface soil layer is eroded to become thin to empty, and the environment develops to the direction of “rock-land mountain” or “rock-desert”. There is the formula for the anti-erosion duration of the soil layer .

$$Ye=Z_0/E$$

In the formula Ye stands for the anti-erosion duration number of a year, Z₀ stands for the effective soil layer thickness(mm), E is the annual eroded depth (mm/year).

In the most of the karst peak-cluster slope in Xichou the soil layer anti-erosion

	I	II	III	IV	V	VI	Total
Erosion grade of intensity	no palpable erosion	slight erosion	middling erosion	strong erosion	stronger erosion	extreme erosion	
Distribution area(km ²)	82	45	81	93	27	7	335
Percentage (%)	24.0	17.8	32.0	36.8	10.7	2.7	100.0
Annual eroded modulus (t/km ² .y)	<46	46–230	230–460	460–740	740–1300	>1300	
Deducted stoneteeth, the eroded depth in fact (mm)		0.08	0.35	0.6	0.8	>1.43	Average 0.542
Annual eroded amount (t)		2250	20000	46500	20250	9100	98100
Percentage (%)		2.3	20.4	47.4	20.6	9.3	100.0

Table 1.12.1 The soil erosion distribution area and the amount of the peak cluster-depression region in the Xichou county.

Note: The soil erosion degree index in the table is worked out according to author's works in the karst mountains region environment in the southeast of Yunnan, synthesized with Cai Zongxin's erosion degree index about the karst area in Guangxi. (1989). Refer to the after mentioned content in the paper and Tab. 1.12.2

year is only 4 - 200 years. They have belonged to the types of dangerous and extremely dangerous erosions. In some parts of the upper peak-cluster slope the stone-teeth or bed rock exposed completely, and the erosion was in a situation of a dilapidate type. The soil erosion area which has belonged to the dilapidate type in Guangxi is up to 18,361 km². It occupies 24% of the total area.

About making out the erosion degree index which fits the karst area

The environment of the karst mountain area has a special character, an especially slow soil formation from the carbonate mother rock, thin soil layer, soil covering discontinuity in the stone-teeth. Although the soil erosion brought about serious harm, the soil erosion modulus is smaller than other non-karst areas in China. In comparison with the soil erosion degree index standard being sued by the Chinese Ministry of water conservancy & electric power after 1984, the soil erosion is less than 700 t/km².year in the most areas of the southern karst mountain, China. It can be divided into a slight erosion level only (the degree index value: 200-2500 t/km².year). The case is not proportionate to that serious harmfulness and erosion latent dangerous degree of the soil erosion in the karst area which has reached a dangerous-destroying type status. Admittedly, the standard of the karst-soil erosion degree index is needed to be made out again. In 1989 Cai Zongxin established the theory of corrosion and weathering in the carbonate rock, residual non-dissolution material to form the karst soil, pro-

pounded the soil-formed modulus value 68t/km².year as the minimum allowable soil eroded quantity, and that the five-grade soil erosion index fits the karst area in Guangxi.

Used for the reference of the means, in accordance with the actual situation of the karst mountain area in the southeast of Yunnan, taking the soil erosion research area of the western typical peak cluster mountain of Xichou as a sample based on the following value: the average corrosion rate of 0.0576 mm/y of the carbonate rock in the area, corrosion modulus 155.5 t/km².y, rock specific gravity 2.7 t/m³, non-dissolution material of karst rock contents 5%, other mixed rock contents 28%, we calculate that the soil-formed modulus is 46 t/km².y, and considering it as the minimum allowable soil eroded quantity volume. And considering synthetically the relative factors of the slope, vegetation cover, latent dangerous of the soil layer anti-erosion year and erosion action type, referring to the grade difference multiple erosion degree index in the non-karst area, the soil erosion intensity index to the graded six degree was made out to fit the peak cluster karst mountain area in Xichou and southeast of Yunnan (Tab. 1.12.2.).

Some scholars discussed the forming process about the weathering crust of the carbonate rock nearby Guiyang (Li jinyang 1991), and propounded the standpoint that mainly the soil-formed action of karst is a different corrosion and selection replacement of the underground water, but not the non-dissolution material residual form karst soil in the carbonate rock. However, the problems are still need to lucubrate and understand fully the soil-formed principle, the migratory process of the material and quantitative analyses, etc.

Erosion grade of intensity		I	II	III	IV	V	VI	Author of degreee index scheme
		tiny erosion	slight erosion	middling erosion	strong erosion	stronger erosion	extreme erosion	
Soil erosion modulus (t/km ² .y)	Guangxi	<68	68-100	100-200	200-500	>500		Cai Zongxin
Soil erosion modulus (t/km ² .y)	Xichou	<46	46-230	230-460	460-700	700-1300	>1300	Author of the paper

Table 1.12.2. Soil erosion degree index in the karst area of Xichou.

Note: The erosion grade of intensity referring in the paper is all based on the index of this table.

Soil erosion types in the karst mountain area

In the karst mountain area there is a variety of the soil erosion types and the various erosion types combination. The hydraulic erosions such as the surface erosion, gully erosion, swill erosion in the rock interval, latent erosion, etc. are the main types; the gravity erosions such as the landslide, rock slip erosion, etc. are the secondary types. Here the typical soil erosion types of the karst peak-cluster of Xichou will be analysed as a sample.

Surface erosion. The splash erosion, sheet erosion and slender rill erosion are included. Their distribution area is the most wide in the research area, occupying 50% of the total area. The erosion intensity vary by the action of factors such as the earth-surface condition, precipitation intensity. It includes the scope of a slight, middling and strong erosion grade.

Splash erosion. Its distribution is broad at the places such as the crest belt of the upper peak cluster slope and the mountaintop, a bare soil surface of a part dry-farming terrace land. Although the karst soil has features of a very heavy texture and strong coagulating power, the splash erosion action is conspicuous, as it is undergone by a rainstorm of a strong rainfall-density, the raindrops kinetic energy is bigger for splashing. The splash erosion causes a mass of soil particles lost stepwise along the slope downwards, so the upper peak cluster slopes and the karst mountaintops can gradually become bare rock conditioned.

Sheet erosion. Distributed in the locations such as sparse thicket and not overgrown slopes, straight plowing dry-land on a relatively thick soil layer-repaired terrace land etc. The erosion intensity may reach the middling and strong grade. For example, at the sheet erosion serious section of the Muzhe mountain and the north peak slope of Dajiechang, the actual measuring intensity is up to 6096 t/km².

Rill erosion. Its distribution is mainly at the location such as a slope tilth and a bare surface-soil on the concave part of the peak slope. Generally, the rill density on the slope

of the karst mountain area is not so high. It often has the shape of a sparse furcation and intersection. However, it has a relatively high erosion volume. Its erosion intensity is higher than the strong level.

Gully erosion. Its distribution is mainly in the thick-layer soil locations such as the slopes and foot slopes of the peak cluster. The distributed proportion in the research area is relatively low, but the erosion action is the most serious. The erosion intensity often belongs to the stronger and extreme grade. Restricted by the factors of topography and soil layer thickness of the karst peak cluster, its shape can be divided into two main types: shallow gully and incised gully.

Shallow gully erosion. Generally, in the bare thick soil part of the nether peak cluster slope and the foot slope the big current of water has washed the broad and shallow groove gullies side by side. The gully breadth is often 1-2 m, the depth <1m. There is gravel at the bottom of a shallow gully erosion location on the slope nearby the Doukan village of the Bengu town.

Incised gully erosion. It is formed by some shallow gullies developed ahead. Its gully-wall is almost erected, gully base reaches the bed rock the stoneteeth has outcropped. The amount and range of the incised gully both is less than a shallow gully. However, the erosion intensity can augment up to an extreme erosion grade. For example, several incised gully developed at the peak cluster slopes in the north of the Benggu reservoir and near the Xiaba wei village, their width is 4 m, and depth 3.5-4 m or the like.

Swill erosion in the rock interval. It is a special erosion form in the karst mountain area. Its distribution is on some karst mountain slopes, with a wide stone-teeth outcropping. On the bare surface slopes that have been denuded long, the relic soil in the rock or stoneteeth interval there is still swilled and eroded by a turbulent runoff to flow together in the rock interval, when heavy rain and rainstorms. But the soil swill erosion is bare when there is a slight and moderate rain, as the rain water infiltrates mainly in soil. It has the an

intensive range of a slight and middling erosion grade, but its harm is so serious that the relic soil is still extinctly eroded until the surface slope becomes a rock desert.

Latent erosion. It is a special erosion form in the karst area, too. In some thick-layer soil places of a karst gentle slope land, table land and depression, the same conformations as a soil cave, blind gully and collapsed hole are formed by the karst latent action of the ground water. Typical samples are those big collapsed holes, each eroded soil volume of more than 1000m³ in the land of the Longtan, Bawei, Shangjinzu village.

Landslide. It often occurs in the belts of local cliff or rock-walls beside highways to be built on steep slopes in a peak cluster. The slope inclination angles of the occurrence place are often in a range of 60-90. The rock layer vertical joint develops well. The rock and soil is in a latent unstable condition. The traffic in some sections of the highway in the research area of Xisa-xinjie, Mozhe, Longzheng is stopped, during the rainy season, due to the action of the road cliff avalanche.

Rock slip. Its occurrence is lesser and its size is small. On 19 September 1974 a rock slip occurred at a fastigate-peak hill nearby the Xinqin village of the Fadou town. One carbonate rock layer slid entirely along the smooth slant occurrence from the hill-top to the middle downwards. It is a type of a shallow layer rock slip. The amount of slide is 360m³, to heap up the foot slope.

A combination erosion type. The main combination types have the following: splash erosion—sheet erosion—rill erosion slope, splash erosion—swill erosion in the rock interval erosion slope, rill—shallow gully erosion slope, shallow gully—incised gully erosion slope, sheet erosion—shallow gully erosion slope, swill erosion in the rock interval—shallow erosion slope, incised gully—latent erosion, etc. Due to different erosion conditions on the slope, the distributed variation of each erosion shape is relative higher. The erosion combination type is different in the small drainage areas of each peak cluster depression.

Soil erosion occurrence and active regularity

Distribution regularity. (1) According to the analysis of the occurrence position of soil erosion types in the karst mountain area, surface erosions and gully erosions are mainly distributed in the belt with the bare desolation slope where the gradient is more than 25, the sparseness sward, the tilth in the same slope strike etc. Latent erosion is main occurred depression place nearby the underground water belt. The landslide and rock slip erosion occur on the unstable slope position in the local steep rock.

(2) According to the analysis of the erosion intensity, the erosion intensity varies relatively widely due to the diversity of synthetic factors among the ground form, slope, the combination proportion between the soil cover and the stoneteeth, vegetation cover. As a rule, in a good cover vegetation place as a hillside, a step land, there is mainly a slight erosion. In addition, in a place with the slope angle more than 40, bad vegetation, relatively deep and bare soil layer in parts, there is a strong erosion. It may go into a stronger and extreme erosion. The middling and strong erosion between the two cases have a widely distribution area, and a maximum proportion of the total erosion volume.

Active regularity. (1) Annual seasonal variety of the soil erosion is outstanding. Influenced by the precipitation condition directly, the erosion accord with the strong precipitation activity. The rain is focused to 5-10 months of the rainy season every year. In the rainy season each type of erosion occur widely and strongly. The erosion volume is above 90% of the total in the whole year.

(2) The whole soil erosion process is the following: Firstly, the erosion is focused on the peak cluster slope; secondly, the erosion material is deposited at the depression place; lastly, the deposited material is lost into the subsurface system through a latent action of the swallow hole, taking the depression as the function of a transfer station.

Soil erosion genesis factor in the karst mountain environment

Tectonics and Geomorphology

The landform in the karst mountain area, especially in the peak cluster area is undulate ruggedly. The relative height difference in the Xichou peak cluster depression is 100-290 m. The statistics of its slopes angle: the slopes that the angle is greater than 35° are above 82.75% of the total slopes. The slope which reaches the maximum repose angle (more than 45°, Tab. 1.12.3.) for loose debris and soil, is up to 41.36% actually. It is advantageous for the activity of gravity erosion and hydraulic erosion.

The research region is located in the northeast of the Wenshan huge rounded rotation and distortion tectonic. It belongs to the uplifting and swelling region from Tertiary. The erosion basis descends widely. Therefore, it provides the physical energy for the erosion activity. The lithologic character of the carbonate rock is mainly hard, pure. The karst formation rate of the soil to the eroded weathering rock is very slow. It will last 17,360 years to weather a thick rock of 1 m, then to form a soil layer less than 10.6 cm. So it makes the anti-erosion fixed number of years of the karst soil very low.

Climate condition

The average precipitation in the Xichou research region is 1300 mm.y. It is mainly focused in the months from 5-10. The precipitation in the rainy season occupies 83% of the whole year. It is often the spate or rainstorm. From 1962 the rainstorm times occupy 88% of the whole year. The maximum value of the daily precipitation intensity is more than 135 mm.date. The maximum precipitation in 1 hour often exceeds 30 mm. According to the field observation data, on the bare slope in the peak cluster with the slope angle of 30 degree with the

soil layer water content of 25.3% the initial erosion precipitation is only 5 mm/30 minutes, the serious soil erosion will occur.

Soil factor

The karst soil formed by carbonate rock weathering and residua has a character of a heavy texturebad perviousness. According to the sampling analysis in the Xichou peak cluster area, the clay granule (with a radius less than 0.005 mm) content is from 65% to 99% high. This causes it easy to form a relatively big soil surface run-off volume. Another reason is that the anti-erosion action decrease for the reaction by the dry-humid-warm paleo-climate, it is evident that the leaching and chemical weathering function, mainly clay mineral, includes kaolinite and vermiculite; and the soil structure is very close and tight, a strongly expanding and shrinking property, softening and fluidity after the saturated water to form a cylindrical shape after an evaporating deaqua-tion. Furthermore, due to the thin soil layer and a smooth contiguity face between the soil and rock, it is very easy to be separated and lost.

Vegetation cover condition

Forest and vegetation is the essential factor to prevent and conserve a good karst environment. Most of the vegetation in the area like calcite is drought-enduring. Due to the vegetation growth on the rock with an advanced root system penetrating into the rock interval, it has an obvious efficiency to prevent the peak cluster slope and anti-erosion. It can be indicated from the experiment observation result of different vegetation slope conditions in the research area. (Tab. 1.12.4.). The vegetation covers rate in the research area decline from 30% to 40.7% in last 30 years. Most of the slope is covered by sparseness bush follow and

Slope angle degree	<25	25-35	35-40	40-45	45-50	50-55	>55
Proportion of slope amount	11.73	5.52	19.32	22.07	19.31	13.79	8.26

Table 1.12.3. The statistics proportion of different slope degrees in the Xichou peak cluster area.

Observation place	Vegetation condition, cover proportion(%)	Date	Precipitation (mm)	Initial intensity precipitation (mm/30 minutes)	Run-off sand content after 10 min. of slope flow (%)
Back slope to Broadcasting station	Higy structure, bush, shallow, grass, 100	1988.6.27	34.3	16.4	0.022
Measuring area I of Huaguoshan	High density Brushwood, 100	1988.6.27	34.3	16.4	0.035
Measuring area II of Huaguoshan	Spareness bush brushwood, 40, 40	1988.6.27	34.3	16.4	0.611
Measuring area III of Huaguoshan	Bare soil, 0	1988.6.27	34.3	16.4	>2.274

Table 1.12.4. The relationship between different vegetation condition and run-off sand content in Xichou peak cluster research area.

bareness slope. It provides a broad space condition for the erosion.

Human being factor

The karst mountain area has a high-density population, the population density in

Xichou is 180.5 person/km². The production and live style cause more unreasonable activity of destroying forest to plantation plowing, culturing on the steep slope, denudation forest for firewood, mining, in building roads leaving around waste residue. It is the main reason of intensifying the erosion growth.

2

South
Karst Studies
China
in W Guizhou
Karst

I

INTRODUCTION

In order to carry out the Protocol of the first session of the China-Slovenia joint committee for scientific and technological cooperation: the project of “Karst Environment Protection and Exploration of Cave Resources” was established, a group of three researchers from the Institute of Geology, Chinese Academy of Sciences (IGCAS) invited by the Karst Research Institute (IZRK) ZRC SAZU visited Slovenia to study on karst caves for two weeks in 1995, paying an official call to the Ministry of Science and Technology of the Republic of Slovenia, IZRK ZRC SAZU and Research Centre, and discussed about further joint research project. The Liupanshui city and its surrounding area were selected as a research area in Guizhou, China. A publication of monograph in English and a round-table scientific conference on the cave genesis in both tropical and subtropical area, the development of cave resources and environmental protection and some contrast research on karst and cave development between the Mediterranean climate area in Slovenia and



Reseachers from the Institute of Geology, Chinese Academy of Sciences and the Karst Research Institute ZRC SAZU at Yezhong plateau, Guizhou (Photo Shi Mengxiang).

subtropical area in South China have been planned to be realised after finishing the field work. Two scientists from IZRK with Chinese colleagues worked in the karst area of West Guizhou in the same year. Followed by the second session of the China-Slovenia joint research project of Karst Environment Protection and the Development of Cave Resources was signed in September 1996 and a group of three consisting of a researcher from IGCAS with two leaders who are in charge of science and technology and agricultural and environment of Liupanshui city visited Slovenia with a special subject: The prevention and control of karst desertification and the development and utilisation of cave resources, aiming at a promoting the transformation of desertification in those of poor Liupanshui area. The researcher left there to go on their special work on "The carbon dioxide content of air and earth in karst area" after visiting group.

Four researchers from IZRK worked in Liupanshui area in 1996. The substance of study included as follows:

1. Surveying of the Tianshengqiao-Natural Bridge of Shuicheng, a cave system of Yanzhidong cave and Xiongjingdong cave of Xinchang, Liuzhi, providing scientific basis for evaluating and developing these caves as a resources of tourist scenic.

2. Karst research for carbonate rocks massif in Yezhong, north bank of Beipanjiang river, including a background of geology and hydrogeology, and an evolution and development of landforms.

3. Making an exploration for the problem of karst desertification, especially for the prevention and cure in the typical victimised area - Taisha, Shuicheng.

4. Making an on-the-spot survey of the profile from Guizhou mountain area with 1000 m a.s.l. to Yunnan plateau 2000 m a.s.l. so as to give a comprehensive understanding of the karst in Yunnan-Guizhou plateau. Along the profile, the karst developed background of some sectors, karstform and landscape and the development of hydrosystem, some well-known show caves and typical karst phenomena, such as Zhijindong cave of Guizhou, the Mabeiehe gorge of Xingyi in Guizhou, Lunan Stone Forest and Wolongdong cave of Jiuxiang, Yiliang in Yunnan have been investigated, covering a limits of karst research area at 25°20'- 26°40'N and 104°-105° E.

2. 1. THE PLATEAU KARST OF EAST YUNNAN AND WEST GUIZHOU

Zhang Shouyue

Physical Geographic and Geological Setting

Physical Geography

The plateau karst of East Yunnan and West Guizhou is located at a scope of 24° 40'-26°40' N and 103°-106° E. It is occupied the second grand terrace in the south among the biggest three grand relief terraces of the giant landform structure in China, Wumengshan and Niushoushan mountain ranges of NNE trend with an elevation of 2400-2500 m, and some 1000-2000 m a.s.l. of big basins, which forming the watershed between Jinshajiang and Wujiang rivers of Changjiang river basin and Nanpanjiang and Beipanjiang rivers of Zhujiang river basin.

With the strongly uplift of the Qinghai-Xizang plateau since late Cenozoic and the settle of the eastern plain of China, the basic outline of modern landform and the regional geomorphologic differentiation were formed. The crustal movements lay a difference of giant geomorphology, the distribution of morphologic units of mountains, plateau and basins are controlled and influenced by the geological structures and petrologic properties.

The plateau surface in West Yunnan keeps well with 2000 m a. s. l. and less un-

dulating terrain and a relatively height of 100 - 500 m in general, being a middle altitude hill and low relief middle altitude mountain.

The plateau faces West Guizhou becomes middle relief and middle altitude mountain, and middle altitude hill with an elevation of 1300 - 1400 m to the Central Guizhou gradually, and reaching 300 - 400 m of a cutting depth on the both side of main river only, show a mountainous landscape.

The difference of river levels between Sanchahe river at the upstream of Wujiang river and Beipanjiang river is 500 - 600 m and the distance from incised gorge of Beipanjiang to watershed occupies about two thirds of the distance between two rivers (Table 1.). The NE-trending uplift in West Guizhou formed the watershed separating the Sanchahe river with U-valley and Beipanjiang river with V-valley. It is shown that both sides of watershed have the different characters on the neotectonic movement.

Climate

The research area belongs mostly to humid climate of subtropical monsoon type (aridity < 1,0), located in south part of the mid-subtropics. The area has an annual pre-

BEIPANJIANG	DISTANCE	WATERSHED	DISTANCE	SANCHAHE
(m)	(km)	(m)	(km)	(m)
1170 (Pingzhai)	17	2300-2400 (Dashan)	11	1650 (Dahebian)
980 (Chahe)	23	200 (Huakouzhai)	16	1590 (Xiabawa)
625 (Shahe)	19	1800-1900 (Duojiào)	13	1150 (Yanjiao)

Table 1. The elements of topographical section between Beipanjiang and Sanchahe rivers

precipitation about 1100 - 1400 mm, concentrating it from May to October and making up 80 - 85 % of the whole year except some 1000 mm of precipitation only on the west edge of east Yunnan plateau. It is a semi-humid climatic area (aridity 1,0-1,5).

The regional climate is influenced by dry-cold air current from north and dry-warm air current of Indian continent in winter and spring. Hindered the warm-wet air current from moving to the west by Wumeng mountain range which is on the border of the west part of East Yunnan plateau, the west part of research area has a climate of low humidity and less precipitation. Most part of the east side of Wumeng mountain area appears a high humidity with plenty of precipitation, forming a precipitation centre of West Guizhou.

Geotectonic geology

The research area is situated in the south-west part of Yangzi block. Its basement consolidated in Late Proterozoic and relatively stable period from Sinian to Middle Triassic, except fissure eruption of Omei basalt in Late Permian.

The Mesozoic and Cenozoic are important periods for the diastrophism, three strong tectonic movement within slab had been occurred. There was Indochina movement in Early Mesozoic, Yanshan movement of Jurassic and Cretaceous and Himalayan movement of Cenozoic, having an appearance of mantle fold, lift and basin structure. It is folded and faulted by the strong tectonic movement in Yanshan period all over China, resulting in overthrust wall by the stress action during the collision and impacting of Pacific, Indian Ocean and Eurasian plates.

After the second episode of Himalayan movement in the end of Miocene, a plain land form was formed and the third episode of Himalayan movement beginning at the end of Pliocene was the tectonic movement of the most great influence upon recent tectonic deformation and geomorphologic evolution of China. The Western China underwent an intense uplift and

a continuing uplift of the plane of denudation formed before Quaternary in Eastern China.

Reaching a rise scope about 1000 - 2000 m from east to west in the research area, the active Xiaojiang fault in north-south trend was developed in the west of the research area, a series of basin structures was developed along the active fault.

There are Shuicheng, Anshun, Qujing, Panxian, Yiliang and Luoping sheets in the research area according to the scale of 1 : 200000 geological maps.

Stratigraphy

In the West Guizhou, the carbonate rock's facies are mainly Carboniferous, Permian and Triassic amounting to several thousand meters in total thickness. Among them, the carbonate rocks of 1715 - 5644 m is in Shuicheng sheet, 2564 - 6170 m in Anshun sheet and 1431-6611 m in Panxian sheet.

Before Carboniferous, the area and the thickness of strata cropped out very small, Lacuna completely or partly from Cambrian to Devonian in many regions.

Carbonate rocks deposits in the East Yunnan can be found in the strata of Sinian, Cambrian and Devonian to Triassic, the total thickness is relatively reduced than in Guizhou, the thickness of carbonate rocks on Qujing sheet is 1282 - 3373 m, Yiliang sheet 3153 - 3738 m and Luoping sheet 3432 - 4599 m respectively.

Dengying group at the upper part of Sinian in the East Yunnan are light colour, sparry dolomite and stromatolite dolomite, being of siliceous in some area.

There are Cambrian system with mainly clastic rocks sandwiched in dolomite, Ordovician developed only clastic rocks of lower series about 100 m in thick, middle and upper series of Silurian with clastic and carbonate rocks, light colour thick bed micrite dolomite, breccia dolomite and biolimestone in middle and upper series of Devonian.

Carbonate rocks is widely developed in East Yunnan and West Guizhou during

Carboniferous to Middle Triassic and separated by noncarbonate rocks, such as clastic rocks with coal in the bottom of Carboniferous, clastic rocks in the bottom of Permian, Upper Permian basalt and coal series and clastic rocks series at the bottom of Lower Triassic, forming three karstific formations of Carboniferous, Permian and Triassic.

Carboniferous of East Yunnan contains coal and clastic series in its bottom, varying in thickness from several metres to over hundred meters, thickness is increasingly to the east and changes to contain Carbonaceous only.

Most of carbonate rocks of Carboniferous in the area are limestone with light colour thick layer, dolomitic limestone with increasing thickness to the east.

There are dark colour carbonate rocks with a large number of chert concretion, reaching a thickness of 1500 m in Shuicheng area. Part of the area has clastic rocks in Lower Permian bottom with coal layer, the thickness ranges from several metres to over hundred meters in the west part and increases to several hundred metres to the east.

The carbonate there consists of Qixia group at the lower part and Maokou group on the upper part, Qixia group characterising as a deep colour limestone with chert concretion and about 100 - 200 m in thick, Maokou group with a thickness varying in 200 - 700 m and increasing from west to east mainly with light colour limestone and chert concretion limestone.

Basalt in the lower part of Upper Permian changes thickness greatly from several ten metres to hundreds and loses in some area, being of 100 - 200 m in thick or even thicker in the coal series and clastic rocks series on the upper part.

All the rocks in the lower part of Lower Triassic are sandstone with purplish red and greyish green colours and mudstone with several hundred metres in thick except the east part of Anshun sheet covering micrite with some 500 m in thick and light colour of thin to mid-thick bed. The upper part of the rocks are limestone, dolomite and breccia with several hundred metres in thick.

From the bottom to the top of Middle Triassic, there are clastic, limestone and dolomite, varying several hundred meters to thousand in thick and limestone with chert concretion and dolomite on the top.

All the continental sediments are scattered since the Late Triassic. A plenty of mammal fossils in the middle and Late Pleistocene were sampled in the cave sediments in West Guizhou.

There are the most abundant in mammal fossils and some cultural excavated from the travertine with light yellow and yellow colours, loam and the breccia at Shilidong in Panxian. The fossils including six orders and thirty-nine species are South China's Ailuropoda-Stegodon fauna of Middle and Late Pleistocene. Flora fossils of Early Pleistocene was excavated in yellow travertine at Dongshan temple in Xuanwei. Pleistocene travertine could be found at the east side of Lunan basin.

Karst of the East Yunnan and West Guizhou Plateau

Within the scope of six hydrogeological maps as mentioned above, karst area reaches to 24.299 km², occupying 55 % in total area of the maps and varying in size from 35 % to 72 % of the map area.

According to the karst zonation of China, the research area belongs to Yangzi block karst area in Porterozoic to Mesozoic carbonate of corrosion and erosion-corrosion region of tropical and semi-tropical humid climate type.

The carbonate rocks system being of same geological time and the same geological history and the characters of crustal movement, it is of similarities on the karst formation, the karst evolution and the space of rock massif.

The differences are determined by some types of karst landscape resulting from the actions of endogenetic and epigenetic forces, some features of karst stage and karst phreatic hydrogeology are represented by the certain karst landscape correspondingly. Therefore, three sub-areas are divided according to the types of karst landscape,

such as East Yunnan (plain-hilly plateau karst), West Guizhou (uvala-qiufeng 1, mountain plateau karst) and Central Guizhou (plain-qiufeng and fenglin 2, mountain plateau karst) (Zhang et al. 1979).

1. Qiufeng: A type of cone karst which is characterised by gently sloping, hemispherical limestone hills, the diameter being times the height. Qiufeng is a transliteration from Chinese.

2. Fenglin: Tower karst and cone karst - a transliteration from Chinese.

East Yunnan karst sub-area

The east border from north to south are the line of Longchang, Panguan, Fuyuan, Shizhong along the provincial boundary of Guizhou and Yunnan. The plateau was formed upwarping continuously since the third episode of the Himalayan movement in the end of Pliocene of the peneplain formed in Pliocene. The movement of fault block differences during uplift caused separation and was out of shape to the peneplain, but still remains the character of plateau surface well.

The hilly plateau surface with an elevation of some 1800 - 2000 m are distributed mostly, several fault blocks varying in uplifting scope forming low relief mountain and fault basin. Although an uneven uplifting of the crust, the height of separated peneplain was distributed from 1800 m to 2300 m, part of sector reaching to 2600 m and the mountain is similar to the hilly plateau surface in morphology, all of them being in wave, only ten to tens meters of the height differences between mountain and valley in shape.

At the top of the mountain are relatively gentle with perfectly round shape and few gulch, developing doline and uvala and covering with red crust of weathering on the surface. The area is always appearing karren field on the top of the mountain and hillslope because of the eroded red soil, it is named as the Stone Forest for some higher karren.

There are undeveloped hydrographic net on the surface, the underground river

system buried not deeply on the surface of hilly plateau, underground river window cave can also be found at the bottom of some dolines, sometimes becoming lakes and underground water of the fault block mountain reaching to a depth of 200 m. Only part of the river at upstream of Nanpanjiang as a base level is the box gorge with a depth about 250 m, and most of the rivers are of a character of light cut plain river, the gradient of longitudinal section in the river bed at upstream of Yiliang is 0,015 %.

The aquifers of carbonate in East Yunnan include Sinian, Devonian, Carboniferous, Permian and Triassic, the total discharge of spring occupy over 99 % of all the springs discharging from various aquifers. The limestone aquifer is heterogeneous and Sinian dolomite is homogeneous, being the best water-bearing bed. The aquifer of Triassic distributes as striped for the folded strata in the east part, most of the karstic forms are contact karst form and the passages develop following the strike.

West Guizhou karst sub-area

The east border along the line of Puding, Liuzhi and Xingyi extending from north-east to south-west. Pliocene peneplain becomes summit plane because of relatively poor preservation, the elevation of 2000 - 2200 m (Shuicheng) decreasing to 1900 - 1950 m (Panxian) gradually from north to south and about 1700 m a.s.l. in Xingyi area, some mountain with relatively high elevation forming by uplifting of fault block.

The character of landform is a step like inclination from NW to SE, the landform is mainly middle relief middle altitude mountain. This is because of neotectonic movement occurring from regional rift along EN-SW direction, decreasing the uplifting area from NE to SE and therefore, developing the river to SE, a series of water falls were developed on tributaries of Nan- and Beipanjiang rivers. The underground river developed well with steps by steps and surface rivers alternate with underground rivers flowing into Nan- and Beipanjiang riv-

ers and some main tributaries with relatively high hydraulic gradient. The former, for instance, Jiulonghe river - Huangnihe river - Nanpanjiang river in Luoping, and the latter, like Daganhe river - Duoyihe river in Luoping and Gesuohe river in Panxian, Wutuhe river in Shuicheng and so on.

The landscapes are uvala-qiufeng mountain plateau karst, being a typical cone karst area. The positive karst landform is peak cluster with main bottom 100 - 150 m in height, 150 - 200 m in diameter of the peak. The peak cluster consists of peak with a slope more than 45 degree and developed doline among them. The density is about 7-8 peaks per square km. Depressions and poljes with relatively large scale can be found along the fault or contact zone with noncarbonate, karstification is deep-seated because of incised river, for example, on a plane of denudation with an elevation of 1500 m at the north bank of downstream of Wutuhe river in Shuicheng, the doline with an area of 700 x 500 m and 200 m in depth was developed.

Wujiadong cave located in Panlong village of east Shuicheng has been explored by China-England Speleological team, the cave is over 400 m in depth being one of the deepest cave in China.

The area distributes karst aquifers mainly Carboniferous, Permian and Triassic, plenty of water occupying 99 % of natural discharge of underground water from various aquifers.

The precipitation and surface water coming from noncarbonate recharge the karst phreatic water and drain into river, the water level and discharge are changed with precipitation. The phreatic water table is controlled by geomorphologic factors, the underground water are buried in a depth of 50 - 100 m or 100 m in the mountain,

except the depth less than 59 m in some large depressions. The water level is changing strongly, and the fluctuation of discharge reaches several tens to hundreds times.

The Central Guizhou Karst sub-area

Only the west part of the sub-area is located within the research area, the plane of denudation formed in early Quaternary with an elevation of 1300 - 1400 m and with a smooth terrain, the wave-like landform in the watershed and the height difference between ridges and valleys are only over ten to tens meters.

The negative karst forms with large scale distribution are polje and corrosive plain, the positive forms are isolated karst cone with a relatively height of 100 - 150 m and sometimes with hum 20 - 30 m in height, it is one of the typical cone karst types.

The area is located at the watershed with strong karstification, the main aquiferous are Permian and Triassic with plentiful karst water resources and smaller buried depth, being of value to develop and utilise.

The underground water is recharged from precipitation, the source of the river is formed mostly by underground river draining to polje or karst plain and very few of them draining to Sanchahe river and Beipanjiang river.

The underground water has small hydraulic gradient at Puding, Anshun, Zhenning and so on because of the wide and gentle landform, recharging surface river to underground river in raining season, the annual fluctuation of discharge for underground river is 3-5 times in general, and the depth of groundwater level are mostly less than 10 m.

2.2. THE KARST ENVIRONMENT AND CAVE RESOURCES OF LIUPANSHUI AREA , GUIZHOU

Shi Mengxiong, Zhang Shouyue

Physical Geography Background

Location and Traffic

Liupanshui is situated in the western part of Guizhou, bordering on the eastern Yunnan. The area has a geographical co-ordinate at 25°20' - 26°55' N and 104°40' - 105°30' E, covering four administrative area of Liuzhi, Panxian, Shuicheng and Zongshan (Fig. 2.2.1.). The area is 9914 km² and with 2.520000 population. It is regions where multi nationalities live in compact communities, including about 640000 in nationalities, like Yi, Miao, Buyi, Gelao, Shui, Hui and so on, which occupy some 26 % of total. The Guiyang - Kunming railway and Yunnan - Guizhou road traverse the area, connecting highway between cities and towns. The new constructed Nanning - Kunming railway and preparing to construct a railway of Neijiang - Kunming and a road of Panxian - Baise will make the area a hub of communication connecting Yunnan, Sichuan and Guangxi.

Geomorphology

The area is located in the central of the Yunnan - Guizhou plateau, being a slope zone of transition from plateau to mountainous region. The relief slopes inclines gently from NW to SE. Miaoling, the main part of mountainous region in the central Guizhou plateau, is the watershed of Yangzhi river and Zhujiang river. The mountains within the boundaries of Liupanshui belongs to Wumeng mountain area, having

several tens mountain peaks with 1700 - 2700 m a.s.l.. The highest in this area is Jiucaiping with 2900 m a.s.l. from north to south, bordering provinces for Yunnan and Guizhou generally. Plateau landscape with smooth terrain is in the west of 2000 -2500 m a.s.l., mountainous region landscape of 1500 - 2000 m in the east, except some areas keeping smooth plateau surface and other mountains becoming fragmented for cutting strongly by the river.

River system

Shuicheng is located in the watershed of Yangzhi river and Zhujiang river, so apart from Sancha river in NE part belongs to Wujiang river system, other river within the area are tributaries of Nan & Beipanjiang rivers - the main river of Zhujiang river system (Fig. 2.2.1.) . Liupanshui area is rich in water resources, according to incomplete statistics, there are 71 rivers with a length of over 10 km, and 14 of them belong to Wujiang river system, 57 for Zhujiang river system of which 44 rivers belong to Beipanjiang tributaries including rivers from north of Yizikong, Laochang and 13 rivers from south belong to Nanpanjiang tributaries (Fig. 2.2.1.). The rivers with an average slope of 0,006 - 0,011 are relatively less at up stream and increasing obviously at down. stream in which the deep cutting valley even reaching to 300 - 500 m, and 1000 m the deepest. The valleys always appear "v" type or box-like with underground flow and waterfall. According to the observation data from hydrostation, the average annual

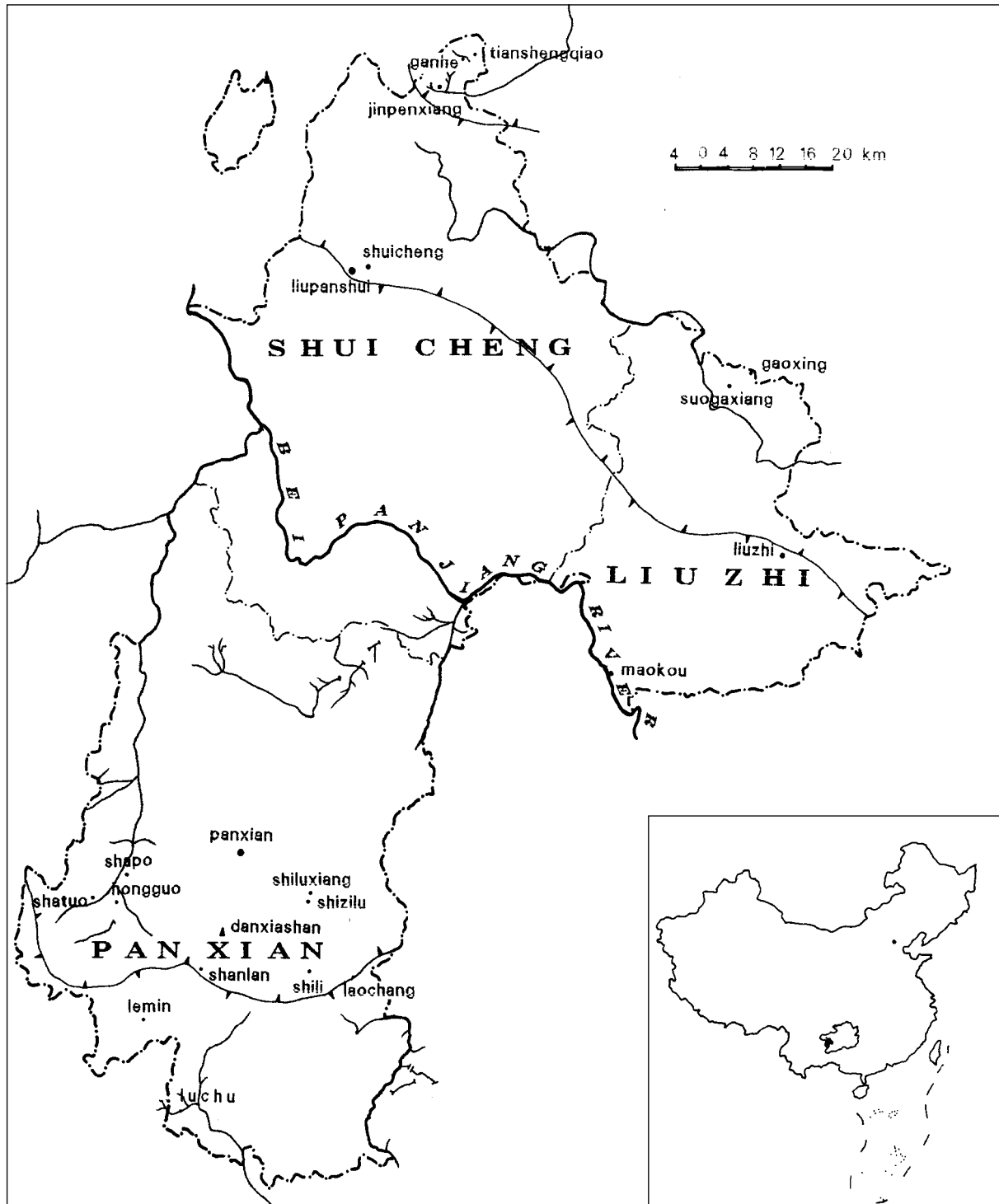


Fig.: 2.2.1. Drainage system and location map

run off of Beipanjiang river is $140,1 \text{ m}^3/\text{s}$. The largest discharge appears in June to September with the extreme value of $2540 \text{ m}^3/\text{s}$. and the minimum discharge is in March and April with an extreme value of $20,4 \text{ m}^3/\text{s}$, and ordinary tributary have an average annual runoff about $10 - 25 \text{ m}^3/\text{s}$.

Surface water and underground river always show a phenomena of replacement, this is also one of the characteristics of karst rivers. In general, rivers in the area have the features of strong abilities in deep cutting, large gradient and rapid current velocity.

	Jan	Feb	Mar	Apr	May	Jun	Jul	Aug	Sep	Oct	Nov	Dec
Liuzhi	15	20	30	100	170	300	279	210	150	140	40	20
Panxian	18	22	29	54	176	277	242	250	183	125	38	17
Shucheng	18	20	21	68	137	236	223	191	150	107	39	17

Table 2. Precipitation (mm/month) in Liupanshui area.

Climate

Being in subtropical zone, the climate is of humid and temperate overcast and raining. The average annual temperature is 12 - 15°C, maximum 20-22°C (July) and minimum 3 - 6°C (January). The climate is influenced by landform greatly because of the mountainous region with higher in NW and lower in SE, having obviously a vertical zonality. There are climate zones divided by elevation and meteorological factors.

ZONE	ALTITUDE	AVERAGE ANNUAL TEMPERATURE
warm	1000-1500 m	18 - 14°C
cool	1500-1900 m	14 - 12°C
cold	> 1900 m	< 10°C

The great changeable climate character, soils and vegetation in the zones make some difference seasons between appearing always midsummer in the valley and cold air in the mountain. The average annual precipitation in the area is over 1000 mm and have a pattern of decreasing from east gradually, but conversely, the evaporation.

From May to October there will be raining season in the area, occupying the rainfall of over 80 % of the year, and dry season from December to next March with about 7 % of rainfall. Tab. 2 shows the meteorological factors.

Tectonics and Hydrogeological Setting

Tectonics

Liupanshui area belongs to the west part of Yangzhi block, it is situated in west Guizhou massif along the east side of Sichuan - Yunnan tectonic zone. The tectonics is mainly linear fold, interbedding

with soluble and insoluble rocks and have a shape of bands appearing in turn. Controlled by tectonics, karstification always developed the some direction with tectonic lines showing distribution of a shape of bands.

According to the direction of tectonics line, the area can be divided into two different tectonic belts. The boundary is from Weining - Suicheng - Liuzhi districts, having Weishui NW tectonic belt with single stable tectonic line on the north and Puan tectonic belt with complex tectonic line to south.

1) Weishui NW tectonic belt with 250 km length and 40 km wide is composed of several parallel faults and of a series brachy - anticlinal and synclinal folds among them, a longer major tectonic is Weishui anticline and Duoque anticline with carbonate rocks of Carboniferous as a axis and Baixing syncline with carbonate rocks of Low Triassic as a axis. The axial of Weishui anticline is 290°- 310°, extending about 50 km with tight fold and slowly at NE wing and steep on SW wing. Duoque anticline extends about 100 km, 10 km wide, with a middle to steep dip angle, developing large faults paralleled the run of the formation. The watershed of Sanchahe river and Beipanjiang river inclines through the anticline. Baixing syncline is an arrested syncline. Wuliudaxiaodong is located the Xinchang massif between the syncline and Duoque anticline. Weichong syncline with a axial of NE, the stratum at core is Jurassic being slowly at NW wing and unsymmetrical anticline with steep SE wing. Suicheng natural bridge was developed in carbonate rocks of NW wing Lower Triassic.

2) Puan tectonic belt: It is an belt of strong interweared tectonics with NW, NE and NNE. Faer tectonic basin is composed of folds and thrust faults, reflecting a multi - direction structure of comprehensive ac-

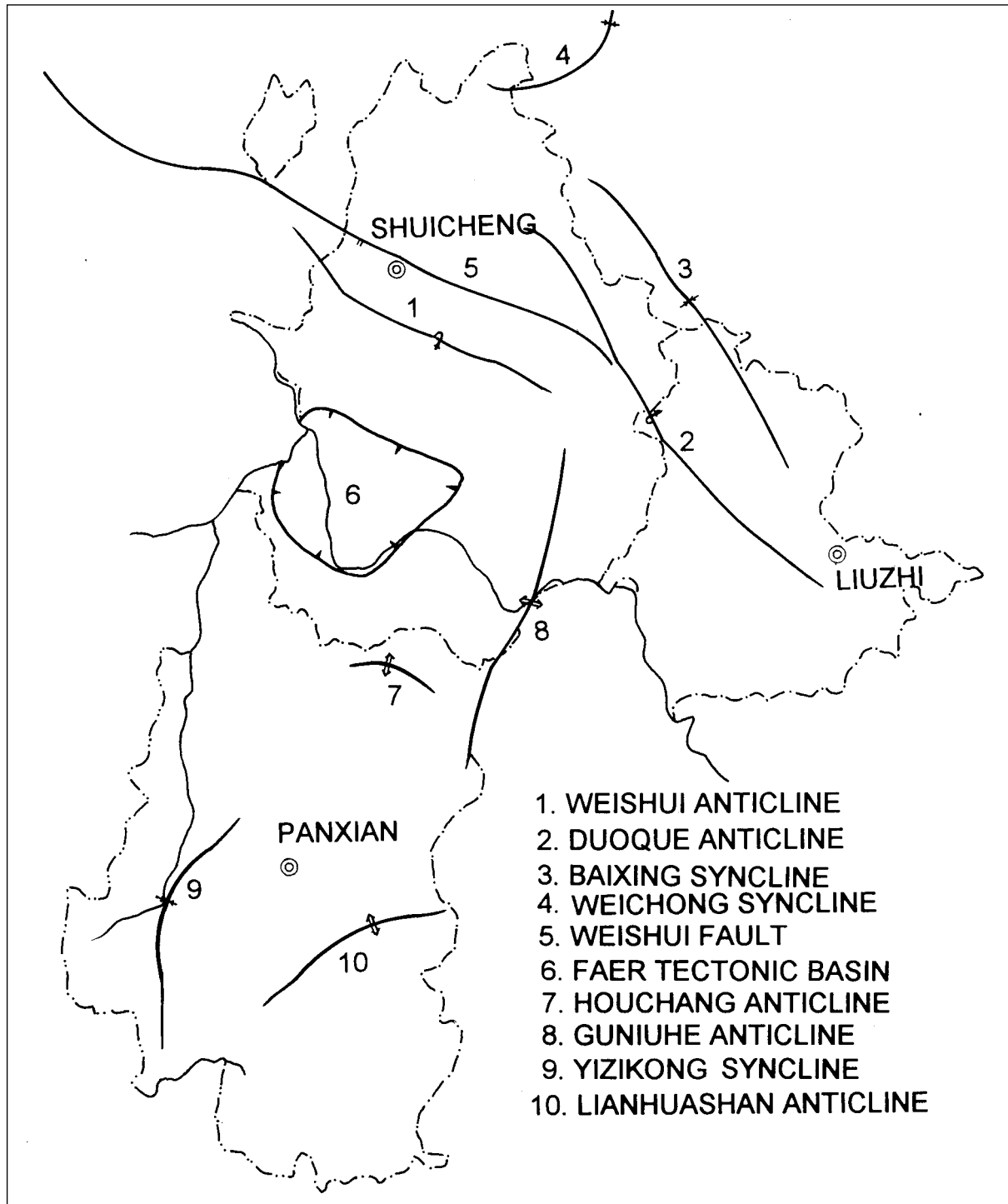


Fig.: 2.2.2. Sketch of structural geology of Liupanshui

tion, having 9 folds over 10 km and 11 faults. Houchang anticline is situated in south part of Faer tectonic basin, axial 325° . The stratum of core part is Mid - Upper Carboniferous with slowly rock bed at both wing and dip angle $10^{\circ} - 20^{\circ}$. Guniuhe anticline is an important part of Puan tectonics, with tight

fold extending to north - south about 50 km, composing of carbonate rocks from Permian to Devonian. Yizikong syncline and Lianhuashan anticline are main tectonics, these folds are composed of carbonate rocks in Permian and Triassic and a little in Devonian and Carboniferous.

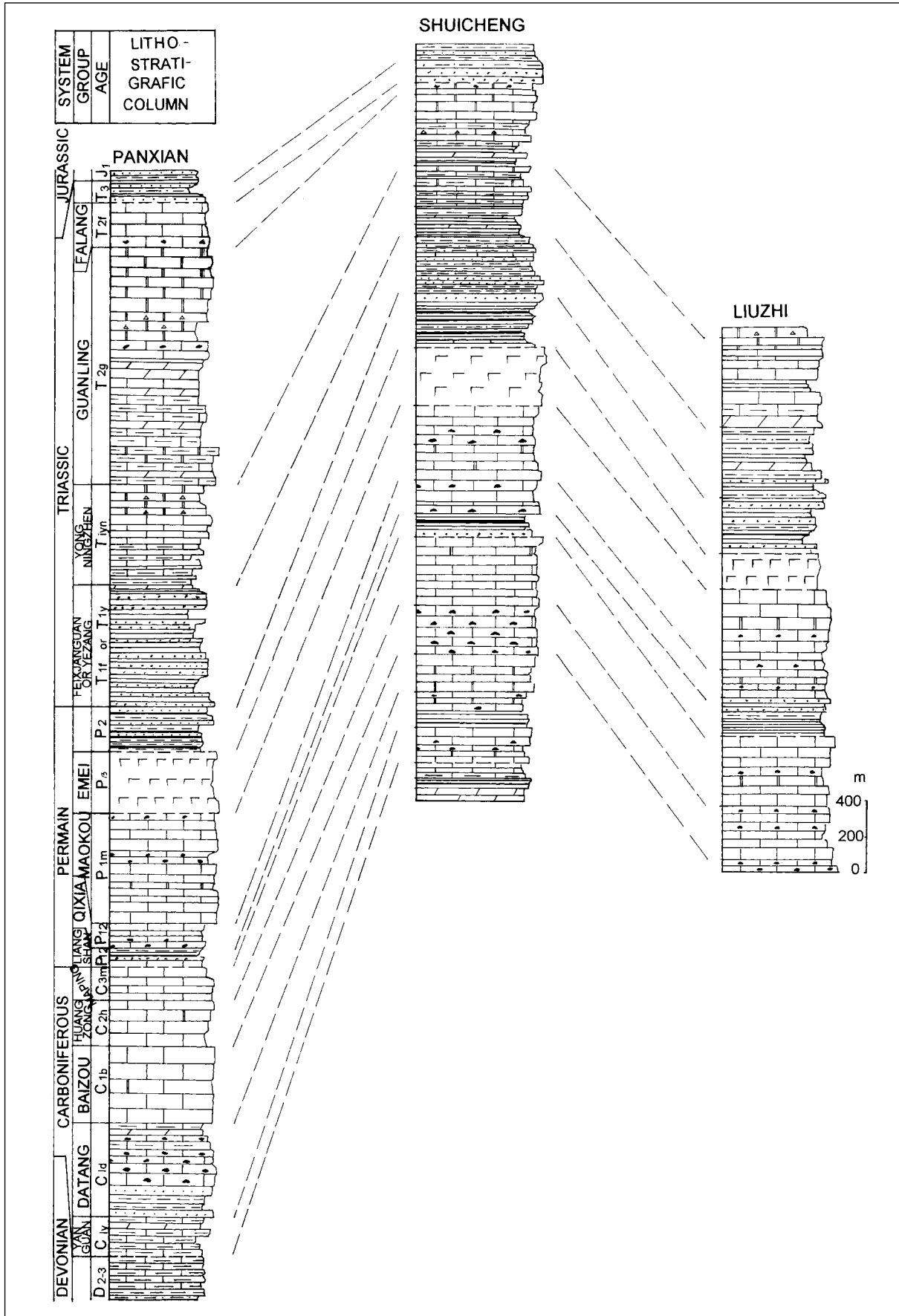


Fig.: 2.2.3. Lithostratigraphic columns of Panxian, Shuicheng and Liuzhi

Aquiferous Formations

The karst water is the most important water resources. The karst water also can be divided into three sub - types by the lithological characters.

1. *The conduit water in carbonate rocks*

The kind of this waters distribute widely, aquifers formations including Lower Permian (P1) and Carboniferous (C) , Middle Triassic (T2) and lower Triassic (T1yn) in Panxian and Liuzhi.

A. Middle Triassic (T2): including Falang group (T2f) and Guanling group (T2g2+3), the lithologic character is mainly mid-thick bedded limestone, argillaceous limestone and dolomite distributed, most of them in a arrested syncline rich in water resources with more than 150 l/s discharge of springs.

B. Lower Triassic Yongningzhen group (T1yn) distributes at the wing of syncline, consisting of thin to mid - bedded limestone, marl, shale, dolomite intercalated with gypsum and breccia, having total thickness from hundred to hundreds m.

C. There are widespread for lower Permian (P1), including Qixia group (P1g) and Moukou group (P1m), thick bedded limestone and black marl sandwiched at the bottom with a thickness of hundreds to thousand. The discharge of spring is about 150 l/s in average. The group have a favourable condition of storing underground water for the tectonics and landforms characters, rich in underground water.

D. Carboniferous (C): There are mid thick bedded limestone on the upper, thick bed massive of dolomite. Limestone and dolomitic limestone in the middle part, thick bed massive limestone at lower part, some layer with flint and strong karstification, the springs with a discharge of about 70 l/s.

2. *The fracture - conduit water in karst carbonate rocks intercalated with clastic rocks*

The group consists of three aquifers, including Middle Triassic (T2) Falang group (T2f) and Guanling group (T2g2+3), Lower

Triassic, Yongningzhen group (T1yn), and Lower Carboniferous to Middle Devonian (C1 - D2-3). The two former groups belong to fracture - conduit aquifer only at Shuicheng. Lower Carboniferous to Middle and Upper Devonian (C1 - D2-3): The lithologic characters in Shuicheng and Panxian are mid - thick bedded argillaceous limestone, marl, limestone intercalated with siliceous rocks, flint layer, shale and basalt of 0,8 m on the top, total thickness of hundreds to thousands without so strong karstification but well developed fracture for flowing out springs with average discharge only 3 l/s.

3. *The karstic fracture water of clastic rock intercalated carbonate rocks*

A. A transition layer of Upper Carboniferous to Lower Permian (C3 - P1): The aquifer distributed in the boundary between Shuicheng and Panxian only, mainly with sandy shale and silicarenite interbedded with limestone, argillaceous limestone and marl of total thickness about 900 m ,with less karstification and undeveloped fracture, so less spring.

B. Middle Triassic Guanling group (T2g1): Only one aquifer in the lower part of Guanling group in Panxian and Liuzhi. The lithological features are mudstone, shale interbedded with argillaceous limestone and dolomite.

Tianshengqiao - Natural Bridge and Cave System In Shuicheng

The geomorphologic unit of area belongs to the low relief (200 - 500 m) middle altitude (about 2000 m) mountain.

Situated at Ganhe village, about 80 km NE from Liupanshui city the tributary of Daganhe river cut here deeply with a strike of NW - SE and the natural bridge crosses above the valley from NE to SW. The bridge surface become a part of the country road between Ganhe and Yantoushang villages. The bridge surface was measured 30 m in both of the length and wide, 15 m of thickness for rock stratum of the roof, 1861m of

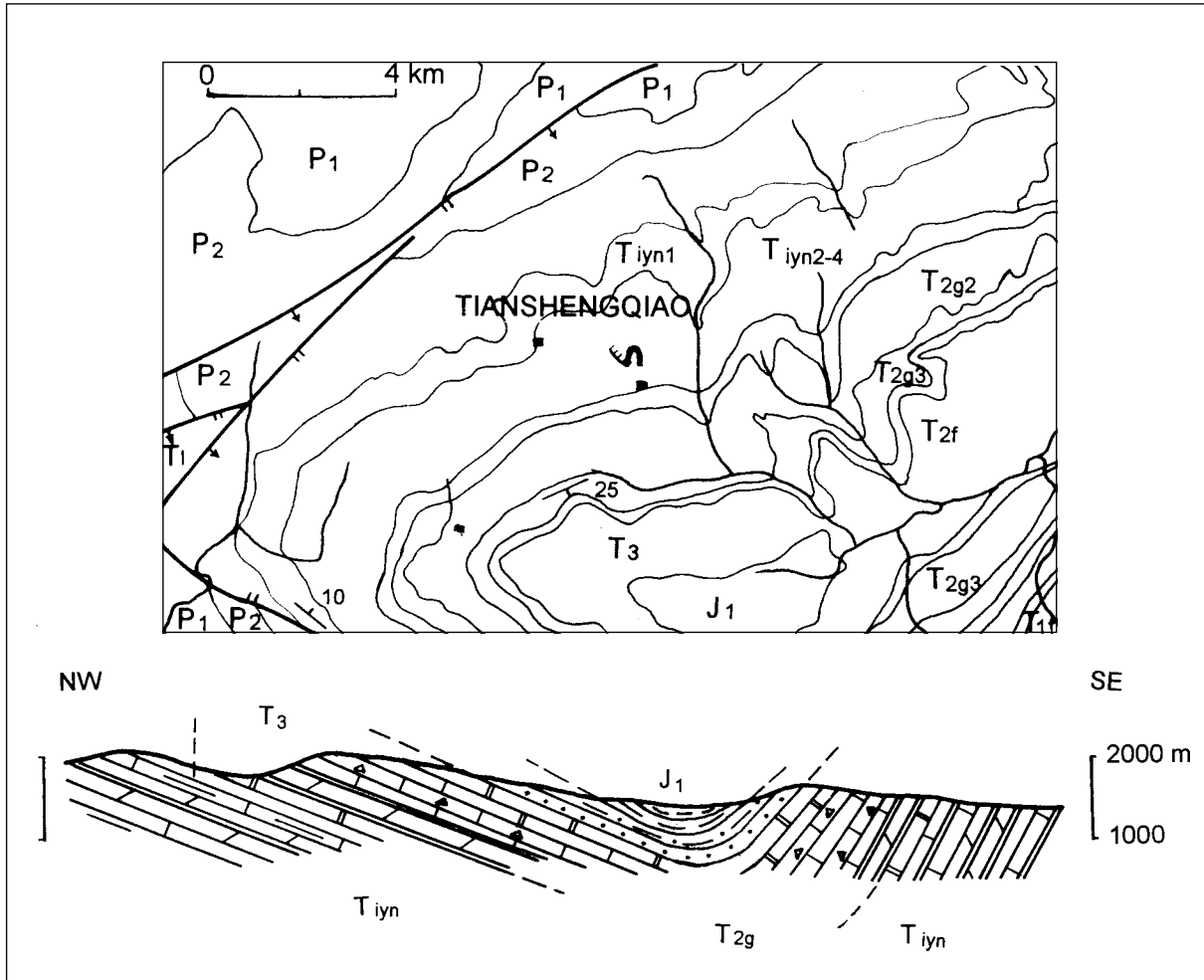


Fig.: 2.2.4. Geological map and section of Tienshengquiao area

elevation from the bridge surface and 1725m from the bottom of the valley, forming a height of 136 m from bridge surface to the bottom. It may be the highest one. There are several caves and small natural bridges around the bridge within an area of 1 km².

Geological setting

Natural bridge cave system Developed in carbonate rocks of Lower Triassic Yongningzhen group (T1yn3) (Fig. 2.2.4.), the bottom of the bridge is seated on the lower part of T1yn3, the rocks are mid-thick bedded grey - purple marl about 30 m in thickness. The natural bridge cave system's tectonic is at NW wing of Weichong syncline. It is an unsymmetrical syncline, appearing gentle on NW wing with a dip 10°-

20° and steep on SE wing with a dip some 60° - 80° (Fig. 2.2.4.)

The natural bridge cave system and it's formation

Natural bridge is developed in the main dry river of the tributary on the west of Daganhe (Fig. 2.2.5.), the total length of the main dry tributary is about 2 km, and the bridge is on the mid stream. Two small natural bridge at down stream and 300m far from the Daganhe, some 1620 m of elevation at the bottom.

Yanzidong cave is a large horizontal cave in research area. The cave situated on the south of natural bridge is a resurgence with elevation of 1725 m. The cave was surveyed 50 m in high and 500 m in length, the most narrow part in cave is less than 10 m and

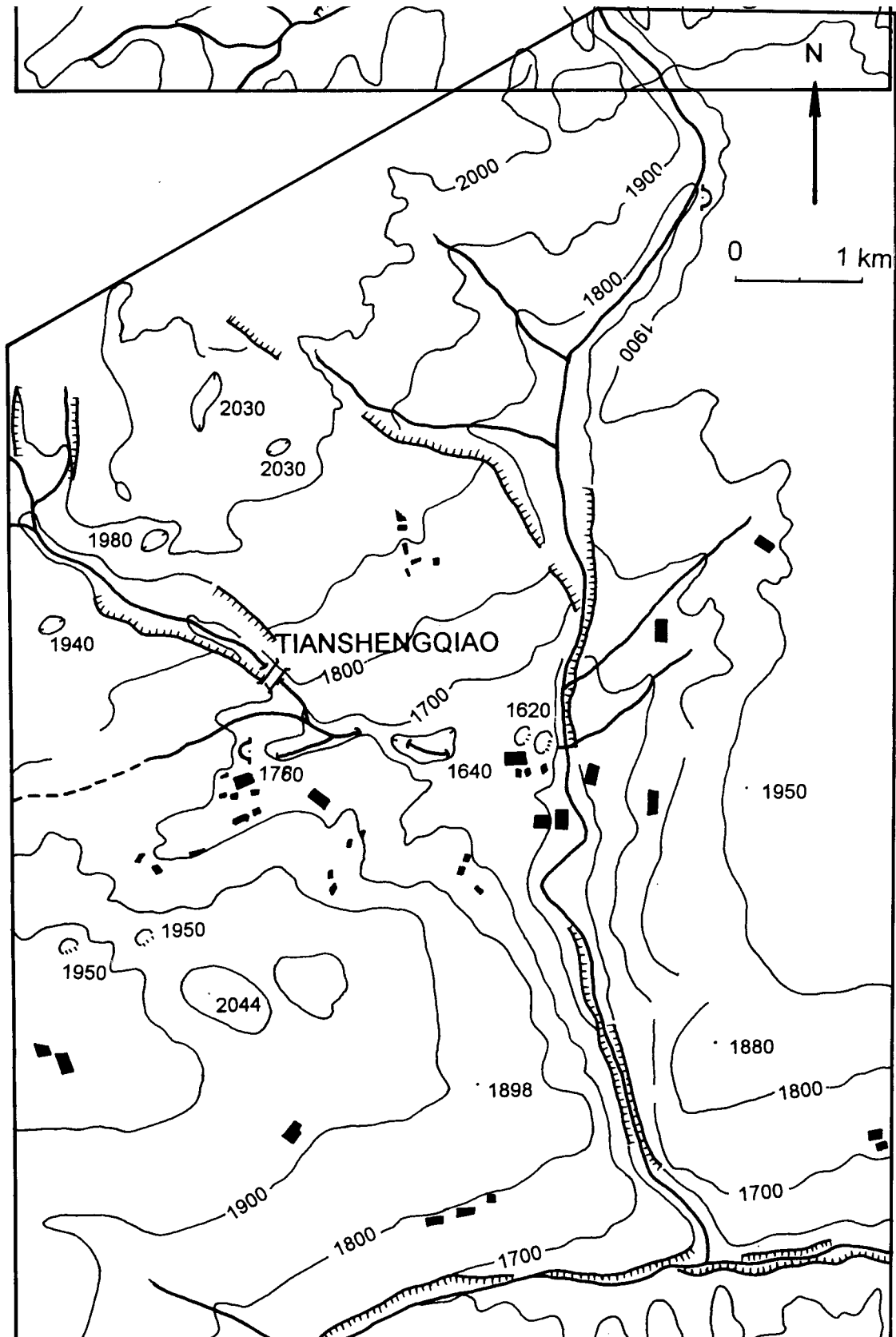


Fig.: 2.2.5. Landform of Tianshengquiao area

widest one 40 - 50 m, the section of cave mouth shows an unsymmetry key hole like and down to underground after running out about 100 m and appears again some 300 m then gathering to the tributary, and then underground again and again and draining to Daganhe toward to the east.

The cave developed in the 4th section of Lower Triassic Yongningzhen group (T₁yn₄) with dolomite of light grey, thin to mid thick argillaceous dolomite, limestone and breccia. The dip of layer is SSE with angle 20 - 25°. Being controlled by the fractures, the cave system especially the older phreatic gallery at right side of ground river shows a chessboard like in plan.

Karst of Yezhong massif

Both west and east sides of the massif are watershed consisting of Upper Permian basalt. In the north, the watershed is

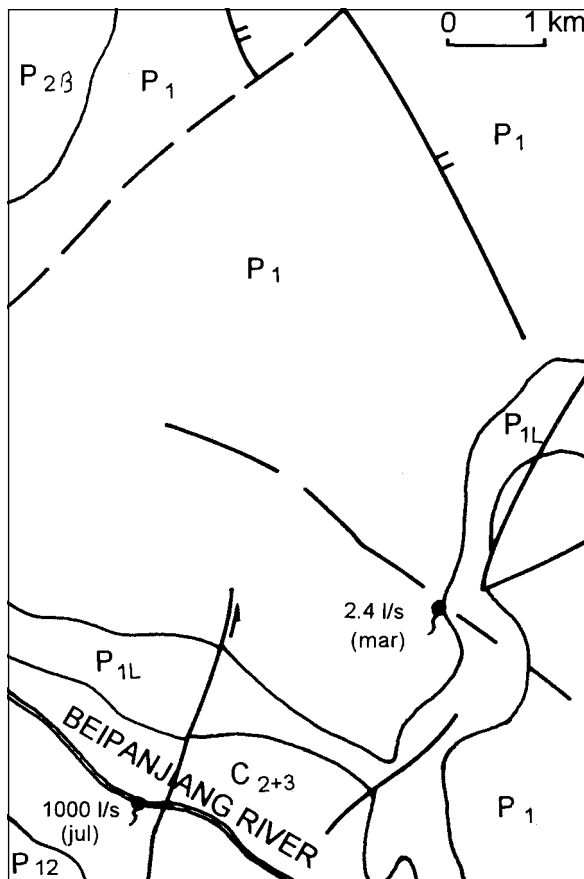


Fig.: 2.2.6. Geological sketch map of Yezhong massif.

landform and the clastic rocks of the bottom of Lower Permian. The boundary of underground water should be the diabase in Lower Permian thick bedded massive limestone with a thickness of 600 m and flint limestone with gentle formation and a dip about 7- 10 degree. Its karstification is controlled by clastic rocks with 150 m in thick at the bottom of Lower Permian(P₁L).

The massif lies to NE wing of Houzi-chang anticline, the axis is NW 325° and rakes to the west, the strata of core is Mid-Upper Carboniferous thick bedded limestone, the Beipanjiang valley developed along the axis, some big discharge and hot springs emerge from the river along NEE-trending fault in Carboniferous limestone.

The carbonate rocks massif hanging high above the base level is the cleuch dissection developing along the fault without big discharge springs and caves along the clastic rocks (P₁L), the massif has been in the vadose zone. A few depressions could be found in the hinterland of the massif with an elevation of 2000 - 2100 m at the bottom and 200 - 300 m in diameter and the deepest one about 70 - 80 m. The area is a typical cone karst landscape, the elevation on the peak top is some 2100 - 2200 m and 50 - 60 m in height of cone in general with a top angle of 110 - 130°.

The evolution of geomorphology can be divided into three phases by the analysis of the plane of denudation. The first phase of denudation plane is composed of cone peaks and depressions or dolines at an elevation of 2100 - 2200 m. The second one is wide valley formed of undercutting on the first plane with 1600 - 1800 m a.s.l. which consisting of a series of poljes and being of permanent or interval surface water. The third one is Beipanjiang gorge, the gorge was formed by the river from the plane of denudation about 1500 - 1600 m a.s.l., undercutting with a depth of 700 - 800 m.

Tourist resources of karst and caves

Carbonate rocks distributed almost all the Guizhou province except south - eastern part, it is one of the typical karst area in

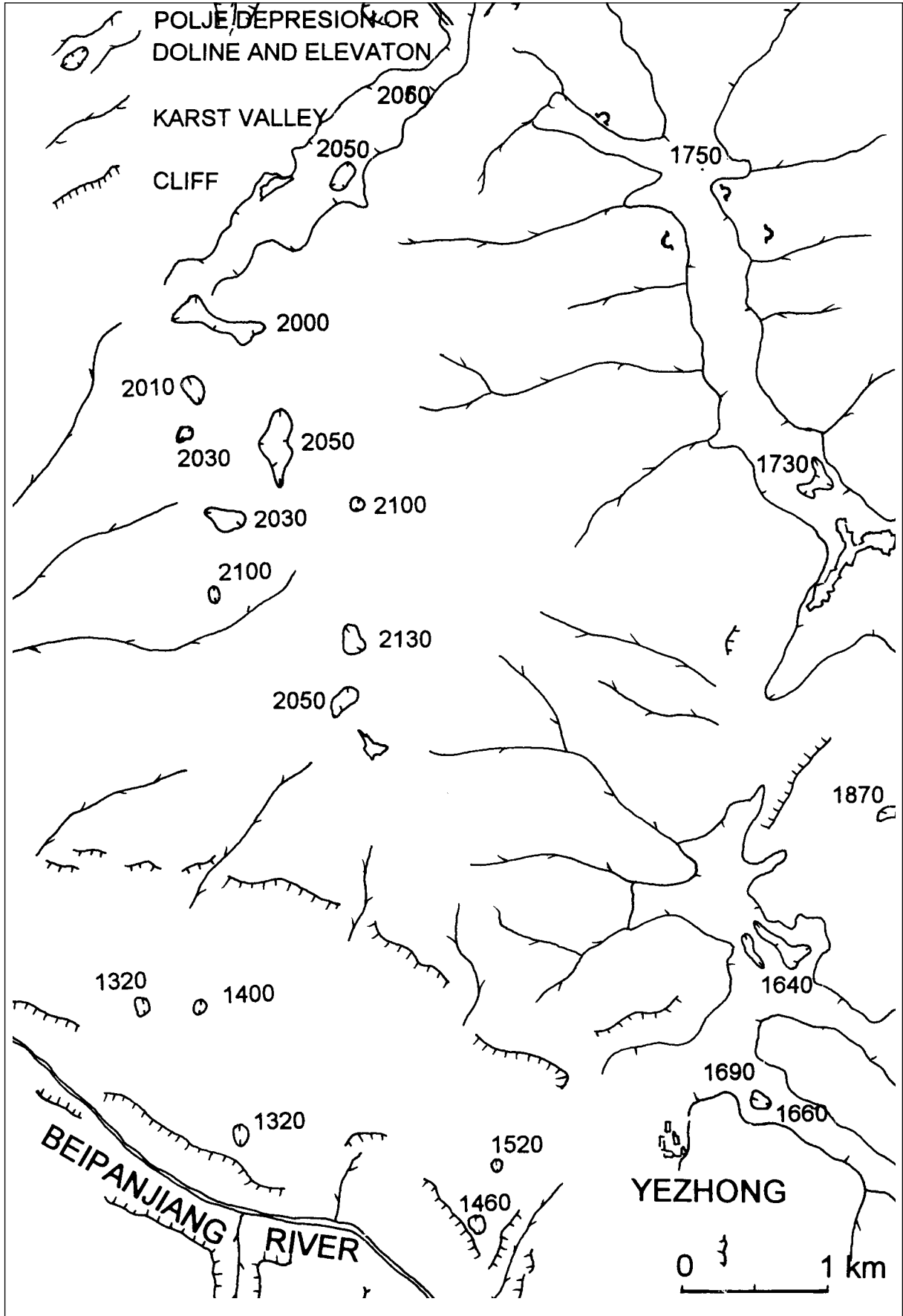


Fig.: 2.2.7. Geomorphological map of Yezhong massif

south China. There are second large chamber in the world of Miaoting with an area of 117,000 m² in Gebihe cave system of Ziyun county and some cave exploring area of Shuanghedong cave in Suiyang county with several km in length, besides the opened noted tour area like Huangguoshu waterfall, Longgong and Zhijindong cave.

Liupanshui area is a potential tourism area not only developing various karst Landforms but also rich in underground karst formations, remaining to be developed for promotion of economical conditions.

The synopsis of the natural scenery in Liupanshui area as follows:

1. Natural Bridge of Shuicheng: As mentioned above, it is the highest highway bridge, with 136m in height, so far all over the world.

2. Doline of Huagaxiang, Suicheng: A huge doline about 3 km from NE of Huagaxiang in SE of Shuicheng is of exploring value, its upper edge lies at 1420 - 1480 m a. s. l. and with a diameter of 250 m at the bottom and an elevation of 1225 m, only 1,25 km far from the Wutuhe river gorge with 800 m a.s.l of river level. The area of doline are 500 x 700 m.

3. Wuliudaxiaodong cave at Xinchang massif of Liuzhi: It is a large cave system, similar to Mammoth cave of USA in geological settings, being of a potential exploring base. At the area distribute mudstone and marl in the middle part of T1yn1 with a wide spread outcrop for a smooth occurrence, covering two underground rivers and Wuliudaxiaodong cave. Therefore, the character of karstification under the massif is a cave system developed in a smooth carbonate rocks under the mudstone.

4. Yegoudong (Feilongdong) cave at Xiongjing of Liuzhi: The cave is developed in limestone of Lower Permian (P1m) with a dip 25°- 30°, measured length 600 m. Plentiful speleothems make the cave more attractive. Besides growing stalagmite and stalactite, there are

drapery, straw, and helictite formed by dripping and spray water. The cave with convenient traffics is a valuable undeveloped show cave.

5. Danxia mountain and Biyundong cave: It is an ancient historical scenic place. Xu xiake - the famous geographer in Ming Dynasty had explored here and gone down in his book "Travels of Xu xiake". A small temple on the Danxia mountain where Xu had been lived. Biyundong and Shuidong caves at SW end of Panxian polje are famous touring site with about 26 carved stone on the both inside and outside the cave, the cave has been arranged as a park and joined in International Show Caves Association (ISCA) in 1995.

6. Beipanjiang is a magnificent undeveloped valley, with several hundreds meters deep, much more tourism resources are waiting for use.

Karst geological disaster

Geological disaster like earthquake, debris flow, earth slide, subsidence, collapse, soil erosion and so on are the productions under specified geological environment. The soil collapse, flooding and desertification are primary geological disaster in karst area because of unique landform, lithological characters and its properties of development and distribution.

Soil collapse

The soil collapse occurs mainly in Shuicheng and Panxian, especially projecting in Suicheng polje.

Suicheng polje presents NW - SE surrounded by mountains, lower in the middle with a length of 28 km and 2 - 3 km wide, developing well in basin's fault structure about 80 faults with various size, NE 60°, NW 290° of fracture and bedding plane. Soil collapse is a direct hateful result for increasing of industries and industrial population consequently rapid supply of industrial and living water and over extracted underground water especially in dry season, causing large extensive descending of groundwater level then soil collapse. There are over 700 soil collapse sites with various size near Laizhidong cave area of the polje

within 2 - 3 km², and some destroyed house and farmland threaten the safety of human being and domestic animal.

Another reason of soil collapse may be very thin (< 10m) Quaternary overburden in Shuicheng polje, It is surveyed that the area with overburden >10 m occurs no soil collapse.

In Putian of Panxian, three new collapse dolines are formed after flooding, one of them become a karst pond because of gathering water for long time.

Another example at Jichangping of Panxian, there are fissures near terrain when pumping test and stop pumping for the safety of houses.

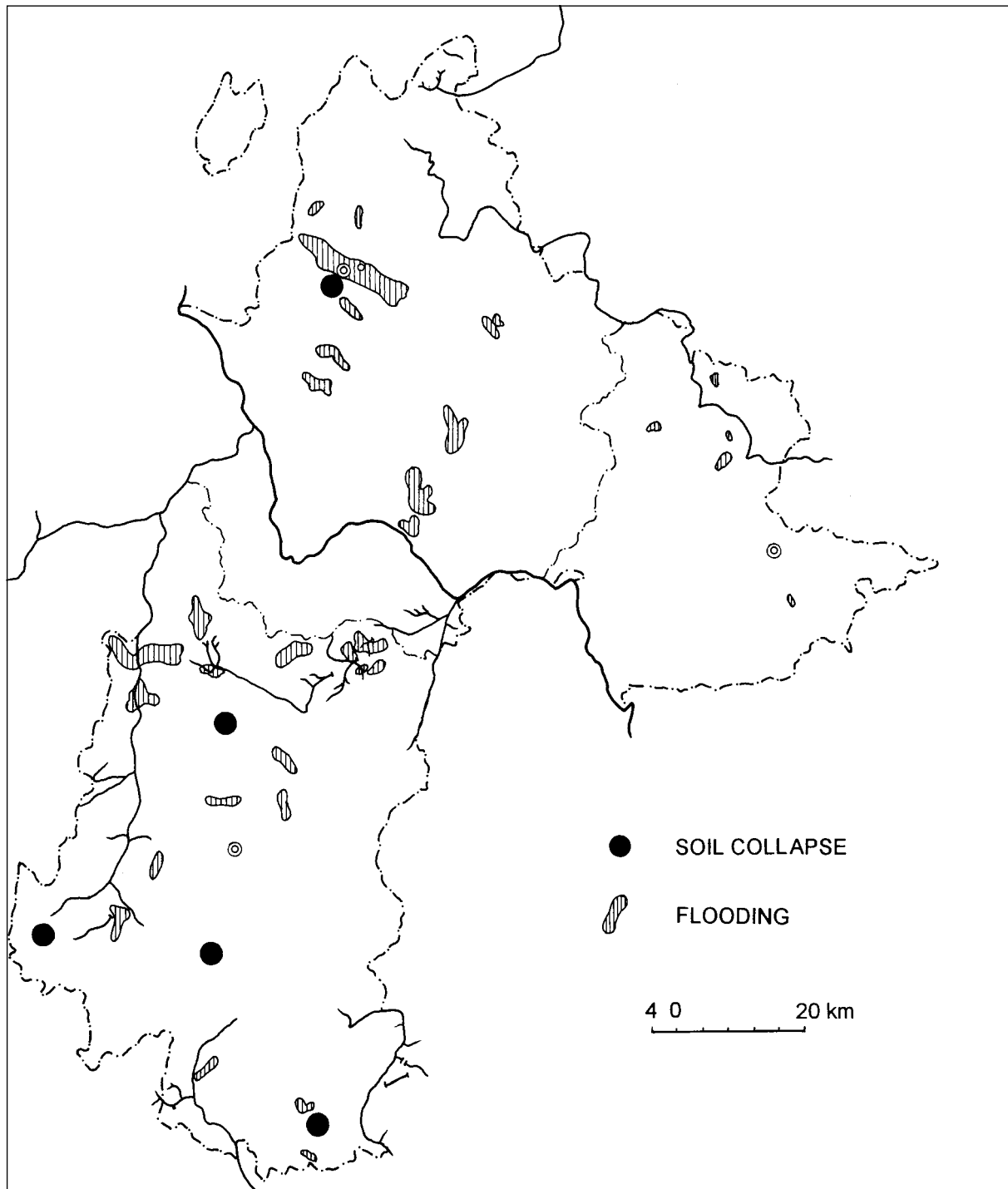


Fig.: 2.2.8. Distribution of soil collapse and flooding of Liupanshui

According to the project, well developed karst fissures and caves with a diameter 2 - 4 m, the ground water level have fallen 24 - 39 m after pumping and a lot of silt was brought about then the surface soil collapse was occurred.

The controlled factors of surface soil collapse in karst area can be summarised according to the examples mentioned above:

1. Karst fissures in subterranean: A size of soil collapse area and space can be limited by developed caves.

2. The factors of motive force resulting in soil collapse are over extracted underground water and built reservoirs causing rapid change of the level of underground water.

3. The thickness of an overburden is also an important condition. (Thickness value is determined by the geological condition.)

Flooding

A relatively high frequency hazard of drought or waterlogging in Guizhou plateau was figured about 20 %. Karst basins

and depressions in Liupanshui area are always flooding caused by torrents of water rushed down the mountain, failed to drain the waterlogged land or remove water to caves impeded from these basins and depressions in raining season.

A series of karst basins and depressions with different sizes which can be calculated a size 500 m (33,4 ha) are some 50 - 60 in Liupanshui area. Another kind of basin distributing in alimentation area of underground water and near the watershed are normally drought for most of the precipitation flowing into deep of subterranean along the karst fissures. Some depressions distributing in draining area for concentrating karst water and surface water are always flooded because of full and block up of terra rossa or humus in fissures and dolines, the flooding duration are lasted 1 - 2 months even half a year.

Desertification

The research area is one of the serious area on desertification in Guizhou. The area



Fig.: 2.2.9. Deforestation, soil erosion and desertification in the Taishaba area (Photo A. Mihevc).



Fig.: 2.2.10. Land use on karst surface in W Guizhou. Terracing of the slopes can prevent soil erosion (Photo A. Mihevc).

of carbonate rocks and area of soil erosion reach to 8865 and 6151 sq.km, occupying 89,42% and 62,04% in total area of Liupan-shui respectively.

The arable land with a slope more than 25 degrees take up to 13.78% and 38500 ha in total arable land.

Taisha - the typical area of desertification is seated on the plane of denudation of 2160 - 2220 m a.s.l.. The Lower Permian carbonate rocks is distributed at the core of anticline with NW 330 trend of axis. It is located on the watershed of both tributaries of Beipanjiang river.

On the plane of denudation, the positive karst forms are qiufeng - a type of cone

karst. The limestone hills are 60 - 80 m high and 110 - 135 degrees of the angle on the hill top. The negative karst forms are shallow plate-shaped doline or uvala with 20 - 30 m in depth. It is bare karst hill without any soil and vegetation except karren. The water table lies down more than 100 - 200 m.

The following treatments have been taken to change the poor economical situation:

1. Emigrating locate people to non-carbonate rocks area with lower elevation;
2. Reforestation for water and soil conservation and reducing arable land;
3. Terracing of the mountain slopes to prevent the soil erosion.

2.3 HYDROCHEMICAL PROPERTIES OF KARST WATER IN LIUPANSHUI

Jin Yuzhang

The characters of karst water records the process in evolution of natural water and provides information for making a through study on the formation and evolution of caves, and the velocity of karstic denudation. It is also the basis of the protection and valuation for ecological environment.

The data discussed on water analysis were collected from field and tested during the expedition in 1996.

Parameters, methods of water analysis and equipment

To conform to the special purpose of speleological exploration, the principle of choosing methods and equipment for natural water analysis in the field are portable and convenient to use, fast and accurate enough to obtain the parameters needed.

The table shows parameters tested, methods and equipment used and their precision concerned.

Description of the water samples and data

The number 9611201 was sampled from the resurgence of Yanzidong cave at Ganhe natural bridge. No.9611262 is the water from epikarst aquifer sampling from a water tank at Taisha village, which is located on the core of the anticline with NE-SE direction near the watershed and the typical area of karst desertification with very thin of soil bed. The samples 9611284 and 9611285 are lied on the valley from Changming to Yezhong, finding clastic rock with coal P1L at the bottom of the valley with a dip angle some 7, covering carbonate rocks massif P1q+m on both side of the valley. It

PARAMETERS	METHOD WITH EQUIPMENT	PRECISION
Temperature (°C)	HACH company	± 0.5 °C
Conductivity (µs/cm)	Model 44600	0.1µs/cm
Total dissolved solid (mg/l)	Conductivity/TDS Meter	0.1mg/l
pH	Digisense pH Meter, Model No. 5994	±0.1pH±1count
CO ₂ in air (mg/l)	Gastec Sample Pump	5-10 %
	HACH Digital Titrator Model 16900-01	
Dissolved CO ₂ (mg/l)	Titration Cartridge (NaOH)	± 1 %
HCO ₃ ⁻ (mg/l)	Titration Cartridge (H ₂ SO ₄)	± 1 %
SO ₄ ²⁻	Titration Cartridge (EDTA)	± 1 %
Cl ⁻ (mg/l)	Titration Cartridge (AgNO ₃)	± 1 %
Ca ²⁺	Titration Cartridge (EDTA)	± 1 %
Mg ²⁺	Titration Cartridge (EDTA)	± 1 %
TH (H ^o)	Titration Cartridge (EDTA)	± 1 %
Aggressive CO ₂ (mg/l)	Titration Cartridge (H ₂ SO ₄)	± 1 %

Table 1. Parameters, methods and equipment, and the precision of water analysis

is one of the type of contact polje. Sample No. 9611286 is a karst spring at the low reach of the valley with a discharge of 2,4 l/s. The 9611287 comes from a small mountain valley on the east part of Yezhong massif, perch ground water formed by resisting of argillaceous sandwiched in a gentle Permian carbonate rocks with very small discharge and never dried up, collecting in a water tank for daily life. The place is 150 m higher than that of main valley.

Physical properties and chemical compositions of the water samples mentioned above are listed on the table below:

The water types in carbonate area are mostly HCO_3^- - Ca^{2+} , Mg^{2+} or HCO_3^- - Mg^{2+} . Ca^{2+} patterns according to the maps of hydrogeological survey (1 : 200000).

The parameters of TDS and TH from basalt and karstic aquifers by each map sheet are listed on the table.

Discussion

1. No. 9611201 was sampled from the cave on the water table, but contains low ions concentration, it was probably got af-

PARAMETER	RESURGENCE	EPIKARST				PERCHED WATER TANK
		water tank	water tank	water tank	spring	
Sample No.	9611201	9611262	9611284	9611285	9611286	9611287
Aquifer	T1yn2-4	P1q	P1q	P1q	P1q	P1q
T(°C)	9.7	8.0	10.2		15.3	16.4
pH	8.25	8.41	8.54	7.64	8.14	8.55
CND($\mu\text{s}/\text{cm}$)	190	320	107.3	600	342	328
TDS(mg/l)	95	159	53.7	300	171	165
TH(H°)	5.25	8.04	5.56	16.42	8.94	9.83
Ca^{2+} (mg/l)	36.00	56.80	18.40	113.60	64.00	66.40
Mg^{2+} (mg/l)	0.98	0.49	13.18	2.44	0	2.44
HCO_3^- (mg/l)	97.60	170.80	61.98	251.32	178.12	180.56
SO_4^{2-} (mg/l)	0	3.82	15.28	68.40	7.64	1.91
Cl^- (mg/l)	4.80	7.20	5.20	18.40	24.00	6.80
DCO_2 (mg/l)	0.60	16.80	4.80	2.60	6.00	1.60
ACO_2 (mg/l)	0	0	6.36	0	0	0

Table 2: The physical properties and chemical composition of karst water in Shuicheng, Guizhou

AQUIFER	PANXIAN			SHUICHENG			ANSHUN		
	pH	TDS(mg/l)	TH(dH°)	pH	TDS(mg/l)	TH(dH°)	pH	TDS(mg/l)	TH(dH°)
T2g2+3	7.1 - 8.2	189.90 - 547.68	8.52 - 20.72						
T1yn				7.4 - 7.9	116 - 209	5.71 - 10.06	7.1 - 7.6	140 - 480	7.74 - 21.77
P2b	5.6 - 8.3	33.14 - 300.43	0.50 - 15.48	6.8 - 7.6	29 - 116	0.64 - 4.28	7.3 - 7.7		8.48 - 18.30
P1m	6.7 - 7.9	120.65 - 276.05	6.05 - 12.71	7.5 - 7.8	119 - 189	6.22 - 9.985	7.3 - 7.6	100 - 210	4.88 11.19
P1q							7.8 - 8.4	190 - 280	9.60 - 13.30
C3m				7.5 - 7.7	147 - 194	8.17 - 10.43	7.3 - 7.7	160	8.42 - 18.30
C2h							7.2 - 7.9	160	8.84 - 22.90
C1				7.4 - 7.8	155 - 227	7.55 - 11.54			

Table 3: The parameters of TDS and TH from basalt and karstic aquifers

ter heavy raining and the water coming from the cave of an allogenic water and with less length.

2. The numbers of 9611262, 9611286 and 9611287 are similar in contents, the latter two samples proved the quantities of typical karst water in Yezhong massif. It is a massif without water, which is suspending highly above the Beipanjiang gorge and set off by the underlying P1L aquiclude, because the ground water of the massif is drained by the main valley developing along a fault and branches and found nothing about good spring. Therefore, there is no spring with high discharge in karst valley which incises the massif, and the composition of the perch ground water or spring

with converging water locally is quite closely with the epikarst water sample No.9611262.

3. No. 9611284 is taken from the water tank of the diversion works, the water sources is probably from the surface.

4. The TDS, TH, CND, Ca^{2+} and HCO_3^- contents of No. 9611285 are much more higher than the others, only a few water samples are similar with it in the past studies, it is probably related to coal mining in P1L and polluted by the waste water of daily use according to the data of low pH value and high concentration of SO_4^{2-} .

5. The contents of TDS, TH and pH of karst water area are higher than those of the water in basalt.

2.4 SPELEOLOGICAL EXPLORATION AT TIANSHENGQIAO - NATURAL BRIDGE, SHUICHENG

Franci Gabrovšek, Andrej Mihevc, Bojan Otoničar, Nadja Zupan Hajna

Introduction

Tianshengqiao - Natural Bridge is situated near the Ganhe village, about 80 km NE from Liupanshui city, NW Guizhou. Bridge is the last remain of once larger cave system of the Ganhe river. Its arch is 15 m thick and 136 m high. There are several caves in vicinity, Swallow cave being the largest of them.

During November 1996, group of researchers from Slovenia and from China worked in the area of Tianshengqiao - Natural Bridge. About 2 km² of the area was mapped and three caves were explored and surveyed (Gabrovšek et al., 1997). Some measurement of main structural elements on the surface and in the caves were done. Water, rock and sediment samples were taken for further lithological and x-ray analyses.

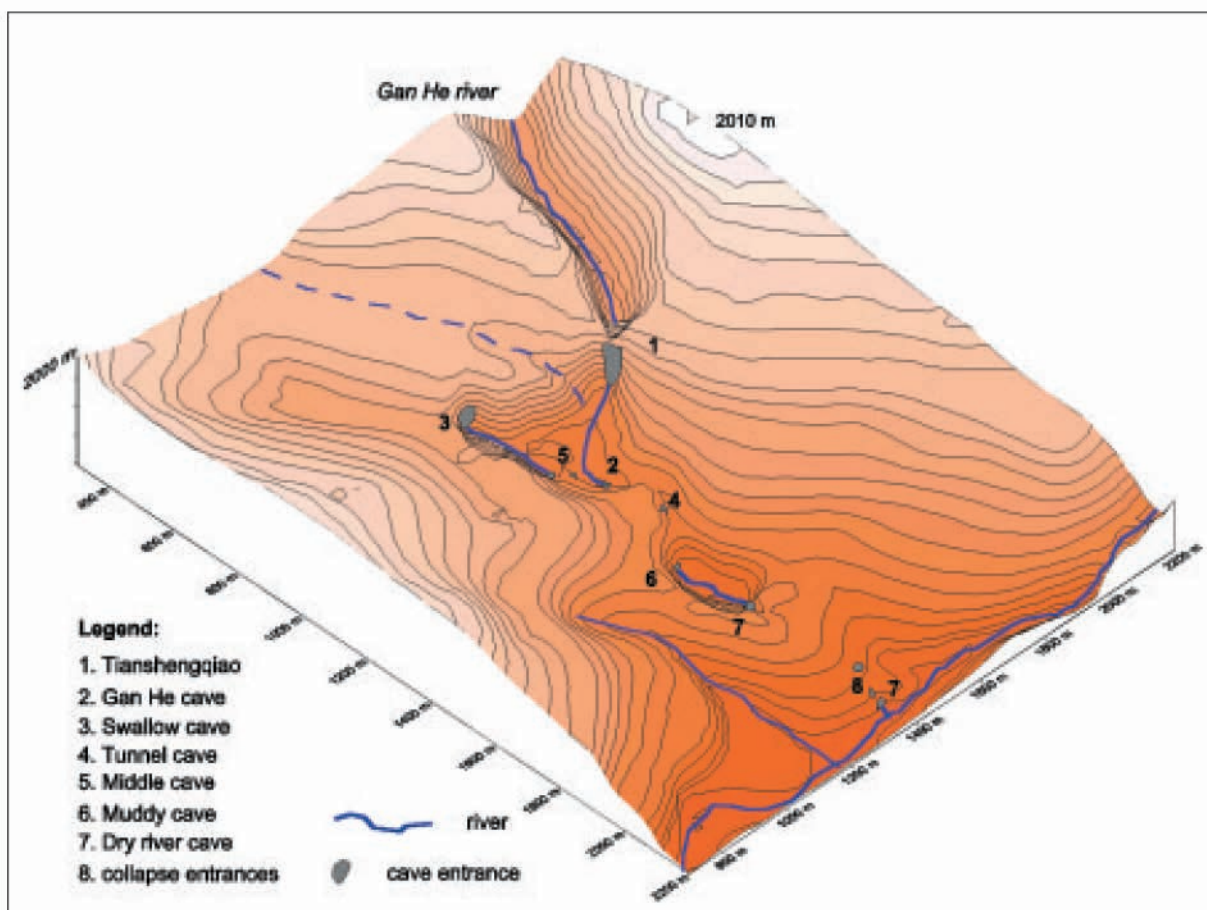


Fig. 2.4.1. Tianshengqiao natural bridge area with caves.

Geomorphology

The area of the natural bridge Tianshengqiao is situated on the southern slopes sweeping from the elevation of 2300 m towards the valley of the Daganhe river in elevation of about 1600 m.

The surface is well karstified, but shows surface fluvial forms, shallow fluvial valleys, canyons, among which the deepest is the canyon of the Ganhe river, which flows under the natural bridge. Doline and closed depressions are on the edge of the plateau only. On the slopes they are only along the rivers, which formed the Tianshengqiao and along the river flowing from the Swallow cave. These depressions are elongated collapse depressions, with steep or vertical walls developed from the disintegrated cave system.

On the upper part of the slope in about 140 m deep canyon of the Ganhe is cut. In

upper part the canyon is formed in limestone, in lower is more marly limestone. Canyon developed from the sinking river cave which ceiling remained only one place as the natural bridge Tianshengqiao.

The altitude of the bridge is 1861 m a.s.l., bridge is about 15 m thick and 30 m wide. It is used for the road connection of the village Ganhe and Yantoushang. From the bridge to the river bellow is 136 m.

Geology

The area belongs to transitional slope of the Yunnan Plateau to Guizhou plateau, which is folded belt composed of a series synclines and anticlines (Maire, Zhang & Song, 1991). In the wider vicinity of the investigated area few hundred to thousand metres thick packages of carbonate, siliciclastic and basalt rocks from Middle Carboniferous to Lower Jurassic in age are present (Zhang & Walthman, 1985).

Lithology

The caves and the natural bridge are developed in dark-grey middle and thin bedded to platy somewhere laminated Lower Triassic micritic limestones and marly limestones with intercalation's of marls and dolomites. Among allochems bioclasts prevail. The most frequent are molluscs (especially gastropods) and ostracodes, in ripples also crinoides. The rocks are characteristically bioturbated and somewhere show mottled structure. Beds often contain clayey dissolution seems and stylolites as well as isolated ripples and laminae mainly of bioclasts. In some places desiccation cracks were noticed. In thin sections pyrite framboids and concentrations of organic matter are visible.

We can conclude that carbonates were deposited in shallow more or less restricted inner part of the carbonate shelf sea where sometimes higher energy events occurred. Occasionally terrestrial influence is evident. Somewhere desiccation cracks indicate emersion conditions.

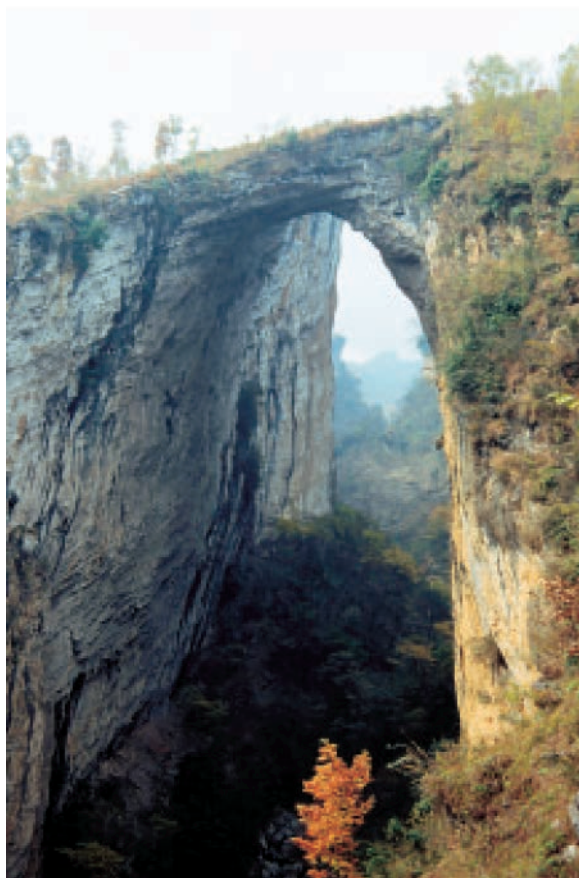


Fig. 2.4.2. Tianshengqiao natural bridge (Photo: A. Mihevc).



Fig.2.4.3. Dark-grey platy internally laminated Lower Triassic marly limestone. The rock is to characteristically bioturbated and shows mottled structure. Long axis of the figure: 1 m. (Photo: B. Otoničar)

Structural elements of the limestone and dolomite beds

In the area beds generally dip toward S-SE, measured directions of dips are from 160° to 170° , with dip angle from 20° to 25° .

Frequency of fissure directions is shown by intensity and length of bars in a rosette (Fig.2.4.4.). The most expressed direction of faults and fissures is about 90° - 270° (E - W). The second place occupies the direction is about 0° - 180° (N - S) and the third one is direction 45° - 225° (NE - SW).

Cave system, the morphology of the channels in the caves and collapse depressions between them are strongly related to directions of all three main faults and fissures directions (Fig.2.4.5.): 1. E-W, 2. N-S 3. NE-SW. The main channels of the caves are developed in first direction, in second and third direction just some parts of main passages are developed.

Hydrology

In the studied area there is a confluence of two underground rivers. First river is Gan He river the second one the river from Swallow cave. To the Natural Bridge water Gan He flows on the surface in the direction NW-SE, after flows below bridge sinks to the ponor of Gan He cave, where reaches the water from Swallow cave which flows also through Middle cave and then to Gan He cave. At low water rivers join underground and flow towards spring which should be out of the area, probably in the main river valley. Only at high waters rivers fill the lower cave galleries and flow on the surface for two times and then flow through the River cave into the main river.

At the time of the visit the discharge of both rivers together was about 100 l/s. The temperature of water in Swallow cave was $9,7^{\circ}\text{C}$ and the temperature of air was $10,4^{\circ}\text{C}$.

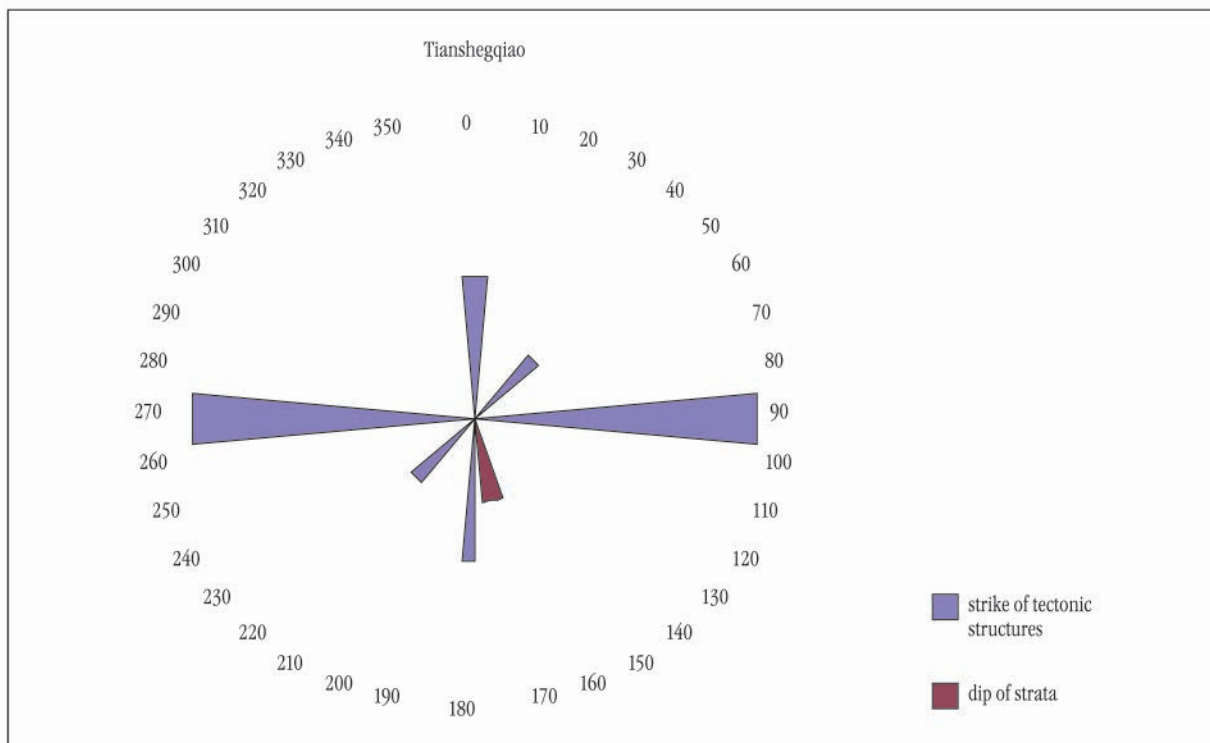


Fig.2.4.4. Dip of strata and strikes of structural zones, intensity is expressed by length of the bars.

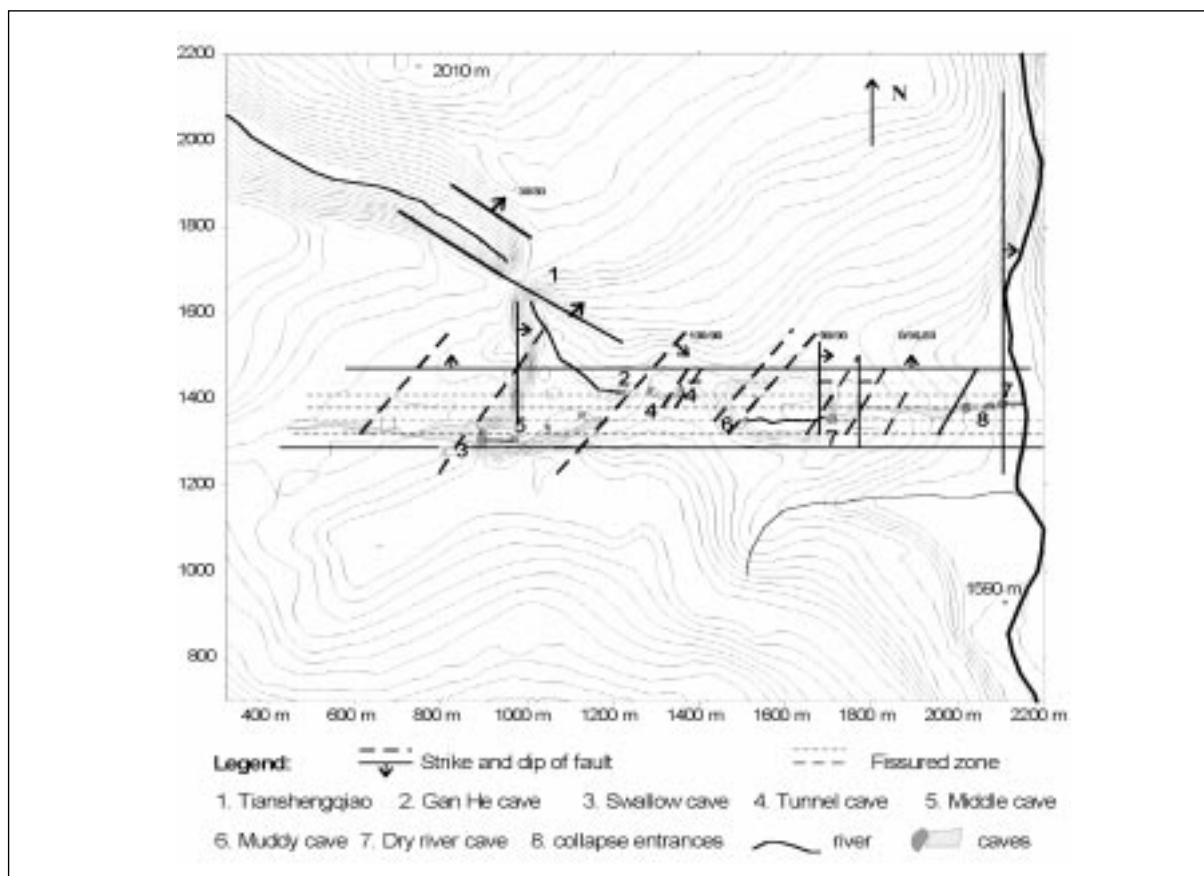


Fig.2.4.5. Tianshengqiao natural bridge area, caves and generalised geological structures of the area.

Caves

In the area of Natural Bridge we visited seven caves but because of the lack of time and equipment we were able to surveyed only three of them.

1. Swallow cave: South of the bridge below the 90 m high wall there is an opening into Swallow cave. In this part of the cave here are the remains of human dwelling and traces of saltpetre production from the cave sediments.

Cave was researched and surveyed upstream for about 500 m, total length of the surveyed part of the cave is 938 m. In the cave two morphological and genetic units can be seen an active narrow, high gallery and a maze of older, phreatic channels.

Active narrow and high gallery which rise in surveyed part for 21 m. Trough this gallery flows river which carries drift wood, among which 40 cm thick and several m

long trunks were found, showing, that this river is a sinking river. The discharge of the river was about 50 l/s. Survey was done upstream until a lake and 3 m high cascade. The canyon is few m wide and about 20 m high, becoming lower upwards.

The main channel is developed along strong structural zone with faults and fissures in E-W direction and in some parts in fissures which form the angle of 45° with it, this is NE-SW direction. The wall rocks consist of thin bedded to platy dark grey in some places obviously bioturbated limestone and marly limestone with dissolution seems and stylolites. Smaller and up to ten cm large scallops are the most prominent features of the cave rocky relief.

Other morphologic unit of the cave is a maze of older, phreatic channels which are about 15 m above the actual stream in the entrance part. The galleries are dipping with strata and they used one bedding-plane for formation. The orientation of these channels is related to two different



Fig. 2.4.6. Entrance to Swallow cave on the left and Tianshengqiao natural bridge on the right. (Photo: A. Mihevc)

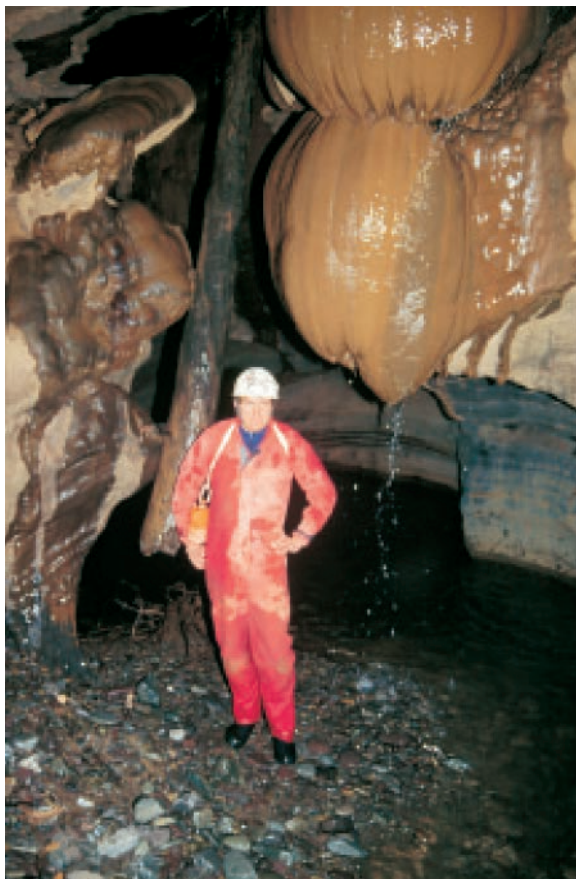


Fig.2.4.7. Our exploration ends at small pool which leads to the step with waterfall. The proof that passage continues and that river in the cave is a sinking river is choked drift wood. (Photo: B. Otoničar)

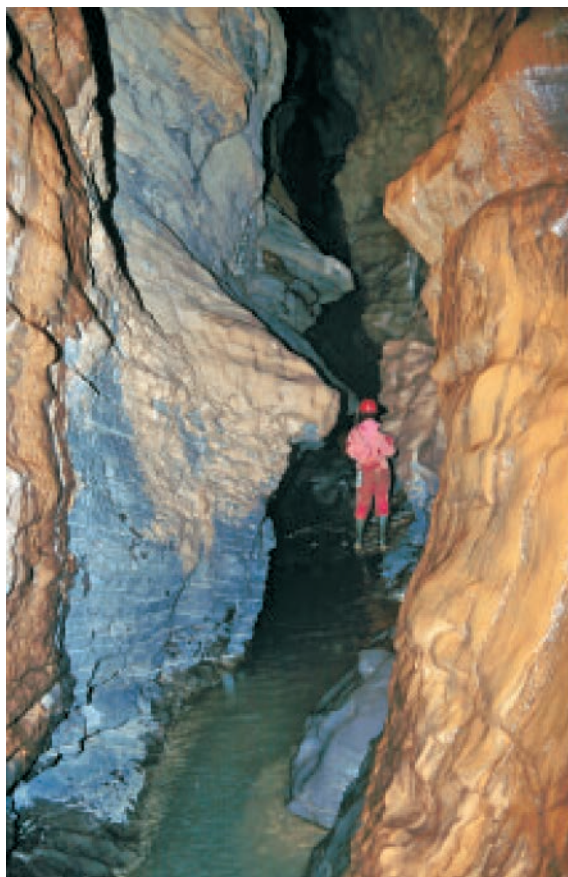


Fig.2.4.8. Main narrow gorge-like passage of the Swallow cave. (Photo: B. Otoničar)

structural zones, the most important is E-W direction and the second one is NE-SW direction. At the entrance part of the cave smaller anastomoses channels are visible along three several metres separated bedding plan partings.

Sediments, gravel, sand and silt were found in upper parts of the cave, indicating older infill of the cave. From the small phreatic channel at the top of high gallery sample of sand mixed by silt was taken. It was analysed by x-ray on the Institute of Mineralogy, University of Ljubljana by the Phillips diffractometer with $\text{Cu}_k\alpha$ ($\lambda = 1,54 \times 10^{-1}$ nm) and automatic divergence slit. The analyse was shown the following mineral composition: quartz, feldspar, chlorite, dolomite, muscovite, calcite, augite and saltpetre (KNO_3). Quartz, chlorite, muscovite, feldspar and augite were brought into the

cave by the stream from noncarbonate rocks. Dolomite and calcite are originated from cave walls.

2. Middle cave: River from the Swallow cave sinks after 50 m of flow on the surface in a cave, which has another entrances further E. We could follow the river in the cave towards east where it probably joins the Ganhe cave.

In the depression where the second entrance to the cave is there is also small canyon, which was dry in the time of the visit. Cave all the time follows the E-W direction, the second entrance is opened along the fissures in N-S direction.

3. Ganhe cave: Gan river flows under the Tianshengqiao and after 200 m sinks in a cave. Entrance to the cave is narrow and



Fig.2.4.9. In some places narrow main passage of the Swallow cave becomes much wider. (Photo: B. Otoničar)



Fig. 2.4.10. Plan and profile of the Swallow cave.

steep. From this cave water flows in at least two directions as mentioned above.

4. Tunnel cave: This is 81 m long cave. Its entrance is in the vertical wall of the can-

yon above its bottom. Cave rises towards east at first, than lowers and opens under the vertical wall again. Cave is a remaining of an old, because of the outside influences much transformed phreatic gallery. In gen-



Fig. 2.4.11. W Entrance to the Middle cave. (Photo: A. Mihevc)

eral cave is also elongated in E-W direction, but in the cave is well expressed also NE-SW direction.

5. Muddy cave: Its entrance is in the lowest part of the second biggest depression in the area. It is temporary spring of the river which flows on the surface for about 200 m and then sinks into the Dry river cave. At the time of the visit it was dry, explored only to the level of the lake of hanging water. Cave follows the dip of bedding plane which is 170/20,25.

6. Dry river cave: Cave is a ponor of the river coming from the Muddy cave. Cave is on the opposite, eastern side of the depression. Cave gallery starts with 20 m high entrance and can be followed for 335 m to the exit at the riverbed of the main river. Most part of the cave is more than 10 m wide and high, and dips evenly for 27 m. Two collapse entrances reach cave in the E part, very near the spring from the cave in the main valley of the area. At the time of the visit cave was dry, some water was in

the pools of trapped water only. At rainy season cave transmits large water quantity.

Galleries are oriented along structural zones in E-W direction, some parts of the

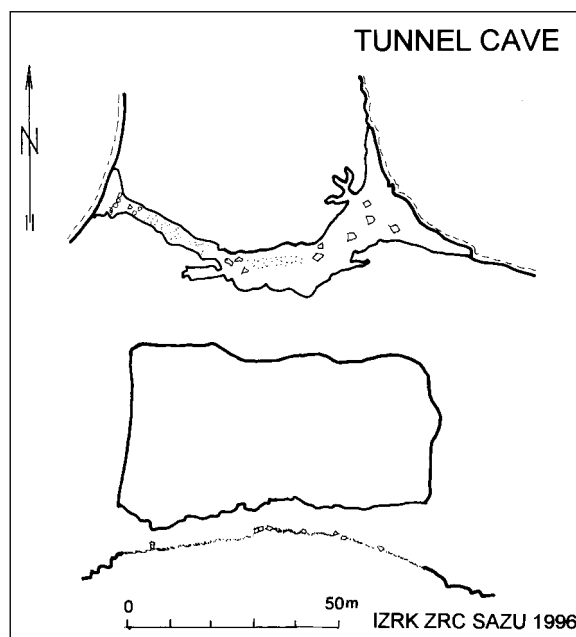


Fig. 2.4.12. Plan and profile of the Tunnel cave.

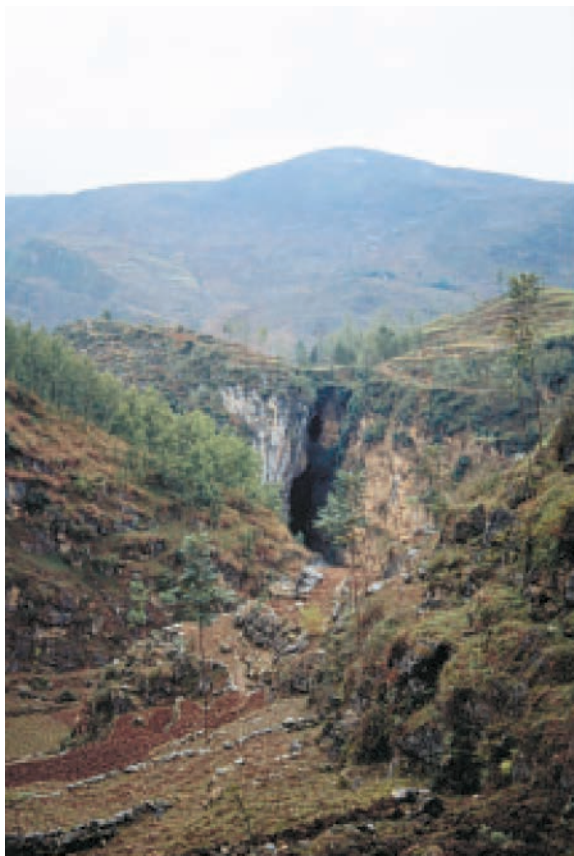


Fig. 2.4.13. Entrance to the Dry river cave is opening at the end of large collapse depression. (Photo: A. Mihevc)

channels also use well expressed N-S direction and NE-SW direction. The collapse entrances are connected to crossing of main

structural zones, where the limestone is more broken.

Conclusions

Natural bridge Tianshengqiao and closed depressions between Swallow cave and the River cave have developed in the limestone sequence which is pure in upper part and more marly in the lower part. Because of the great gradient caused by the downcutting of the main river both Gan He river and the Swallow cave river start to sink in the karst. First galleries probably followed the bedding planes and followed the dip. Some of the phreatic small cross section and with old sediments filled galleries can still be seen in the Swallow cave. Opening of the karst laterally to the valley of the main river made sinking of the rivers possible. Rivers probably formed narrow and high underground galleries. Collapses elongated along the main structures in E-W direction occurred. Collapse depressions were latter connected in elongated canyon like depression, with some tunnel caves and the Tianshengqiao bridge as the remains of the previous cave system.

The Tianshengqiao cave system presents an interesting case of the speleogenesis and gives an opportunity for many new cave research and discoveries.

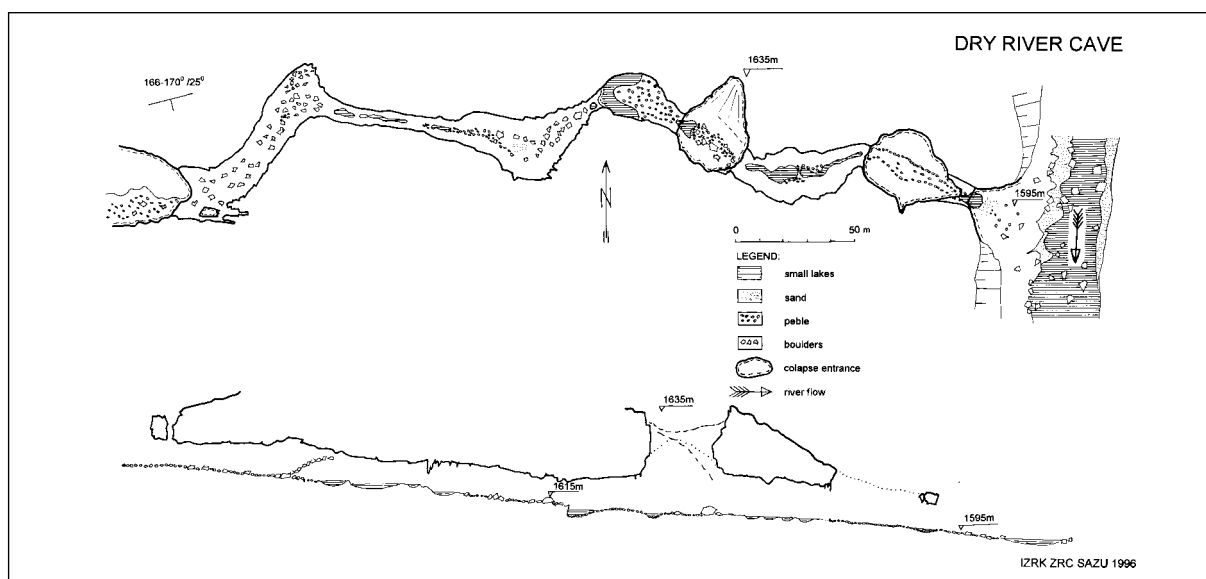


Fig. 2.4.14. Plan and profile of the Dry river cave.

2.5. KARSTOLOGICAL RESEARCH OF THE CAVE BY XINGCHANG VILLAGE

Franci Gabrovšek, Andrej Mihevc, Bojan Otoničar, Nadja Zupan Hajna

Geomorphology

Cave developed in relief of cones and depressions. In this surface valley like depressions and smaller closed depressions developed. Peaks of the cones are at 1900 m a.s.l. and the bottoms of depressions at 1700 m a.s.l. There are also larger depressions, they are deeper, with bottoms at 1600 m.

Entrance to the cave is below the steep slope of a karst cone, which below it continues to the large cockpit. Slopes of cones and the cockpit are inclined to 40°. There is some soil in the bottoms of depressions. In larger and deeper depression some surface streams appear. These depressions are being flooded too.

Geology

Lithology

The cave and its surroundings lie in Lower Permian crinoide limestone and porous grainy dolomite. Where limestone is present, the partly leached stems of crinoids protrude from the weathered cave walls; foraminifers, brachiopods, bryozoas, corals and spines of Echinoidea - sea urchins - are also visible.

In the passage on the west side of the entrance doline, opposite the main passage and stratigraphically somewhat below the level observed in the main passage, a nearly black micritic limestone appears.

Similar sediments can be observed above the cave, where limestone gradually

prevails over dolomite. In this part we observed only small irregular lenses of coarse-grained dolomite. Directly above the cave, in dark micritic limestone, we found interesting thin laminas and ripples of crinoids and foraminifers (Fig. 2.5.1.). Limestones are of the packstone and wackestone type and are recrystallised in places. Among the allochems, bioclasts and peloids - mainly micritized bioclasts - prevail. The most frequent fossils are echinoderms, primarily crinoids, and fusulinid foraminifers, dasycladacean algae fragments, individual corals, gastropods and bryozoas, while fragments of various indefinable tests also appear.

The matrix is mostly micrite, which can be washed, recrystallised or selectively dolomitized. Drusy mosaic spar may be present in places.

Among structures, we observed the previously mentioned laminae of individual bioclasts in micrite. Allochems are frequently oriented with their longer axis parallel to the stratification. In places, distinct bimodality is noticeable in the samples. Rarely grains of framboidal pyrite are presented.

The structure of the dolomite is euhedral to subhedral (Fig. 2.5.2.), the grains indicate a zone distribution of impurities. In some places in dolomite, there are remains of micrite and undolomitized crinoidal plates (selective dolomitization) (Fig. 2.5.2.).

Somewhat higher above the cave, stylolitized limestone with nodules and lenses of black chert (Fig. 2.5.3.) appear. Fossil remains are well preserved here, especially crinoids and fusulinids.



Figure 2.5.1: Various bioclasts redeposited in micrite; among them we observe fusulinid foraminifers, crinoidal plates, various indefinable tests and rare brachiopod spicules. Lower Permian – limestone directly above the cave. Long axis of the figure: 1,25 cm. (Photo: B. Otoničar)



Figure 2.5.2: Coarse grained dolomite in which most of the cave has developed. The grains are chiefly subhedral with well seen zonation. The large grains represent non-dolomitized crinoidal plates – selective dolomitization. Lower Permian. Long axis of the figure: 1 cm. (Photo: B. Otoničar)



Figure 2.5.3: Bedded stylolitized fusulinid-crinoidal black limestones with nodules of black chert. Lower Permian – broader vicinity of the cave – the beds are stratigraphically above the cave. (Photo: B. Otoničar)

Rock similar to that described above can also be found in the cave’s broader surroundings.

The limestones described above were deposited in the middle and outer shelf.

Primarily limestones of the packstone type with more or less rounded grains oriented parallel to the stratification represent rather higher energy shallow water banks or shoals. Limestones of the packstone type

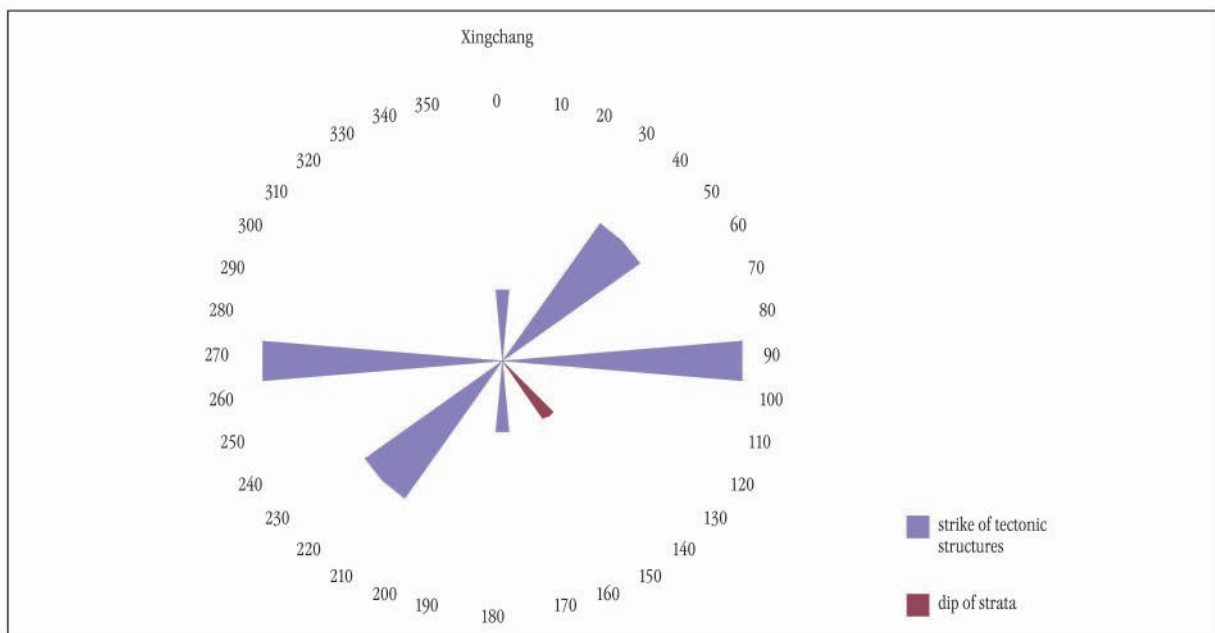


Fig.2.5.4. Dip of beds and strike of tectonic structures, intensity is expressed by length of the bars.

with distinct macrofossils are probably sediments of the marginal parts of patch reefs or beds flanking the build-ups. Micritic limestone with bioclastic laminae and ripples was deposited in shallow water marine conditions with open circulation close to the wave-base. Periodically during higher energy events fossils were redeposited into this sediment. Limestones with chert were probably deposited in somewhat deeper water in the surroundings of build-ups on the shelf slope.

Structural elements

Carbonate beds generally dip toward SE. Entrance part and the end part of the cave

generally follow the dip of strata 140/20-35. The middle part of the cave follows the strong vertical fissured zone E-W. NE - SW and N - S directions of tectonic structures are also expressed (Fig. 2.5.4).

Clastic sediments

Sediment samples were taken for further mineralogical analyses, two on the slope above village Xingchang and one in the cave.

Yellow loam from middle part of the cave contains predominantly quartz, some montmorillonite, muscovite and chlorite, kaolinite and goethite are present in traces.

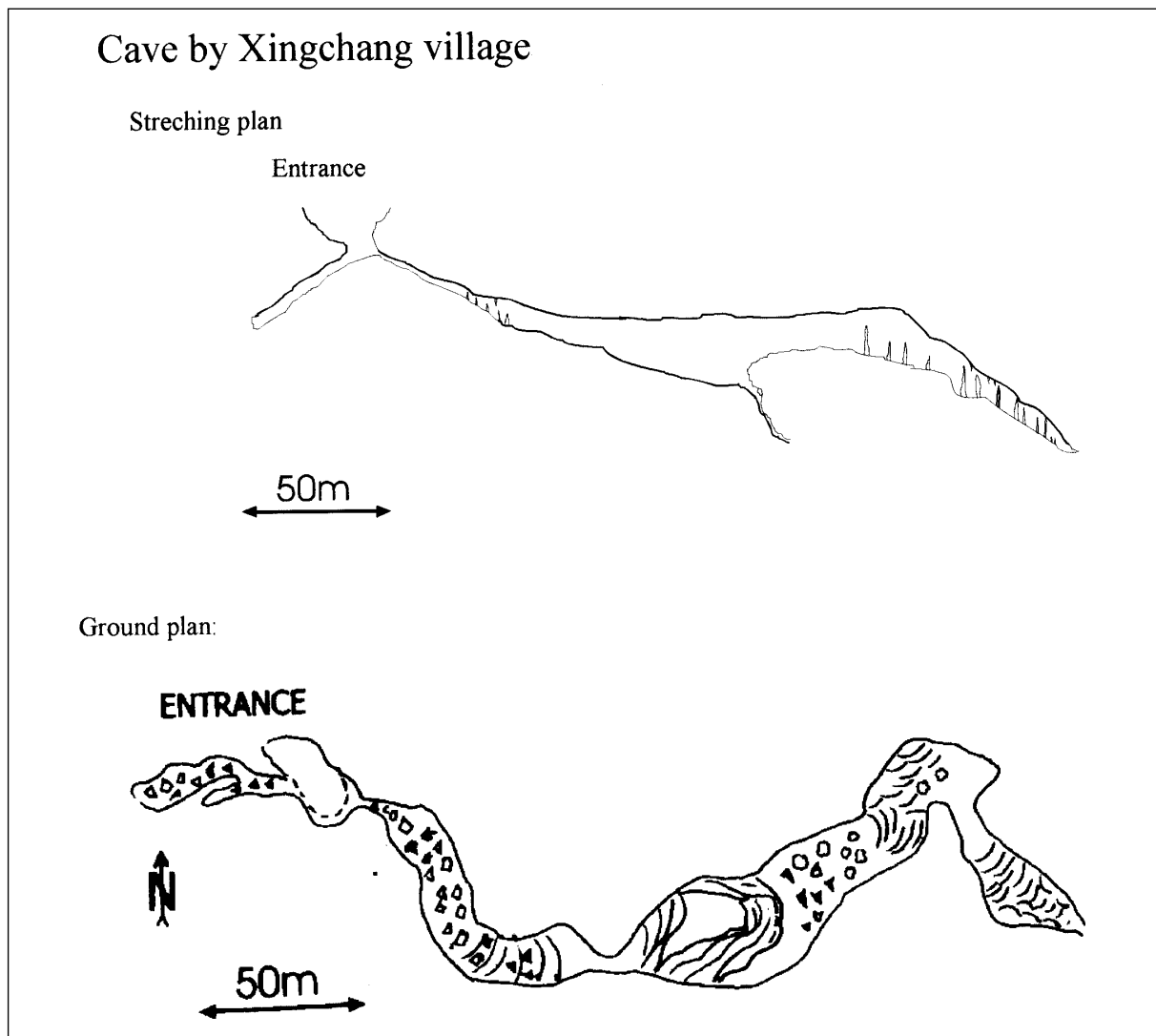


Fig. 2.5.5. Stretching profile and ground plan of the cave by Xingchang village.

Accumulation of yellow weathered loam on slope above village was mixed with some chert pebbles comprises mostly quartz, and very small amount of montmorillonite, muscovite, chlorite and kaolinite.

Yellow loam on the slope above road which was under construction that time consists mostly of quartz, and little of montmorillonite, muscovite, gibbsite, chlorite and kaolinite.

Regarding on mineral composition yellow loam on the surface and in the cave have had the same origin. They probably originated from weathered rests of limestones rich with chert nodules (Fig. 2.5.3.).

Cave

Geographical position: The entrance of the cave lies in a smaller collapse doline which is located on 1720 metre above sea level, NW from the Xingchang village, on slope above karst polje.

Basic data about the cave:

Length: 541m

Depth: 99m (between highest and lowest points of the cave)

Horizontal length: 510m

Stretching in E-W direction: 330m

Stretching in N-S direction: 90m

Description of the cave:

On the bottom of the collapse doline with diameter of 20 m are two entrances, one of the eastern longer passage and the other of the shorter western passage (Fig. 2.5.5.).

Eastern passage:

The narrow and low entrance in the eastern passage becomes after few metres widely opened and follows the bedding plane parting dip under the inclination of 20° . In this part numerous fossils (especially crinoid stems) jut out of the weathered cave walls. At the beginning ceiling is lower than 1m, but highness of the passage monotonously increases and after 100m passes into largest hall in the cave (50X40X20m). On the bottom of the hall is an entrance that leads into series of short vertical steps that



Fig.2.5.6. The stalagmite in the western passage of the cave by Xingchang village.

end (continue) with narrow muddy channel (unmeasured) 30m below the hall. Channel is already below the level of the flooding waters.

The hall is on the eastern side break off with flowstone barrier. Up to 10m high and up to 25m wide passage is covered with flowstone and proceeds towards NW from the hall. After 100m channel turns towards SE and continues with flowstone slope. At the bottom of the slope is the most remote and the deepest measured point of the cave. The final parts of the cave are beautifully decorated by numerous and various forms of flowstone.

Western passage:

Western passage is developed along vertical E-W oriented fissured zone. Ten metre high entrance is triangular in shape and the walls diverge into fissure on the roof. The passage steeply descend toward W under the inclination of 35° . The bottom is covered by gravels and the walls are bare.

2.6. LITHOLOGIC CHARACTERISTICS OF YEZHONG PLATEAU

Bojan Otoničar

Introduction

We investigated lithological properties of carbonate rocks of the Yezong plateau, which is typical conical karst area, and of the northern bank of the Beipanjiang river, that cut into the plateau.

The oldest rocks included in the research were Upper Carboniferous limestones which were subsequently karstified and covered by lower coal series, which we will not treat lithologically here. These rocks were followed by Lower Permian mixed carbonates and siliciclastic beds

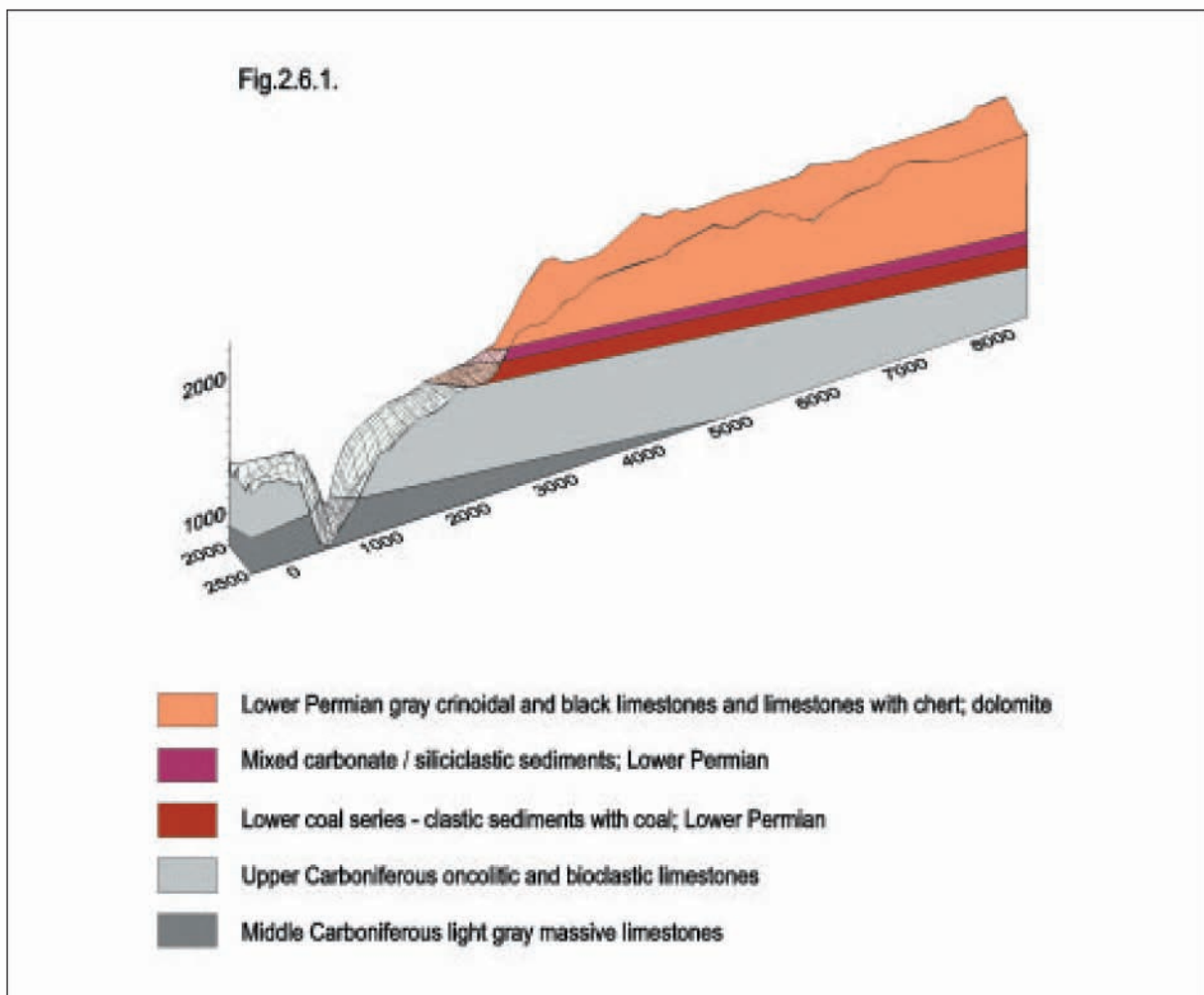


Fig.2.6.1. Lithostratigraphic sketch of Beipanjiang river canyon and Yezong plateau

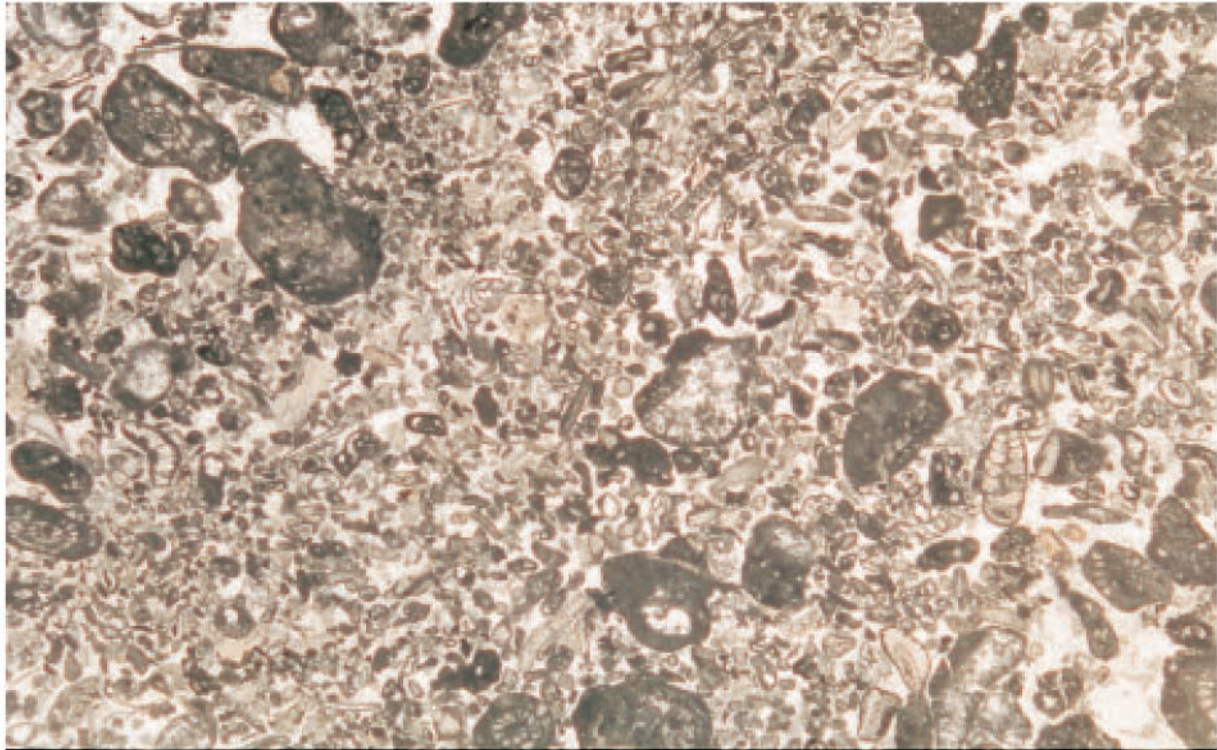


Figure 2.6.2: Poorly sorted bioclastic grainstone. Bioclasts of various origins (algal plates, foraminifers, etc.) are more or less micritized, partly rounded and poorly sorted. The origin of large allochems is not entirely clear, although they do point to micritized and otherwise modified bioclasts (fusulinid foraminifers are noticeable). The outer shelf high energy sand bars. Upper Carboniferous. Long axis of the figure: 1 cm. (Photo: B. Otoničar)

which pass into Lower Permian limestone (Figs. 2.6.1., 2.2.3., 2.2.6.). Over the another paleokarst surface upper coal series and basalts occur in the topmost part of the profile and are also not a part of lithologic research. The total thickness of the rock included in the research of the Yezhong plateau area is about 1000 m. We assessed the main lithologic types of rock in the field, and took samples for microscopic research of the most characteristic ones.

Rock research in the main profile was combined with field observations and informational sampling in some other areas. In other locations in the broader vicinity of the Yezhong plateau we also examined Upper Carboniferous oncolite limestones, Lower Permian transitional strata and Lower Permian limestones and dolomites.

Profile from the top of the Beipanjia river canyon and the road above the reserve management (Fig.2.8.3.)

In the lower part of the Upper Carboniferous part of the profile, thick bedded light gray primarily sparry limestones with small oncoids, peloids, bioclasts and intraclasts prevail in which the quantity of basic components varies. We can observe the alternation of some similar basic lithofacies among which laminated biointraoncosparite limestones, biosparite-fusulinid limestones, and biosparite limestones with large corals (height: up to 10 cm; diameter: 2 cm), foraminifers, and crinoids, prevail.

Limestones are often laminated, and contain laminae and ripples primarily of small oncoids and partly rounded fossil de-

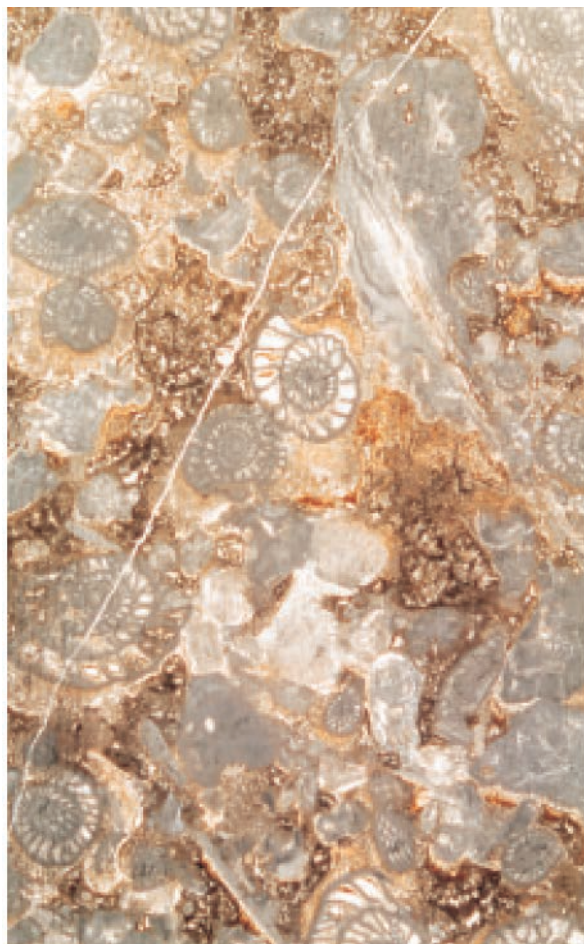


Figure 2.6.3: Pedogenically altered fusulinid crinoidal limestone. We observed secondary brownish micrite (calcrete) in which an alveolar-septal fabric is noticeable. In the lower parts of the bedrock remains we also observe stalactitic vadose cement. Upper Carboniferous. Long axis of the figure: 1,25 cm. (Photo: B. Otoničar)

bris, especially crinoids. A bimodal distribution of clasts is also characteristic.

Fusulinid foraminifers, plates of crinoids, bivalve tests and algal debris are frequent among fossils. Gastropods and, in some beds, solitary corals up to 2 cm in diameter, occur sporadically. In some thin sections, we observed *Tubiphytes*. Characteristic micritisation (Fig. 2.6.2.) and coating of bioclasts can be observed under a microscope as well. Sometimes it is difficult to differentiate clusters of micrite from the matrix and from various irregular micrite coats.

In microscopically examined samples mainly drusy mosaic spar occurs, while isopachous fringing A cement occurs less

often. Crinoidal plates are surrounded by syntaxial rim cement.

The lower part of the Upper Carboniferous part of the profile is divided from the upper by belt of dark limestones with foraminifers, crinoidal plates and individual corals.

The limestones are of the packstone type. Bioclasts prevail among the allochems, but oncoids of the algal ball type and peloids are present as well. Among bioclasts, foraminifers, primarily fusulinids (Fig. 2.6.3.), crinoidal plates, algae, individual gastropods and fragments of various tests and corals are present. Bioclasts are frequently micritized and coated (Fig. 2.6.3.).

The micritic matrix is frequently imperceptible due to the dense packing of particles. In some places it is partially washed, recrystallised or dolomitized. Crinoidal plates may be surrounded by syntaxial rim cement. In some microscopically examined samples, we observed pyrite and tiny calcite veins.

In the belt of dark limestones, thinner lenses of breccia, up to approximately 0.5 m thick, with stylolitic seams occur also. Among other things, we find clasts of colonial corals in it.

In the thin sections (Fig. 2.6.3.) directly beneath the breccia, the matrix is represented by a brown secondary pedogenic micrite with a clotted, indistinct alveolar-septal and in some places a laminated fabric; rhizolites (Fig. 2.6.4.) and brown pellets also occur. The described features are characteristic of beta calcretes (Tucker & Wright, 1990). In the host rock micritized fusulinids and peloids prevail (Fig. 2.6.3.). Some stalactitic vadose cement can be observed on the lower sides of the clasts, or on the ceilings of the infilled voids in the host rock (Fig. 2.6.3.).

Lighter sparry limestones with foraminifers in which, in some places, colonial corals and individual gastropods and crinoids are found, succeed the beds of dark limestone. The limestone is micritic in some places.

This limestones are succeeded by micritic and then by sparry limestone of the grainstone type with small oncoids and

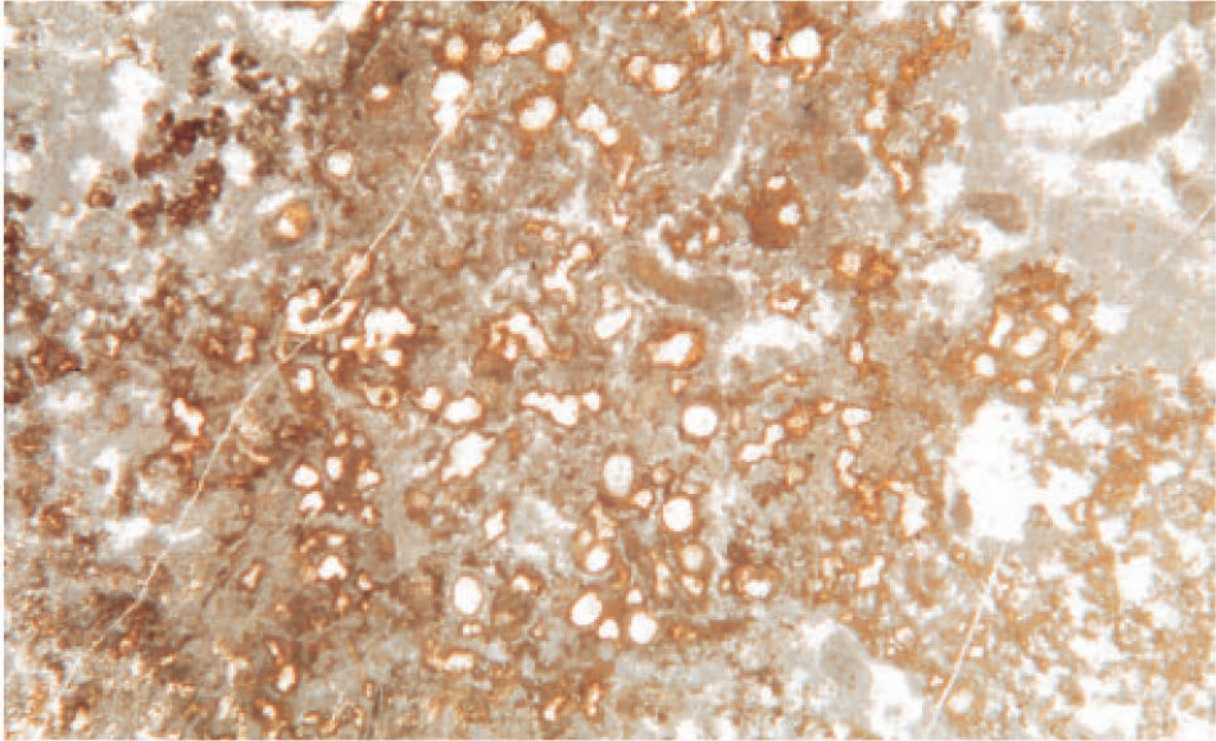


Figure 2.6.4: Lower part of the same thin section as in figure 2.6.3. Rhizolites, indicating pedogenic alteration of the bedrock and/or sediment. Upper Carboniferous. Long axis of the figure: 0,75 cm. (Photo: B. Otoničar)

limestones with rounded bioclasts and oncoids of the algal ball type. We can observe two generations of sparite cement in the thin sections; an A generation of fringing calcite and drusy mosaic spar.

In some places the limestones are graded and have a bimodal distribution of allochems (Fig. 2.6.5.). Larger allochems, up to a few centimeters in size, have micritized margins and in some places could be coated. Higher up, grainy limestones, that is densely packed biomicrite of the packstone type (Fig. 2.6.6.) occur. Fusulinid foraminifers and crinoidal plates prevail among the fossils. The matrix is difficult to determine, only around the crinoidal plates is there a clearly defined syntaxial rim cement.

Limestones of the grainstone type appear in this part of the profile (Fig. 2.6.7.) as well. In them micritized bioclasts, different peloids, primarily irregular in shape, up to 0.5 cm irregular clots of micrite and/or oncoids of the algal ball type and grapestone, predominate. The main component among fossils is represented by micritized

and coated fusulinid foraminifers but crinoidal plates and gastropods also appear. Most peloids were probably formed by micritization and coating of bioclasts and grapestones since, in the majority of them, a poorly preserved inner texture is still visible. Some forms of the micritic clots are similar to *Tubiphytes*. All allochems are more or less well-rounded. Here the allochems are also surrounded by isopachous fringing A cement, while all of the remaining interparticle pores are filled with drusy mosaic spar.

A few meters below the coal series is a distinct bed with irregular concentric, up to 5 cm large, oncoids (Fig. 2.6.8.). Very distinct ones are also to be found on the opposite side of the canyon, at an aerial line distance from the described profile of about 10 km. Large oncoids, probably belonging to the same horizon, were also found by the bridge across the Beipanjiang river. We microscopically examined two samples from this area, of which clotted micrite and micritization and coating of allochems, es-

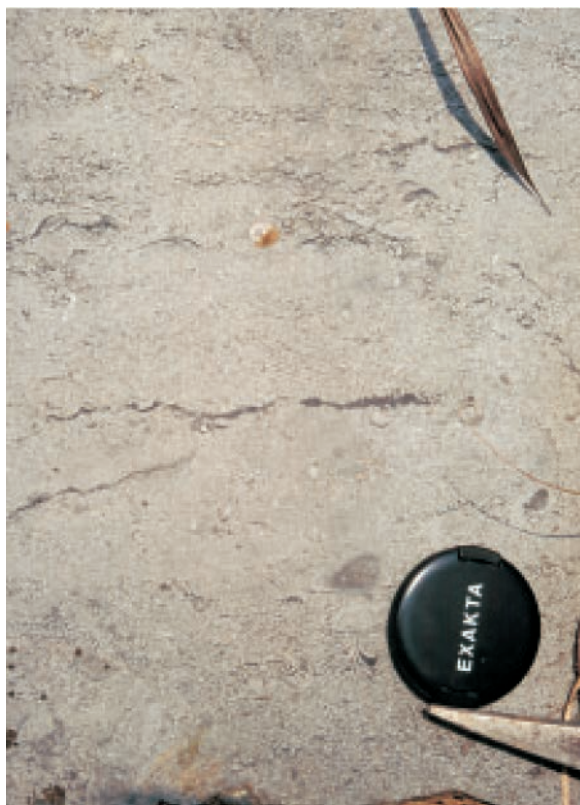


Figure 2.6.5: Poorly laminated and graded bioclastic - intraclastic limestone. Upper Carboniferous. Long axis of the figure: 30 cm. (Photo: B. Otoničar)

pecially bioclasts, is characteristic (Fig. 2.6.9.). Fusulinids are most common among fossils, but green algae and individual gastropods also appear. Among oncoids (Fig. 2.6.9.), ones with an inner spongy fabric and an indistinctly laminated denser micritic coat and oncoids of the algal ball type prevail.

The described limestones are succeeded by a lower coal series, where thinner beds of coal, which are sometimes exploited in small mines in which only a few miners are employed, appear between mudstones and sandstones. The lower contact between Upper Carboniferous limestones and Lower Permian clastics is expressed by paleokarst which we did not observe in the field as it was covered by slope gravel. Transition beds succeed the coal series (Fig. 2.6.10.) which we studied closely some 10 kilometers south-west of the described profile. In these beds black limestones alternate with mudstones, marlstones, and sandstones (Fig. 2.6.10.). Transition beds are succeeded by lighter Lower Permian limestones with crinoids, foraminifers, corals, gastropods, brachiopods and individual patches of co-

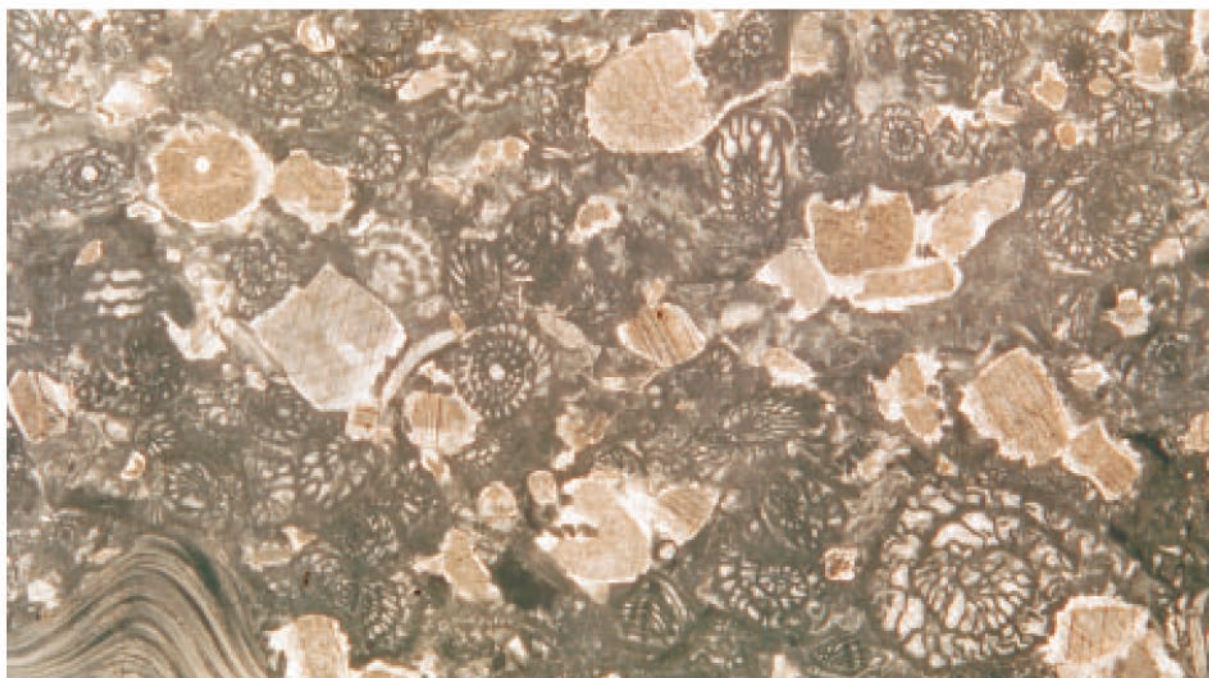


Figure 2.6.6: Fusulinid crinoid packstone. Syntaxial rim cement is visible around the crinoidal plates. Upper Carboniferous. Long axis of the figure: 1,25 cm. (Photo: B. Otoničar)

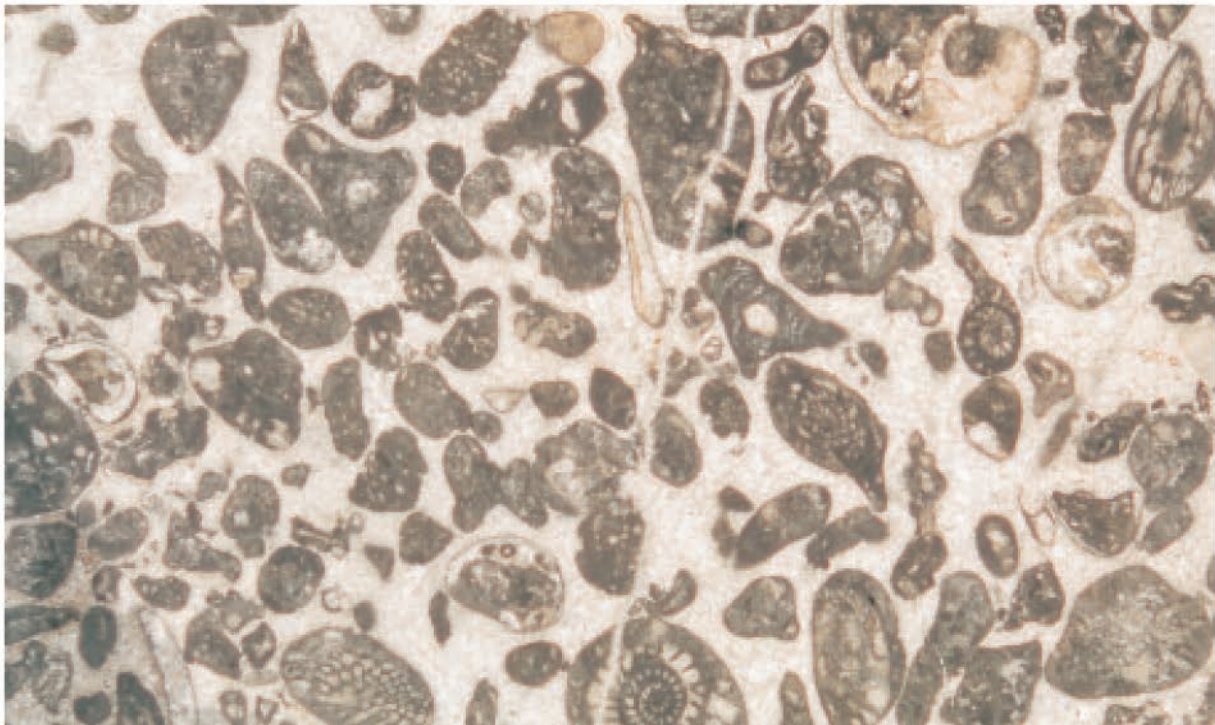


Figure 2.6.7: Well sorted bioclastic peloidal grainstone. Bioclasts (fusulinids, gastropods, and individual crinoidal plates) are partly rounded, micritized, and some are even coated. Allochems cemented into clots – grapestones and oncoids of the algal ball type also appear. High energy shoals of the outer shelf. Upper Carboniferous. Long axis of the figure: 1,25 cm. (Photo: B. Otoničar)

lonial corals. Chert also appears in the lower part of the limestones.

The microscopically examined black limestone of the transitional beds represents a characteristic organic dark-brown to black laminated densely-packed biomicrite limestone of the wackestone type.

Fragments of partly deformed tests of bivalves, ostracods, individual gastropods and brachiopods, and individual crinoidal plates appear.

The tests are oriented parallel to the stratification, which emphasizes the laminated structure. Black organic matter and pyrite are present in the micritic matrix.

Zhongzhai

In the vicinity of the Zhongzhai karst valley (Fig. 2.8.3., 2.8.9.), stratigraphically somewhat above the transition beds, bedded and frequently laminated light gray crinoide limestones and darker micritic

limestones, in which gastropods and ostracods can be seen in some places, alternate. Leached crinoids are also visible in some cavern walls.

In general these limestones are somewhat more micritic than the previously described Upper Carboniferous limestones. Biomicrite and/or pelbiosparite (washed and/or recrystallised) are mostly of the wackestone and packstone type.

Bioclasts and peloids prevail among allochems. Ornamented faecal pellets occur in limestones where there is noticeable bioturbation. Bioclasts are more or less micritized, probably a large part of the peloids formed with complete micritization of bioclasts (Fig. 2.6.11.). We observed indistinct coatings around some allochems. The allochems are fractured and broken in some samples.

Among the fossils, fusulinid foraminifers, crinoidal plates, bryozoas, ostracods, various micritized bioclasts and fragments of various indefinable tests, are present.



Figure 2.6.8: Bed with undulate laminated macrooncoloids of over 5 cm in diameter. Upper part of Upper Carboniferous limestones. Long axis of the figure: 70 cm. (Photo: B. Otoničar)

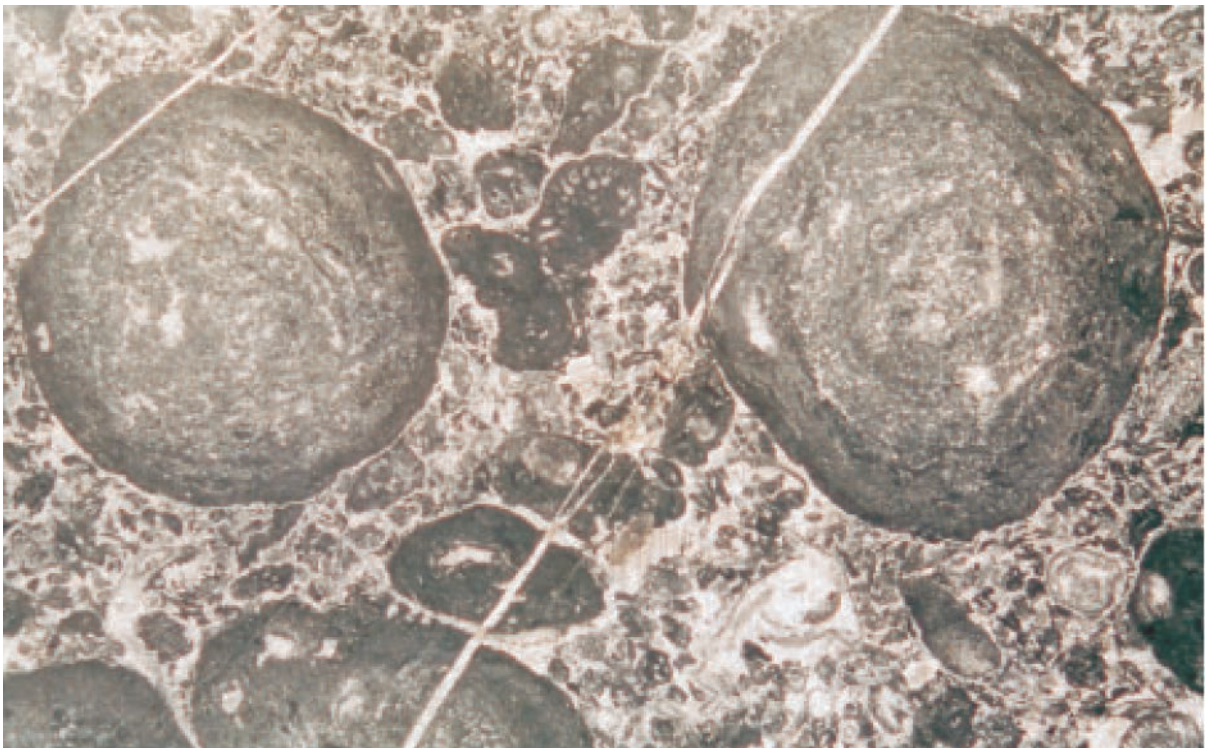


Figure 2.6.9: Peloidal oncolite packstone/grainstone. Irregular peloids of various size, micrite and fossil clots, and various micritic oncoloids and chips of the above-mentioned allochems pass into each other and are difficult to define accurately. Larger oncoloids with spongy inner fabric and denser, poorly laminated coat are the most distinctive. The bimodal allochem distribution is characteristic. Upper Carboniferous. Long axis of the figure: 1,25 cm. (Photo: B. Otoničar)



Figure 2.6.10: Mixed siliciclastic-carbonate transition beds between lower coal series and Lower Permian limestones. Long axis of the figure: 4 m. (Photo: B. Otoničar)

The microscopically examined samples are inhomogeneous due to bioturbation, only in some places can an indistinct lamination be observed. In one sample fine grains of framboidal pyrite, filling some of the chambers of fusulinid foraminifers (Fig.2.6.11.). The samples examined under a microscope were dark brown to black as well.

As mentioned, the matrix is mainly micrite, although clotted micrite may appear. Syntaxial rim cement appears around crinoidal plates. In some places patches of more or less impure drusy mosaic calcite and microspar are seen.

Majiachong (Fig. 2.8.3)

Stratigraphically higher, more or less in the same area and relatively close to the contact of limestones and the second coal series and basalts, on more or less micritic dark limestones with thick calcite veins, lie

lighter crinoide limestones which pass into black limestone with chert in the upper part of the observed profile.

The lower bituminous limestones are essentially biomicrites of the wackestone type (Fig.2.6.12.). They contain fragments of various tests (bivalves, ostracods, algae, bryozoas, gastropods) and individual crinoidal plates. Among the others allochems we also observed tiny medium to well-rounded dark peloids in thin sections. Black stylolitic seams are also characteristic (Fig.2.6.12.).

Crinoide limestones higher in the profile are mainly very densely packed pelbiosparite/micrite of the packstone type (fig.2.6.13.). Partly micritized crinoids and foraminifers dominate among fossils. Individual algae also occur (Dasycladaceae). Among other grains, peloids are frequent, oncoids of the algal ball type and intraclasts also appear. Crinoidal plates are in some places surrounded by syntaxial rim cement.

Contacts between the described limestones and upper coal series and/or basalts

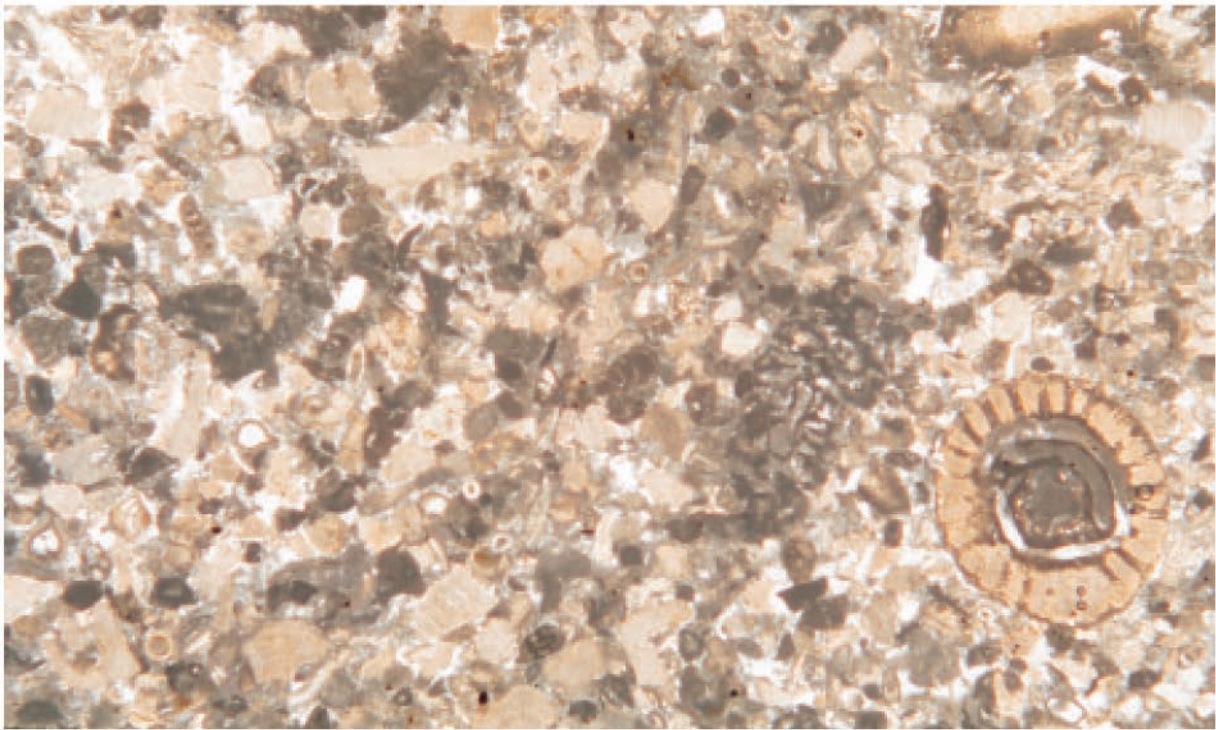


Figure 2.6.11: Peloidal bioclastic grainstone. Peloids are mostly irregular and poligenetic (micritized fossils, various micrite clots, faecal pellets, etc). Among bioclasts, various foraminifers appear, among these fusulinids, crinoidal plates and individual indefinable tests, are the most distinctive. Lower Permian. Long axis of the figure: 0,75 cm. (Photo: B. Otoničar)

are paleokarstic, although paleokarst forms could not be observed in the field due to the fact that they are covered by the weathering product of sandstones and basalts. Flowstone, seen on the surface in the upper profile, may be consistent with this paleokarstic phenomena.

Taishaba

Some ten kilometers towards the NE from the Yezhong plateau, and stratigraphically probably somewhere in the middle between the upper and lower coal series and/or basalts, we geologically surveyed the terrain around the village of Taishaba (Fig. 2.2.9.). We took some informational samples for microscopic analysis.

Thick-bedded limestones are of a similar appearance in a whole area and are medium to dark gray, more or less micritic and contain crinoids. Breccia-calcrudite, followed by black limestones with chert, is of

interest in the lower part. Above these limestones, lighter micritic limestones with algae and individual laminated crinoids, individual patches of colonial corals (up to 10 cm in diameter), gastropods, ribbed fine bivalve tests and foraminifers appear. The limestones lying over the cherts have a mottled appearance due to selective dolomitization.

Microscopically, the samples are of the wackestone or packstone type. Because the matrix is partially washed or recrystallised, it is often difficult to distinguish micrite from micritized grains. In some places we observed clotted micrite.

Among the allochems, we observed peloids of different origin (angular, partly-rounded recrystallised grains, micritized bioclasts, small oncoids of the algal ball type, various clots of micrite, and pellets, intraclasts (partly recrystallised biomicrite) and faecal pellets.

Among fossils, foraminifers, crinoidal plates, various indefinable thin tests and in-

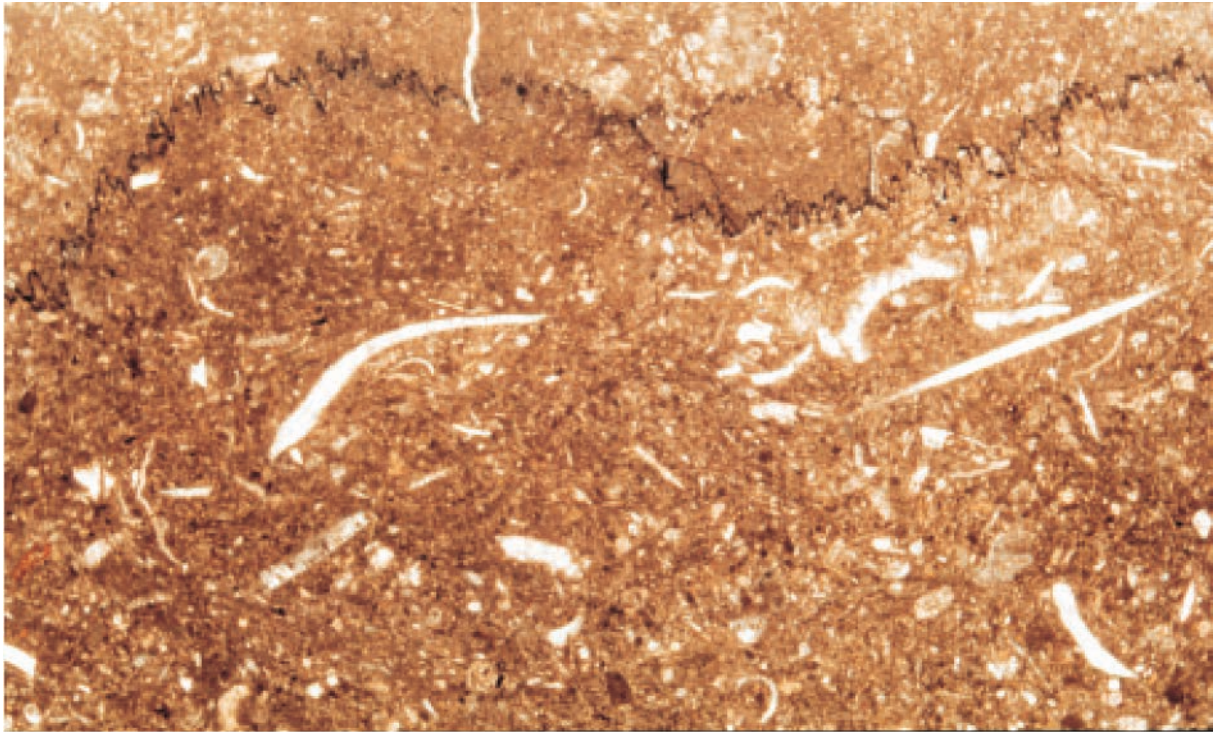


Figure 2.6.12: Bioclastic wackestone/packstone. Among allochems larger and smaller debris of various fossils (gastropods, algal plates, etc), rarely peloids are presented. Due to the fine fraction of the grains, it is difficult to recognize the matrix, as it is probably a fine fraction of debris of various allochems. The sample is cut by a marked stylolitic seam. Lower Permian. Long axis of the figure: 1 cm. (Photo: B. Otoničar)

dividual algae, appear in thin sections. Bioclasts are coated in some places.

Crinoidal plates are frequently surrounded by impure syntaxial rim cement. Under a microscope, in some parts of the thin sections, the selective dolomitization of micrite is visible. In such cases we observed euhedral to subhedral dolomite crystals which have impurities distributed inside in zones.

Conclusion

Despite the limited research time, we can, based on field data and microscopic analyses of informational samples, draw some of conclusions.

We recognized the high variegation of rocks, in terms of lithology and microfacies, and also in terms of depositional environments and diagenesis. Carbonates are rep-

resented primarily by limestones, which are sometimes substituted by coarse, grainy dolomite. In Lower Permian limestones, nodules and lenses of the chert also appear. Generally speaking, Lower Permian limestones are similar to Upper Carboniferous limestones, although the former have more micritic limestones, deposited in somewhat less agitated depositional environments.

In the somewhat higher energy outer parts of shallow shelf seas, primarily pure thick bedded limestones of the grainstone and packstone type were deposited. Bioclastic limestones were deposited on open shelves, on banks or on shoals, which separated the calmer parts of the middle shelf from the outer somewhat deeper areas of the slope, and in the vicinity of build-ups or small patch reefs. Although we did not notice build-ups or mounds morphologically in the field, some facies, which are characteristic of their cover and flanking

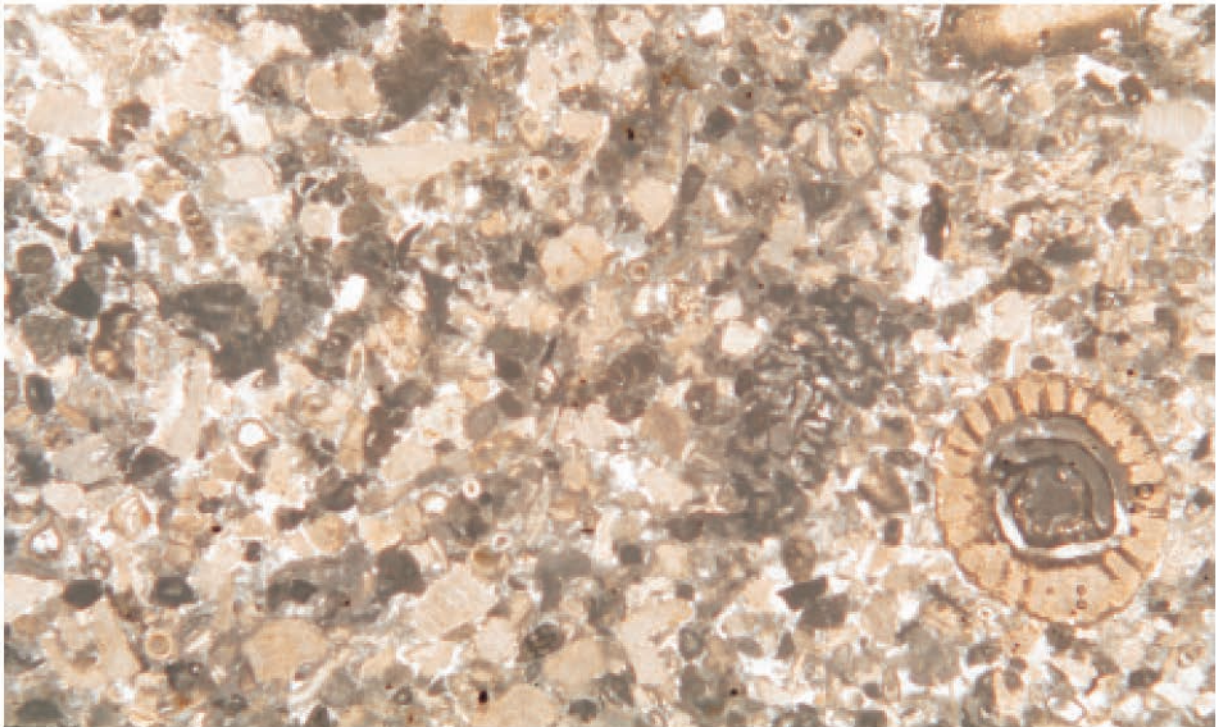


Figure 2.6.13: Crinoidal packstone. Allochems (bioclasts and peloids) are densely packed. Among bioclasts besides crinoids different foraminifers and Dasycladaceae appear. Lower Permian. Long axis of the figure: 1,25 cm. (Photo: B. Otoničar)

beds (biogenetic grainstone and packstone), indicate them. Crinoids, bryozoas, *Tubiphytes*, and also algae and corals, thrived in outer, higher energy shelf environments. These organisms could also build up to form banks, small reefs of various forms and composition and patch reefs, from which they were periodically redeposited into the rather calmer environments. There different organisms micritized bioclasts, coated them and adhered them and their debris into different clots with carbonate cement.

Bioclastic sedimentation was particularly abundant in the area of normal wave activity. Under these conditions, limestones of the grainstone type with rounded bioclasts were deposited. They represent the layers which have been deposited on the highest parts of the shelf margin.

The more rarely present micritic limestones were deposited in calmer areas in the vicinity of the build-ups, behind the barriers or somewhat deeper on shelf slopes.

Some darker limestones of the packstone and wackestone type were probably deposited in bars and shoals of the middle shelf behind the main barriers (shallow lagoons and bays). Bioturbation and *in situ* production of carbonate grains is characteristic of these conditions.

Oncolite limestones with macrooncolites in the upper part of the Upper Carboniferous were deposited in very shallow water with a rather limited circulation, although not so much as to prevent grains from turning over in conditions of slow sedimentation of carbonate mud (possibly under tidal influences). Similar sediments can be found in tidal channels, where they formed under the influence of the tidal currents. A shorter subaerial exposure of the carbonates, approximately in the middle of the Upper Carboniferous part of the profile, is indicated by pedogenically altered limestones with rhizolites, alveolar-septal fabric and stalactitic vadose cement. In this part we noticed dolomite only beneath pedogeni-

cally altered limestones and this possibly represents dolomitization in the zone where freshwater and seawater mixed.

Individual varieties of carbonate do not have a visible effect on morphological forms of large dimensions. They have a greater effect on small morphological forms, which is especially discernible in dolomite areas and areas where mixed carbonate-siliciclastic beds outcrop. The strongest effect on morphology in the research area have clastic

rocks of the coal series which, in the otherwise steep slopes of the Beipanjiang river canyon, constitute structural terrace a few hundred meters wide. The bottoms of some “hanging” karst valleys are also composed of the rock mentioned. The soil cover on this rock is usually very thick. Chert in limestone also has an effect on soil cover development and also indirectly on karst processes. The same is true of mixed carbonate-siliciclastic bed areas.

2.7. SOME GEOMORPHOLOGIC OBSERVATIONS OF THE CONE KARST RELIEF IN WEST GUIZHOU

Andrej Mihevc

Some geomorphologic observations of the cone karst relief in West Guizhou are described. The cone examples are taken from old surfaces of high plateaux at an altitude of over 2000 m, from parts of the relief which have gone through rejuvenation due to rivers sunken into canyons or karst plains.

The morphology of singular cones and their connecting into relief units with intervening depressions are described. The relief develops entirely as karst, with underground drainage, and the depressions sink

most rapidly, while the cones remain as more resistant rock in between.

Cones are visually dominant in the landscape, although the fastest dissolution processes are of the rock in the depressions. Their growth therefore determines the distribution of the cones, while their form is determined by karstic denudation and slope processes. Cone distribution, slope inclinations, the distribution and form of lapiaz and structural lines thus only indirectly characterise the most intensive and dominant processes which take place at the bottom of the depressions.



Fig. 2.7.1. Karst cones, fenglings at Bajizhai (Photo A. Mihevc).

Cone karst characteristics

Karst relief spreads across a large part of southern Chinese territory. We find very different types of relief in this area. Undoubtedly cone karst with depressions in between is the most characteristic type.

Cone karst, irrespective of whether it takes the form of singular cones or towers (fenglin) on a karst flood plain or karst cones with a common base and depression in between (fengcong), aroused the interest of researchers some time ago. Cone karst was studied by Chinese and foreign geomorphologists (Zhang et al. 1987; Zhu Xuewen 1988; Yuan Daoxian 1985; Lin Yushi 1995; Habič 1970, Williams 1985, Ford & Williams 1989).

While travelling across the karst in south-west China, we were able to observe the characteristic cone relief in the provinces of Guizhou and Yunnan. We were primarily interested in the distribution of cones, their relation to geologic structures and the relation between depressions and morphologically more pronounced cones, which are in essence residual features. Cone karst is especially interesting when compared to the Dinaric karst (Habič 1992), where the cone relief is less pronounced and sink-holes are the most pronounced feature among the depression forms.

In the field we were able to observe only the basic relief characteristics, rockiness, small forms and cone distribution, due to a lack of time. We chose the most characteristic types of cone karst relief. On a karst plain at the city of Suicheng we observed an isolated cone, a fenglin in the middle of the plain. On the Yezhong plateau we observed two different areas with cone relief of the fengcong type, on the highest part of the plateau at the settlement of Maichong and at the edge of the plateau over the Beipanjiang river canyon.

Fenglin on the Shuicheng karst polje

We chose a small cone with a double peak near the village. The cone stood by itself at the bottom of the polje, which lies at

an altitude of approximately 1860 m. A new road passes the southern slope of the cone, and part of the cone is used as a quarry. We measured the slope inclinations and the cone shape.

The approximately 25 m high cone is a corrosion remainder of the cones at the bottom of the polje near the village of Bajizhai. The process of lateral corrosion removed and diminished their density in the middle part, while there are some at the fringes of this large, structurally conditioned elongated plain.

The cone had a double peak divided by a pass located approximately 8 m lower. The cone slopes are steep, the greatest inclinations being 55°. The cone slopes have an inclination lower than 30° at their base, while in the central part the inclination ranged between 30° and 40°. Lower inclinations were measured for the cone ridge and the pass between the two peaks.

Small relief forms on the cone are mostly lapiaz and rain rills. They indicate that the cone surface was exposed to precipitation water for a long time. A few small, up to 5 m deep vertical shafts were found on the cone ridge. It was not possible to determine whether they are cave shafts or simply cracks widened by corrosion.

Since the cone is used as a quarry, work in it exposed up to 1.5 m deep pockets of red-brown soil between two rock blocks. Based on preserved subcutaneous forms on rock blocks we can assume that the soil depth on the pass between the two peaks was lowered between rocks by around 1 m. Farm animals graze on the steep slopes, while on the less steep slopes between the cone peaks corn and some other agricultural crops were sown. We were not able to define the amount of soil removal by observing subcutaneous corrosion surfaces.

Karst cone – depression relief on the Yezhong plateau

The Yezhong plateau is a vast levelled surface, dissected into cones and depressions lying between them. The relief is located around 2000 to 2200 m high, the de-

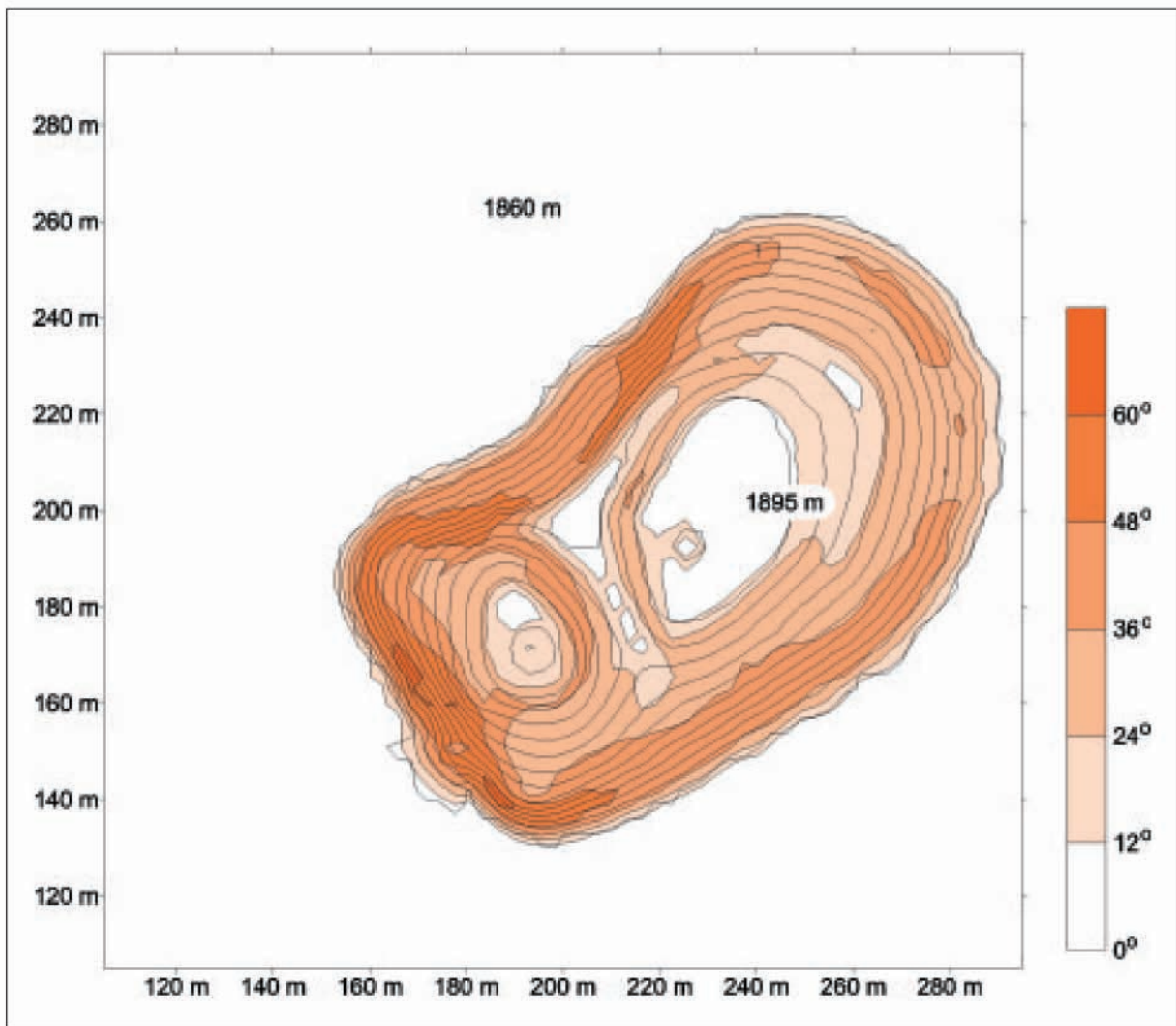


Fig. 2.7.2. Map of distribution of the slope inclinations on the Bajizhai fenglin.

pressions are of various depths. The usual karst relief had an amplitude of around 200 m, some structurally conditioned forms, dry valleys, and valleys are up to 300 m deep. The Beipanjiang river cut into the plateau and bared an approximately 2000 m packet of carbonate rock. The bottom of the gorge lies at 700 m.

In general, we distinguish three types of karst relief in this area (Fig. 2.8.3.).

1. Beipanjiang river canyon is a typical canyon formed by the rising of the relief in connection with the newest tectonic phase of the development of this territory. The canyon slopes are mostly very steep, in some places the walls of the canyon are completely vertical, and the biggest walls are up to 500 m high. The wall shapes, their

inclinations and fall zones depend on lithologic characteristics of the limestone and how broken down they are. The river cut into massive thick bedded Permian limestone in which the steep canyon sections are found. In Lower Permian limestone with coal beds and marl the slopes are the steepest, forming a structural terrace up to 2 km wide with an inclination of approximately 20°. Massive Carboniferous limestone, in which the narrowest and frequently vertical part of the canyon formed, lies beneath them.

2. The Yezhong plateau relief formed in Permian limestone and limestone with chert. The plateau is dissected into cone relief with depressions and valleys in between the cones. The surface is 2000 to

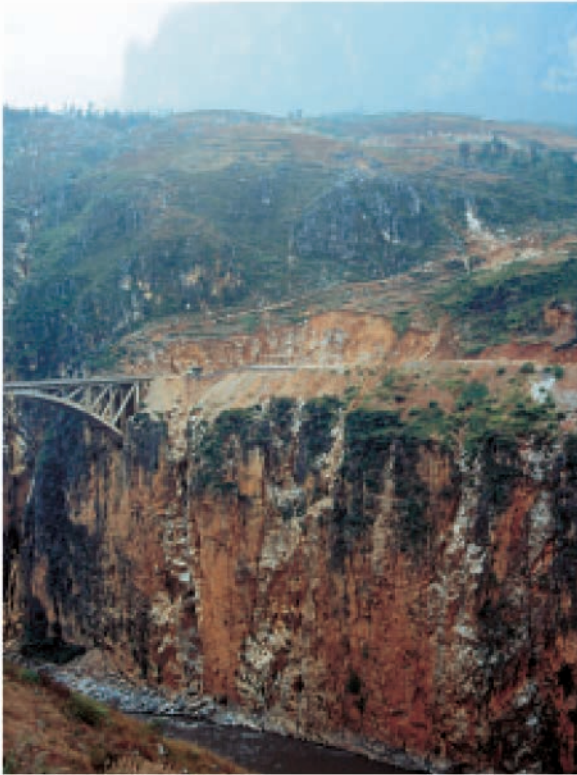


Fig. 2.7.3. Characteristic view of the Beipanjiang river canyon (700 m a.s.l) cut into Yezhong plateau (2200 m a.s.l). There are vertical walls in Permian and Carbon limestones, in less resistant Lower Permian beds with coal series a structural terrace was formed (Photo A. Mihevc).

2200 m high. The surface of the cones is rocky, soil is only to be found at the bottom of depressions or on more level slopes between the cones. There are no surface flows in the whole area.

3. Large karst depressions on the plateau formed in areas with exposed Lower Permian coal beds. An indistinct karst relief with valleys and plains developed on them. The underground drainage is characteristic, a thick soil cover has however remained on the surface. The cones developed in the form of residual fenglins in limestones which are stratigraphically above the limestones of coal series, for example by the village of Zhongzhai (Fig. 2.8.9.).

Karst surface at the village of Majiachong

The relief of the plateau at Majiachong village is dissected into cone peaks and intervening depressions. The cone surfaces are rocky with belts of soil between the rocks. More soil covers smaller inclinations and depression bottoms. Due to new soil erosion, the exposed cones have traces of subcuta-



Fig. 2.7.4. View of Yezhong plateau. Cone peaks are approximately 2250 m above sea level (Photo A. Mihevc).



Fig. 2.7.5. View of cone peaks on Yezhong plateau (Photo A. Mihevc).

neous erosion, although it is not possible to estimate the amount of erosion, as it differs.

This relief is a part of the oldest leveling of this area. The cone peaks are around 2250 m above sea level, depression bottoms at around 2000 m. The relative height of the cone peaks is around 200 m (Fig. 2.8.18.).

The cone slopes are inclined to 55° and the relief in between, that is moderate valleys, to 15° - 20°. The depressions between the cones are somewhat elongated in the NW - SE direction and transversally to this direction. In the lower part of the cone slopes larger inclinations occur in these directions, in the upper part the largest inclinations are distributed around the whole cone. The largest inclinations appear in the middle of the cone slopes.

Cones on the canyon edge at Natural Reserve administration centre

On the edge of the canyon small cones developed on a morphologically distinct,

around 2 km wide terrace. They formed in limestone which lay beneath coal series and in which the lower part of the Beipanjiang river canyon also developed (Fig. 2.8.6.). The area of cones is small, with a size of 300 x 300 m. 5 separated cones formed on this relief with a depression in between.

The cone surface is rocky, with belts of soil among the rocks. The surface between the cones is covered with a thick layer of weathering product. The soil is eroded due to human impact. Singular blocks are up to 2 m high, signs of breaking off block peaks were found approximately 20 cm below the peaks. Up to 1 cm deep rain rills have developed on the broken surfaces. In some places there are holes several metres deep.

The cones are around 100 m above the surrounding relief. The cone peaks are around 1500 m above sea level, and the terrace edge is roughly 1400 m above sea level. Below the edge the vertical walls up to 500 m high and steep talus cones incline towards the river which flows at approximately 750 m above sea level.

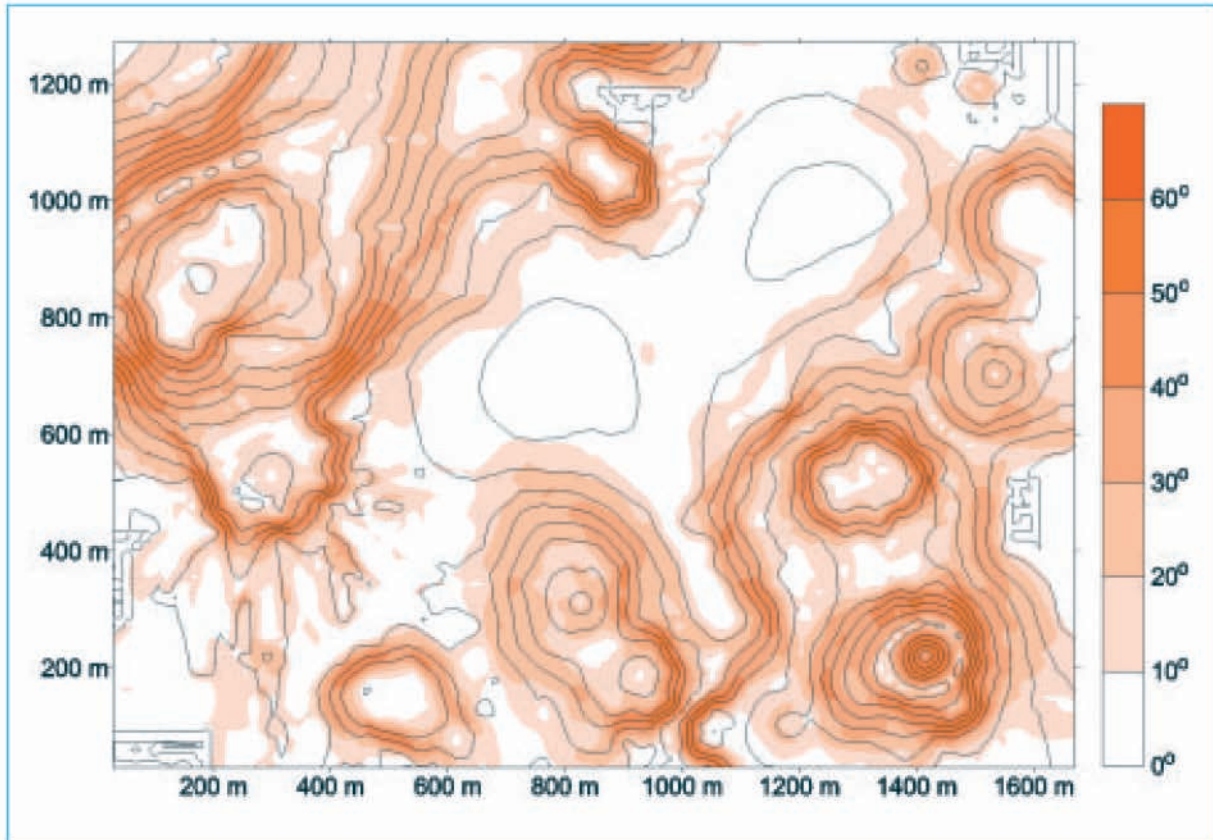


Fig. 2.7.6. Map of inclinations at the village of Majiachong.



Fig. 2.7.7. Cones formed on the terrace in the Beipanjiang canyon (Photo A. Mihevc).



Fig. 2.7.8. Cones formed at the edge of Beipanjiang river canyon are influenced only by canyon slope processes (Photo A. Mihevc).

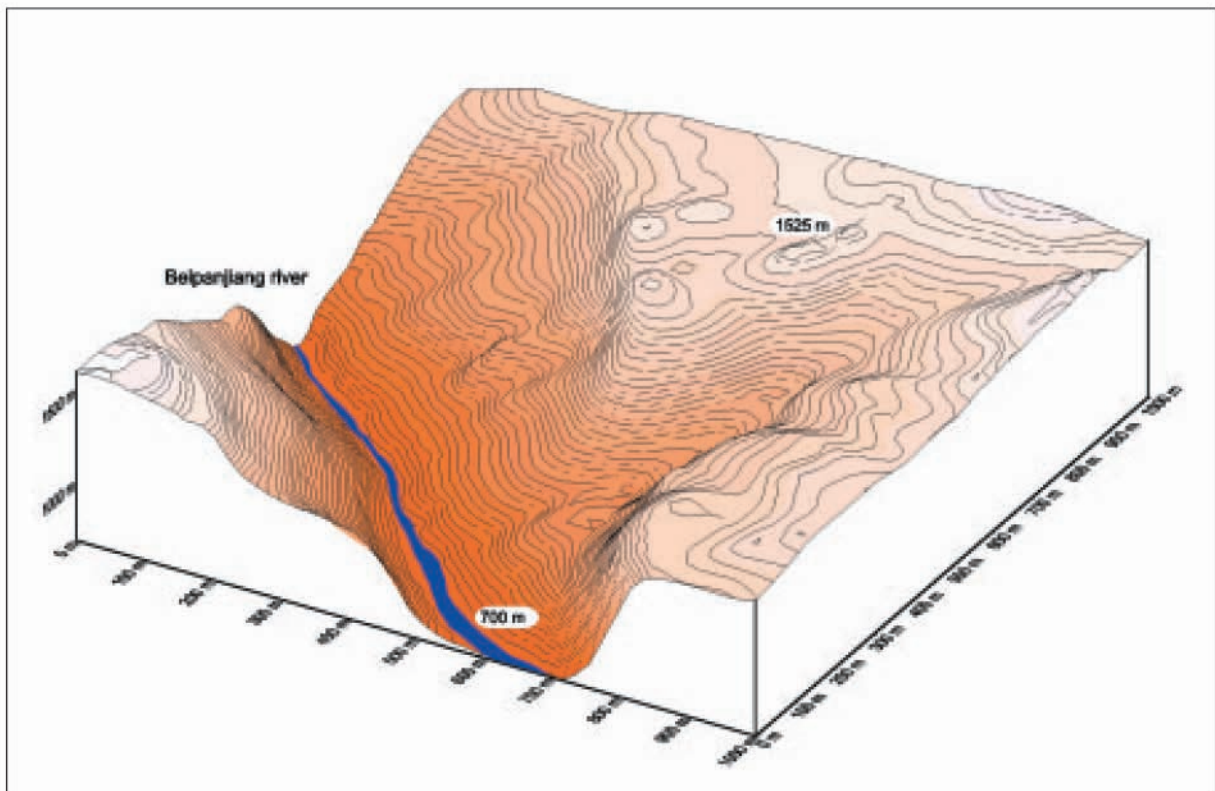


Fig. 2.7.9. Model of relief with cone peaks above Beipanjiang river canyon.

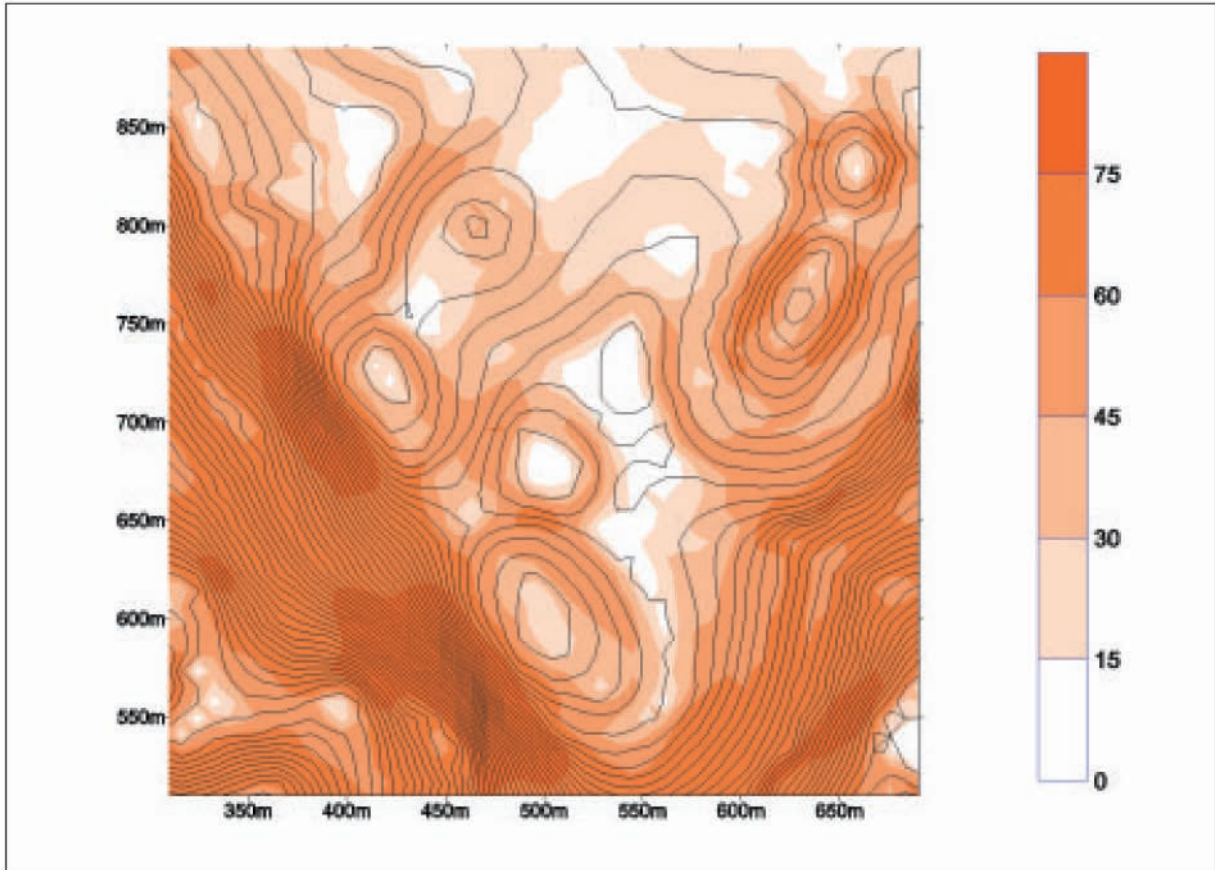


Fig. 2.7.10. Map of inclinations of cone karst above the canyon.



Fig. 2.7.11. Surface at elevation of about 1400 m in Xichou, S Yunnan. Level of the ground water is now deep below the surface and there are only thin soils on the surface (Photo A. Mihevc).



Fig. 2.7.12. Leveled surface is a relict of the karst plain that developed in the level of the ground water. Slope transformation of the fenglin cones is very slow, so the sharp transition from the cone to the plain is still visible (Photo A. Mihevc).

The cone slopes incline to 37° , the relief in between and moderate valleys incline to $15^\circ - 20^\circ$. Larger inclinations appear on the canyon edge and in places where the canyon cuts off parts of cones. The inclinations in these areas are $60^\circ - 90^\circ$. The canyon walls cut off parts of cones or depressions between them. The canyon, 700 m deep, does not affect the shape of the cones, the effect reaches only to a few metres from the edge of the walls.

Cone karst on the high elevations differ from the karst features in lower positions, in E Yunnan, Xichou area, for instance. Lower position means different climatic conditions and different relation between water table and karst surface and gradient in karst.

There are different stages of development of the relief in Xichou. Large area was levelled in elevation of about 1400 m. Plain shows it was formed in the water table level where only some about 100 m high fenglin remained. The surface is without any sur-

face water and has very thin soil cover. Slopes of the cones are even more stony.

On the edge of this surface valley like depressions or karst poljes developed. These youngest features are at elevation at about 1100 m. There are many karst springs and caves at the foot of the slopes in them, but there are also level dry, non active caves in higher levels or the slopes cut caves, that have been filled with allochthonous non-carbonate sediments.

Conclusion

It is not possible to reach significant morphological conclusions based on a few cone measurements in various karst environments. Cones are the visually dominant feature in the West Guizhou karst, although the fastest process is rock dissolution in depressions. Their growth and distribution are therefore determined by cone distribution, while their form is determined by



Fig. 2.7.13. Valley like elongated depression between cones are result of youngest phase of karst development, their bottoms being at elevation of about 1100 m (Photo A. Mihevc).



Fig. 2.7.14. Closed depressions, karst poljes are also formed in elevation of about 1100 m. Several of them are inundated for longer periods during the year (Photo A. Mihevc).

karst denudation and slope processes. Cone distribution, slope inclinations, distribution and forms of lapiaz and structural lines thus only indirectly characterise the most intensive and dominant processes which take place at the bottom of depressions.

Cone relief at the village of Majiachong represents a part of the oldest relief in which the river cut a canyon 1500 m deep. The cones in this area are up to 200 m high, and the cone slopes are very steep. This indicates that the depression bottoms are still lowering.

Cone relief on the edge of the plateau formed on a structural terrace in the middle of the Beipanjiang river canyon and is much younger, which is probably the reason why the cones are only up to 100 m high. Characteristic of this relief is that despite its position near the canyon, there are no signs of the canyon determining cone

formation. The effect is visible only where mechanical effects of crumbling of the 500 m high walls of the canyon also affect the cones. This insensitivity to the vicinity of the canyon points to vertical drainage, corrosion in the subcutaneous karst zone being the most important for cone and other surface features formation. It explains also the absence of surface water flow which would create fluvial forms in the relief.

The cone slope inclinations depend on the relation between lowering of the depressions between the cones and slope processes. The slopes can be grouped into those slopes which are a part of the depression and those which are part of the cone. The depression slopes display a greater dependence on structural lines, primarily fracture zones, while the slopes of the cones as residual forms show less structure control both in their inclination and direction.

2.8. EFFECT OF GEOLOGICAL STRUCTURAL ELEMENTS ON GENESIS OF CONE KARST, EXAMPLES FROM NORTHWEST GUIZHOU

Nadja Zupan Hajna

Introduction

During field research of the cone karst of NW Guizhou I attempted to answer the following question: Does a correlation exist between the distribution of cones and geological structural elements, primarily rock deformation in fault zones. It is known that a series of cone summits adheres to the geological structure (Daoxian, 1991; Song and Liu, 1992; Sweeting, 1992) and that the shape of individual cones depends on the

distribution of geological elements such as, for example, strata dip, fault presence and varying lithology. I have attempted to explain why cones are positioned at their exact location and not a few meters away next to the same structure. I did this in the field by measuring of geological elements. A cone is a slope reaching a height from a few meters to a few hundred meters and divided from the others by a depression. In essence a cone is a remnant of rock that is disappearing due to karst relief denudation. The



Fig. 2.8.1. Work in the stone-pit and road construction cut the cone at Bajiazhai, Liupanshui and expose disintegrated P_1 limestone and dolomite beds. In the stone-pit two karst pocked filled by red soil are opened (Photo. N. Zupan Hajna).

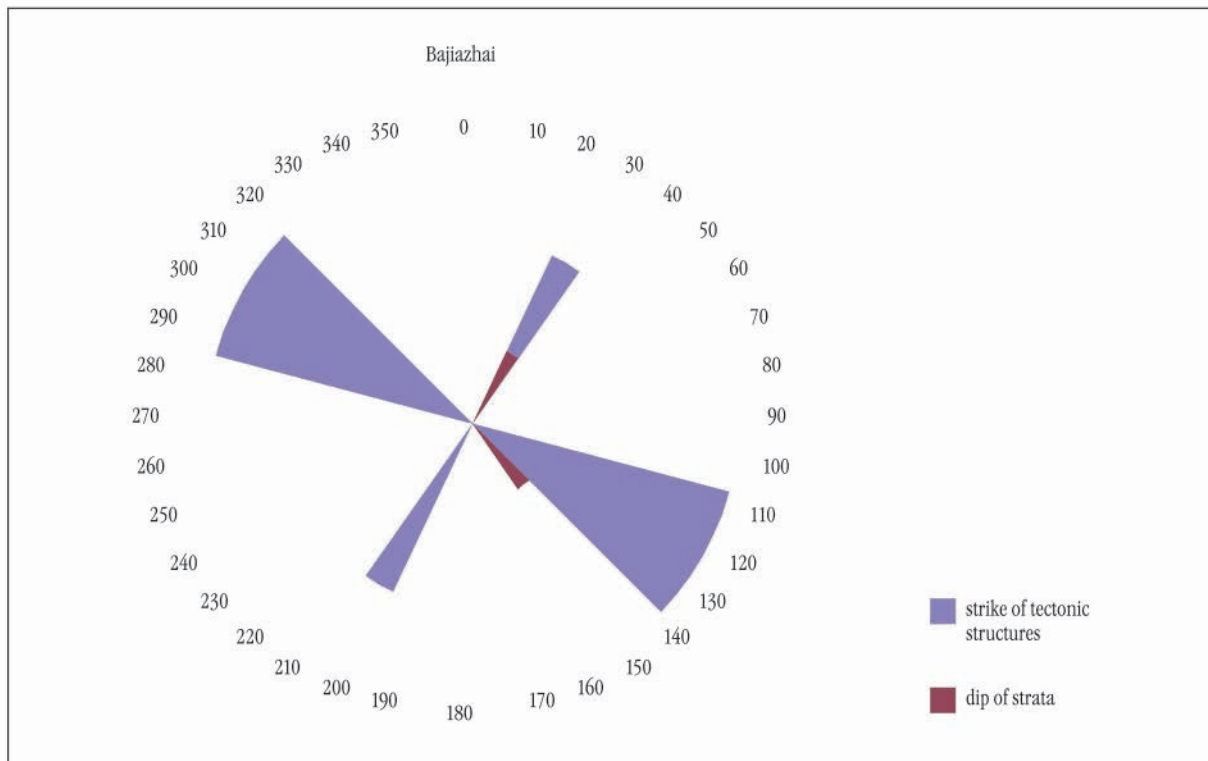


Fig. 2.8.2. Dip of beds and strikes of tectonic structures on a cone near the village Bajiazhai near Liupanshui. Intensity is expressed by length of the bars.

depressions in between are lowered in relation to groundwater level and conform to it. The cone or rock remainder can develop and remain at the same location where its summit was protected from weathering by an impermeable cover or more resistant carbonate sequence or in a location where it is limited by more tectonically deformed rock. Tectonic deformations weaken the mechanical hardness of the rock, undermining its structure and thus exposing it to mechanical and also chemical weathering. In this way the rock, which is more mechanically disintegrated, will in most cases yield to stronger weathering and consequently the relief will lower faster in that particular area.

Measurements of geological structural elements were carried out on the chosen terrain in the vicinity of the city Liupanshui, in the village of Bajiazhai, then north of the town in the area of the Tianshengqiao natural bridge, east of the town cave near the village of Xingchang, south of the town near the village of Taishaba, near the village of Majiachong and in the karst valley near the

village of Zhongzhai on the Yezhong plateau, and on the slopes of the Beipanjiang river canyon. The frequency and intensity of the measured structural elements with the length of the data series is presented in the article in the form of charts.

Bajiazhai

The city of Liupanshui lies in a karst depression at 1850 m above sea level and is surrounded by cone summits. There are a number of cone summits at the bottom of the depression so that the city lies between them. In the immediate vicinity of the city, in the small village of Bajiazhai, the construction of a road and a smaller excavation have cut off parts of the cone with two peaks leaving its inner structure well exposed (Fig. 2.8.1.).

The cone is structured of Early Permian limestone, which is quite well dolomitised. In the lower part of the cone, the strata dip towards the south-east 140/10-15, and in the upper part of both peaks towards the

north-east 30/30. The layers are heavily fractured in different directions, a fissured zone in the direction of 290°-110° is most distinct across the second peak, and across the pass between both cone peaks in the direction 310°-130°. On the northern side, where the cone was cut off for a small stone-pit, planes of faults running in two directions are clearly visible: the first in the direction 290°-100°/90 and the second in the direction 210°-30°/70-75.

Beipanjiang

The Beipanjiang river canyon is cut into the Yezhong karst plateau, which is over 2000 m above sea level. The cones on the plateau are over 2200 m above sea level (Fig. 2.8.3.), the river Beipanjiang flows at 800 m above sea level (Fig. 2.8.4.).

We are able to view rock from the middle of the Carboniferous to the late part of the Early Permian. At the bottom of the canyon there is limestone and dolomite from the middle of the Carboniferous which is light-colored, in thick strata and massive. They are followed by Late Carboniferous limestone in thick strata of the Maiping formation, which are thickly crystallized and very pure. They are followed by paleokarst, and then by the Early Permian Lianshan formation, with flint sandstone and a coal series containing coal of poor quality. This is followed by Early Permian strata of the Maukou formation which in regard to their age belong to the late part of the Early Permian. Over this limestone, main paleokarst developed. Basalt spread over this rock in the Late Permian. The main direction of the fault zones, fractures and strata dip in the area of Yezhong plateau are presented in Fig. 2.8.5.

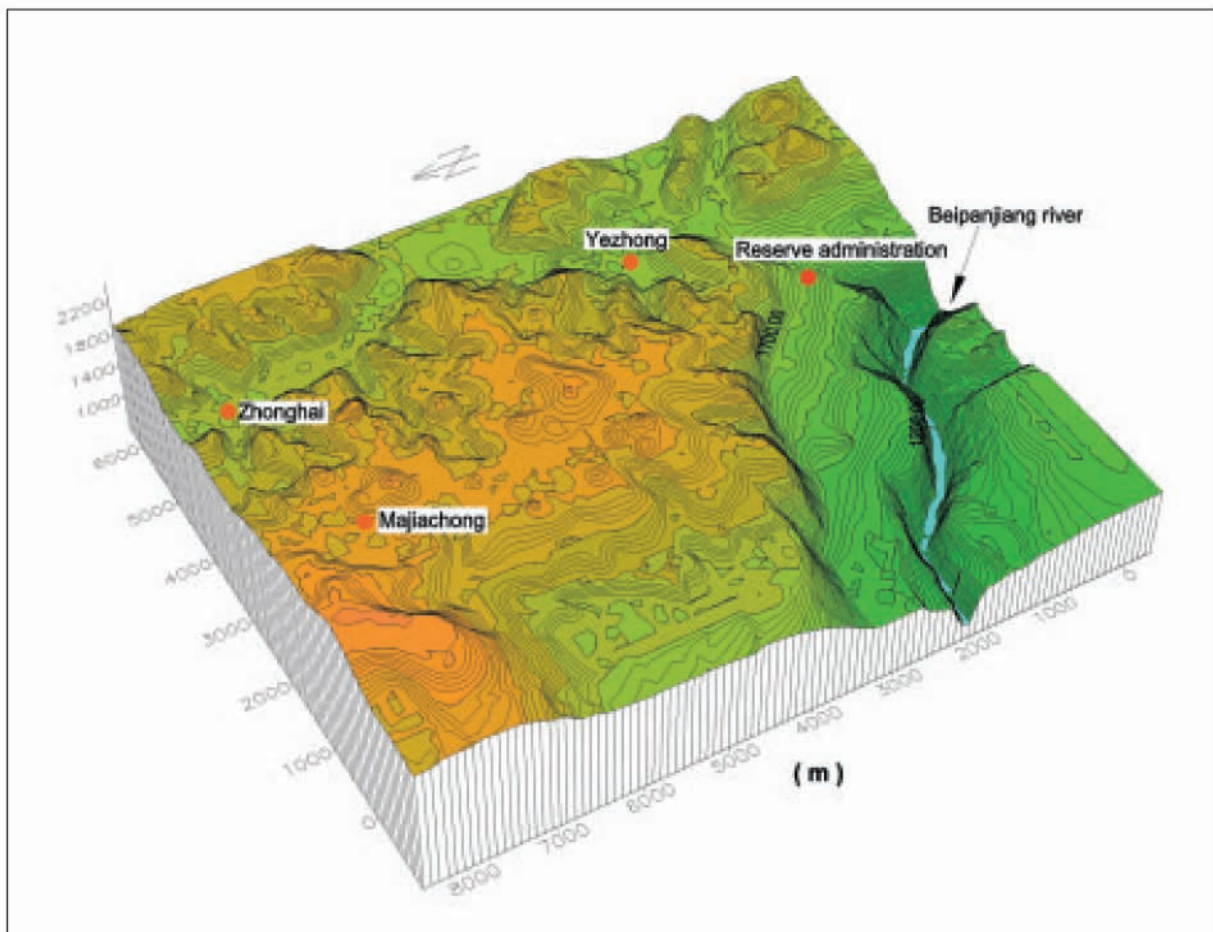


Fig. 2.8.3. Yezhong karst plateau with cone karst above the canyon of the Beipanjiang river with the location of significant points marked.



Fig. 2.8.4. The canyon of the Beipanjiang river is cut 1400 m deep into the high plateau Yezhong, the canyon direction in this part is NW-SE (Photo. N. Zupan Hajna).

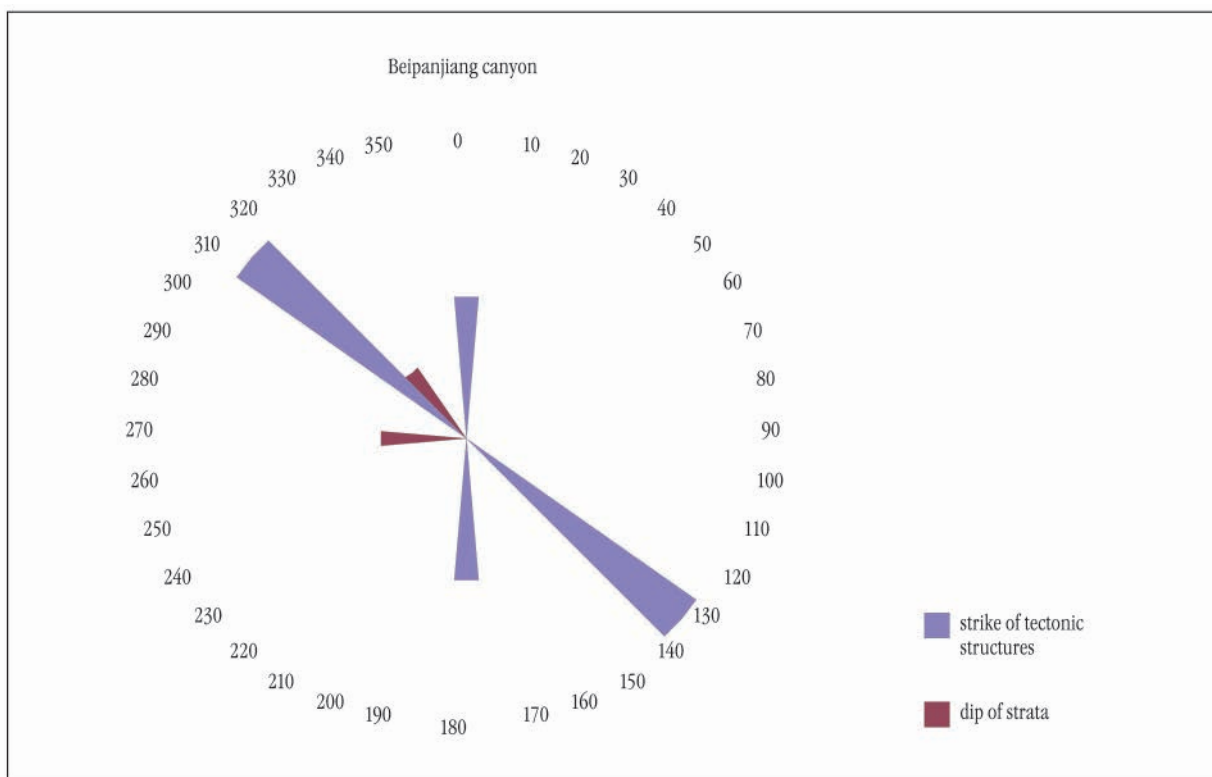


Fig. 2.8.5. Dip of beds and strikes of tectonic structures in the Beipanjiang canyon. Intensity is expressed by length of the bars.



Fig. 2.8.6. Low cone summits are located on the structural terrace below Monkey reserve administration, at the beck upper part of the canyon is seen and the top of the Yezhong plateau (Photo. N. Zupan Hajna).

Near the bridge

The canyon across the Beipanjiang river follows a NW-SE direction, the fissures and parallel faults in the canyon wall run in the same direction. Faults in the N-S direction are also visible. To the west the canyon still follows an E-W direction, but further on takes a turn at the fault zone in the direction NE-SW. Faults and fault zones oriented NE-SW are characteristic of all Chinese neotectonics. The layers in the incline of the canyon dip toward W and NW, with dips 270/20, 310/20, 320/15.

Below the monkey reserve administration

On the structural terrace, around the middle of the canyon incline, at 1500 m above sea level and immediately at the edge of the river canyon, there are low cone summits (Fig. 2.8.6.).

The orientation of the canyon edge here is NW-SE, a very strong fissured zone on the structural terrace lies in the direction 310°-130°. Karren up to 50 cm deep have developed in this zone. A weaker fissured zone was also found on the structural terrace in a N-S direction. Fractures in the NW-SE direction are most pronounced between cones and across the cone located at the edge of the canyon. In this fissured zone, deep karren have formed on the cones and on the edge of the structural terrace above the canyon (Fig. 2.8.7.).

On the southern side of the canyon, above the structural terrace below which the canyon begins, a fracture zone in the NW-SE direction is clearly visible in the walls of a large sinkhole (Fig. 2.8.8.).

Zhongzhai

On the north-eastern side of the Yezhong plateau, near Zhongzhai village, we found

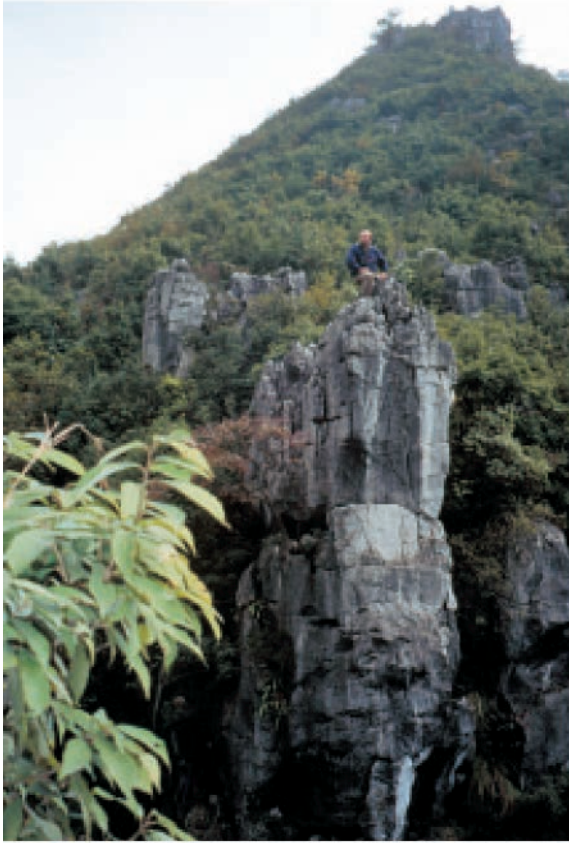


Fig. 2.8.7. Deep karren by the fractures in the NW-SE direction directly next to the edge of the structural terrace that overhangs the 700 m deep Beipanjiang river canyon (Photo. N. Zupan Hajna).

the entrance to a karst valley. The valley lies approximately 1750 m above sea level and is surrounded by cone summits over 2000 m high (Fig. 2.8.9.).

There are individual 100 m high cones scattered around the bottom of the valley (Fig. 2.8.10.). In the area we traversed, the valley was generally oriented in a N-S direction, with side valleys connecting to it from the east and west sides (Fig. 2.8.11.).

The valley descends in stages towards the Beipanjiang canyon (Fig. 2.8.12.). There is no large water flow in the valley but small flows, which soon disappear in the valley bottom, run from side valleys.

Four general fault zone directions N-S, NE-SW, NW-SE, and E-W have affected the valley's orientation and the formation of cone summits in the valley bottom and edges. This part of the Yezhong plateau is structured of Early Permian limestone dolomitised in some places and also containing chert. The layers dip to the S-W, 240/10 (15) in the eastern and southern parts of the valley and, in the south-eastern part of the valley, to the SE, 150/5 (Fig. 2.8.13.).

A large number of large and small cave entrances in the slopes of the cones in the

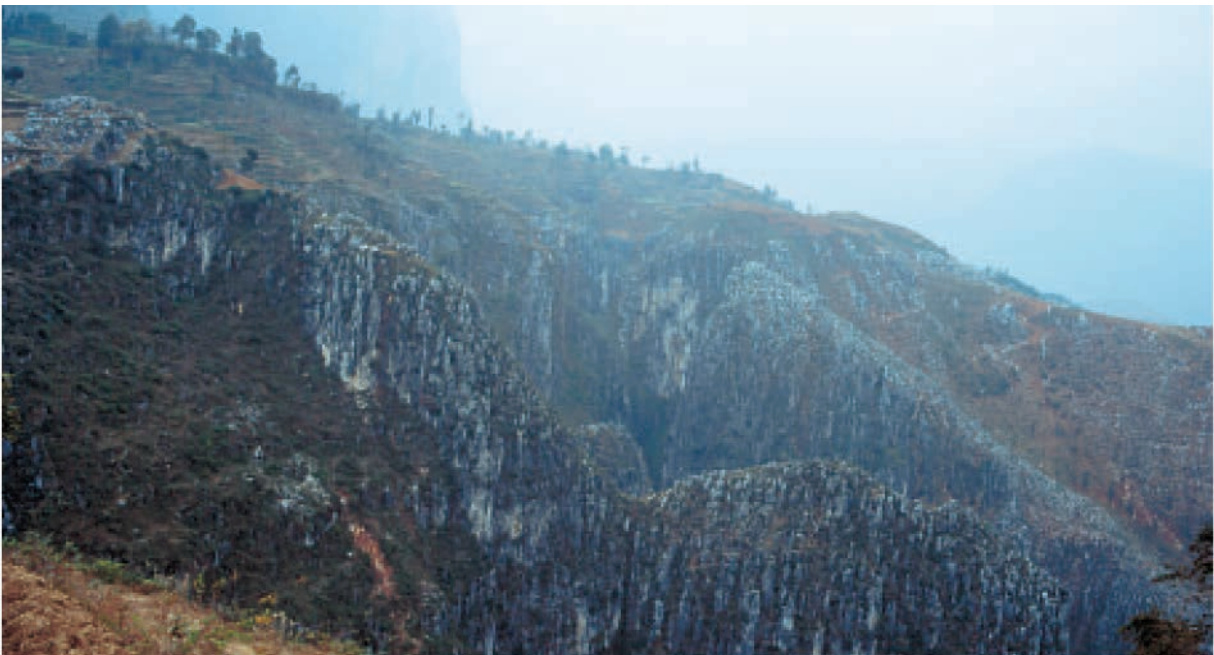


Fig. 2.8.8. A strong fissured zone in the NW-SE direction in the limestone on the structural terrace of the southern slope of the Beipanjiang river canyon (Photo. N. Zupan Hajna).

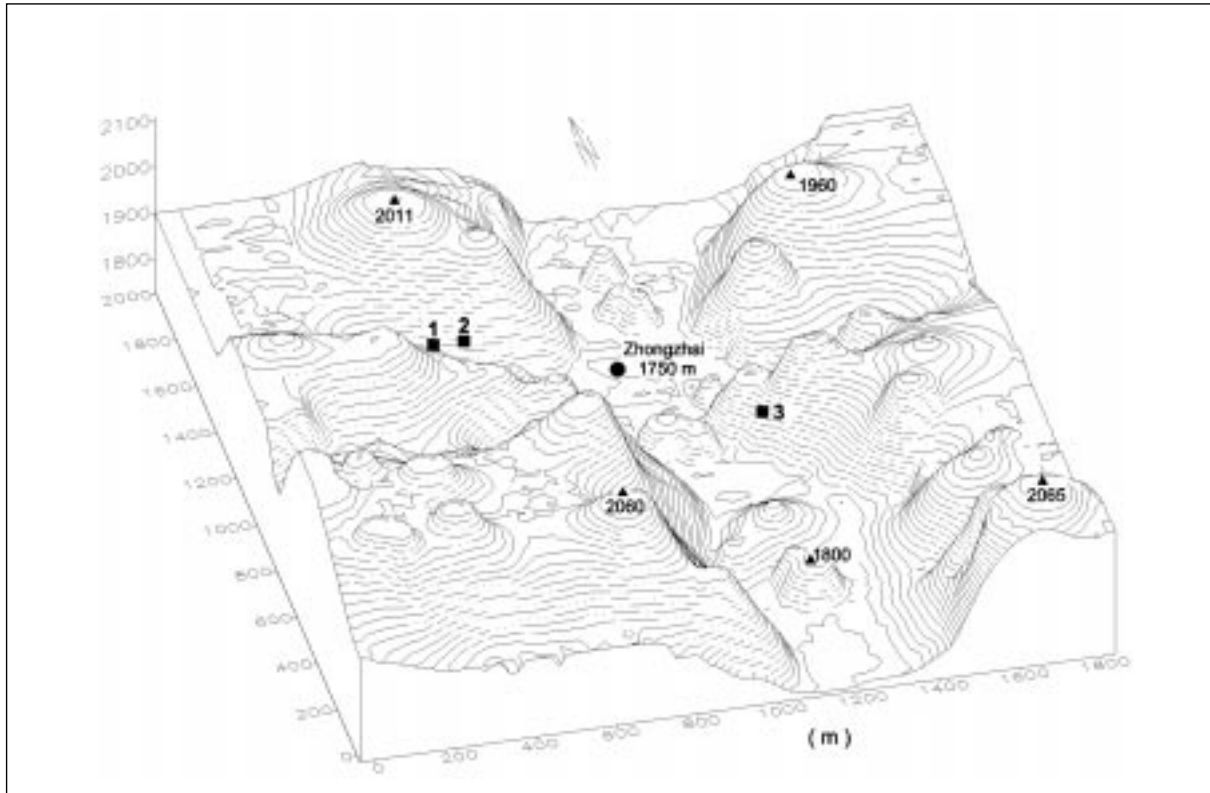


Fig. 2.8.9. Karst valley by the Zhongzhai village 1750 m above sea level surrounded by cone summits over 2000 m high. Legend: 1 - Cave I, 2 - Cave II, 3 - Cave III.



Fig. 2.8.10. About 50 m high cones are scattered along the bottom of the Zhongzhai valley (Photo. N. Zupan Hajna).



Fig. 2.8.11. The Zhongzhai valley has generally N-S direction (Photo. N. Zupan Hajna).



Fig. 2.8.12. The Zhongzhai valley descends towards the Beipanjiang river canyon (Photo. N. Zupan Hajna).

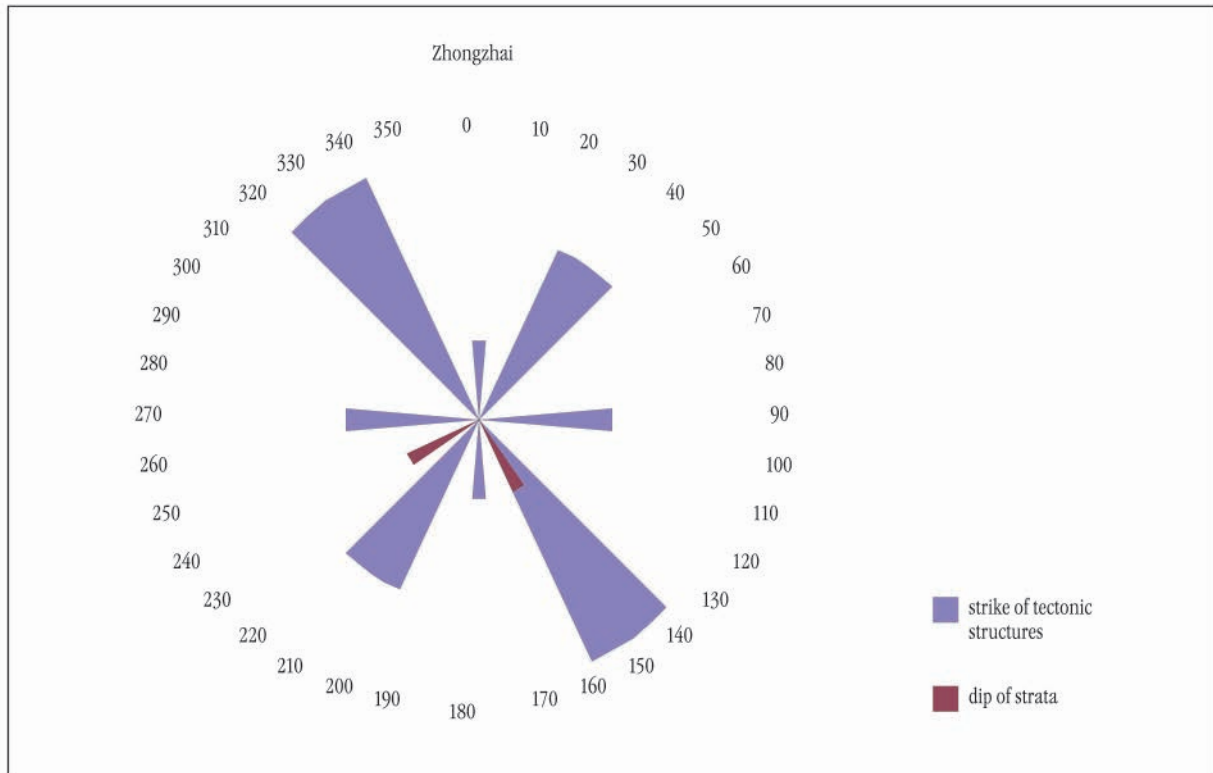


Fig. 2.8.13. Dip of beds and strikes of tectonic structures in the Zhongzhai karst valley. Intensity is expressed by length of the bars.

main valley and side valleys are visible. The entrances are located at the following heights: first at the bottom of the valley at the contact of the cone base and valley bottom, the second at about 100 m above the valley bottom, and the third at about 200 m above the valley bottom. There is water in the caves at the valley bottom, while the caves in the valley slopes show signs of past groundwater levels.

Side valley

There is a small creek spring near the road leading from a plateau over 2000 m above sea level near the Majiachong village through a smaller side valley to the main valley near Zhongzhai village. About 100 m above the valley bottom, in its northern slope, two cave entrances showed promise of leading to a larger cave (Fig. 2.8.14.).

The first, Cave I., terminated after a few meters in a passage filled with sediments. We measured the cave and drew a map of it. We also measured the directions of the



Fig. 2.8.14. Large cave entrance in the slope of the side valley (Photo. N. Zupan Hajna).

geological structures. The second cave, Cave II., was essentially a huge abri filled to the top with sediments.

Cave I.

The cave passage is oriented to the north and follows the fractures in a N-S direction, which is clearly visible from the entrance to the end of the cave. The cave entrance opens in the fractures in a NW-SE direction 330° - 150° to 320° - 140° , that is in the direction of the side valley. Lesser fractures in the E-W direction are also nicely visible. The cave ends blocked with sediments, there are also large quantities of remains of old conglomerate on the walls. The cave ceiling is leveling, which points to the fact that the cave was once filled to the top with sediments.

Cave II.

The entrance to the cave is located in a wall that runs in the same direction as the fractures, that is E-W, approximately 100 m above the valley floor. It is a wide escarpment filled with allochthonous sediments of a yellow color.

Main valley

In the area where the side valley described connects to the main valley, at Zhongzhai village, the creek submerges in a smaller depression below a cone through which a fault cuts with a dip of 130/70 (Fig. 2.8.15.).

A cone approximately 100 m high rises on its southern side. It is structured of a light-colored, thick-layered limestone in the lower part, and in the upper part of a darker, stratified limestone with individual sheets of chert. The limestone layers dip in the SW direction, the strata dip is 240/10. This cone is interesting because the entrance into the smaller cave lies in its slope and also due to the fact that it is bisected by a longitudinal opening with a few meters wide vertical walls (Fig. 2.8.16.).

The trough is limited by its surfaces in the E-W direction and is filled to the top

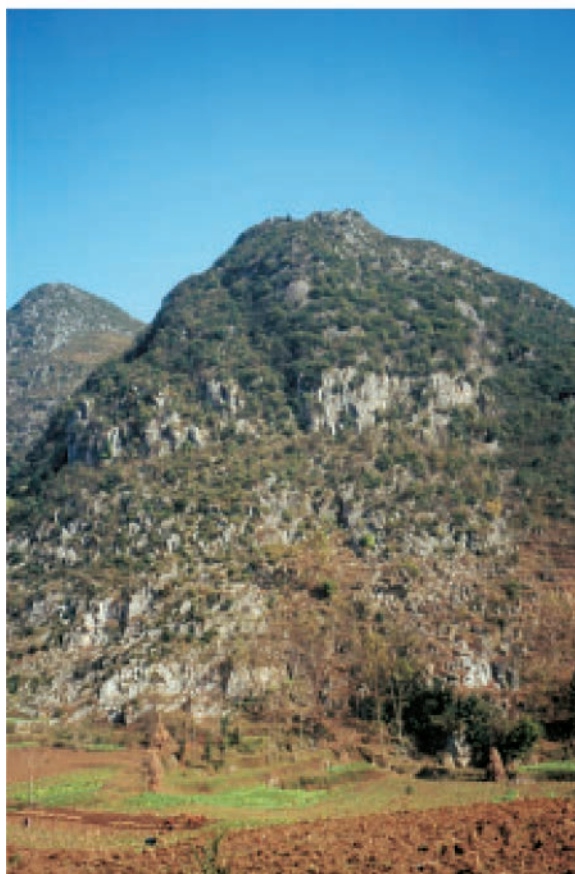


Fig. 2.8.15. A fault with a dip of 130/70 cuts the cone above the swallow-hole of the periodical creek (Photo. N. Zupan Hajna).

with autochthonous and allochthonous mechanical sediments. In the short time available we were not able to establish whether it is a smaller tectonic opening filled with sediments from the surface or a roofless cave passage filled with sediments. To the north, on the lower part of the cone, an area of 1 m deep karren had developed on its summit in a fissured zone in the E-W direction. On the pass between the area mentioned and the crest which rises towards the east and summits over 2000 m high, we find a clearly visible broken zone in the N-S direction. The fissured zone is especially evident on the neighboring cone with deep karren in the lower part where the limestone is more stratified (Fig. 2.8.17.).

Cave III.

The entrance to the cave is located in the middle of the slope of a cone with a



Fig. 2.8.16. The cone with Cave III. and 'roofless cave' on the top of the summit, Zhongzhai (Photo. N. Zupan Hajna).



Fig. 2.8.17. Fissured zone in the E-W direction are especially evident with karren in the thick stratified limestone (Photo. N. Zupan Hajna).

trench and a fracture zone in the direction 320° - 140° . The short cave passage lies in the E-W direction. The wall is cracked with small fractures in the 210° - 30° direction. The cave is 8 m long, and terminates in gray conglomerate that fills the passage to the top.

Majiachong

The valley by the village Majiachong on the Yezhong plateau follows a NE-SW direction (Fig. 2.8.18.).

The bottom of the valley is 2000 m above sea level, the highest cone summits around it are over 2200 m above sea level (Fig. 2.8.19.). There are individual cones at the bottom of the valley. The early Permian limestone which this area is structured of, came into contact with Early Permian basalt on the north-eastern edge of the valley. We climbed to some of the summits to the south of the village and these were from 180 to 260 m high.

The highest reaches a height of 2265 m, there are passes at various heights between the cone summits. The dip of the limestone layers here is $300/20$. The lower parts of the cone summits, below the pass at a height of 2100 m, are formed of layers of dense black limestone, the upper part of the layers of white limestone with lenses of chert. The contact between them is heavily tectonised. There is a high density of calcite veins in the black limestone at the contact represented by a vein of crystal calcite approximately 10 cm thick. In pockets and over large areas on the cone slopes a brown weathered deposit, rich with quartz, was found.

The main fissured zone across the cone has a NW-SE direction, 310° - 130° , and a weaker fissured zone in the N-S direction, running in the 350° - 170° direction. Black limestone at the bases of the cones, below the pass, are fractured in the NE-SE direction, 250° - 70° , the limestone was crushed between the faults of the same orientation (Fig. 2.8.20.).

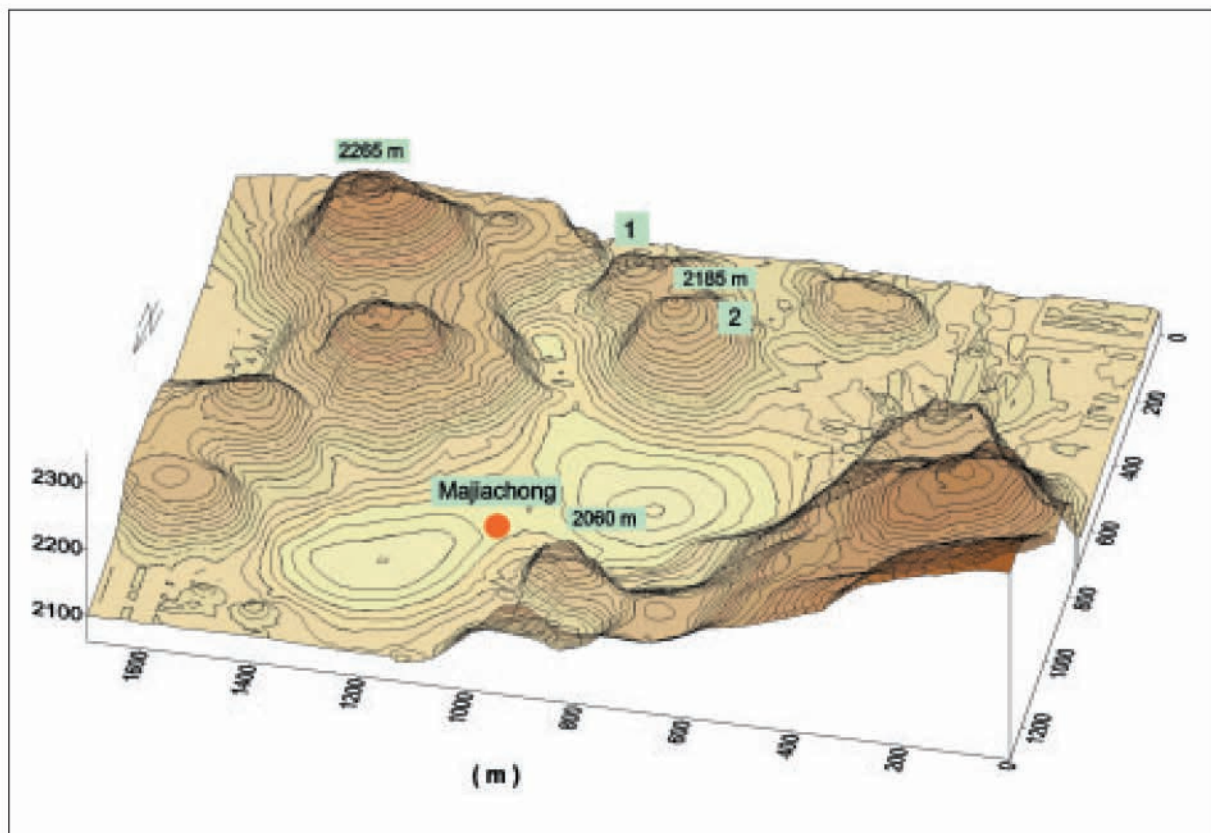


Fig. 2.8.18. Valley by Majiachong village 2000 m above sea level is lying in the NE-SE direction. Legend: 1 - Cone I, 2 - Cone II



Fig. 2.8.19. Majiachong valley encircled by cone summits over 2200 m high (Photo. N. Zupan Hajna).

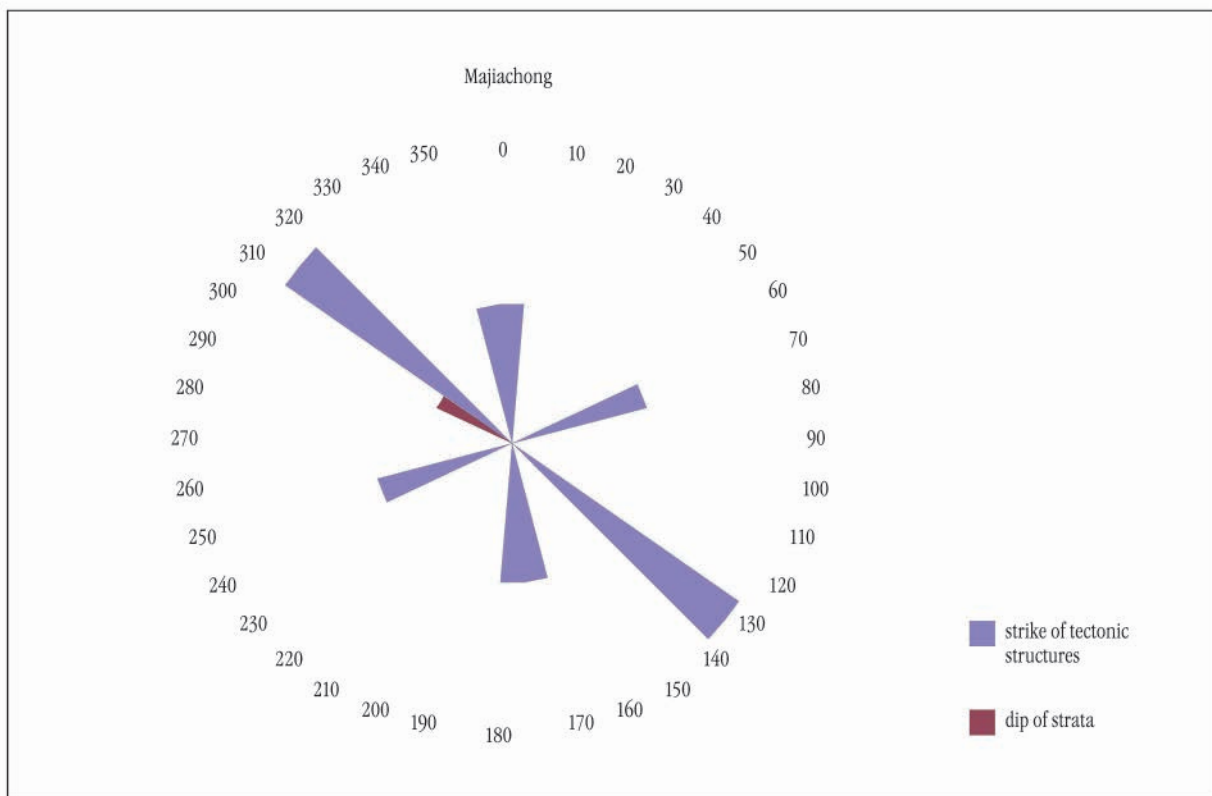


Fig. 2.8.20. Dip of beds and strikes of tectonic structures in the Majiachong valley, Yezhong plateau. Intensity is expressed by length of the bars.

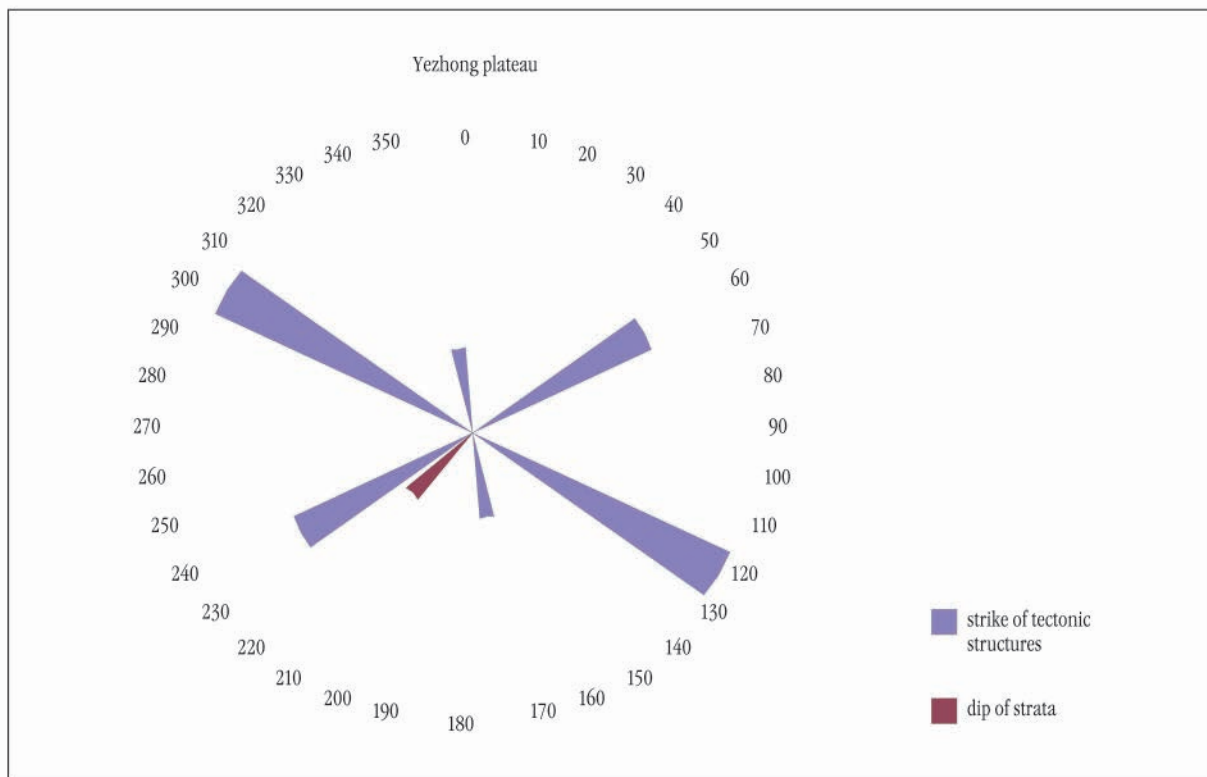


Fig. 2.8.21. Dip of beds and strikes of tectonic structures on the Yezhong plateau, between the village of Majiachong and the Beipanjiang river canyon. Intensity is expressed by length of the bars.

The following structural elements have been measured from the Majiachong village towards the Beipanjiang canyon, that is towards the SE, over the Yezhong plateau with its cone summits which reaches over 2000 m above sea level limestone strata dip 230/18; and three main fracture directions, the first, N-S, which turns to 350°-170°, the second, NW-SE and the third, NE-SE (Fig. 2.8.21.).

Taishaba

At Taishaba, south of the city of Liupanshui, on a plateau over 2000 m high, cone karst has developed in Early Permian beds. A creek flows past the village, but was dry during our stay. We followed its bed to the swallow-hole in the lowest depression between the cone summits. At the last swallow-hole, fractures in the NE-SW direction, 210°-40°, were evident.

In Early Permian limestone, from which the cones at the north-eastern edge of the

village are structured, the strata dip is towards the SW. The dip of the strata is between 200/20-25 and 220/20. A strong fissured zone is evident and cuts the cone in the NE-SW direction, 230°-50° (Fig. 2.8.22.).

The direction of the main fissured zone across the pass between the cones is N-S. The two cones are limited by weaker fractures in the E-W direction on the northern and southern side. Both fissured zones divide the two cones where all three mentioned directions of tectonic deformations cross. The rock there is crushed.

Conclusion

The measurements of individual geological structures indicated that the passes between individual cones usually occur at the intersection of a number of differently oriented fault zones or in zones with heavily disintegrated rock. As rock is crushed it also becomes less resistant, therefore this is where more intense dissolution happens.

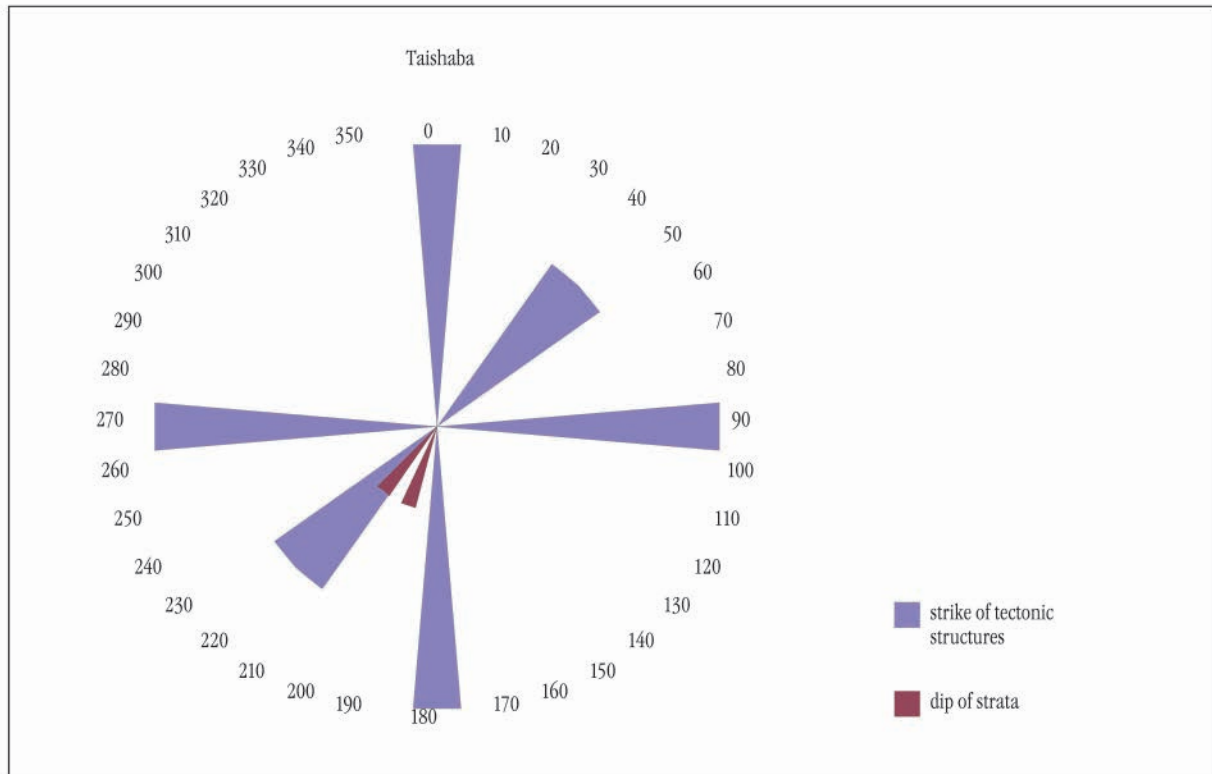


Fig. 2.8.22. Dip of beds and strikes of tectonic structures at Taishaba village. Intensity is expressed by length of the bars.

This form of dissolution is nevertheless weaker than the dissolution which takes place simultaneously at the groundwater level at the base of the cone. The groundwater level regulates the development of the level area between the cones and thus divides them. The plain may be flooded occasionally, according to the water level variation. Dissolution processes form the cones which may be divided by a flood plain, by passes or cockpits which develop in zones with heavy tectonic breaking of the rock, and thus where selective corrosion is stronger. Cones with separate summits and

the same base may develop, the rock is lowered between the summits because zones with more disintegrated rock are located there. In passes and depressions between the cones, a heavier accumulation of mechanical sediments or soil is often present, additionally accelerating carbonate rock dissolution.

We may conclude that where a cone forms, that is where rock remains, depends to a greater extent on the distribution of fault zones and to a lesser extent on the differences in rock lithology, the main process being selective corrosion.

2.9. CLASTIC SEDIMENTS FROM KARST OF SOUTHEAST YUNNAN AND NORTH WEST GUIZHOU

Nadja Zupan Hajna

Introduction

Sediments in the karst relief and caves of south-east Yunnan and north-west Guizhou seemed interesting to me for the reason that they do not differ in colour from sediments in the karst of Slovenia. Sediments and soils in the karst of Slovenia and south China are mainly red and yellow. These facts resulted my interest in mineral composition of karst sediments in south China. The basins of south China are in a great part filled by a thick layer of red sediments. Red soil developed in a tropical climate of sediments originated from the

weathered remains of non carbonate rocks, schist, sandstones, Upper Permian basalt, Eocene lake sediments etc. (Zhang 1984). Some of them don't exist in that part of China anymore. Weathered remains are enriched on silico-ferrous minerals like quartz, opal, amorphous silica, goethite, hematite, sericite, siderite etc. (Maire & Pomel 1995). Sediments are not captured just in big basins but also in smaller depressions of cone karst and in caves.

The relief of SE Yunnan is in great part covered by thick layer of red soil probably developed from basalt and Eocene sediments (Zhang 1984). Clastic sediments,

SAMPLE	LOCATION	A.S.L.	FIELD DESCRIPTION
SF	Stone Forest, behind the hotel	1800 m	red soil
LIU 1	Bajiazhai, pocket	1850 m	red loam
LIU 2	Bajiazhai, pocket	1850 m	yellow sand
BAI 1	Baipanjiang, near the Bridge	960 m	brown loam
BAI 2	Baipanjiang, southern side	1350 m	red- brown soil
ROB 1	Baipanjiang, terrace edge	1510 m	yellow loam
ROB 2	Baipanjiang, terrace edge	1510 m	red loam
ROB 3	Baipanjiang, karren on cone	1565 m	brown soil
ROB 4	Baipanjiang, Monkey's Head	1620 m	red soil
ZHO 1	Zhongzhai, Cave II.	1850 m	sand, loam
ZHO 2	Zhongzhai, Cave III.	1830 m	sand, pebbles
ZHO 3	Zhongzhai, in front of Cave III.	1830 m	loam, limonite crust
ZHO 4	Zhongzhai, roofless cave	1850 m	laminated loam
MAI 1	Maijachong, Cone I.	2150 m	brown loam
MAI 2	Maijachong, Cone II.	2150 m	brown soil
MAI 3	Maijachong, main road	2150 m	basalt
TAI 1	Taishaba, pass between cones	2270 m	brown soil
TAI 2	Taishaba, cone slope	2270 m	red-brown soil
TAI 3	Taishaba, swallow-hole	2195 m	yellow-brown soil
XIN 1	Xingchang, Cave	1720 m	yellow loam
XIN 2	Xingchang, slope above village	1800 m	yellow weathered loam
XIN 3	Xingchang, slope above road	1820 m	yellow loam

Table. 2.9. Location and field description of samples analysed by x-ray diffraction technique.

found in the karst relief of NW Guizhou, are in most cases of a brown colour and originate from weathered basalt, quartz sandstone and rock of the coal series.

The samples in which was defined mineral composition represent clastic sediments that differ very much in terms of colour, texture and consistency. The quantities of each sample were small due to transport limitations. Beside the samples of clastic karst sediments of south-east Yunnan and north-west Guizhou, samples of basalt and quartz sandstone were also taken. These are the two most common forms of non-carbonate rock in this area which come into contact with carbonate rock and are thus the possible original rock for their formation. Altogether we took 22 samples from across a vast area (Table. 2.9.). For this reason we gained an impression only of their composition and not of their origin.

X-ray of the samples was performed at the Institute of Geology at the Faculty of Natural Sciences and Technology in Ljubljana with a Phillips diffractometer using the x-ray diffraction technique. The shoot-

ing conditions were a $\text{Cu}_k\alpha$ anode, automatic divergence slit, the area of shooting was at angle 2θ from 4° to 70° and the size of the step was 0.02. All the samples contained so many different minerals that the reflections covered each other thus making it difficult to define them. It was not possible to determine lower reflections in some cases and we assume that these belong to the minerals that were scarcer in the samples. Plagioclases, feldspar, mica minerals and phosphates were in such a low quantity that their precise determination was not possible. The quantity of minerals is given in their respect to the height of the main peak of particular mineral and it is relative. Mineral composition of samples is represented in Fig. 2.9.8..

South-west Yunnan (Lunan and Xichou)

One third of Yunnan province consists of carbonate rock, mostly from the Late Paleozoic and Triassic. In Lunan area, the



Fig. 2.9.1. Red soil covers slopes of the cone summits, yellow-coloured clastic sediments can be residue of sediments from denuded cave (Photo. A. Mihevc).

karst relief is covered with a thick layer of red soil beneath which stone forests have developed in Lower Permian limestone and dolomite. The height above sea level in this area varies from 1100 to 1950 m. Upper Permian basalt has covered Lower Permian carbonate rock and Eocene lake sediments. These rocks are the possible source rock for the development of the red soil.

From Lunan to the south, the plateau becomes cut through with valleys, the cone summits on plateau are encircled and partly covered by red soil. Xichou, which lies in the far south-eastern part of Yunnan, is an area of cone karst and has formed in Lower and Upper Paleozoic limestone and dolomites. It has an ear-like pattern of carbonate rock, large depressions lie in the middle of the ear-like structure and small ones on the edge (Song Lin Hua & Liu Hong 1992). Red soil covers the summits and slopes of the cone summits. Yellow-coloured clastic sediments can be found in caves, in some places at the bottom of depressions, and sometimes in irregular patches on the slopes of cones (Fig. 2.9.1.). The yellow colour of the sediments indicates that the sediments were not in the oxidation zone during the warm climate, preventing iron oxides from transforming into hematite and turning red. The presence of yellow-coloured sediments in patches and their colour point to the possibility that they used to be cave sediments which have subsequently surfaced.

Lunan Stone Forest

Sample SF

Sample SF consist of red soil from the Lunan Stone Forest (Fig. 2.9.2.) containing individual chips of weathered limestone. It was taken behind the hotels in construction-pit.

The sample is mostly comprised of quartz 96 %, chlorite 2 %, muscovite 1 %, kaolinite and hematite are present in traces. The minerals present do not indicate the origin of the sample, since these are minerals present in the weathered product of dif-



Fig. 2.9.2. In some places red soil covers limestone karren almost to the top, Lunan Stone Forest, behind the hotels (Photo. N. Zupan Hajna).

ferent parent rocks. The quartz probably derives from Eocene lake sediments and the hematite points to the fact that the sediment was formed in a warm climate.

North-west Guizhou (Panxian and Liupanshui)

The province belongs to the eastern part of the Yunnan-Guizhou plateau, 75 % of the area is carbonate rock of the Carboniferous, Permian and Triassic ages.

The oldest rock in north-west Guizhou is of the Middle Carboniferous and is represented by light-coloured massive and thick-layered limestone and dolomites. The Lower Permian begins with quartz sandstone and marl, in some places containing thin layers of poor quality coal. These are succeeded by black limestone with marl and schist, and above the Lower Permian



Fig. 2.9.3. Weathered basalt from the Yunnan-Guizhou plateau, from the border between provinces of Yunnan and Guizhou (Photo. N. Zupan Hajna).

lies grey and white limestone which is dolomitised in some places. The Lower Permian ends with vast paleokarst. The Upper Permian begins with thin-layered dark grey and black limestone interchanging with main coal layers, marl and schist, and quartz sandstone; all of the layers are covered with basalt. Basalt is followed by rock from the Lower Triassic, with red marl at the bottom, followed by grey limestone and dolomites. The Middle Triassic is represented by breccia limestone with marl and schist at the bottom. Clastic sediments, found in the karst relief and caves in NW Guizhou, most probably originate from weathered basalt (Fig. 2.9.3.) and quartz sandstone.

Shizilu

In the south-eastern part of Guizhou, south of the city of Panxian, the karst polje Shizilu lies 1680 m above sea level. It is surrounded by cone summits up to 200 m high. The cone karst of this area is composed of

Lower, Middle, Upper Carboniferous limestone, Lower Permian limestone and marl with some coal and Upper Permian basalt and marl with main coal layers and at the end Lower Triassic sandstone. A sinking creek flows across the polje carrying weathered remains of previously mentioned rocks with it. Polje is covered by grey-yellow sediments and on the slopes of the cones red soil prevailed (Fig. 2.9.4.). The cave Huoshao is located between two passes, 1750 m above sea level. Basalt, quartz and limestone pebbles were found in the cave. Many flow-stone pallets and helectites, nice calcite crystals up to 2 cm in size, which grew in line with the water level, were found at the end of the cave.

Most of the sediments from the karst surface of NW Guizhou were investigated in the vicinity of the city of Liupanshui. The samples were taken from the stone-pit near the small village of Bajiazhai, and north of the city from Swallow Cave next to the natural bridge Tianshengqiao, from the cave and the surface around the village of Xingchang,



Fig. 2.9.4. Karst polje Shizilu is covered with grey-yellow sediments but on the slopes of the cones red soil prevailed (Photo. N. Zupan Hajna).

from the surface around the village of Taishaba and of Majiachong and from caves and the surface around the village of Zhongzhai, and from the slopes of the Beipanjiang river canyons. From the above a review of clastic sediments that occur on the Yezhong plateau, which has an average height of 2000 m, and above Beipanjiang river was made (Fig. 2.8.3.).

Bajiazhai

In the small village of Bajiazhai by the city of Liupanshui at 1850 m above sea level, two samples from a cone with two summits cut by the construction of a road and by a stone-pit were taken. The structure of The cone is built of Lower Permian limestone which has become quite dolomitised (Fig. 2.8.1.). Two karst pockets were open in the wall, both filled with red loam, where it contacted with the rock large quantities of yellow sand were found .

Sample LIU 1

Sample is red loam from a karst pocket from a cone with two summits. Sample con-

tains quartz 32 %, montmorillonite 41 %, gibbsite 9 %, dolomite 7 %, kaolinite 4 %, chlorite 3 %, and hematite 3 %. This red loam is probably residue of well developed paleosol.

Sample LIU 2

Sample is yellow sand from the contact between red loam and neighbouring rock. Yellow sand contains mostly dolomite 89 %, in quantity succeeded by quartz 7 %, calcite, gibbsite and mica 1 %, kaolinite, plagioclase and hematite were in traces. Regarding on mineral composition, this yellow sand is result of dolomite weathering in the contact with red loam.

Tianshengqiao

In Swallow cave near big natural bridge, Tianshengqiao, about 15 m above the actual stream a maze of older phreatic channels is filled by sediments. Gravel, sand and silt indicat older infill of the cave. From the small phreatic channel at the top of high gallery sample of sand mixed by silt was taken.

Sample SWC

Sample from Swallow cave is comprised of quartz 65 %, feldspar 9 %, chlorite, dolomite 5 %, muscovite 4 %, calcite 35 %, augite 3 % and niter (saltpetre) 3 %.

Quartz, chlorite, muscovite, feldspar and augite were brought into the cave by the stream from noncarbonate rocks. Dolomite and calcite are originated from cave walls.

Beipanjiang

The Beipanjiang river canyon is cut into the karst plateau Yezhong which is over 2200 m high. We can trace carbonate rock and two coal series from the Middle Carboniferous to the late part of the Upper Permian in the approximately 1400 m deep canyon. Basalt covered all this rock in the Upper Permian. Various clastic sediments could be found on the surface and in caves. On the surface brown-yellow and red soil and in the caves grey and yellow sand, loam and pebbles are most common sediments.

Sample BAI 1

Sample of brown loam was taken from a fracture which was subsequently widened by corrosion, beside the New bridge crossing the river at 970 m above sea level. The brown loam contained quartz 60 %, montmorillonite 22 %, chlorite 5 %, hematite 3 %, and calcite, muscovite, kaolinite, goethite and feldspar at 2 % each.

Sample BAI 2

In the southern part of the canyon, on a structural terrace 1350 m above sea level, we found a larger accumulation of red-brown soil (Fig. 2.9.5.) with quartz nodules and limonite collections in it. Soil sample Bai 2 contained quartz 47 %, goethite 16 %, chlorite 13 %, hematite and kaolinite 8 % each, phosphate 5 % and gibbsite 4 %.

Individual low cone summits have formed on a structural terrace around 1500 m above sea level. Varicoloured clastic sediments were found between fractures



Fig. 2.9.5. In the southern part of the Beipanjiang river canyon, on a structural terrace 1350 m above sea level, a larger accumulation of red-brown soil (Fig. 2.9.5.) with quartz nodules and limonite collections in it exists (Photo. F.Gabrovšek).

running across the structural terrace and summits in diverse directions. We took samples of yellow and red loam from between two cones on the edge of Beipanjiang river canyon. The positions of the two samples were only a few meters apart. Sample of brown soil from a fracture in a cone located above the two samples was also taken. The next sample of red soil was taken from the part where the structural terrace starts to rise towards the slope of the Yezhong plateau, that is from karren below the reserve administration.

Sample ROB 1

Sample of yellow loam is very likely the weathering product of quartz sandstone which could be found up the slope of Yezhong

plateau. Sample comprised of quartz 88 %, chlorite 7 %, kaolinite 2 %, mica, goethite, hematite and gibbsite 2 % each.

Sample ROB 2

Sample of red loam containing quartz 80 %, chlorite 11 %, kaolinite and gibbsite 3 % each, hematite 2 % and goethite 1 %.

Sample ROB 3

Sample of brown soil from a karren on the cone, by the edge of the canyon, comprised of quartz 70 %, montmorillonite 14 %, calcite 5 %, chlorite 3 %, gibbsite 2 % and dolomite, mica, kaolinite feldspar, goethite and hematite 1 % each.

Sample ROB 4

Sample of red loam from karren near The Monkey's Head, below the reserve administration, comprised of quartz 63 %,

chlorite 13 %, goethite 9 %, gibbsite 8 %, kaolinite 5 %, and phosphate 3 %.

Samples ROB 1 and ROB 2 have almost the same mineral composition, they were taken just few meters apart and their colour is different. They are probably weathered remains of quartz sandstone which is located further on the slope of canyon and it belongs to Permian coal series. Samples of red-brown loam and soil, including samples BAI 1 and 2, have very similar mineral composition which shows on formation in tropical climate.

Zhongzhai

The karst valley near the village of Zhongzhai at 1750 m above sea level is surrounded by cone summits at a height of over 2000 m. Two caves have large entrances in a small valley connecting to the northern slope of the Beipanjiang river canyon by the Majiachong road.



Fig. 2.9.6. Pebbles mixed with yellow sand in the entrance part of the Cave II. (Photo. N. Zupan Hajna).

Cave I.

In at the entrance in Cave I. Holocene gravel and fallen rocks were found and also, on the bottom, lightly attached rubble with individual animal bones. There are remains of conglomerate on the walls of the cave pointing to the fact that the cave was filled with sediments to the ceiling. The sediments are composed of cobbles 10 cm in size, sand and loam. The ceiling is leveled where it is in contact with the sediment.

Cave II.

Cave II. is filled with allochthonous yellow-coloured sediments to the roof. Layers of pebbles (Fig. 2.9.6.), sand and laminated loam exchange. There are a number of stalactites, hanging at the entrance part.

Sample ZHO 1

Sample is of yellow laminated loam from Cave II., which was located beneath the layer with pebbles and contains quartz 55 %, chlorite 23 %, montmorillonite 8 %, feldspar 5 %, goethite 4 %, kaolinite and augite 2 % each.

Cave III.

The entrance to Cave III. is in a cone located on the eastern slope of the main valley by the village of Zhongzhai. In the cave is a large quantity of white decaying flowstone and some fallen rocks. The profile of the sediment at the end of the cave is 2 m high, the matrix connecting the small pebbles are sandy, cementation is weak.

Sample ZHO 2

The mineral composition of the conglomerate sample from Cave III. is quartz 36 %, montmorillonite 32 %, calcite 19 %, feldspar 3 %, chlorite and plagioclase 2 % each and kaolinite and goethite 1 % each.

The cone with Cave III. is bisected by a wide longitudinal opening with vertical walls. The opening, formed by fractures running in an E-W direction, is filled almost

to the top with mechanical sediments. Pebbles, sand and loam in belts with higher concentrations of limonite are covered by fallen blocks and gravel from the slope of the cone. Whether this is a small tectonic opening filled with sediments from the surface or a roofless cave passage filled with sediments to the top could not be determined in such a short period of time. We took two samples from this location.

Sample ZHO 3

The was a sample of the brown loam with pebbles and limonite crust in a longitudinal opening of the same height as the entrance to Cave III, the minerals in the sample were as follows: quartz 48 %, goethite 37 %, chlorite 8 % and montmorillonite 6 %.

Sample ZHO 4

The second was a sample of the laminated loam from the trench directly beneath the pass. The sample contains quartz 59 %, montmorillonite 21 %, goethite 10 %, chlorite 7 %, feldspar 2 % and kaolinite 1 %.

Last two samples have little different mineral composition like previous one specially in a differ goethite content.

Majiachong

Near the village Majiachong, in the southern part of the valley on a plateau over 2000 m above sea level, on a cone summit we found patches of brown weathered deposit, probably quartz sandstone or from 'in situ' limestones rich with chert nodules. The accumulation of this weathering deposit was bigger depressions and on level parts of the slope. Samples were taken on Cone I and Cone II (Fig. 2.8.18.).

Sample MAI 1

Sample of the brown soil was taken on the Cone I, 2150 m above sea level. Sample contains quartz 46 %, goethite 22 %,

kaolinite 20 %, chlorite 10 % and montmorillonite 1 %.

Sample MAI 2

Sample of the brown sandy loam with bigger pieces of quartz sandstone was taken on the Cone II, 2185 m above sea level (Fig.2.9.7.). Sample contains quartz 65 %, montmorillonite 18 %, muscovite 3 %, chlorite 4 %, kaolinite 7 %, chlorite 4 %, muscovite and gibbsite 3 % each and hematite 1 %.

These two samples are different in mineral composition specially in the regards of containing goethite and also gibbsite. Maybe the origin is for both the same from weathered quartz sandstone or from 'in situ' limestones rich with chert nodules but the diagenesis of these two deposits was different.

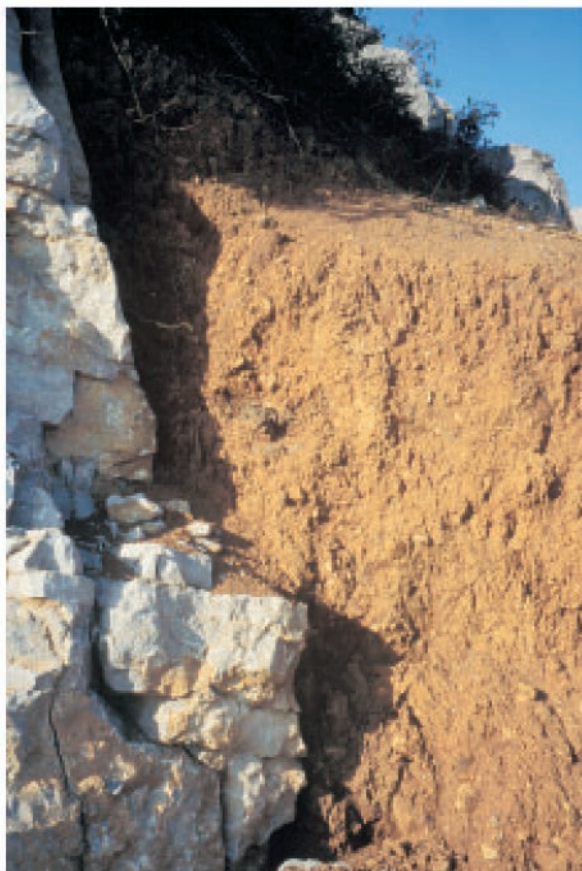


Fig.2.9.7. Brown sandy loam with bigger pieces of quartz sandstone in karst pocket on the Cone 2 (Photo N. Zupan Hajna).

Sample MAI 3

Sample Mai 3 was taken at the contact of Lower Permian limestone and basalt and was originally thought to be basalt though this subsequently proved not to be the case. The mineral composition of the sample is quartz 47 %, plagioclase (anorthite) 18 %, chlorite 15 %, augite 11 %, muscovite and ilmenite 4 % each and kaolinite 2 %.

Taishaba

Three samples of varicoloured and variously textured sediments from cones in the vicinity of the village of Taishaba were taken. Plateau surrounding of Taishaba is over 2200 m above sea level overlay with cones. In the depression between them lies bigger accumulation of soil and slopes of cones are almost bare, there is some soils captured among karren.

Sample TAI 1

Sample Tai 1 is from brown soil from the pass between the first and the second cone behind the school. The sample contains quartz 87 %, chlorite 5 %, muscovite 3 %, kaolinite and gibbsite 2 % each, plagioclase 1 % and hematite is in traces.

Sample TAI 2

Sample Tai 2 is red-brown soil from the lower part of the slope of the third cone behind the school. The sample contains quartz 80 %, chlorite 12 %, muscovite and gibbsite 2 % each, kaolinite and feldspar 1 % each, dolomite and hematite are in traces.

Sample TAI 3

Sample Tai 3 is loam from the swallow-hole beneath the village. The sample consists of quartz 83 %, goethite 8 %, chlorite 4 %, gibbsite 3 % and mica 2 %.

Mineral association in samples of all localities is almost the same and represents the soil formation in tropical climate.

Xinchang

Xingchang village is situated cone-depression karst type 1600 m to 1900 m above sea level. Samples of yellow loam were taken on the cone slope above village Xingchang and in the cave below village.

Sample XIN 1

Yellow loam from middle part of the cave contains quartz 94 %, montmorillonite 3 %, muscovite 1 % and chlorite, kaolinite and goethite are in traces.

Sample XIN 2

Accumulation of yellow weathered loam on slope above village was mixed with some chert pebbles comprises quartz 92 %, montmorillonite 4 %, muscovite and chlorite 2 % each and kaolinite 1 %.

Sample XIN 3

Yellow loam on the slope above road consists of quartz 92 %, montmorillonite 3 %, muscovite and gibbsite 2 %, chlorite and kaolinite 1 %.

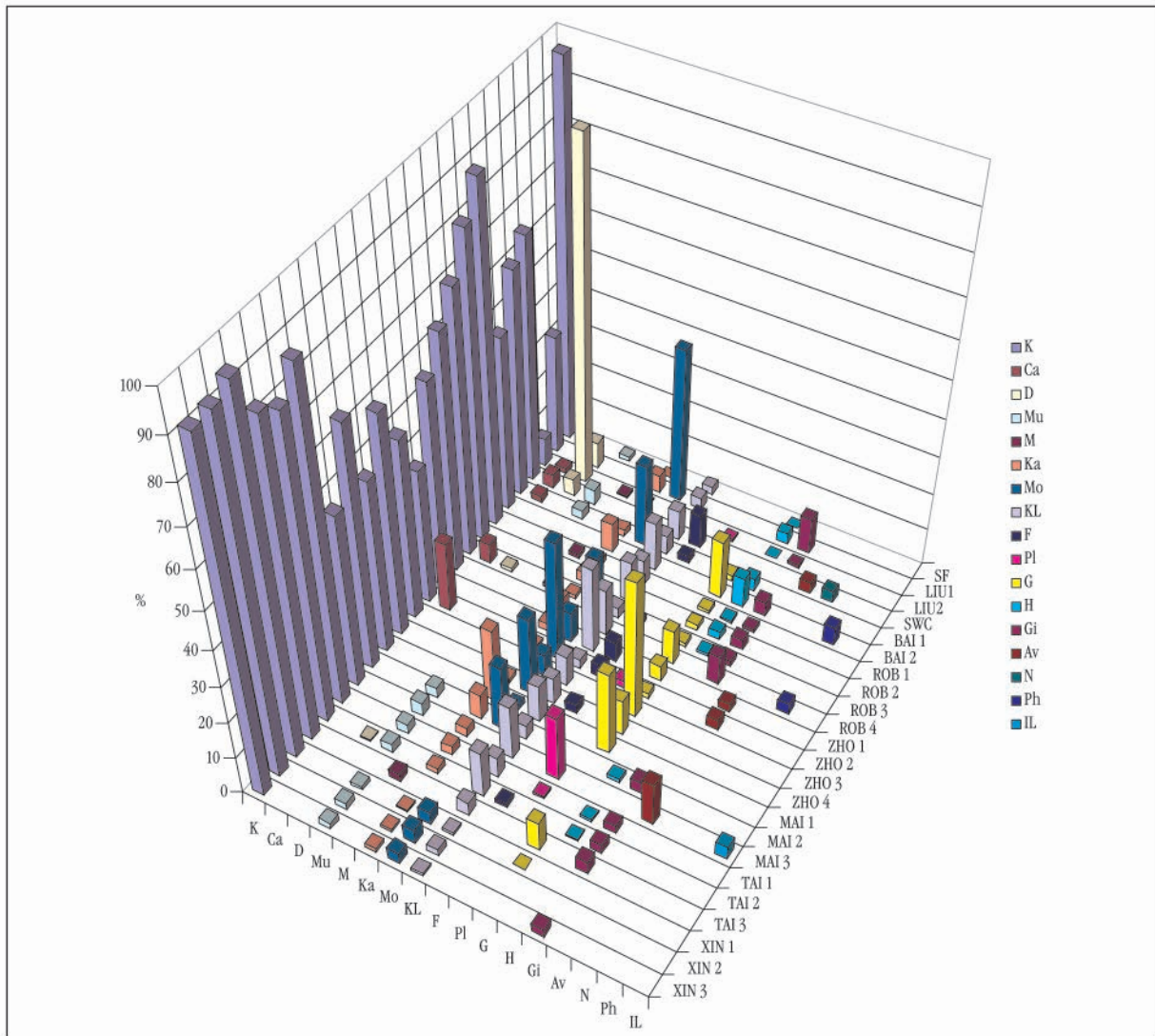


Fig.2.9.8. Mineral composition of samples from SE Yunnan and NW Guizhou.
Legend: SF, LIU 1, LIU 2, SWC, BAI 1, BAI 2, ROB 1, ROB 2, ROB 3, ROB 4, ZHO 1, ZHO 2, ZHO 3, ZHO 4, MAI 1, MAI 2, MAI 3, TAI 1, TAI 2, TAI 3, XIN 1, XIN 2, XIN 3 are samples;
 minerals: K - quartz, Ca - calcite, D - dolomite, Mu- muscovite, M - mica, Ka - kaolinite, Mo - montmorillonite, KL - chlorite, F-feldspar, PL - plagioclase, G - goethite, H - hematite, Gi - gibbsite, Av - augite, N - niter, Ph - phosphate, IL - ilmenite.

Regarding on mineral composition yellow loam on the surface and in the cave have had the same origin. They probably originated from weathered rests of limestones rich with chert nodules (Fig.2.5.3.).

Conclusion

The samples represent very different clastic sediments, that is in terms of colour, texture and consistency. As they represent a large area and they are few in number, the information concerning their mineral composition offers only a small insight into their origin (Fig.2.9.8.). A large number of the minerals in the samples are secondary, formed during the processes of weathering, and some of them are primary minerals which often have their origin in quartz sandstone and are the insoluble remainder of limestone rich in chert. The mineral hematite and gibbsite indicate the formation of sediments in a tropical climate.

As already pointed out in the introduction, karst sediments in Slovenia and in southern China are of the same colour, in mineral composition they differ primarily in 'additional' minerals, which is understand-

able. Quartz is the most common and profuse mineral in the sediments, in Slovenia as well as in the samples described. This is because it is the most resistant mineral and represents the remainder of the weathering of a large number of various rock types. The aluminosilicates are also resistant, but in time transform into clay minerals and chlorites, which are the most common minerals to form during weathering processes and are widespread, which is why we find these minerals in sediments in Slovenia and also in southern China. The primary minerals are different, they are most commonly heavy minerals which are characteristic of the rock of origin and this varies from case to case. Thus we find in the sediments of the southern Chinese karst, minerals that are characteristic of basalt weathering and other minerals that are rare in sediments in the karst of Slovenia. I did not have enough samples to allow me to draw more important conclusions concerning the origin of sediments in SE Yunnan and NW Guizhou and their mineral composition.

The colour of the sediments is more a reflection of the conditions under which the sediment formed and survived and less of their mineral composition.

2.10. LAND USE IN MOUNTAINOUS KARST AREAS

Andrej Mihevc

Presented below are some traditional forms of land use in mountainous areas of the Chinese karst in the provinces of Yunnan and W Guizhou. The bottoms of karst depressions, where there is more soil and where the soil is continuous, are utilized as small or large fields. If irrigation is possible, rice paddies are prevalent; corn, tobacco, hemp and cotton grow where there is no water for irrigation.

The soil cover is not continuous on the slopes, but the surface is nonetheless cultivated. The prevailing form of cultivation is digging and turning the soil with special narrow shovels and the planting of individual plants, mostly corn, between stone blocks. We find this type of use on slopes with an incline of around 40°. Pressure on the land is increasing and this causes the colonization of areas with poor natural conditions to continue.

Introduction

Carbonate rock is spread over 1/10 of China's territory, or 910,000 km², which is double the area covered with loess. In the provinces of Guanxi, Guizhou, Yunnan, and in parts of the provinces of Sichuan, Hubei, Guangdong, Hunan, Shandong and Hunan, which have a population of a few hundred million, typical karst developed in carbonate rock.

In most karst areas agriculture is impeded due to the natural features of karst, resulting in karst areas being poor, sparsely settled and underdeveloped. The main limitations on agricultural use are soil defi-

ciency and/or rocky surface and aridity of the surface caused by karst water movement characteristics.

Karst in China extends from the tropical belt to the temperate climate, from humid monsoon climates to the semi-arid to arid interior and from the coast to a height of 5000 m above sea level. The largest part of the karst lies in the tropical and subtropical monsoon climate where corrosion plains by the rivers in the lowlands and karst towers (fengling) are characteristic. The plains are covered with a thick layer of alluvial deposits and the vicinity of water sources makes intensive irrigation arable farming possible. Higher relief is characterized by vast plateaus with cone summits and doline-like depressions and karst plains. The surface is very rocky, except at the bottom of depressions and water is far below the surface, allowing irrigation only at the bottom of plains where karst flows appear.

Difficulties concerning water and soil are a very obvious and significant limiting factor for development in the karst of mountainous SW China and are caused by the marked monsoon climate and water and soil difficulties brought about by karst relief processes.

The poor natural conditions are made worse by some negative effects of overburdening karst areas which have triggered heavy degradation processes. Although settlement of the mountainous SW Chinese karst is relatively low in comparison with settlement of lowlands, the area appropriate for agricultural use is nevertheless overburdened which is the cause of expansion

to new land on which agricultural activity is barely possible.

Research of agricultural land use in karst relief is important from two perspectives. It can point to the manner in which it may become possible to improve or enlarge arable land in karst areas and at the same time prevent the negative effects of agricultural practices. It may also assist in expedient planning of future land use.

The other important aspect of research lies in the possibility of comparing existing intensive land use in the Chinese karst with intensive land use in the Mediterranean karst in Europe. These comparisons can assist us in studying the history of agricultural systems.

Methods of work

During our stay we traveled across the Chinese countryside and were able to observe agricultural land use in karst areas. Due to lack of time we were able to observe only some forms, so we primarily observed the adaptation of agriculture to a scarcity of water resources and soil.

In this area we observed the utilization of karst relief forms, evaluated the intensity of recent erosion and attempted to evaluate the amount of removed soil by comparing chipped rocks and subcutaneously formed rock surfaces.

We also observed some semi-industrial karst resource uses, for example the production of lime, stone-pits, coke, and charcoal. These uses in a way complement life in the country and have an important effect due to their dispersion.

Due to lack of time we were not able to satisfactorily measure and spatially evaluate these phenomena, which is why the above described observations can only serve to draw attention to phenomena.

Traditional land use and relief degradation

The SW Chinese mountainous karst can be morphologically described as high pla-

teau karst dissected by cone hills and sinkholes similar to depressions, dry valleys, large or small karst plains. Large karst areas are often cut through by deep canyons of allogenuous rivers that only cross karst. There are no surface water bodies, all precipitation percolates into the karst, karst springs are present on the fringes of plateaus of larger karst depressions.

The climate of this part of China is subtropical with a characteristic monsoon interchange of rainy and dry seasons. The amount of precipitation and the temperatures depend on the height above sea level at which the area is located. Despite the considerable amount of precipitation, the relief is dry in its depth because of the long



Fig. 2.10.1. Karst plain in Guizhou province. At the bottom of the karst plain there are thick layers of loamy soil. The submerging creek that crosses the plain has cut a series of terraces into it. The field is intensively used, the main crop being rice. Settlement is limited to the agriculturally inferior fringe of the plain (Photo A. Mihevc).

dry seasons and water runoff. Droughts are frequent and because of water scarcity irrigation is mostly limited to only the lowest parts of the karst.

Settlements are established primarily only in advantageous areas, on the edges of plains, on the bottom of large karst plains or closed depressions. There was enough arable land in these areas and karst springs or groundwater near the surface provided an adequate water supply. The growth of large connected settlements was possible here.

The two main limiting factors for life in the karst are soil and water. We find soil and water in karst areas only at the bottom of karst basins, plains or large plains by karst rivers. Higher and more dissected karst indicates a scarcity of both of the basic resources needed for agricultural land use in karst areas.

Settlement also expanded to agriculturally less adequate areas, where the surface is prevalently rocky, where there is less soil and the water sources are distant. Such areas cover vast expanses in high plateau karst. Although they are not significant in

terms of population size and density, their significance lies in the vastness of the area of karst which they cover.

It is difficult to determine the settlement of new karst territories and colonization in terms of time-scale. Three periods of rapid population growth are characteristic of China, but there have also been sudden declines in population size, usually as a consequence of bad harvests or periods of instability, or even both at the same time. The process of mountain colonization and population expansion to less favorable areas still continues. The reason for this is a sharp increase in the size of the population, which has doubled in the last 40 years. Houses continue to be built in remote areas and new arable land is being created.

In mountainous and hilly areas water rapidly sinks into the ground, it is also the case in areas where deep karst has developed that most water flows are deep beneath the surface. The water emerges at the edge of the karst in large springs, where it is abundant. It is possible to moderate the lack of water through hydrotechnical works.



Fig. 2.10.2. Characteristic landscape of cones with depressions in between. Settlements are sparse due to the rocky surface and limited water resources (Photo A. Mihevc).



Fig. 2.10.3 Construction of new house in the Yezhong plateau area at around 2000 m above sea level (Photo A. Mihevc).

The lack of soil is a stronger limiting factor. Soil forms more slowly on limestone than on other rock. The reason for this is that the rock is being dissolved and carried away in the form of a solution and the insoluble remainder is small. The consequence of this is that on the rocky surface, insoluble remainders accumulate in the fractures, and among them we find large bare rocks. Soil scarcity also increases the speed of precipitation runoff causing the surface to be more arid than we would assume from the quantity of precipitation.

Yellow-brown washed soil, more like loam, prevails on rock surfaces and is preserved in fractures in the subcutaneous zone widened by corrosion. Organic material is sparse and the top humus layer of the soil is thin due to rapid decay of organic material and heavy washing. The consequence is low retention capacity of the soil and rapid surface water runoff.

There is a larger amount of soil on karst rock which has a higher level of insoluble remainder in the rock or where the soil was

brought onto the limestone from elsewhere. Erosion processes may be triggered quickly on such rock and despite the fact that the absolute amount of removed soil is small, the effect is greater because they remove a larger proportion of the existing soil.

We can evaluate the proportion of new erosion triggered by man by observing soil erosion on slopes and the accumulation of soil in depressions. Observing forms of subcutaneous corrosion in rills and forms which develop in surface rocks which are exposed to atmospheric effects is also an important method. We can presuppose the former soil cover of these rocky surfaces and erosion in the recent past from the diffusion of subcutaneous forms.

Some cases of land use in karst of China

The examples of agricultural land use described apply to the provinces of Guizhou and Yunnan. Examples are described



Fig. 2.10.4. Forest fires are common in second half of winter. They are set on purpose, to create a grazing land (Photo A. Mihevc).

of land use in different relief areas in W Guizhou and E Yunnan: at the bottom of a karst plain near the city Liupanshui; at the bottom of the small karst plain Shizilu; at the edge of a plain near the Dadong cavern; and also on the highest parts of a high Yezhong plateau near the village of Taishaba; near the village of Majiachong; and at the edge of the Yezhong plateau above the Beipanjiang river canyon. Further examples of land use near the city of Xichou in Yunnan are also described.

The karst plain of Shuicheng lies at around 1880 m above sea level and is up to 3 km wide and over 10 km long. The flat bottom of the plain is covered by thick soil and several small rivers flow across it and occasionally flood the bottom of the plain. The structurally conditioned edge of the plain passes into an old dissected level area which is up to 300 m high. The bottom of the plain is flat, although individual cone hills (fengling) appear in a number of places. On one of them, barely 10 m high, the old town of Shuicheng has established

itself. Today the small town lives in the shadow of the rapidly developing new center – Liupanshui.

The bottom of the plain is cultivated, rice and vegetables grown on small plots primarily to sell at the Liupanshui market, prevail. The natural bottom of the plain has been changed by irrigation systems.

The soil on the plain is brown anthropogenic, and probably a few meters thick. Beside the bottom of the plain, surfaces where irrigation is not possible are also farmed as are the surfaces of the slopes of fenlings between clints where yellow-brown soil is present in corrosionally widened cracks.

Because of the rapid growth of the city, the nearby ironworks and cement factory and new roads, there are many evident stone-pits, earthworks and new embankments which have drastically altered the natural bottom of the karst depression and its water conditions.

The Shizilu karst plain by the city of Panxian is a dry valley situated 1700 m above



Fig. 2.10.5. The karst plain of Shuicheng, near the village of Bajiazhai. The large plain is farmed intensively because of the soil and the possibility of irrigation. Vegetables for sale at the nearby town market are important. The plants are treated with chemicals (Photo A. Mihevc).



Fig. 2.10.6. The Shizilu karst plain. The bottom is turned into terraces, which are irrigated. Slopes with an incline of 30° or less are cultivated. On steeper or rockier surfaces bushes and trees grow, the trees do not reach full size because they are cut for firewood. The trees, which have golden brown leaves, are Ginkgo Biloba (Photo A. Mihevc).

sea level and enlarged by corrosion. Its bottom is covered with thick Quaternary deposits in which creeks have cut a number of terraces. Two smaller creeks flow to the bottom, into each other and then submerge in a swallow-hole at the edge of the plain. There is also a great deal of silt around the swallow-hole, indicating rapid washing of sediments underground.

The bottom of the dry valley is cultivated and turned into terraced fields for rice. The creek bed is narrowed and strengthened. The creek is dammed in its upper flow and channeled for terrace irrigation. The slopes above the bottom, in the lower part where the incline is, are first changed into horizontal and higher up into sloping terraces. The smallest terraces are only a few square meters in size. The terraces are created in places where there is enough soil and the incline is below 15-20°. Slopes with larger inclines do not have terraces, the soil in rills is dug and turned with shovels. The rills in the lower part show signs of chipped rock

at the top, the rock is then used to build terraces or stacked in piles.

The comparison of rocks with subcutaneous and surface corrosion form showed that up to 0.5 m of soil was removed from the slopes. This soil might have been washed away or may have been used for terracing.

Land cultivation near Dadong Cavern in Panxian region. The cavern has a large entrance 20 m above the plain by the creek swallow-hole west of the city of Laochang. The bottom of the valley by the swallow-holes is irrigated, and rice grows in the fields. The slopes above it are utilized for growing corn as they are very rocky. Despite the slight incline, no terraces are present due to the rockiness, the soil between rills is cultivated using shovels.

The highest karst in Guizhou is on a high plateau which stretches from Yunnan to W Guizhou. The Yezhong plateau is between 2000 and 2400 m above sea level in the area of the Beipanjiang river gorge south of the



Fig. 2.10.7. The swallow-holes of the creek at the bottom of the Shizilu plain are surrounded by a great deal of silt indicating washing underground. The completely altered water regime of the channeled creek adds to this (Photo A. Mihevc).



*Fig. 2.10.8: Corn field on the slope beneath the entrance to Dadong Cavern, Panxian.
(Photo A. Mihevc).*



Fig. 2.10.9. The vicinity of the village of Taishaba. This area is highly settled because of a relatively large amount of soil. Fields are cleared of rocks, the rocks are stacked into dry walls and terrace scarps. The scarps are only a few years old, indicating the fight against soil erosion and also the increasing pressure on land (Photo A. Mihevc).

city of Liupanshui. This part of the plateau has an average annual temperature of 11-19° and receives from 900 to 1500 mm of precipitation.

The karst plateau is dissected into numerous valleys, oblong depressions and karst plains. Positive relief forms, groups of summits or fengcongs, dominate the landscape, causing the relief to appear dissected with height differences between the bottoms of depressions and the summits of up to 300m. The plateau is also crossed by the Beipanjiang river, which has carved a canyon 600 to 700 m above sea level, thus creating 1700 m in height differences.

Despite the relatively poor climatic conditions, dissected relief, soil and surface water scarcity, the karst relief is utilized up to the cone summits.

Taishaba is a small settlement located by the main road of the dissected relief on the Yezhong plateau around 2300 m above sea level. The flatter parts of the depression between the cone summits are converted into large fields. Inclined slopes are terraced, terraces become smaller as the incline increases, and are built below an incline of 20°-30°. Above the terraces slopes are dug between rills below an incline of 33°-45°. Only more steeply inclined slopes are not cultivated, although they are overgrown with bushes and other vegetation which is used for collecting firewood, grazing animals or picking edible plants or cattle feed.

Between the village of Majiachong and the edge of the Beipanjiang river canyon on a high plateau is the dissected karst relief of cone hills and an oblong depression between them. The summits are up to 2300 m above sea level. The bottoms of the depressions, large dolines and cockpits are 2100 m above sea level. The inclines of the summit slopes are mostly greater than 45°. The relief is structured of thick bedded limestone and in some places limestone with chert.

The area is settled in the form of scattered farms and some small villages. Large villages exist only on the edge of the plateau, near the contact with non-carbonate rock in dry valleys. This settlement is a few



Fig. 2.10.10. At the bottom of a large depression by the swallow-holes of an intermittent creek, much silt has formed in the karst loam. Heavy erosion is probably the consequence of the altered hydrological characteristics of the upper layer of soil, which is no longer capable of water retention. The runoff is thus rapid and washing into the karst is intense (Photo N. Zupan Hajna).

centuries old. The settlements continue to expand, new homes are also being built in previously unsettled areas. Water supply is difficult, the water is accumulated in cisterns dug in the ground or from a few small creeks in surface water collectors.

The bottoms of depressions or flatter areas between the summits, primarily where there is chert in limestone, more soil has formed and this can be ploughed. The terraces are small, in some places only a few meters long and wide. Soil on steeper slopes is turned by hand, on the steepest and shady slopes cattle are grazed or the area is over-

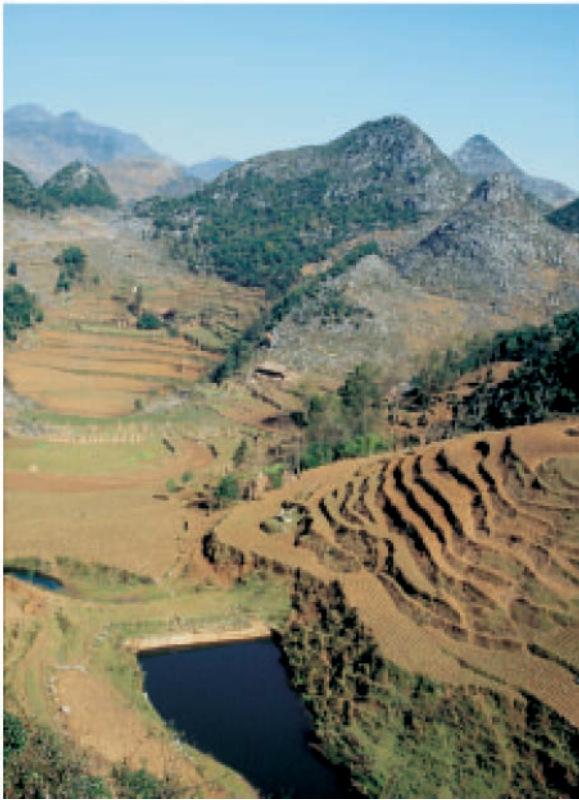


Fig. 2.10.11. Yezhong plateau. Accumulation of water in bed of small creek in the side of a large sink-hole (Photo A. Mihevc).

grown with bushes or trees. There are no longer any old trees.

The Beipanjiang river has cut a canyon, up to 1700 m deep, in the Yezhong plateau. The canyon is cut into two levels by a vast structurally-conditioned terrace. In the lower part of the canyon above the river, there are vertical walls up to 500 m high or steep slopes where agricultural land use is practically impossible. Three different kinds of monkey have remained in the area for this reason: *Presbytis F. Franciosi*, *Macaca M. Mulata*, and *Macaca Thibetana*, as well as the wild sheep, *Naemorhedus Goral Griseus*.

Despite the relatively sparse population in the protected area of the natural park of the Beipanjiang river canyon, which extends across 20 km², around 2500 people live there. In the reserve a natural, relatively well-preserved forest grows, the walls are bare. There is a vast shelf, around 2 km wide, with an incline of about 20°. The shelf is formed of rock in which layers of limestone interchange with layers of coal and marl. A thicker layer of soil has developed



Fig. 2.10.12. Yezhong plateau. Large fields can be ploughed using draught cattle. Because of water scarcity, the prevailing plant in the fields is corn (Photo A. Mihevc).

on this rock and the relief is cultivated intensively.

The surface has been converted into small terraces and the prevailing crop is corn. Cultivation has caused soil erosion which, judging by the exposed subcutaneous forms, has removed a layer of soil up to 1 m thick from the whole surface. Rocks have thus reached the surface and were at first broken off, but the erosion has progressed rapidly. Small rain rills cut into the subcutaneous and broken surfaces of rocks indicate the period of the first erosion and the breaking up of the tops of the rock chunks.

In the vicinity of the city of Xichou in South Yunnan, the karst plateau is located at an altitude of 1500–1800 m and cut into it are low valleys and large karst plains with the bottom at a level of around 1300 m. Because of the lower position, the climate is warmer and the area is more densely settled than the higher plateaus. The dry season is more pronounced and the difficul-

ties concerning water supply are greater.

The bottoms of karst valleys have flowing submerging rivers, making them appropriate for irrigation and growing plants that need a large amount of moisture. There is no flowing water on the slopes and on the higher plateau. The water supply is based on water reservoirs dug into the ground and sealed with cement. Flatter slopes are formed into terraces in places where there is some soil. The construction of terraces has not yet been completed and was begun following a government program in the last decade. Steeper or rockier areas are farmed by turning the soil between rills.

Other karst land uses with important environmental impacts

A strong impact of the degradation of the natural landscape is caused by other traditional or new activities. They are signifi-



Fig. 2.10.13. Water reservoir by the village of Miandze, Xichou. The fissures widened by corrosion and filled with loam were used, this is indicated by the subcutaneous forms on the wall. (Photo A. Mihevc)



Fig. 2.10.14. Charcoal is produced in underground stoves. The furnaces are located where there is enough wood and where the terrain is less rocky (Photo A. Mihevc).



Fig. 2.10.15. Pile for producing coke. The escape of gases rich in sulfur oxides is visible. (Photo A. Mihevc)

cant because of their spatial extent, as we find them even in areas which are difficult to access by transport.

Charcoal production is an important complementary activity. Charcoal is used in cooking, heating and forging. It was more common in the past while today it is being replaced by coal and coke. Charcoal is an important product especially in mountainous areas where forests are still preserved.

Trunks up to 15 cm thick are the most suitable for charcoal production, these are burned in furnaces with a chamber, chimney and a side access dug into the ground. During the time of “The Great Leap Forward” (at the beginning of the sixties), each village had to produce iron. For this, primitive furnaces were built and they used wood charcoal for smelting. This is how the last remains of the forests were ruined. Today the effect of charcoal production is less, although it does hinder reforestation as does the use of slash and burn to create grazing land.

Charcoal production is today less extensive than coke production. Thin layers of black coal often lie between the limestone of the Chinese karst. This is exploited in small mines and burnt in furnaces similar to the ones used for charcoal production to produce coke. Coke is burned primarily close to the roads, thus allowing the produced coke to be distributed by truck to users, ironworks or large settlements where it is used in households.

Coke production is a major air polluter as the coal used in the process contains a lot of sulfur. In places where coke is used for a longer period of time, the gases completely destroy the nearby vegetation.

An important product of the karst areas is lime. Lime-kilns are established beside the road close to important users (i.e. larger settlements). Coal and coke are most commonly used for burning, lime is sometimes produced during coke burning.

The production of lime also heavily pollutes the environment with sulfur dioxide



Fig. 2.10.16. Traditional form of lime-kiln. Coke is used for burning (Photo A. Mihevc).

emissions. Even more noticeable are the many stone-pits which strongly degrade the visual appearance of the landscape. Because stone-pits, lime-kilns and coke furnaces are often located in valleys near roads, this is where the negative effects of these activities are concentrated and they create a specific form of landscape degradation.

Conclusion and comparison with Mediterranean karst land use

The main limiting factors in land use in the South Chinese karst are scarcity of soil (i.e. rockiness), high degrees of incline, and scarcity of water.

Soil is preserved at the bottom of plains, at the bottom of depressions or where limestone contains additions of other rock like chert, allowing the soil to form. Soil in depressions, especially smaller ones, has to a great extent been washed from the slopes. It is possible to evaluate the degree of ero-

sion through history from the expansion of subcutaneous corrosion forms on rocks that now lie exposed.

Fields with larger quantities of soil are ploughed. Small fields and plots which are only a few meters long by a few meters wide are also ploughed. Smaller surfaces are cultivated by hoeing or with special narrow shovels. In this way even narrow belts of soil between rocks, sometimes as little as 20 cm wide, can be cultivated. The smallest plots can accommodate only one agricultural plant – for example one cornstalk, one tobacco plant or one hemp plant. In such places the broken tops of rocks are heaped in small stacks or piles.

Terraces are less common in karst areas. Most of them situated at the bottom of larger karst depressions, where irrigation is still possible and the dominant crop is rice. Where irrigation is not possible, terraces are built to sustain cattle farming which is easier and to prevent erosion. Terraces are built on slopes with an incline of



Fig. 2.10.17. New centre of the area, Liupanshui is growing on the edge of large karst polje (Photo A. Mihevc).

30° or less. Steeper slopes are usually so rocky that there is not enough soil on them to build terraces. Inclined terraces are often built on steeper slopes. The terraces are fairly horizontal in the direction of the steepest incline of the slope, but they descend to the side with a slighter inclination.

In the area of Yunnan the terraces on non-irrigated surfaces with rocky stacked scarps are newer, at the most 20 years old, this implies the increase of the pressure of population on the land and the fight to prevent soil erosion.

Settlement patterns are various, from urban settlements in karst and large villages to dispersed settlement in small villages. Small villages and individual homes seem to be the newest form of colonization of previously unsettled karst land. They are usually on the edges of depression bottoms – dolines or cockpits. Fields for cultivation are at the bottom, slopes where soil is only present in cracks between rills are also cultivated. Steeper or rockier slopes are used for grazing pigs or cattle, and sometimes goats or sheep. For this purpose these surfaces are burnt and thus cleared of bushes.

Water is necessary for drinking and also for irrigating agricultural land. Small karst springs have clean potable water and are

often protected. Water from larger sources is used for irrigation. On plains, numerous vertical shafts connecting to groundwater or drilled wells are used for pumping water. Water is retained on the surface as long as possible.

The largest amounts of water are required for rice growing, which is why it this is grown at the bottom of plains where water is abundant, as are sugar cane and vegetables. Where irrigation is not possible, corn, hemp tobacco and other plants prevail.

The comparison of land use in karst areas, primarily of terrace and scarp building, points to some common features of karst in some parts of China and Mediterranean karst. The comparison is interesting because karst in China is agriculturally overburdened due to hand cultivation, land interventions in karst areas are still very new in some places. Intensive land use is being abandoned in the Mediterranean karst, in contrast to China where it has not reached its peak extent or intensity. Understanding agricultural land use and observing the natural processes which are triggered by it can assist in the reconstruction of past processes in karst areas, understanding them in the present and planning suitable future use.

2.11. CONCLUSION - CONTRAST THE KARST OF CHINA WITH SLOVENIA

Zhang Shouyue, Andrej Mihevc, Bojan Otoničar

Karstification is controlled under the time and space by physical geographic, geological backgrounds and its developing history, while the differences of karstification and its results are reflected by the karst phenomenon. The development and evolution of karst in China and Slovenia might be contrasted through following aspects.

1. Carbonate formation: Carbonate rocks in Slovenia are mainly shallow water shelf carbonates of the Mesozoic and Paleogene age. An important influence on karst development had Cretaceous to Eocene flysch beds that presently separate different mostly carbonate thrust and extended nappes. In Chinese karst area carbonate formation were developed from Proterozoic to Mesozoic and are mainly the carbonate rocks of Palaeozoic to Early Mesozoic in stable continental block, which is of very high thickness and with non-carbonate deposit constantly.

Modern carbonate mudstones generally have porosity of around 60 to 70 % with very surficial deposits having even higher porosities. Porosity values for grainstones range from 40 to 50 %. These initial porosities in both shallow-water carbonate sediments and deep-water chalks with increasing age and/or deepening burial depth of the sediments by the compaction and diagenesis and are influenced by the compositions and texture of rocks. Therefore the original porosity of carbonate formation shows the older geological age, the lower of original porosity generally.

In North China, the intercrystal porosity of dolomite in Sinian system is less than 1 %. The porosity of Devonian-Carbonifer-

ous carbonate rocks in Guilin area presents 1,79 % in dolomite and 0,67 - 0,78 % in limestone.

The effective porosity of Triassic limestone in Sichuan are 0,49 - 1,53 % and 0,92 - 8,25 % in dolomite. It is clearly that the karstification is developed more favourable in Mesozoic-Cenozoic by porosity - one of the voids for karst development.

2. The main geological structures and landform features of Slovenia were formed mostly in Cretaceous and Tertiary and they are the products of the last stages of the Alpine orogeny. All megatectonic units of western Slovenia, where most of the Slovenian karst is developed, belong to the Dinarides and consist of thrust and extended nappes with directions of structural elements W-E in the Southern Alps and Inner Dinarides, and NW-SE in the Outer Dinarides (Placer, 1996). Together with formation of the nappe structure flysch deposition started since Cretaceous and had been finished till Eocene. Towards south and south-west the carbonate basement is overlain by younger and younger flysch beds, what is an evidence of the migration of the flysch basin in that direction (Placer, 1996). Placer (1996) also considers that significant faults that strike NW-SE, SW-NE, W-E and N-S were started during Mesozoic and later often reactivated. Although Gams (1965) considers that the karst morphology in Slovenia is obviously young we should reconsider this statement on the basis of the above presented ascertainments.

In the end of Palaeozoic, the Mainland China except the part of Qinghai, Xizang are oceanic crust, most of the area have

been become as the continental crust. The strong crust movement of Cenozoic belongs to the landmass change in the plate, presenting mantle fold, rift, magmatic action and basin structure and so on. There are Yanshan period mantle fold which was developed in Jurassic and Cretaceous all over China, the geological structure of Chinese karst area was laid in this period and also the beginning of new period of karstification. The mantle fold of Himalayan period was mainly in West China. The modern geomorphic outline of China was settled basically beginning from the end of Pliocene and going on for the present neotectonic period. The third episode of Himalayan movement beginning from the end of Pliocene made the rising of West China strongly, and the raising of peneplane and the plane of denudation, and the descending of plane formed before Quaternary in East China, the Quaternary with huge thickness was deposited at the same time.

It is quite evident that karstification of East China was undergone a long period since late Cretaceous, while new karstification period in Slovenia was begun from Late Tertiary, but they had been influenced by the raising of earth's crust and the differential movement of block.

3. Climate factor is closely related to karstification, so the karstification under different climate zone is a problem of common interest to be discussed. Slovenia belongs to the Mediterranean climate zone and a transition area between the climate of Mediterranean and continent. With an annual average precipitation between 1200 and 3500mm, the major part of the Dinaric and the Alpine karst territory receives annually above 1500mm. The basic features of the Mediterranean climate is low rainfall in Summer, but most of the Dinaric karst area appears as the transition climate with well-distributed rainfall. According to the data from Ljubljana river basin, all the rainfall are between 100 and 130mm for each month, except with rainfall less than 100mm in February, July and August.

In Alpine karst area of north part, there are annual average rainfall more than

2000mm and accumulated snow throughout the year, forming relatively large caves which was influenced by the glacier of Quaternary.

Owing to the comprehensive actions of raising the Qinghai-Xizang plateau strongly and atmosphere circulation, the East Asian monsoon have been strengthened since several million years. Therefore, the Mainland China has been resulted in the basic features of monsoon limit, which is less precipitation with dry and cold in winter and much more rainfall with damp and hot in summer. In the tropical and subtropical area of South China, there is humid climate with a aridity less than 1,0, annual average temperature 14° - 24°C and annual rainfall 800 - 1600 mm, reaching to 1800 - 2000 mm in part of precipitation centres and increasing the temperature and precipitation gradually towards to south.

Carbonate rocks area in North China belongs to mid- and warm-temperate zone with dry and sub-humid climate, having the aridity between 1,0 and 1,5, annual average temperature from 6° to 14° C and annual rainfall about 400 - 800 mm. The annual rainfall couldn't be well-distributed due to the feature of East Asian monsoon climate, only part of the precipitation could be fully involved in the karstification and another part would flow into the river quickly. For example, the annual rainfall in East Yunnan and West Guizhou area is some 1100 - 1500 mm, among them, 75 - 85 % are concentrated in between May and October and occupy frequently 50 % of annual rainfall in between June and August.

According to the analysis for carbon dioxide in soil air, the results measured in different karst area of Slovenia in November show that most of the CO₂ content within 50cm under the surface are between 10000 and 25000 ppm, the highest even can be found from 30000 to 64000 ppm, while in China, the CO₂ contents measured from soil air are several thousands in general, the highest result about 18500-24000 ppm only can be found in tropical rainforest. It is clearly that high CO₂ content of soil air in Slovenia is widespread and is bound up with rainfall and its distribution.

The contrast from climate factor shows that the water run-off is of important significance as a major factor of karstification and depends to the rainfall and its distribution. The annual rainfall in Slovenia is generally more abundant and well-distributed than in China's, it is the great favourable condition to develop modern karstification.

4. The results of karstification display karst landscape and caves. Each karst cycle corresponding to the raising of landmass can be divided into different evolution stages. Under the conditions of similar climate zone, the karst phenomenon are similar for periods of relative stability of landmass or for periods of strong uplifts.

Karst landscapes in Slovenia are generally on stages of the disintegration of positive landform, appearing to deep doline developed on the surface of plateau, undeveloped surface water system and many caves formed by vertical influent from vadose zone - doline karst.

Karst area in China due to many cycles of karstification ever since the Cretaceous and its east part influenced by strong raises of Qinghai-Xizang plateau since the end of Tertiary, some denudation planes of different period were developed under differential movement of blocks and mainly uplift with different raising scope and the denuded surfaces at the same period lower gradually from west to east. So some landscapes in continuous carbonate rocks distributed area from Yunnan plateau to South China sea can be seen, such as from plateau karst which is mainly positive landform to peaks and dolines or depressions, and karst plane, isolated peak and peak forest which are mainly negative karst morphology. Peak forest on the ocean could be seen in Xialongwan Bay within Vietnam in Beibuwang Bay.

It was found on speleoarchaeological studies in Slovenia that 30 sites of Mid and Upper Palaeolithic belong to Late Pleistocene, and no earlier cave archaeological sites could be found. Dating by U-Series from caves, there are several tens samples from 6 caves dated as Mid-Pleistocene.

The speleoarchaeological sites in China, there are about 49 sites belong to Late

Pleistocene, Mid-Pleistocene from 19 sites and cave fauna sites could also be found in Early Pleistocene and Pliocene. The method of U-series was mainly used to date the speleothems. All the data of dating ages are Mid, Late Pleistocene, thus couldn't be discussed further. Without any Quaternary continent glacial sheet could be found and therefore, the karstification haven't been influenced by continental glacial sheet.

The main limiting factors in land use on the karst in China and Slovenia are scarcity of soil (i.e. rockiness) and scarcity of water. Soil is preserved at the bottom of plains, at the bottom of depressions or where limestone contains additions of other rock like chert, allowing the soil to form. Soil in depressions, especially smaller ones, has to a great extent been washed from the slopes.

Smaller surfaces are cultivated by hoeing or with special narrow shovels. In this way even narrow belts of soil between rocks can be cultivated. Terraces are less common in karst areas of China. Terraces are built on slopes with an incline of 30° or less. In the area the terraces with rocky scarps are newer, indicating the increase of the pressure of population on the land and the fight to prevent soil erosion.

The terrace and scarp building started in Mediterranean karst in antiquity. Intensive land use is being abandoned in the Mediterranean karst, in contrast to China where it has not reached its peak extent or intensity. In Slovene karst the artificial and natural reforestation returned forest vegetation to more than 50% of the karst areas.

The most intensive and dominant processes take place at the bottom of depressions, but cones or groups of cones are visually dominant feature in the West Guizhou karst. Cones studied had different topologic positions, dimensions, development and age.

Cone relief at 2200 m a.s.l. represents the oldest relief in which the river Beipanjiang cut a canyon 1500 m deep. The cones in this area are up to 200 m high and the cone slopes are very steep, with inclination angles 30° - 50°.

Cone relief in the middle of the Beipanjiang river canyon is much younger,

with cones only about 100 m high. In spite its position near the canyon, there are no signs of the canyon determining cone formation, cutting them by retreat of 500 m high walls. This points that vertical drainage, corrosion in the subcutaneous karst zone is the most important for cone and other surface features formation.

Cone features on Slovene Dinaric karst are different, cones are much lower and not so steep. More pronounced are the flat or slightly inclined surfaces in which dolines are incised.

REFERENCES

- Barnabary, J.P, R., Maire, S. Zhang et al., 1991: Gebihe'89 Karsts de Chine. Deuxieme expedition speleologique franco - chinoise, PSCJA et Institut de Geologie de Academia Sinica.- *Karstologia - Memoires* 4.
- Bögli, A., 1981: Solution of limestone and karren formation.- *Karst geomorphology*, ed. M.M. Sweeting, *Benchark Papers in Geology* 59, 64-89, Hutchinson Ross Publishing Company.
- Chen Zhi Ping, Song Lin Hua and M.M. Sweeting, 1983: The Pinnacle Karst of the Stone Forest, Lunan, Yunnan, China: an example of sub-jacent karst.- *New Direction in Karst, Proceedings of the Anglo-French Karst Symposium*, Edited by K. Paterson and M.M. Sweeting.
- China Lunan Stone forest karst research group, 1997: *China Lunan Stone forest karst research*, Yunnan science publishing house.
- Chinese Academy Geological institute karst research group, 1979: *China Karst Research*, Scientific Publishing House.
- Day, M., 1987: Slope from, erosion, and hydrology in some Belizean karst depressions; in: *Earth Surface Processes and Landforms*, Vol.12, 497-505.
- Dzulynski, S., E. Gil, J. Rudnicki, 1988: Experiments on kluftkarren and related lapies forms.- *Z. Geomorph. N.F.* 32, 1, 1-16, Berlin - Stuttgart.
- Dusar, M., S. Chang, 1991: East Yunnan 1991 geological and speleological reconnaissance of the east Yunnan karst (P.R.China).- *Belgian geological survey, Professional paper*, 4(248).
- Fiol, L., J.J. Fornós, A. Ginés, 1996: The role of biokarstic processes on the development of "solutional" rillenkarrren: an experience on Jurassic carbonate rocks of Mallorca.- *Karren Landforms*, 63-64, Palma.
- Ford, D., P. Williams, 1989: *Karst Geomorphology and Hidrology*.- U. Hyman, p.601, London.
- Ford, D., J.N. Salomon, P. Williams, 1996: Les "Forets de Pierre" ou "Stone forests" de Lunan.- *Karstologia* 28, 28/2, 25-40.
- Ford, D., J.N. Salomon, P. Williams, 1997: The Lunan Stone forest as a potential world heritage site.- *Stone forest a treasure of natural heritage, Proceedings of International Symposium for Lunan Shilin to Apply for World Natural Heritage Status*, 107-123, China environmental science press.
- Fornós, J.J., A. Ginés /eds./, 1996: *Karren Lanforms*.- Universitat de les Illes Balears, Palma.
- Forti, F., 1972: Le "vaschette di corrosione". Raporti tra geomorfologia carsica e condizioni geolitologiche delle carbonatiti affioranti sul carso triestino.- *Atti e memorie*, 11/1971, 37-66, Trieste.
- Forti, F., 1977: Studio geomorfologico delle scannellature carsice (rillenkaren) sulle rocce carbonatiche calcaree del carso triestino.- *Mondo sotterraneo*, anno 1, 8-14, Udine.

- Gabrovšek, F., Yuzhang Jin, B. Otoničar, Shi Mengxiong, Zhang Shouyue, A. Mihevc, N. Zupan Hajna, 1997: Speleological exploration at Tianshengqiao - natural bridge, Shui cheng, NW Guizhou, China.- Proceedings of the 12th International Congress of Speleology, 1, vol. 6, 32-35, La Chaux-de-Fonds.
- Gams, I., 1965: Speleological characteristics of the slovene karst. *Naše jame* 7, 41-50, Ljubljana.
- Gams, I., 1971: Podtalne kraške oblike. Summary: Subsoil karst forms.- *Geografski vestnik* 43, 27-45, Ljubljana.
- Gams, I., 1980: Poglavitni dejavniki kemične erozije na karbonatnih kamninah slovenskega dinarskega in alpskega krasa. Summary-Factors and dynamics of corrosion of the carbonatic rocks in the dinaric and Alpine karst of Slovenia.- *Geografski vestnik*, 38, 11-68, Ljubljana.
- Gams, I., 1988: Hydrogeographic review of the Dinaric and Alpine karst in Slovenia with special regard to corrosion. - Problems of karst hydrology in Yugoslavia, *Mems. Serb. Geog. Soc.* 13, Beograd.
- Gams, I., 1993: Karst denudation measurements in Slovenia and their geomorphological value.- *Naše jame* 35, 31-35, Ljubljana.
- Gams, I., 1997: Climatic and lithological influence on the cave depth development.- *Acta carsologica* 26/2, 321-336, Ljubljana.
- Gao Daode, Zhang Shichong & Bi Kun etc., 1986: Karst in South Guizhou, China; Guizhou People's Publishing House.
- Glew, J.R., D.C. Ford, 1980: A simulation study of the development of rillenkarren.- *Earth surface processes* 5, 25-36.
- Gospodarič, R., P. Habič, 1976: Underground water tracing. Investigations in Slovenia 1972 - 1975.-1- 309, Ljubljana.
- Habič, P., 1968:Kraški svet med Idrijco in Vipavo. Summary-The karstic region between the Idrijca and Vipava rivers.-1-243, Ljubljana.
- Habič, P., 1980: S poti po kitajskem krasu. Summary: From the way to the Cinese karst.- *Geografski vestnik* 52, 107-122, Ljubljana.
- Habič, P., 1981: Nekatere značilnosti kopastega krasa v Sloveniji. -*Acta carsologica* IX, 5-21, Ljubljana.
- Habič, P., 1993: Kras and karst in Slovenia.- *Naše jame*, 35, 12-18, Ljubljana.
- Habič, P., J. Kogovšek, 1992: Sledenje voda v kraškem zaledju Krupe v JV Sloveniji. Summary-Water tracing in the Krupa karst catchment, SE Slovenia.- *Acta carsologica*, 21, 35-76, Ljubljana.
- Habič, P., J. Kogovšek, M. Bricelj, M. Zupan, 1990: Izviri Dobličice in njihovo širše kraško zaledje. Summary-Dobličica springs and their wider karst background.- *Acta carsologica*, 19, 5-100, Ljubljana.
- Hantoon, P.W., 1997: Definition and characteristics of Stone forest epikarst aquifers in south China.- Proceedings of 12th International Congress of Speleology, Vol. 1, Symposium 8, 311-314, La Chaux-de-Fonds.
- Knez, M., 1994: Freatični kanali v Veliki dolini (Škocjanske jame, Slovenija). (Phreatic Channels in Velika dolina, Škocjanske jame (Škocjanske jame Caves, Slovenia)).- *Acta carsologica*, 23, 64-72, Ljubljana.
- Knez, M., 1995: Pomen in vloga lezik pri makroskopskih raziskavah karbonatnih kamnin, v katerih so oblikovani freatični kanali.- *Annales, Anali za istrske in mediteranske študije*, 7, 127-130, Koper.
- Knez, M., 1996: Vpliv lezik na razvoj kraških jam. (Primer Velike doline, Škocjanske jame). Summary: The Bedding-Plane Impact On Development Of Karst Caves (An Example Of Velika Dolina, Škocjanske Jame Caves). Znanstvenoraziskovalni center SAZU, 14, 186 str., Ljubljana.
- Knez, M., 1997a: Karst Cave Development from the Bedding-plane Point of View (Škocjanske jame Caves, Slovenia).- *Proc. 30th Int. Geol. Congr.*, vol. 24, 86-105, VSP, International Science Publishers, Zeist, Nietherland.

- Knez, M., 1997b: Speleogenesis of phreatic channels in bedding-planes in the frame of karst aquifer (Škocjanske jame Caves, Slovenia).- Proc. 12th Int. Cong. Speleology, vol. 2, 279-282, La Chaux-de-Fonds, France.
- Knez, M., 1997c: Prvi rezultati raziskav kamnine v treh lunanskih kamnitih gozdovih (Yunnan, Kitajska). Summary: First results of rock research in three Lunan Stone forests (Yunnan, China).- Acta Carsologica, 26/2, 431-439, Ljubljana.
- Kogovšek, J., 1984: Vertikalno prenikanje v Škocjanskih jamah in Dimnicah. Summary - Vertical percolation in Škocjanske jame and Dimnice.- Acta carsologica, 12 (1983), 49-65, Ljubljana.
- Kogovšek, J., 1997: Nekatere značilnosti prenikajoče vode na lunanskem krasu, Yunnan, Kitajska. Summary: Some properties of the percolation water in the karst of Lunan, Yunnan province, China.- Acta carsologica 26/2, 441-456.
- Kogovšek, J., A. Kranjc, 1988: Opazovanje kislosti padavin v Postojni v letih 1985-87. Summary - Precipitation acidity observations in Postojna (1986-87).- Geografski vestnik, 60, 21-29, Ljubljana.
- Kogovšek, J., H., Liu, M., Petrič, 1997: Properties of underground water flow in karst area near Lunan in Yunnan Province, China.- Tracer Hydrology 97, 255-261, Rotterdam.
- Kranjc, A., 1989: Recent Fluvial Cave Sediments, Their Origin and Role in Speleogenesis.- Dela SAZU, Razred za naravoslovne vede, Dela 27, 167 p., Ljubljana.
- Liu Xing, 1998: ESR dating and its geological significance of travertine in the stone forest, Yunnan province; Carsologica sinica, 17, 1, 9-14, Beijing.
- Maire, R., Zhang Shouyue, Song Shixiong, 1991: Genese des karsts subtropicaux de Chine du sud (Guizhou, sichuan, Hubei).- Gebihe 89, Grottes et karsts tropicaux de Chine Meridionale, Karstologia memoires, 4, 162-186.
- Mangin, A., 1984: Pour une meilleure connaissance des systemes hydrologiques a partir des analyses corrélatoire et spectrale.- Journal of Hydrology, 67, 25-43, Amsterdam.
- Mangin, A., 1997: Some features of the Stone forest of Lunan, Yunnan, China.- Stone forest a treasure of natural heritage, Proceedings of International Symposium for Lunan Shilin to Apply for World Natural Heritage Status, 68-70, China environmental science press.
- Mihevc, A., 1994: Kitajski kras. Summary: China Karst.- Geografski obzornik, 3-8, Ljubljana.
- Moses, C.A., H.A. Viles, 1996: Nanoscale morphologies and their role in the development of karren.- Karren landforms, 85-96, Palma.
- Novak, D., 1991: Novejša sledenja kraških voda v Sloveniji po letu 1965. Summary-Recent tracings of karstic waters in Slovenia.- Geologija, 33, 461-478, Ljubljana.
- Perna, G., 1996: Evolution of karren in the Alto Garda area (Trentino, North Italy).- Karren Landforms, 381-396, Palma.
- Placer, L., 1996: tectonic structure of southwest Slovenia.- International workshop Postojna '96: The role of impact processes in the geological and biological evolution of planet Earth, Eds. K. Drobne, Š. Goričan, B. Kotnik, 137-140, Ljubljana.
- Salomon, J.-N., 1997: Comparaison entre les "Stone forests" du Lunan (Yunnan-Chine) et les Karsts a "Tsingy" de Madagascar.- Stone Forest, a treasure of natural Heritage (Song, L., Waltham, T., Cao, N., Wang, F., Eds.), 124-136, Beijing.
- Slabe, T., 1990: Skalne oblike v dveh poligenetskih jamah visokega krasa. Summary: Rocky features in two polygenetic caves of high karst.- Acta carsologica 19, 165-196, Ljubljana.
- Slabe, T., 1994: Dejavniki oblikovanja jamske skalne površine. Summary: The factors influencing on the formation of the cave rocky surface.- Acta carsologica 23, 369-398. Ljubljana.
- Slabe, T., 1995, Cave Rocky Relief and its Speleogenetical Significance.- Zbirka ZRC, 10, 128 p., Ljubljana.
- Slabe, T., 1997: Karst features discovered during motorway construction in Slovenia.- Environmental Geology 32/3, 186-190, Springer-Verlag.

- Song Lin Hua, 1986: Origination of stone forest in China.- *International Journal of Speleology* 15 (1-4), 3-33, Trieste.
- Song Lin Hua, Liu Hong, 1992: Control of geological structures over development of cockpit karst in south Yunnan, China.- *Tübingen Geographische Studien*, 109, 57-70, Tübingen.
- Song Linhua, He Yueben, Feng Yan, 1993: Ground water tracing in Wulichong surface drainage system Mengzi county, Yunnan province.- *Proc. of 11th International Congress of Speleology*, 227-229, Beijing.
- Song Linhua, Li Yuhui, 1997: Definition of Stone forest and its evolution in Lunan County, Yunnan, China.- *Stone forest a treasure of natural heritage, Proceedings of International Symposium for Lunan Shilin to Apply for World Natural Heritage Status*, 37-45, China environmental science press.
- Song Linhua, Wang Fuchang, 1997: Lunan Shilin Landscape in China.- *Proceedings of 12th International Congress of Speleology*, Vol. 1, Symposium 8, 433-435, La Chaux-de-Fonds.
- Standard Methods for the examination of water and wastewater., 1992. 18th edition
- Sweeting, M., 1992: Tectonics and fluvial denudation in the formation of cone karst, with particular reference to South China. *Tübinger Geographische Studien*, 109, *Proceedings of the Karst Symposium - Blaubeuren*, 45 - 56, Tübingen.
- Sweeting, M. M., 1995: *Karst in China. Its Geomorphology and Environment.* -Springer-Verlag, XI+265 str., Berlin, Heidelberg, New York.
- Šebela, S., 1996: Results of Tectonic Measurements in the Stone Forest, Lunan, China.- *Acta carsologica*, 25, 437-450, Ljubljana.
- Trudgill, S. T., 1986: Limestone weathering under a soil cover and the evolution of limestone pavements, Malham district, north Yorkshire, UK.- *New directions in karst*, Ed.K. Paterson and M.M. Sweeting, *Proceeding of the Anglo-French karst symposium*, 461-472.
- Tucker, E.M. & Wright, V.P., 1990: *Carbonate sedimentology.*- Blackwell Scientific Publications, 482 p., Oxford.
- Waltham, A. C., 1984: Some features of karst geomorphology in South China.- *Cave Science*, *The transactions of the British Cave Research Association*, 11, 4, 185-198, Somerset.
- Water and Electricity Survey & Plan Institution of Quijing, Yunnan, 1993: Hydrogeological map. (Unpublished)
- Weng Jintao, 1987: *Karst and carbonate rocks in Guilin*; published by Chongqing publishing house.
- Williams, P., 1985: Subcutaneous hydrology and the development of doline and cockpit karst. *Z. Geomorf.* 29, 4, 463-482. Berlin.
- Yu Yinbiao, Yang Baoguo, 1997: Paleoenvironment during formation of Lunan Stone Forest.- *Stone forest a treasure of natural heritage, Proceedings of International Symposium for Lunan Shilin to Apply for World Natural Heritage Status*, 63-67, China environmental science press.
- Yu Jinbiao, Yang Lizheng & Zhang Haisheng etc., 1990: *Typical Study on Developmental Regularity of Karst in China - assessment and utilization of water resources in the Southern Puding, Guizhou Province.* Scientific Publishing House. 108-116
- Yuan Daoxian, 1997: A global perspective of Lunan Stone forest.- *Stone forest a treasure of natural heritage, Proceedings of International Symposium for Lunan Shilin to Apply for World Natural Heritage Status*, 68-70, China environmental science press.
- Yuan Daoxian, 1991: *Karst of China.*- Geological Publishing House, 224p., Beijing.
- Yuan Daoxian, Cai Guihong, 1988: *The Science of Karst Environment*, Chongqing Publishing House, Chongqing, China, 59-71.
- Zhang Faming, Geng Hong, Li Yuhui, Liang Yongning, Yang Yanhua, Ren Jian, Wang Fuchang, Tao Honglin, Li Zhongde, 1997: *Study on the Lunan stone forest karst, China.*- Yunnan Science and Technology Press, pp. 155.

- Zhang Faming, Wang Fuchang, Wang Huiji, 1997: Lunan Stone forest landscape and its protection and conservation.- Stone forest a treasure of natural heritage, Proceedings of International Symposium for Lunan Shilin to Apply for World Natural Heritage Status, 71-77, China environmental science press.
- Zhang Shouyue, 1983: The development and evolution of Lunan Stone Forest.- *Carsologica Sinica*, 3, 2, 48-55 (in Chinese).
- Zhang Shouyue, 1984: The development and evolution of Lunan stone forest.- *Carsologica Sinica* 1984, 3(2).
- Zhang Shouyue, 1987: Research of China karst.- Karst Research Group, Institute of Geology, Academia Sinica, (ed) Science Press, Beijing.
- Zhang Shouyue, 1997: Stone forest in China and pinnacle karst in Madagascar.- Stone forest a treasure of natural heritage, Proceedings of International Symposium for Lunan Shilin to Apply for World Natural Heritage Status, 78-80, China environmental science press.
- Zhang Shouyue, J.P. Barnaby, 1988: Guizhou '86. Premiere expedition speleologique franco - chinoise. PSCJA.- Lyon et Institut de Geologie de Academia Sinica. *Spelunca - Memoires* (16).
- Zhang, D., T, Walthman, 1985: Guizhou. Manuscript copy.
- Zhang Zhigan, 1980: Karst types in China.- *GeoJournal*, 4,6, 541-570.
- Zhang, S., 1997: Stone Forest in China and Pinnacle Karst in Madagascar.- Stone Forest, a treasure of natural Heritage (Song, L., Waltham, T., Cao, N., Wang, F., Eds.), 78-80, Beijing.
- Zhu Xuewen 1988: Guilin Karst. -Shanghai scientific & Technical publishers, 1-188, Shanghai.
- Zupan, N., 1991: Flowstone datations in Slovenia.- *Acta carsologica* 20, 187-204, Ljubljana.